School of Medicine
Institute of Infection and Immunity
Ysgol Meddygaeth
Adran Heintiau Imiwnedd

Human γδ T cell-based immunotherapy for breast cancer

Hung-Chang Chen

Thesis presented for the degree of
Doctor of Philosophy

September 2015

Cardiff Institute of Infection & Immunity
School of Medicine, Cardiff University

DECLARATION

This work has not been submitted in substance for any other degree or award at this or any other university or place of learning, nor is being submitted concurrently in candidature for any degree or other award.

Signed …… (candidate) Date: ……

Statement 1

This thesis is being submitted in partial fulfilment of the requirements for the degree of PhD.

Signed …… (candidate) Date: ……

Statement 2

This thesis is the result of my own independent work/investigation, except where otherwise stated. Other sources are acknowledged by explicit references.

Signed …… (candidate) Date: ……

Statement 3

I hereby give consent for my thesis, if accepted, to be available for photocopying and for inter-library loan, and for the title and summary to be made available to outside organisations.

Signed …… (candidate) Date: ……

Statement 4: Previously approved bar on access

I hereby give consent for my thesis, if accepted, to be available for photocopying and for inter-library loans after expiry of a bar on access previously approved by the Academic Standards & Quality Committee.

Signed …… (candidate) Date: ……

To my Parents, Brother and Grandparents,
who have selflessly supported me throughout my pursuit of knowledge

ACKNOWLEDGEMENTS

Firstly, I must express sincere gratitude to my supervisor, Dr. Matthias Eberl, for tremendous support, guidance and encouragement throughout my PhD. Your patience in correcting and editing my thesis was invaluable. Thank you for listening to all my ideas even when they were somewhat left-field. Additionally, thank you for constantly ingraining the importance of setting up rigorous experiments using "endless" controls. I would also like to express my great appreciation to Prof. Bernhard Moser, for your inspiration and thoughtful support especially during my writing-up period. Additionally, many thanks go to my co-supervisor, Dr. Richard Clarkson, for your critical advice. Learning and developing as a scientist in such a wonderful and nurturing environment, alongside your great minds, has been a fantastic and rewarding experience.

A massive thank you goes to all the members in Moser/Eberl group; Chris Tyler, Anna Rita Liuzzi, Dr. Chan-Yu Lin, Dr. Wajid Khan, Dr. Michelle McCully, Paul Collins, Ann Kift-Morgan, Dr. Ida Jackson, Dr. Martin Davey, Dr. Matt Morgan, Dr. Joanne Welton, Dr. Jingjing Zhang, Andy Thomas, Dr. Luke Piggott, Yasmin Shanneik and Dr. Riaz Jannoo, for their constant support, help and discussions. I have always enjoyed many happy hours with you inside and outside of the lab. I gratefully acknowledge all the help from: Prof. Awen Gallimore, Dr. Ann Ager, Dr. Garry Dolton, Dr. Emma Kempshall and Ellyn Hughes for setting up the animal study; Dr. John Bridgeman, Dr. Chia-Te Liao and Tamsin Dockree for lentiviral constructs; Dr. Thomas Herrmann and his group for FPPS shRNA constructs; Dr. Aled Clayton and Dr. Jason Webber for confocal microscopy; Dr. Emmanuel Scotet, Dr. Ulrich Jarry and Dr. Noémie Joalland for collaboration in setting up T cell adoptive transfer model; Dr. Catherine Naseriyan for cell sorting; Prof. Robert Weinberg for providing HMLER cells; Dr. Fariba Navid for hu14.18K322A antibodies; Dr. Daniel Olive for BTN3A blocking antibodies and Dr. Hassan Jomaa for synthetic HMB-PP. I would also like to thank Dr. David Rhodes for including me in the BTN3 and PPL study. I sincerely appreciate the generous support from Tenovus PhD Studentship, Government Scholarship for Study Abroad from the Taiwanese Ministry of Education and Cardiff CR-UK Centre Development Fund. Without all your invaluable support, this thesis could not have been completed.

I would like to thank my thesis examiners, Prof. Francesco Dieli and Prof. Andrew Godkin, for their time and insightful questions to enhance and improve this thesis. I would also like to acknowledge Dr. Alan Parker for chairing the *viva* and making it a smooth and pleasant journey.

I am grateful to my flatmates and friends here in Cardiff. Many thanks to Alison, Chris, Chia-Te, Sophie, Huiyu, Duarte and Bei for their consistent support and consideration outside the lab. I have enjoyed all the moments without holding a pipette because of you. Thank you for your consideration when I messed around at home and experimented, even exploding an egg all over the microwave oven. I would like to sincerely thank my friends, Bonnie, Yu-Chen and Chin-Hsuan, who are thousand and thousand miles away in Taiwan. Thank you for picking up the call, even past midnight, and for all your consistent support, listening and encouragement. I would also like to sincerely acknowledge my mentor, Prof. Shuen-Kuei Liao, for taking me into scientific research and looking after my development thereafter.

Lastly, I would like to express my great appreciation to my family for their endless and selfless love and encouragement. Thank you for always being there and letting me know that I would always have someone to rely on, no matter what happens. Without all your support I would not have had the bravery to pursue a PhD overseas, so far from home.

ABSTRACT

Scientific background. The inherent resistance of breast cancer stem cells (CSCs) to existing therapies has largely hampered effective treatments for advanced breast cancer. My research aimed at establishing novel immunotherapy approaches efficiently targeting CSCs by harnessing human γδ T cells as non-MHC-restricted killer cells and simultaneously as APCs to induce tumour-specific $CD8^+$ T cell responses.

Approach. An experimental model allowing reliable distinction of CSCs and non-CSCs was set up to study their interaction with γδ T cells and $CD8^+$ T cells. FluM1 and CMVpp65 viral epitopes were used as surrogates for yet-to-be-discovered CSC-associated antigens.

Results. Stable sublines with characteristics of CSCs and non-CSCs were generated from *ras*-transformed human mammary epithelial (HMLER) cells as confirmed by their (*i*) distinct expression profiles of CD24, CD44 and GD2, (*ii*) mesenchymal- and epithelial-like characteristics, (*iii*) differential growth patterns in mammosphere culture and (*iv*) distinct tumourigenicity, self-renewal and differentiation in NSG mice. The resistance of both CSCs and non-CSCs to γδ T cells could be overcome by inhibition of FPPS through pretreatment with zoledronate or FPPS-targeting shRNA, resulting in increased cytotoxicity and APC function of γδ T cells. CSCs presenting FluM1 or CMVpp65 exhibited stronger resistance to antigen-specific $CD8^+$ T cells as compared to their non-CSC counterparts. Of note, pretreatment of Flu M1- or CMVpp65-presenting CSCs with γδ T cell conditioned supernatant significantly increased surface expression of MHC class I and ICAM-1 by both CSCs and non-CSCs as well as their susceptibility to $CD8^+$ T cell-mediated killing. Moreover, using the humanised anti-GD2 monoclonal antibody, Hu14.18K322A, a specific direction of γδ T cell responses against CSCs could be achieved. In addition to their direct cytotoxicity and ability to modulate the susceptibility of CSCs and non-CSCs to $CD8^+$ T cell-mediated killing, γδ T cells concomitantly functioned as APCs to initiate *de novo* tumour-specific cytotoxic $CD8^+$ T cell responses.

Conclusions. My findings identify a powerful synergism between MHC-restricted and non-MHC-restricted T cells in the eradication of both CSCs and non-CSCs, thus establishing a powerful positive feedback loop for the eradication of residual cancer cells survived from killing by γδ T cells. My research suggests that novel immunotherapies

may benefit from a two-pronged approach combining γδ T cell and $CD8^+$ T cell targeting strategies that triggers effective innate-like and tumour-specific adaptive responses.

PUBLICATIONS AND PRESENTATIONS

Publications

Chen H-C, Jarry U, Bridgeman JS, Khan MW, Shanneik Y, Piggott L, Li J, Herold MJ, Herrmann T, Gallimore AW, Wooldridge L, Scotet E, Clarkson RW, Moser B and Eberl M. Synergistic targeting of breast cancer stem cells by human γδ T cells and cytotoxic $CD8^+$ T cells. (in preparation)

Rhodes DA, **Chen H-C**, Price AJ, Keeble AS Davey MS, James LC, Eberl M and Trowsdale J. Interaction of BTN3A1 with the cytoskeletal adaptor periplakin and the activation of γδ T cells. ***J Immunol*** 194: 2390, 2015

Khan MW, Curbishley S, **Chen H-C,** Thomas A, Pircher H, Mavilio D, Steven N, Eberl M and Moser B. Expanded human blood-derived γδ T cells display potent antigen-presentation functions. ***Front Immunol*** **5**: 344, 2014

Chen H-C, Dieli F, Eberl M. An unconventional TRAIL to cancer therapy. ***Eur J Immunol*** 43: 3159, 2013

Presentations

Chen H-C, Clarkson R, Herrmann T, Eberl M. Synergistic Targeting of Breast Cancer Stem Cells by Human γδ T Cells and Cytotoxic $CD8^+$ T Cells. **6^{th} γδ T Cell Conference**, Chicago, IL, USA, 16 - 18 May 2014 (oral presentation)

Chen H-C, Clarkson R, Herrmann T, Eberl M. Synergistic Targeting of Breast Cancer Stem Cells by Human γδ T Cells and Cytotoxic $CD8^+$ T Cells. ***Bright Sparks in Immunology,*** **BSI Congress 2013**, Liverpool, UK December 2-5, 2013 (oral presentation)

Chen H-C, Clarkson R, Herrmann T, Eberl M. Synergistic Targeting of Breast Cancer Stem Cells by Human γδ T Cells and Cytotoxic $CD8^+$ T Cells. **ECSCRI Targeting Cancer Conference 2013**, Newport, Wales, UK July 24-26, 2013

Chen H-C, Piggot L, Clarkson R, Eberl M. Sensitization of Breast Cancer Cells to γδ T Cell-Mediated Cytotoxicity by Suppression of the Apoptosis Inhibitor c-FLIP. **5th International γδ T Cell Conference 2012**, Freiburg, Germany, May 31-Jun 2, 2012

LIST OF ABBREVIATIONS

ANOVA – Analysis of variance
ADCC – Antibody dependent cell cytotoxicity
ALDH – Aldehyde dehydrogenase
APC – Allophycocyanin
APCs –Antigen presenting cells
BM – Bone marrow
BSA – Bovine serum albumin
BTN3 – Butyrophilin 3
CD – Cluster of differentiation
CSC – Cancer stem cell
CMV – Cytomegalovirus
CTL – Cytotoxic T lymphocytes
Cy – Cyanine
DAMPs – Damage associated molecular patterns
DAPI – 4', 6-diamino-2-phenylindole
DC – Dendritic cell
DMAPP – Dimethylallyl pyrophosphate
DNA – Deoxyribonucleic acid
ds – double stranded
EDTA – Ethylenediaminetetraacetic acid
EphA2 – Ephrin receptor A2
EMT – Epithelial-mesenchymal transition
EPCR – Endothelial protein C receptor
ER – Estrogen receptor
FACS – Fluorescence-activated cell sorting
FcR – Fc receptor
FCS – Foetal calf serum
ffluc – Firefly luciferase
FITC – Fluorescein isothiocyanate
Flu M1 – Influenza virus matrix protein M1
FPPS – Farnesyl pyrophosphate
FSC – Forward scatter
GD2 – Disialoganglioside 2
Gluc – *Gaussia* luciferase
Her2 – Human epidermal growth factor receptor 2

HLA – Human leukocyte antigen

HMB-PP – (*E*)-4-hydroxy-3-methyl-2-butenyl pyrophosphate

HMLE – Human mammary epithelial cell

HMLER – *Ras*-transformed human mammary epithelial cell

hTERT – Human telomerase reverse transcriptase

ICAM-1 – Intercellular adhesion molecule-1

IF – Immunofluorescence

IFN-γ – Interferon-γ

IL – Interleukin

i.p. – Intraperitoneal

IPP – Isopentenyl pyrophosphate

i.v. – Intravenous

LMP2 – Epstein Barr virus latent membrane protein-2

LN – Lymph node

LPS – Lipopolysaccharides

LT – Large T antigen

mAb – Monoclonal antibody

MEP – Methylerythritol 4-phosphate

MHC – Major histocompatibility complex

MFI – Mean fluorescent intensity

MPS – Mononuclear phagocyte system

nBP – Nitrogen-containing bisphosphonate

NCR – Natural cytotoxicity receptor

NK – Nature killer

NKG2D – Natural-killer group 2, member D

NSG – NOD scid gamma (NOD.Cg-Prkdc^{scid} Il2rg^{tm1Wjl}/SzJ)

PAMPs – Pathogen associated molecular patterns

PBMC –Peripheral blood mononuclear cells

PBS – Phosphate buffered saline

PCR – Polymerase chain reaction

PE – Phycoerythrin

PerCP – Peridinin chlorophyll

pHH3 – phospho-histone H3

PHA – Phytohaemaglutinin

PI – Propidium iodide

PMA – Phorbol 12-myristate 13-acetate

PR – Progesterone receptor

RPMI – Roswell Park Memorial Institute

rpm – revolutions per minute

RT – Room temperature

s.c. – Subcutaneous

SSC – Side scatter

ST – Small T antigen

SV40 – Simian virus 40

TCR – T cell receptor

TGF-β – Transforming growth factor β

TLR –Toll-like receptor

TRAIL –Tumour necrosis factor-related apoptosis inducing ligand

TN – Triple negative

TNF-α – Tumour necrosis factor-α

Treg –Regulatory T cell

ULBP – UL16-binding protein

TABLE OF CONTENTS

LIST OF FIGURES

LIST OF TABLES

Chapter 1. Introduction

1.1. Breast Cancer

1.1.1. Epidemiology of breast cancer

According to GLOBOCAN 2012 (Ferlay *et al.*, 2015), breast cancer is currently the second most common cancer in the world. Growing from an estimated 1.38 million new cancer cases diagnosed in 2008 to an estimated 1.67 million new cancer cases diagnosed in 2012, which accounts for 25.2% of estimated total new cancer cases diagnosed in 2012, breast cancer remained the most common cancer diagnosed in women. The incidence rates of breast cancer vary considerably across the globe, ranging from 27 per 100,000 population in Middle Africa and Eastern Asia to 96 per 100,000 in Western Europe. In the UK, the incidence rate increased from less than 60 per 100,000 in the 1980s to about 90 per 100,000 in 2010. A similar increasing trend can be observed all over the world, especially in more developed regions, indicating that breast cancer as a growing problem in the UK and other more developed countries. With 522,000 deaths in 2012 worldwide, breast cancer ranks as the fifth most frequent cause of death from all cancers. In the UK, breast cancer accounted for 7% of all deaths from cancer and thus ranked 3rd most common cause of cancer in 2012 (Cancer Research UK). Despite the alarming increase in incidence rates, the mortality rate in the UK dropped from around 30 per 100,000 in 1985 to 15.2-18.1 per 100,000 in 2008, reflecting encouraging advances in early detection and adjuvant therapy over past decades. However, although overall survival of breast cancer patients is improving and has doubled in the last 40 years, the survival of breast cancer patients dropped significantly, depending on the stage of disease when diagnosed, with the 5-year survival rate of patient diagnosed with stage IV breast cancer during 2002-2006 being as low as only 15% (Cancer Research UK). These numbers indicate that there remains an unmet need for the development of more efficient treatments for patients with breast cancer, especially those at advanced stages.

1.1.2. Heterogeneity of breast cancer and clinical classification

Most breast tumours originate from epithelial and glandular epithelial tissue and thus are denoted as carcinoma and adenocarcinoma, respectively. However, some breast cancers may also present as sarcoma, which are derived from cells of muscle, fat or connective tissue. The development and progression of breast tumours have been described as a

linear process with multiple steps (Bombonati and Sgroi, 2011). Derived from the epithelium in the milk ducts, mutated cells with clear abnormality in the morphology of nucleus and cytoplasm, which is extensively used in the diagnoses for distinguishing neoplastic cell from normal cells, begin to grow rapidly without control and build up a compact mass restricted within the lumen by surrounding intact basal membranes. This progress has been characterised as a sequential transition typically from epithelial ductal hyperplasia (UDH), flat epithelial atypia (FEA) and atypical ductal hyperplasia (ADH), and eventually to ductal carcinoma *in situ* (DCIS). Similarly in the lobules, the transformation starts from atypical lobular hyperplasia (ALD) and subsequently progress to lobular carcinoma *in situ* (LCIS). As DCIS and LCIS keep accumulating more mutations and may thus evolve to acquire further malignant transformations, they develop to break out from the constraining basal membranes for invasion into surrounding tissues, and are then characterised as invasive ductal and lobular carcinoma, respectively. Together, lobular and ductal subtypes contribute to the majority of patients diagnosed with invasive breast cancer. Particularly, the ductal subtype accounts for 80% of diagnosed preinvasive and invasive breast cancers (Bombonati and Sgroi, 2011).

Breast cancer can be further classified into different subtypes for the purpose of prognosis by immunohistochemistry (IHC) examinations for the expression of estrogen receptor (ER), progesterone receptor (PR) and human epidermal growth factor receptor 2 (Her2) (Nielsen *et al.*, 2004). Currently, IHC staining of ER, PR and Her2 is used in routine diagnosis to classify breast tumour subtypes and provide prognostic and predictive information. Depending on the expression of ER, PR and Her2, breast cancers can be categorised into three major subtypes, namely ER^+/PR^+ (hormone receptor positive; HR^+), $HR^-/Her2^+$ and triple negative ($ER^-/RP^-/Her2^-$; TN). Each subtype is characterised by different histopathological features, prognosis and responses to different breast cancer therapies.

Exceeding this histological classification, the molecular and biological complexity of breast cancer with tremendous inter- and intra-tumour heterogeneity was further revealed by gene expression profiling (Perou *et al.*, 2000). In the human mammary gland, there are two distinct lineages of epithelial cells; the basal (and/or myoepithelial) cells that constitute the outer layers of the mammary ducts, and the luminal epithelial cells that line the insides of the mammary ducts. Through a large microarray study of 65 breast tumour

samples collected from 42 patients, Perou *et al.* introduced the concept of cell lineage on top of the traditional ER classification, and demonstrated that heterogeneous breast tumours could be precisely classified into four molecular subtypes: (*i*) luminal A, (*ii*) luminal B, (*iii*) $Her2^+$, and (iv) basal-like tumours (Perou *et al.*, 2000; Sorlie *et al.*, 2001; Sorlie *et al.*, 2003; Sotiriou *et al.*, 2003; Hu *et al.*, 2006).

Most breast cancers are luminal tumours, in which luminal A and B tumours account for 40% and 20% of breast cancer, respectively. While sharing similar characteristics in overexpression of ER, ER-responsive genes and a gene expression signature representative for luminal epithelial cells, luminal A and B tumours are distinct in their expression of Her2 and proliferation-related genes. ER^+ luminal A tumours are characterised by their high level expression of ER- and PR-associated genes, low level expression of proliferation-related genes and lack of Her2 expression (Perou *et al.*, 2000; Sorlie *et al.*, 2001; Loi *et al.*, 2007; Voduc *et al.*, 2010). Oppositely, luminal B tumours show strong expression of Her2 and proliferation-associated markers, *e.g.* Ki67, with decreased ER expression and absence of PR expression (Carey *et al.*, 2006). Her2 tumours account for 10-15% of breast cancer and show a characteristic lack of expression of both ER and PR (Carey *et al.*, 2006; Voduc *et al.*, 2010). Basal-like tumours share large similarities with TN tumours in terms of their genetic makeup and tumour behaviours (Nielsen *et al.*, 2004; Cleator *et al.*, 2007; Foulkes *et al.*, 2010). Together they account for around 15-20% of breast cancers, and both show a poorly differentiated and aggressive feature histologically with necrosis often being observed in these tumours.

1.1.3. Treatment of breast cancer and current obstacles

By defining the molecular subtype of the tumour, the treatment for each patient can be personalised with precision by choosing the most suitable and effective therapy currently available. For example, patients with tumour expressing ER and PR are likely to benefit from hormone therapy with tamoxifen and aromatase inhibitors (Ignatiadis and Sotiriou, 2013). Although carrying a generally worse prognosis with higher risk of recurrence and metastasis as compared to luminal tumours, $Her2^+$ breast cancer patients may benefit from therapies directly targeting Her2 such as trastuzumab (Herceptin) and lapatinib, but less so from endocrine-based therapies. Most importantly, TN and basal-like tumours, which lack expression of all three receptor targets and are therefore insensitive to standard drugs,

have significantly poorer clinical prognosis compared to the estrogen receptor-positive luminal A and luminal B tumours, and targeted therapy is currently limited (Rouzier *et al.*, 2005). In the absence of better options, patients with TN and basal-like tumours are currently treated with a combination of surgery, radiation therapy and chemotherapy using standard cytotoxic agents such as doxorubicin and paclitaxel, and hence suffer from associated short-term and long-term side effects. Although novel approaches are urgently needed for treating such resilient cancers, only few potential targets for TN and basal-like tumours including EGF receptor, αB-crystallin and cyclin E have been identified so far (Yehiely *et al.*, 2006).

Besides the need for better targeted therapies for TN and basal-like tumours, metastasis and recurrence after therapy remain major setbacks in improving outcomes. Nearly 30% of all patients with early stage breast cancer develop recurring disease, which in most cases is metastatic (Gonzalez-Angulo *et al.*, 2007). Treatment options for both metastasis and recurrence are very limited, and therapeutic efficacies are mostly disappointing. In addition, frequent drug resistance represents a major obstacle in treating breast cancer patients. For example, a substantial proportion of patients with localised disease, and most patients with advanced disease who initially respond to tamoxifen, subsequently develop *de novo* or acquired resistance (Early Breast Cancer Trialists' Collaborative, 2005; Chang, 2012). However, the mechanisms underlying the development of drug resistances in breast cancer are yet totally clear. Recently, the emerging concept of cancer stem cells (CSC) has linked this minor subset of pluripotent cells within the bulk tumour to the initiation of primary tumours and distant metastasis, disease relapse and recurrence as well as drug resistance (Pinto *et al.*, 2013; Luo *et al.*, 2015; Mitra *et al.*, 2015). Thus, novel approaches specifically targeting CSCs, including immunotherapies harnessing immune cells against CSCs, may provide a safe and effective way to treat breast cancer patients and improve outcomes.

1.2. Cancer stem cells

1.2.1. Heterogeneity of tumour

To explain the heterogeneity observed within a tumour, the classical clonal expansion model for carcinogenesis proposed that normal cells may become transformed by stochastically accumulating distinct combinations of gene mutations during the process of tumourigenesis. These transformed and malignant cells may share equal or similar tumourigenicity and expand clonally, thereby giving rise to a heterogeneous tumour (Nowell, 1976). The more recent cancer stem cell hypothesis arose from the similarities observed between normal stem cells and tumourigenic cells with regard to their unique ability to divide asymmetrically for self-renewal, and to give rise to different daughter cells, a non-tumourigenic differentiated cells and a tumourigenic CSC retaining its pluripotency, by asymmetric division. In contrast to the clonal expansion model, the CSC hypothesis applies and emphasises the hierarchy within a tumour based on the concept that not all transformed cells are equally tumourigenic (Reya *et al.*, 2001; Campbell and Polyak, 2007). However, these two models are not mutually exclusive. During the long period of tumourigenesis, it is conceivable that the initial CSC may further diverse into different subsets by acquiring new sets of distinct gene mutations, which allows the maintenance of CSC properties with further modification in their malignancies, and subsequently contribute to the diversity within a tumour by clonal expansion of these different CSC-like subsets (Visvader and Lindeman, 2008; Beck and Blanpain, 2013).

1.2.2. Phenotypical and functional characterisation of breast cancer stem cells

Bonnet and Dick provided the first experimental evidence for the existence of CSCs in a human acute myeloid leukaemia xenotransplantation model in NOD/SCID mice by defining surrogate markers for potential CSCs (Bonnet and Dick, 1997). A minor population of cells with a $CD34^{+}$ $CD38^{-}$ phenotype was identified to exhibit superior tumourigenic capacity as compared to the bulk of the leukaemia cells (Bonnet and Dick, 1997). In extension of this pioneering work, serial transplantation of specific cell populations in immunodeficient mice comprehensively encompasses the most important CSC-like properties including tumourigenicity, self-renewal and pluripotency in a single experiment, and is now considered as the golden standard for the identification and characterisation of CSCs from different haematological malignancies and solid tumours of different origins, including breast cancer (Smalley *et al.*, 2013; Kreso and Dick, 2014).

Using this standard approach, Al Hajj *et al.*, were the first to identify a small population of highly tumourigenic cells from breast cancer lesions as $CD44^+$ $CD24^-$ ESA^- $lineage^-$ cells (Al-Hajj *et al.*, 2003). Following from this observation, similar highly tumourigenic CSC populations have been identified in different malignancies such as brain (Singh *et al.*, 2004), colon (O'Brien *et al.*, 2007; Ricci-Vitiani *et al.*, 2007), melanoma (Schatton *et al.*, 2008) and pancreatic cancer (Hermann *et al.*, 2007), by the use of a broad panel of putative markers for CSCs, reflecting the huge diversity of CSCs across different types of tumours. In addition to the definition as $CD44^+$ $CD24^-$ cells, CSCs within breast tumours have been characterised phenotypically by the use of cell surface markers such as CD90 (Lu *et al.*, 2014), CD133 (Wright *et al.*, 2008) and GD2 (Battula *et al.*, 2012; Liang *et al.*, 2013), and functionally by specific enzyme activity, *e.g.* aldehyde dehydrogenase 1 (ALDH1) (Ginestier *et al.*, 2007), alone or in combination. Wright *et al.* showed that both $CD44^+$ $CD24^-$ and $CD133^+$ cell populations derived from *BRCA1* deficient mouse mammary tumours exhibited comparable tumourigenicity and stem cell-associated gene expression profiles, suggesting the existence of heterogeneous CSC populations within tumours (Wright *et al.*, 2008). Similarly, Hwang-Verslues *et al.* showed that the specificity of proposed markers including CD44/CD24, ESA, CD133, CXCR4 and PROCR for the identification of CSCs varied considerably across a panel of human breast cancer cell lines and specimen (Hwang-Verslues *et al.*, 2009). Furthermore, Ginestier *et al.* showed that $ALDH^+$ and $CD44^+$ $CD24^-$ $lineage^-$ populations overlapped minimally by only 0.1-1.2% in four breast cancer samples examined (Ginestier *et al.*, 2010). Functionally, $ALDH^+$ and $CD44^+$ $CD24^-$ $lineage^-$ populations showed distinct tumourigenicity, with the minor population of cells with overlapping expression profiles exhibiting strongest tumourigenicity, suggesting that at least two inter-converting CSC populations may co-exist within a tumour and subsequently contribute to intra-tumour heterogeneity. Putative CSC subpopulations were further linked to epithelial-mesenchymal transition (EMT), a phenomenon governing embryogenesis, development and organogenesis (Kalluri, 2009; Thiery *et al.*, 2009). While breast CSCs typically show a mesenchymal-like (EMT-like) morphology with a $CD44^+$ $CD24^-$ $EpCAM^-$ $CD49f^+$ expression profile and are functionally more quiescent but more invasive, CSCs with an epithelial-like (MET-like) morphology and a distinct $ALDH^+$ $EpCAM^+$ $CD49f^+$ expression profile appear to be functionally more active and possess the capacity for self-renewal (Biddle *et al.*, 2011; Liu *et al.*, 2012). This interpretation is supported by the observation that MET-like CSCs are found to reside predominantly in the centre of a

tumour, whereas EMT-like CSCs typically sit at the invasive front where they may drive tumour dissemination and metastasis (Liu *et al.*, 2012).

Taken together, these findings reveal that there is no universally applicable CSC marker for all subtypes of breast cancer. Given the substantial heterogeneity within every single breast tumour, it is likely that more than one population of tumourigenic CSCs, concomitantly exist intra-tumourally, with different levels of tumourigenicity and differentiation. Moreover, breast CSCs between different tumours are indeed distinct and thus contribute to inter-tumour heterogeneity. Notwithstanding these obstacles, different subpopulations of breast CSCs share functional similarities, which provides us with a window of opportunities to study the biology of CSCs and CSC-like cells and their interaction with the immune system.

1.2.3. Cancer stem cells, epithelial-mesenchymal transition and metastasis

Metastasis is a complex process involving both genetic and epigenetic changes when cells derived from the primary tumour translocate to a new distant site (Hanahan and Weinberg, 2011). During this process, cancer cells have to overcome numbers of hurdles. First, in response to stresses such as hypoxia (Yang *et al.*, 2008) and inflammation (Wu *et al.*, 2009a), some tumour cells residing at the invasive front of the primary tumour may lose their cell-cell adhesion capacity and dissociate themselves from the bulk tumour through EMT. Once receiving environmental cues like TGF-β, such cells may eventually lose their surface expression of E-cadherin, which is involved in the formation of adheren junctions between cells, and instead acquire expression of N-cadherin, vimentin and fibronectin, which participate in the determination of cellular polarity and rearrangement of the cytoskeleton (Xu *et al.*, 2009a). This series of events subsequently leads to a distinct change from cells with apical-basal polarity and cuboidal-like morphology to cells with asymmetric polarity and enhanced motility and invasiveness (Vincent-Salomon and Thiery, 2003). In addition, EMT has been proposed to concomitantly induce stem cell-like properties in procuring differentiated cells (Mani *et al.*, 2008; Morel *et al.*, 2008; Scheel and Weinberg, 2012). Acquisition of the stemness could largely benefit the survival of disseminated cells in the circulation and seeding at distant sites (Medema, 2013). These EMT-like malignant cells can then invade into the nearby basement membrane and blood/lymphatic vessels by degradation of extracellular matrix (ECM)

through releasing a variety of enzymes including diapeptidases, arginases, acid phosphatases, cathepsin, and matrix metalloproteinases (MMPs) (Deryugina and Quigley, 2006; Struckmann *et al.*, 2008). Circulating tumour cells frequently can protect themselves from the attack of immune cells (Chouaib *et al.*, 2014) and the fluid pressure caused by the blood flow through strategies including induction of platelet aggregation to form a tumour-platelet complex (Tsuruo and Fujita, 2008). During this process, only a few circulating tumour cells penetrating through the wall of a blood vessel (extravasation) or the lymphatic system will successfully be transported to an appropriate organ site, where they colonise to form a new metastatic mass by inducing angiogenesis and adapting to the new microenvironment (Hanahan and Weinberg, 2011). This new soil is now known as "pre-metastatic niche", which is believed to be prepared ahead of time for metastatic deposition of tumour cells (Psaila *et al.*, 2006). The acquisition of stem-like properties through EMT endows CSCs with a great plasticity to adapt to, and colonise, the new microenvironment (Medema, 2013).

1.2.4. Intrinsic resistance of CSCs to chemotherapy, radiotherapy and immune surveillance

CSCs have been as well characterised for their innate resistance to chemotherapeutic drugs (Dean *et al.*, 2005), radiation (Rich, 2007) and immune surveillance (Kawasaki and Farrar, 2008; Schatton and Frank, 2009; Chouaib *et al.*, 2014) and may thus be a major driver of disease recurrence after treatment.

Conventional stem cells and CSCs share many properties including their expression of ATP-binding cassette (ABC) transporters, active DNA repair capacity and intrinsic resistance to apoptosis, which in combination lead to their resistance to cancer therapies. Goodell *et al.* found that ABCG2, also termed BCRP (breast cancer resistance protein), which was originally identified in mitoxantrone-resistant cells, has the ability to pump out the dye Hoechst 33342, resulting in a characteristic unlabelled "side population" detected by flow cytometry, which predominantly consists of CSCs (Goodell *et al.*, 1997). ABCB5, another ABC transporter, was also found to have the ability to mediate chemoresistance in stem-like tumour cell populations in human malignant melanoma (Schatton *et al.*, 2008). By expression of these ABC transporters, CSCs obtain a unique capacity to export a wide range of cytotoxic drugs and thus acquire multidrug resistance

(MDR). Increased activation of the DNA damage checkpoint has been characterised in CSCs derived from human glioblastoma. Although having similar susceptibility to ionising radiation compared to non-CSCs, CSCs respond to these double stranded DNA damages more efficiently by their elevated basal expression of active checkpoint kinases such as CDK1, CDK 2 and rad17 (Bao *et al.*, 2006). Piggott *et al.* showed that suppression of the apoptosis inhibitor cellular FLICE-Like Inhibitory Protein (c-FLIP), an antagonist of caspase-8 and caspase-10, preferentially sensitises breast CSCs to the anti-cancer agent tumour necrosis factor (TNF)-related apoptosis inducing ligand (TRAIL), suggesting enhanced endogenous resistance of breast CSCs to apoptosis and their potential to escape from immune surveillance (Piggott *et al.*, 2011).

In addition, similarly to mesenchymal stem cells (Le Blanc and Ringden, 2007; Uccelli *et al.*, 2008), CSCs also exhibit a suppressive immunomodulatory nature (Schatton and Frank, 2009). Schatton *et al.* showed that malignant melanoma-initiating cells (MMICs) characterised by ABCB5 expression (Schatton *et al.*, 2008) significantly suppress secretion of interleukin-2 (IL-2) by mitogen-stimulated PBMCs and skewed the normal T-cell mediated response by inducing the secretion of the suppressive cytokine IL-10 by autologous PBMCs in co-culture (Schatton *et al.*, 2010b). Similarly, glioblastoma CSC-like cells suppress the proliferation and IL-2 and interferon (IFN)-γ secretion by T cells upon non-antigen-specific stimulation with mitogen and anti-CD3/CD28 (Di Tomaso *et al.*, 2010; Wei *et al.*, 2010b). By the secretion of immunosuppressive cytokines and growth factors such as TGF-β and VEGF, CSCs isolated from different type of tumours including breast cancer (Shipitsin *et al.*, 2007), glioblastoma (Bao *et al.*, 2006; Wei *et al.*, 2010a) and melanoma (Schatton *et al.*, 2010b) can thus induce anergy of antigen-reactive lymphocytes. Expression of programmed death-ligand 1 (PD-L1) and secretion of galectin-3 allows CSCs to directly suppress antitumour immunity by inducing apoptosis of cancer-reactive T cell clones (Wei *et al.*, 2010b). In addition to direct suppression of immune responses, MMICs showed the capacity to induce functional regulatory T (Treg) cells (in terms of IL-10 secretion) from PBMCs in co-culture *via* their potent expression of B7.2 and 4-1BBL (Schatton *et al.*, 2010b). Similar induction of Treg cells was observed in co-culture of PBMCs with CSC-like cells derived from glioblastoma (Wei *et al.*, 2010b).

Apart from suppressing immune responses, CSCs may develop strategies to escape from immunosurveillance. Through down-regulated expression of tumour-associated antigens, *e.g.* MART-1 and NY-ESO-1, as well as of MHC class I and II and co-stimulatory molecules such as CD80, CD86 and CD40, CSCs can escape from MHC-restricted T cells (Di Tomaso *et al.*, 2010; Schatton *et al.*, 2010b). Similarly, CSCs can down-regulate their expression of NKG2D ligands to evade cytotoxicity by non-MHC-restricted NK cells and γδ T cells (Todaro *et al.*, 2009; Di Tomaso *et al.*, 2010).

Selective eradication of CSCs by different therapeutic strategies has been reported to effectively inhibit experimental tumour growth (Bao *et al.*, 2006; Schatton *et al.*, 2008; Chan *et al.*, 2009; Gupta *et al.*, 2009; Majeti *et al.*, 2009). Thus, it is conceivable that successful therapy of breast cancer requires complete eradication of CSCs within a tumour by rebalancing the tumour microenvironment with adequate sensitising strategies and/or adjuvants to recreate effective and specific anti-CSC immunity. Such CSC-targeting therapies are likely to lead to better outcomes by efficiently preventing disease relapse and harnessing long-lasting anti-tumour immunity. For this purpose, γδ T cells, which can function effectively as both non-MHC-restricted innate-like killer cells and professional APCs, are particularly attractive targets to complement and restore the MHC-restricted surveillance and boost anti-CSC adaptive immune responses.

1.3. γδ T cells

1.3.1. γδ T cells as the third arm for immune protection

Set aside from conventional αβ T cells and B cells, γδ T cells constitute an "unconventional" lymphocyte population with distinct functions that are complementary to those of B cells and αβ T cells. γδ T cells comprise different subsets defined by the expression of different combinations of γ chains and δ chains of the TCR. These different γδ T cell subsets exhibit distinct features with regard to tissue tropism, anatomical location, antigen specificity and function (Bonneville *et al.*, 2010; Vantourout and Hayday, 2013). Uniquely, γδ T cells exhibit both specified adaptive features for the expression of rearranged (yet non-MHC-restricted) T cell receptors (TCRs), and innate-like functions of NK cells and myeloid cells (Bonneville *et al.*, 2010; Vantourout and Hayday, 2013). Functionally, they show surprising plasticity (Bonneville *et al.*, 2010; Vantourout and Hayday, 2013; Lafont *et al.*, 2014) to act as (*i*) efficient killer cells recognising a broad spectrum of infected cells and cancer cells through their TCR and innate receptors such as NKG2D (Bonneville *et al.*, 2010; Vantourout and Hayday, 2013; Lafont *et al.*, 2014); (*ii*) as immune modulators providing help to B cells, DCs, monocytes and neutrophils for their specialised functions (Tyler *et al.*, 2015); (*iii*) as APCs to polarise helper CD4 T cells and initiate cytotoxic CD8 T cell responses (Moser and Eberl, 2007, 2011); and (*iv*) as regulatory cells suppressing immune responses (Wesch *et al.*, 2014).

1.3.2. γδ T cell subsets as defined by combination of TCR γ and δ chains

During their development in the thymus, γδ T cells acquire their TCR diversity through V(D)J recombination mediated by recombination activating gene (RAG). As compared to αβ T cells and B cells, γδ T cells have a relatively simple repertoire of Variable (V) gene segments available for rearrangement of both Vγ and Vδ chains (Adams *et al.*, 2015). In humans, rearrangement of the Vγ chain is restricted to seven functional Vγ gene segments (Vγ2, Vγ3, Vγ4, Vγ5, Vγ8, Vγ9 and Vγ11) out of total twelve Vγ gene segments on chromosome 7p15. Similarly, only three (Vδ1, Vδ2 and Vδ3) out of eight Vδ gene segments are frequently used for the rearrangement of the Vδ chain. As the Vδ gene locus sits within the Vα gene locus on chromosome 14p11-12, the remaining five Vδ gene segments (Vδ4, Vδ5, Vδ6, Vδ7 and Vδ8,) are shared for the use in rearrangement of both Vα and Vδ chains, possibly explaining their less frequent usage in rearranged Vδ chains. Of note, a pairing bias of Vγ with Vδ chains has been observed in γδ T cells localising to

different peripheral tissues in both mice and humans (Table1.1) (Pereira and Boucontet, 2004; Bonneville *et al.*, 2010). In the mouse, γδ T cells constitute only a minor fraction of thymocytes and circulating lymphocytes in the spleen, lymph nodes and peripheral blood, but are significantly enriched in epithelial tissues including epidermis and mucosa of the digestive and reproductive tracts (Goodman and Lefrancois, 1988; Borst *et al.*, 1991). In contrast, human γδ T cells constitute only a relatively small population of up to 10-20% of total T cells in the intestinal epithelium (Borst *et al.*, 1991). While human γδ T cells in most peripheral tissues, especially epithelial tissues, majorly express a Vδ1 chain, γδ T cells in blood predominantly express a Vδ2 chain preferentially paired with a Vγ9 chain (Triebel *et al.*, 1988a; Triebel *et al.*, 1988b; Borst *et al.*, 1989; Casorati *et al.*, 1989; Borst *et al.*, 1991). This apparent link between unique tissue distribution by different subset of γδ T cells led to the hypothesis that γδ TCRs with each specific combination of Vγ and Vδ chain may be restricted to recognise conserved (self-) antigens of only low variability, as opposed to the broad specificities of αβ TCRs and immunoglobulins (Janeway *et al.*, 1988). The tissue tropism of different γδ T cell subsets may thus largely depend on the prevalence of different target antigens in different tissues.

Table 1.1. Distribution and repertoire of γδ T cells in humans and mice

Peripheral location	Predominant usage (and pairing, if applicable) of Vγ and Vδ gene segments
Human	
Blood	Vγ9/Vδ2*
Dermis	Vδ1
Gut epithelia	Vδ1 and Vδ3
Liver	Vδ1 and Vδ3
Spleen	Vδ1
Thymus	Vδ1
Mouse	
Adult thymus	Diverse
Dermis	Vγ4[♯]
Epidermis	Vγ5/Vδ1
Gut epithelia	Vγ7/Vδ4, Vγ7/Vδ5, Vγ7/Vγδ6 and Vγ7/Vγδ7
Liver	Vγ1/Vδ6.3, Vγ4 and Vγ6
Lung	Vγ4 and Vγ6
Lymph nodes	Diverse
Spleen	Vγ1 and Vγ4
Uterovaginal epithelia	Vγ5/Vδ1

*Lefranc and Rabbitts' nomenclature for human γδ TCR; [♯]Heilig and Tonegawa's nomenclature for mouse γδ TCR. Adapted from (Hayday, 2000; Bonneville *et al.*, 2010)

1.3.3. Antigen recognition by different subsets of γδ T cells

Most γδ T cell antigens remain obscure, which severely impinges on our progress in understanding γδ T cell responses. However, significant advances have been made in identifying ligands for human γδ T cells. Vγ9/Vδ2 T cells recognise phosphoantigens (Constant *et al.*, 1994; Tanaka *et al.*, 1994), which have been studied extensively. Other human $V\delta2^{+}$ and $V\delta2^{neg}$ T cells have been described to recognise foreign antigens derived from bacteria and virus as well as self-antigens expressed on stressed and transformed cells (Table 1.2). Some $V\delta1^{+}$ T cells have been reported to exhibit alloreactivity to certain polymorphism of MHC molecules including HLA-A2, HLA-A24 and HLA-B27 (Ciccone *et al.*, 1989; Spits *et al.*, 1990), and to recognise MHC class I chain-related proteins, *e.g.* MICA and MICB (Groh *et al.*, 1998; Xu *et al.*, 2011). In addition, some $V\delta1^{+}$ T cells show autoreactivity to CD1c and CD1d molecules and recognise CD1d tetramers loaded with α-galactosylceramide (αGalCer) (Uldrich *et al.*, 2013) or sulfatides (Bai *et al.*, 2012; Luoma *et al.*, 2013). Interestingly, although the exact ligand(s) is currently unknown, $V\delta2^{neg}$ T cells (including $V\delta1^{+}$, $V\delta3^{+}$ and $V\delta5^{+}$ T cells) were observed to expand extensively in patients with cytomegalovirus (CMV) infection and exhibit strong cross-reactivity against CMV-infected cells and intestinal tumour cells (Halary *et al.*, 2005). A $V\gamma4/V\delta5^{+}$ T cell clone established from PBMCs of a CMV-infected patient showed specificity for endothelial protein C receptor (EPCR), a protein that resembles CD1d in its capacity to bind phospholipids (Willcox *et al.*, 2012). Interestingly, the recognition site of EPCR by Vγ4/Vδ5 TCR is outside the potential lipid binding pocket, suggesting that EPCR itself rather than lipid as the ligand for Vγ4/Vδ5 TCR. In mouse, a broad diversity of antigens for the recognition by different subset of γδ TCRs has been reported (Table 1.3). Despite these advances, only a small number of proposed γδ T cell ligands have actually been confirmed biochemically and/or structurally.

Table 1.2. Antigens recognised by γδ TCR in human and mouse

γδ T cells	Origin	Antigen	Reference
Vδ1*	IELs	MICA and MICB	(Groh *et al.*, 1998; Xu *et al.*, 2011)
Vδ1 and Vγ4/Vδ1	Clones and primary cells from blood	HLA-A2, -A24 and -B27	(Ciccone *et al.*, 1989; Spits *et al.*, 1990)
Vγ1.4/Vδ1 and Vγ2/Vδ1	Clones and primary cells from blood	CD1c	(Porcelli *et al.*, 1989; Faure *et al.*, 1990; Spada *et al.*, 2000)
Vδ1 and Vγ5/Vδ1	Primary cells from blood and clone transduced with Vγ5/Vδ1 TCR	CD1d tetramers loaded with αGalCer	(Uldrich *et al.*, 2013)
Vδ1	Blood	CD1d tetramers loaded with sulphatide	(Bai *et al.*, 2012; Luoma *et al.*, 2013)
Vδ1	Clones from Lyme arthritis synovial fluid	Lipohexapeptides	(Vincent *et al.*, 1998)
Vδ2	Blood, TILs and T-lymphoma cell line transduced with γδ TCR	ULBP4	(Kong *et al.*, 2009)
Vδ2	Primary cells from blood	hMSH2	(Dai *et al.*, 2012)
Vγ9/Vδ2	Clones and primary cells from blood	Phosphoantigens (IPP, HMB-PP)	(Constant *et al.*, 1994; Tanaka *et al.*, 1995; Hintz *et al.*, 2001)
Vγ9/Vδ2	Clones and primary cells from blood	F_1-ATPase associated with apolipoprotein A-I, ApppI or phosphoantigens as nucleotide derivatives	(Scotet *et al.*, 2005; Mookerjee-Basu *et al.*, 2010; Vantourout *et al.*, 2010)
Vγ9/Vδ2	Clones and primary cells from blood	Tetanus toxoid	(Kozbor *et al.*, 1989; Holoshitz *et al.*, 1992)
Vγ9/Vδ2	Clones and primary cells from blood	OXY, DXS2 or Rv2272 peptides	(Xi *et al.*, 2011; Xi *et al.*, 2013)
Vγ1.3/Vδ2	T hybridoma cell line transduced with γδ TCR	Histidyl-tRNA synthetase	(Bruder *et al.*, 2012)
Vγ4/Vδ5	Clone from blood	EPCR	(Willcox *et al.*, 2012)

*Lefranc and Rabbitts' nomenclature; adapted from (Vantourout and Hayday, 2013; De Libero *et al.*, 2014).

Table 1.3. Antigens recognised by γδ TCR in mouse

γδ T cells	Origin	Antigen	Reference
Vγ1[#] (clones)		Cardiolipin and apolipoprotein H	(Born *et al.*, 2003)
Vγ1 (clones)		Insulin peptide (B:9-23)	(Zhang *et al.*, 2010)
Vγ1-Jγ4/Vδ5		Phycoerythrin	(Zeng *et al.*, 2012)
Vγ1/Vδ8	NX6	Cyanine 3	(Zeng *et al.*, 2014)
Vγ2/Vδ5	Hybridoma LBK5	I-E^k	(Matis *et al.*, 1989)
Vγ2/Vδ8 (clone)		HSV glycoprotein I	(Johnson *et al.*, 1992)
Vγ4/Vδ4	1G9	4-hydoxy-3-nitrophenylacetyl	(Zeng *et al.*, 2014)
Various	Hybridomas G8 and KN6	H2-T10, -T22 and -T27	(Crowley *et al.*, 1997; Shin *et al.*, 2005)

[#]Heilig and Tonegawa's nomenclature for γδ TCR. Adapted from (Vantourout and Hayday, 2013; De Libero *et al.*, 2014).

1.3.4. Phosphoantigens as ligands for recognition by Vγ9/Vδ2 T cells *via* TCR

Due to their preferential localisation in blood, circulating human Vδ2^{+} T cells are much easier to obtain than predominantly tissue-residing Vδ2^{neg} T cells, and the early identification of phosphoantigens as specific agonists that induce activation and expansion of Vδ2^{+} T cells has allowed extensive studies of this γδ T cell subset *in vitro* and *in vivo*. Phosphoantigens are by far the best characterised class of agonistic molecules activating γδ T cells in human and non-human primates (Eberl *et al.*, 2003; Riganti *et al.*, 2012; Harly *et al.*, 2014), starting from the observation that Vγ9/Vδ2 T cells expand rapidly and considerably in the peripheral blood of patients infected with *Mycobacterium tuberculosis*. By the use of mycobacterial extracts, which is highly active in stimulating Vγ9/Vδ2 T cells *in vitro*, the actual reactive ligand of Vγ9/Vδ2 T cells within these extracts was narrowed down to a small lectin-binding compound resistant to proteases (Pfeffer *et al.*, 1992) but sensitive to periodic acid oxidation and to alkaline phosphatase treatment (Constant *et al.*, 1994). In addition, the bioactivity of this compound was found to depend essentially on the presence of phosphate moieties (Schoel *et al.*, 1994). Following from these findings, isopentenyl pyrophosphate (IPP), a product of isoprenoid biosynthesis, and its derivative dimethylallyl pyrophosphate (DMAPP) were the first identified phosphoantigens produced both in microbial and mammalian cells (Tanaka *et al.*, 1995). However, microbial IPP levels often do not reach the minimum required for effective T cell activation *in vitro*, which ruled out a major role for IPP itself in infections (Jomaa *et al.*, 1999). Instead, it became apparent that only extracts from bacteria possessing a newly discovered, alternative pathway of IPP synthesis were capable of stimulating Vγ9/Vδ2 T cells but not extracts from bacteria utilising the classical mevalonate pathway of IPP synthesis. The final demonstration that the non-mevalonate pathway was indeed the source of the natural Vγ9/Vδ2 T cell ligand came from genetically engineered *E. coli* strains (Eberl *et al.*, 2003), which ultimately led to the identification of a novel microbial metabolite, the IPP precursor (*E*)-4-hydroxy-3-methyl-2-butenyl pyrophosphate (HMB-PP), as the most potent agonistic ligand for Vγ9/Vδ2 T cells (Hintz *et al.*, 2001).

Apart from bacterial extracts, a broad spectrum of tumour cells, mainly lymphoma, was observed to be stimulating Vγ9/Vδ2 T cells both *in vitro* (Fisch *et al.*, 1990; De Libero *et al.*, 1991) and *in vivo* (Malkovska *et al.*, 1992). Based on the observation that the mevalonate pathway is frequently dysregulated with increased expression of rate limiting enzyme, HMG-CoA reductase, in haematological malignancies (Harwood *et al.*, 1991)

and mammary carcinoma (Asslan *et al.*, 1999), Gober *et al.* hypothesised that accumulation of IPP in tumour cells might be the target for Vγ9/Vδ2 T cells (Gober *et al.*, 2003). Indeed, manipulation of the mevalonate pathway in normal and malignant cells with statins that inhibit HMG-CoA reductase or with aminobisphosphonates (nBPs, analogues of pyrophosphates) such as pamidronate and zoledronate that inhibit farnesyl pyrophosphate synthase (FPPS) significantly abrogates or enhances, respectively, Vγ9/Vδ2 T cell responses to different cancer targets (Kunzmann *et al.*, 1999; Kunzmann *et al.*, 2000; Gober *et al.*, 2003). The concept of intracellular IPP accumulation as signal for Vγ9/Vδ2 T cells was eventually experimentally proven by elegant approaches based on mass spectrometry (Monkkonen *et al.*, 2007; Roelofs *et al.*, 2009; Benzaid *et al.*, 2011). By screening *in vitro* a large panel of cancer cell lines derived from haematological malignancies and carcinomas of different origins, Idrees *et al.* further confirmed that inhibition of FPPS by pretreatment of cancer cells with zoledronate at sub-lethal doses is sufficient for effective enhancement of their potential to stimulate Vγ9/Vδ2 T cell responses, including cytotoxicity and cytokine secretion (Idrees *et al.*, 2013).

With their potent anti-resorptive effects, nBPs such as alendronate (Fosamax), pamidronate (Aredia) and zoledronate (Zometa/Aclasta) have been widely used in treating postmenopausal osteoporosis and tumour-induced osteolysis, including metastatic breast cancer. Kunzmann *et al.* first described an expansion of Vγ9/Vδ2 T cells in patients with multiple myeloma, hyperparathyroidism or osteoporosis receiving intravenous injections of nBPs (Kunzmann *et al.*, 1999), and proposed a role for these cells in mediating the flu-like acute phase responses frequently seen in nBP-treated individuals (Reid *et al.*, 2010). Indeed, activation of Vγ9/Vδ2 T cells and monocytes, which serve as efficient APCs for the presentation of nBPs to Vγ9/Vδ2 T cells (Roelofs *et al.*, 2009), were found to be key determinants of the acute phase response in osteoporosis patients (in the absence of infection and cancer as confounding conditions) treated with zoledronate (Thompson *et al.*, 2011; Welton *et al.*, 2013b).

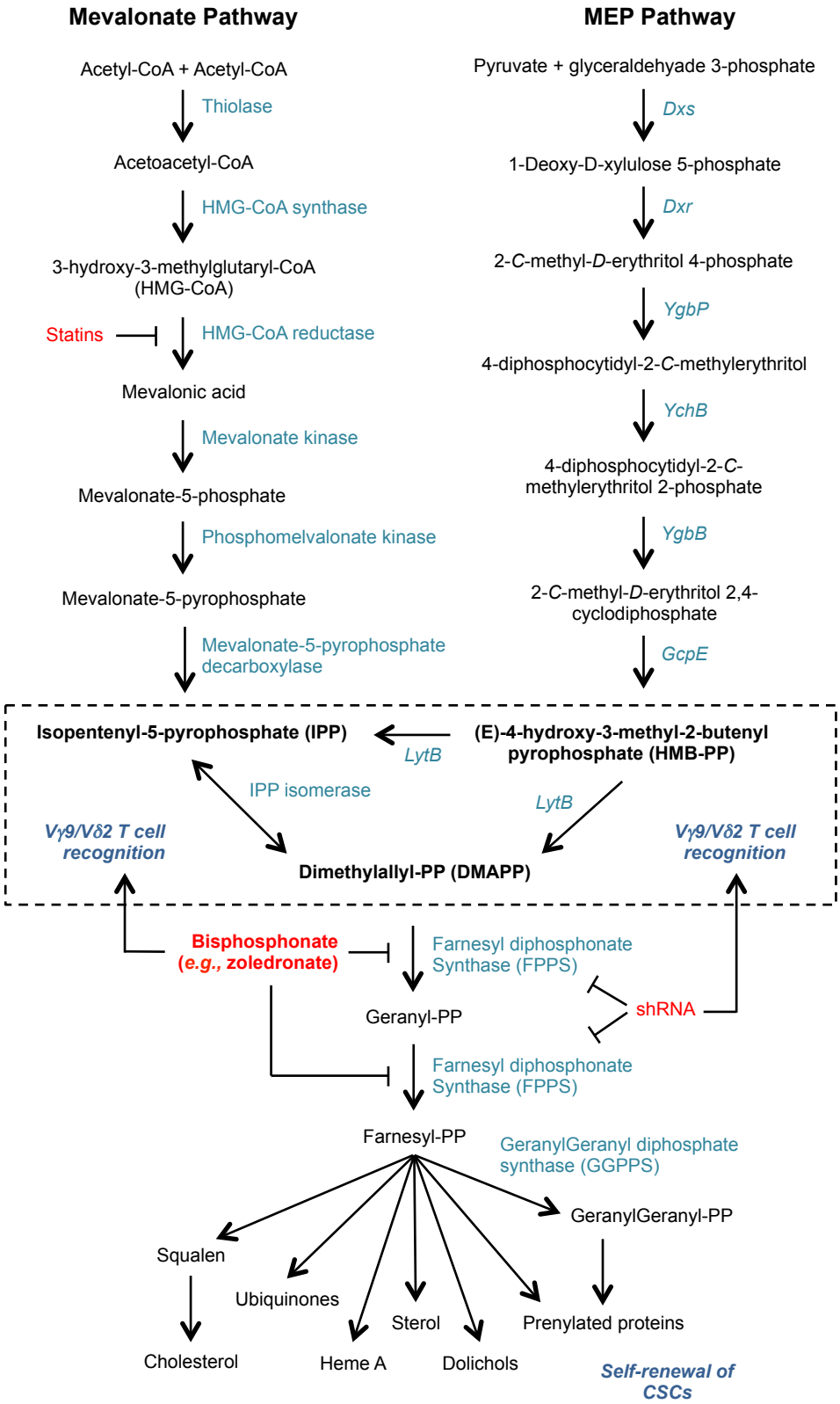

Figure 1.1. Mevalonate and MEP pathways of isoprenoid biosynthesis and their implication in activation of Vγ9/Vδ2 T cells. Mevalonate and MEP pathways are vital for the biosynthesis of isoprenoid products such as cholesterol. The two pathways are mutually exclusive (except in *Listeria monocytogenes*). The MEP pathway is found in many bacteria, in chloroplasts of plants and plastids of apicomplexan protozoa (*e.g.* malaria parasites). Instead, the mevalonate pathway is used by all eukaryotic cells in their cytoplasm, and by those bacteria that do not use the MEP

pathway. While HMB-PP is the most potent agonistic ligand of Vγ9/Vδ2 T cells, IPP and DMAPP as well serve as ligands for activation of Vγ9/Vδ2 T cells but with lower bioactivity. Thus, statins and nBPs, which inhibit HMG-CoA reductase and FPPS, respectively, provide a good opportunity for therapeutically modulating the susceptibility of cancer cells to Vγ9/Vδ2 T cell-mediated cytotoxicity.

1.3.5. Presentation of phosphoantigens to Vγ9/Vδ2 T cells by BTN3

Although the first phosphoantigens were already identified more than 20 years ago, the molecular mechanisms of how they actually stimulate Vγ9/Vδ2 T cells is only now becoming clear. Morita *et al.* initially showed that stimulation of Vγ9/Vδ2 T cells by exogenous phosphoantigens required an extracellular presentation machinery that does not involve antigen uptake, classical MHC class I and II pathways and CD1 family proteins (Morita *et al.*, 1995). Later, this unknown phosphoantigen-presenting molecule on the cell surface was characterised to be species-specific to humans and higher primates (Miyagawa *et al.*, 2001; Kato *et al.*, 2003; Green *et al.*, 2004). The first interesting candidate proposed was mitochondrial F_1-ATPase, which translocates to the cell surface for the presentation of exogenous and endogenous phosphoantigens in the form of nucleotide conjugates (Scotet *et al.*, 2005; Mookerjee-Basu *et al.*, 2010). This model provided an intriguing notion of how damaged and transformed cell possibly convert metabolic stress signals to activate Vγ9/Vδ2 T cells. However, the fact that phosphoantigens need to be conjugated to ATP to become ”presented” by F_1-ATPase (Vantourout *et al.*, 2010) suggests that this molecule may not be directly involved in presenting phosphoantigens to Vγ9/Vδ2 T cells and may rather play a role in shuttling phosphoantigens across the cell membrane.

More recently, butyrophilin 3A1 (BTN3A1; CD277) was identified as the molecule that is likely to present both exogenous and endogenous phosphoantigens to Vγ9/Vδ2 T cells (Harly *et al.*, 2012; Vavassori *et al.*, 2013; Sandstrom *et al.*, 2014; Rhodes *et al.*, 2015). With three isoforms (A1, A2 and A3), BTN3A proteins share a highly conserved B7-family immunoglobulin-like extracellular domain composed of an IgV domain at the N-terminus and a membrane-proximal IgC domain at the C-terminus, connected to a single transmembrane domain. This transmembrane domain links to a cytoplasmic B30.2 (PRYSPRY) domain in BTN3A1 and BTN3A3 but not BTN3A2 (Rhodes *et al.*, 2001; Palakodeti *et al.*, 2012). BTN3A proteins are widely expressed by tissue-resident

macrophages, monocytes, lymphocytes, NK cells, endocrine tissues, epithelial cells in breast, colon, intestine and kidney, and endothelial cells stimulated by DCs (Compte *et al.*, 2004; Rhodes *et al.*, 2015). Interestingly, enhanced expression of BTN3A was observed in tumours such as breast and colon cancer, suggesting their possible involvement in the recognition of cancer cells by Vγ9/Vδ2 T cells (Rhodes *et al.*, 2015). Functionally, BTN3A and related butyrophilin-like proteins have been reviewed to exhibit diverse roles in modulation of immune responses by either activating or inhibiting immune cells (Abeler-Dorner *et al.*, 2012; Arnett and Viney, 2014). The first line of evidence showing the role of BTN3A in presenting phosphoantigens to Vγ9/Vδ2 T cells came from the observation that an agonistic mouse anti-BTN3A antibody (clone 20.1) induced a conformational change of BTN3, which triggered an intracellular signalling cascade mimicking phosphoantigen-mediated activation of Vγ9/Vδ2 T cells (Figure 1.2) (Harly *et al.*, 2012; Palakodeti *et al.*, 2012; Decaup *et al.*, 2014). In contrast, an antagonistic anti-BTN3A antibody (clone 103.2) was found to abrogate the activation of Vγ9/Vδ2 T cells by stabilising the inactive conformation of the BTN3A molecule on the cell surface (Figure 1.2) (Harly *et al.*, 2012; Palakodeti *et al.*, 2012).

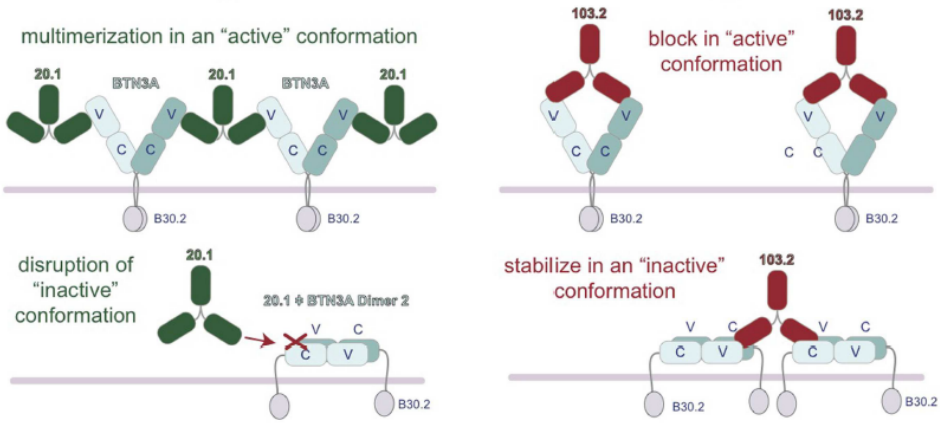

Figure 1.2. Proposed action model for agonist 20.1 and antagonist 103.2 anti-BTN3A antibodies in stimulating Vγ9/Vδ2 T cells (Gu *et al.*, 2014). Without stimulation, BTN3 molecules form an inactive head-to tail dimer conformation. 20.1 antibodies disrupt this inactive conformation and induce the mutimerisation of BTN3 molecules by linking each BTN3 molecule at the IgV domain to form an active conformation, which activates Vγ9/Vδ2 T cells. On the contrary, 103.2 antibodies efficiently abrogate the activation Vγ9/Vδ2 T cells by stabilising the inactive conformation and blocking the formation of the active conformation.

Currently, there are two conflicting models proposed to explain how BTN3 molecules actually present phosphoantigens to Vγ9/Vδ2 T cells (Figure 1.3) (De Libero *et al.*, 2014; Gu *et al.*, 2014; Harly *et al.*, 2014). Vavassori *et al*. firstly described that for the recognition of phosphoantigens by the Vγ9/Vδ2 TCR, BTN3A1 molecules bind IPP and HMB-PP on their extracellular groove, similarly to classical antigen presentation *via* MHC or CD1 molecules (Vavassori *et al.*, 2013). However, observations from other laboratories have contradicted this direct presentation model by showing that instead of binding to the outer groove of the extracellular IgV domain as reported by Vavassori *et al.*, IPP and HMB-PP actually bind to the intracellular B30.2 domain (Wang *et al.*, 2013; Hsiao *et al.*, 2014; Sandstrom *et al.*, 2014; Rhodes *et al.*, 2015). Of note, the binding affinity of HMB-PP to the purified B30.2 domain was found to be at least 1,000 fold higher than that of IPP, in close agreement with the 10,000 fold higher bioactivity of soluble HMB-PP on cultured Vγ9/Vδ2 T cells compared to IPP (Hsiao *et al.*, 2014; Sandstrom *et al.*, 2014; Rhodes *et al.*, 2015). Similarly to the 20.1 agonistic antibodies, binding of phosphoantigens to the B30.2 domain is believed to induce the active conformation change responsible for the stimulation of Vγ9/Vδ2 T cells through the extracellular domain, and concomitantly to reduce the mobility of BTN3A1 at the cell surface for stable presentation to Vγ9/Vδ2 T cells (Harly *et al.*, 2012; Sandstrom *et al.*, 2014). These two models may seem contradictory but actually are not necessarily mutual exclusive. As negative charged phosphoantigens are unlikely to cross the cell membrane in a passive manner, an unknown transporter on the cell surface is required to internalise exogenous phosphoantigens for the binding to intracellular B30.2 domain. In this case, although with low affinity, direct binding to the extracellular IgV domain might compromise the internalisation of phosphoantigens in certain situations and provide more rapid screening of infected or transformed cells by Vγ9/Vδ2 T cells (De Libero *et al.*, 2014).

Apart from BTN3A1 itself as the main protein that directly interacts with phosphoantigens, additional molecules may be required and contribute to the activation of Vγ9/Vδ2 T cells by phosphoantigens. Riano *et al.* showed that a human-specific molecule(s) encoded on chromosome 6 is essential for successful activation of Vγ9/Vδ2 T cells in the presence of phosphoantigens (Riano *et al.*, 2014). However, it will be challenging to narrow down this list of potential candidates, given the extensive number of immune-related genes on chromosome 6 including the MHC locus with MHC class I and class II, MHC-like genes

(MICA, MICB), genes involved in antigen processing (*e.g*. TAP and TAP binding protein, cytokines (TNF-α, LT-α) and the BTN family. By yeast-two-hybrid screenings, Rhodes *et al.* demonstrated that binding of periplakin, a cytoskeletal adaptor, to a region upstream the B30.2 domain is necessarily involved in the presentation of phosphoantigens by BTN3A molecules to Vγ9/Vδ2 T cells, possibly by recruiting and stabilising the dimerisation of BTN3A molecules on the cell surface (Rhodes *et al.*, 2015). These findings suggest that the presentation of phosphoantigens by BTN3A molecules is complex and involves additional molecules that remain to be identified.

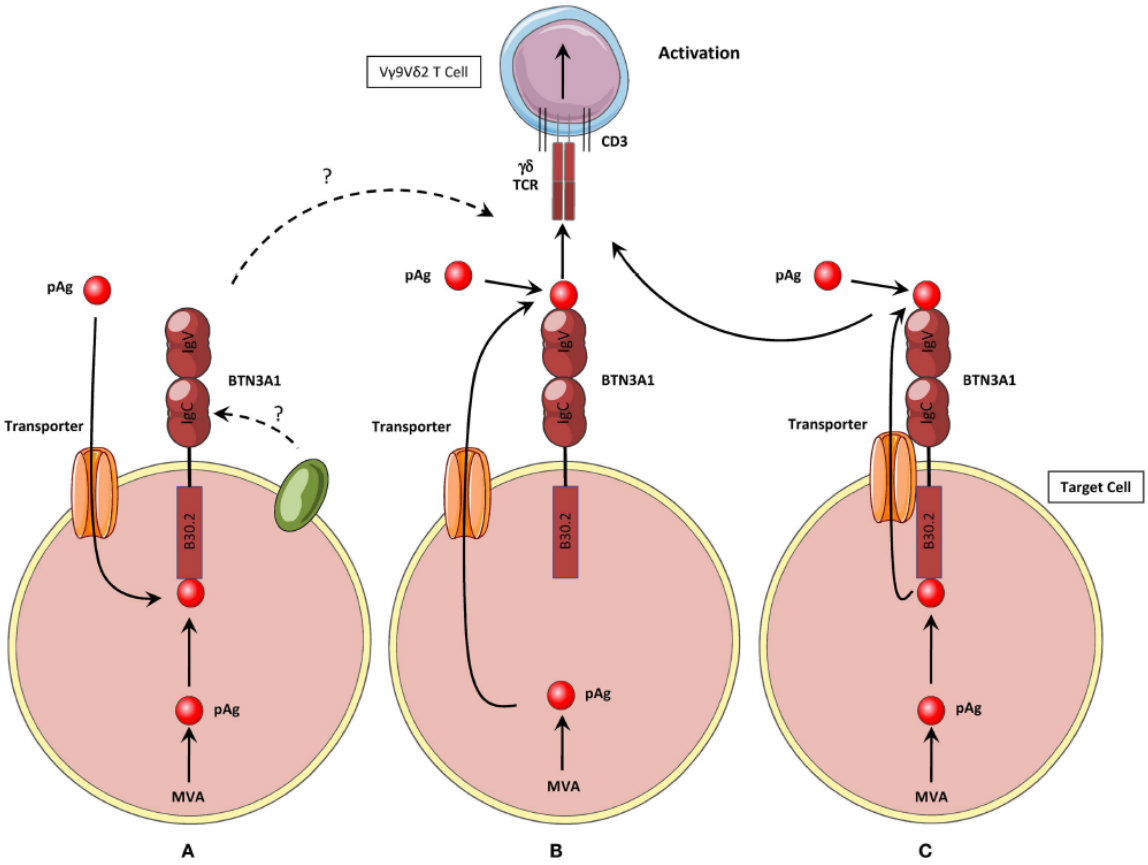

Figure 1.3. Currently proposed models for the presentation of phosphoantigens to Vγ9/Vδ2 TCR by BTN3A molecules on the cell surface (Harly *et al.*, 2014). **(A)** Endogenous phosphoantigens and exogenous phosphoantigens internalised by unknown membrane transporter(s) bind to the intracellular B30.2 domain of BTN3A1 and induce conformational changes at the extracellular domain, which may modify the distribution and multimerisation of active BTN3A molecules on the cell surface in association with currently unidentified molecular partner(s). **(B)** Exogenous phosphoantigens and endogenous phosphoantigens translocated by unknown membrane transporter(s) are loaded onto the extracellular IgV domain of BTN3 molecules for classical MHC-like presentation to Vγ9/Vδ2 T cells. **(C)** Combining the hypotheses described in (A) and (B), endogenous phosphoantigens firstly bind to the B30.2 domain for induction of BTN3A1 reactivity and then become exported by unknown membrane transporter(s) and loaded onto the extracellular IgV domain.

1.3.6. Stimuli activating Vγ9/Vδ2 γδ T cells

In addition to stimulation of phosphoantigens through the TCR, γδ T cells also express a wild range of innate-like receptors recognising stress-induced surface markers, pathogen-associated molecular patterns (PAMPs) and damage-associated molecular patterns (DAMPs) (Rey *et al.*, 2009).

Most γδ T cells express the C-type lectin family receptor nature killer group 2D (NKG2D), often in conjunction with other NK receptors including NKp30, NKp44 or NKp46, which allow them to recognise a broad range of stressed and transformed cells in a TCR-independent fashion (Hudspeth *et al.*, 2013). The importance of NKG2D for γδ T cell mediated immune surveillance is particularly apparent in mouse models of carcinogenesis (Girardi *et al.*, 2001) and cytotoxicity against human cancer cells (Corvaisier *et al.*, 2005; Viey *et al.*, 2005; Nedellec *et al.*, 2010b), although there is increasing evidence that NKG2D also plays a role in the detection of infected cells (Qin *et al.*, 2009; Bessoles *et al.*, 2011). As an activatory receptor, human NKG2D recognises and binds MHC class I related proteins (MICA and MICB) and UL16-binding proteins (ULBP1-4) and induces the cytotoxicity and cytokine secretion of γδ T cells in response to infected and transformed cells (Groh *et al.*, 1998; Corvaisier *et al.*, 2005; Wrobel *et al.*, 2007; Kong *et al.*, 2009; Xu *et al.*, 2011). Like NK cells, γδ T cells also express NKG2A and immunoglobulin-like transcript 2 (ILT2), which both deliver inhibitory signals upon recognition and binding to MHC class I molecules, allowing them to recognise transformed cells with defective MHC class I expression (Nedellec *et al.*, 2010a). This action greatly complements the frequent failure of MHC-restricted surveillance mediated by cytotoxic $CD8^+$ T cells. The expression of DNAX Accessory Molecule-1 (DNAM-1/CD226) allows γδ T cells to recognise PDGF- and VEGF-related receptors (PVR/CD96) and Nectin-2 expressed by myeloid leukaemia blasts (Gertner-Dardenne *et al.*, 2012) and Necl-like-5 expressed by hepatocarcinoma cells (Toutirais *et al.*, 2009), and exhibit potent cytotoxicity.

1.3.7. Memory of Vγ9/Vδ2 T cells

Although γδ T cells function in an innate-like manner, the observation that they respond and expand more rapidly and in stronger magnitude to secondary mycobacterial infection suggests the existence of memory-like adaptive immunity in Vγ9/Vδ2 T cells (Shen *et al.*,

2002; Chen and Letvin, 2003). Indeed, like αβ T cells, Vγ9/Vδ2 T cells can be classified into four different subsets including naïve T cells (T_{naive}), central memory T cells (T_{CM}), effector memory T cells (T_{EM}) and terminally differentiated effector memory T cells (T_{EMRA}), according to their $CD45RA^+$ $CD27^+$, $CD45RA^-$ $CD27^+$, $CD45RA^-$ $CD27^-$ and $CD45RA^+$ $CD27^-$ phenotype, respectively (Dieli *et al.*, 2003). Each of these Vγ9/Vδ2 T cell memory subsets exhibits distinct functions in response to stimulation by phosphoantigens (Table 1.4) (Dieli *et al.*, 2003; Angelini *et al.*, 2004; Battistini *et al.*, 2005). Upon stimulation, Vγ9/Vδ2 T cells are believed to differentiate sequentially from T_{naive}, to T_{CM}, T_{EM} and finally T_{EMRA} cells (Dieli *et al.*, 2003). Functionally, T_{naive} cells display a lymph node (LN) homing phenotype and are predominantly found in LN; T_{CM} cells are thought to represent an antigen-primed subset predominantly found in peripheral blood with the ability to respond rapidly to restimulation in the draining LNs; T_{EM} and T_{EMRA} cells represent functionally matured subsets that patrol peripheral inflammatory sites and exert immediate cytotoxicity or cytokine secretion. Of these effector cells, T_{EM} cells exhibit a strong ability to secrete IFN-γ but not cytotoxic molecules, and their lack of NCR expression suggests that this subset is mainly activated through the TCR. As opposed to T_{EM} cells, T_{EMRA} cells show only low levels of IFN-γ secretion and proliferation upon stimulation but release abundant amounts of cytotoxic molecules. The broad expression of NCRs by T_{EMRA} cells leads to the speculation that this subset differentiates to acquire a wider spectrum for recognising targets at inflammatory sites. Of note, different from effector αβ T_{EMRA} cells, which have a short life span and are typically only found during ongoing inflammatory responses, cytotoxic γδ T_{EMRA} cells exhibit surprising persistence *in vivo* and are largely enriched in inflammatory tissues (Dieli *et al.*, 2003). This enhanced survival suggests the potential of potent efficacy in adoptive transfer of effector γδ T cells or *in vivo* expansion of γδ T_{EMRA} and T_{EM} cells in cancer patients treated with zoledronate and IL-2 (Dieli *et al.*, 2007; Santini *et al.*, 2009; Meraviglia *et al.*, 2010; Welton *et al.*, 2013a).

Table 1.4. Phenotypic and functional characteristics of different Vγ9/Vδ2 T cell memory subsets

	T_{naive}	T_{CM}	T_{EM}	T_{EMRA}
Memory phenotype	$CD45RA^+$ $CD27^+$; $CD45RO^-$	$CD45RA^-$ $CD27^+$; $CD45RO^+$	$CD45RA^-$ $CD27^-$; $CD45RO^+$	$CD45RA^+$ $CD27^-$; $CD45RO^+$
Chemokine and homing receptors	CCR7 and CD62L	CCR7 and CD62L; 25% positive for CCR5 and CXCR3	$CCR7^{lo}$ and $CD62L^{lo}$; CCR2, CCR5, CCR6 and CXCR3	CCR5 and CXCR3
Localisation in periphery	Predominant subset in LN	Predominant subset in blood	Inflammatory sites	Inflammatory sites
Function upon stimulation:				
• *Proliferation*	Intermediate	High	Low	None
• *IFN-γ secretion*	None	Low	High	Low
• *BLT esterase*	None	Minimal	Low	High
• *Perforin*	–	–	Low	High
• *NK receptors*	–	–	$NKG2A^{lo}$ and $CD94^{lo}$	$CD16^+$, $CD94^+$, $NKG2A^+$, $CD158^+$, $NKAT2^+$

–: Data not provided in the references listed
Table summarised from data shown in (Dieli *et al.*, 2003; Angelini *et al.*, 2004; Battistini *et al.*, 2005)

1.3.8. Functional plasticity of effector Vγ9/Vδ2 T cells against cancer

Depending on the culture conditions, γδ T cells can be polarised to function as (*i*) cytotoxic effector clearing infected and transformed cells, (*ii*) immune modulators secreting pro-inflammatory cytokines such as IFN-γ and TNF-α and interacting with other immune cells for induction and enhancement their maturation and specific function, and (*iii*) APCs to prime and induce adaptive $CD4^+$ and $CD8^+$ T cell immunity (Lafont *et al.*, 2014; Tyler *et al.*, 2015).

γδ T cells have been well documented for their profound ability against a wide spectrum of solid tumours and haematological malignancies including breast cancer (Beck *et al.*, 2010; Meraviglia *et al.*, 2010; Benzaid *et al.*, 2011; Capietto *et al.*, 2011), bladder cancer (Yuasa *et al.*, 2009), colon cancer (Corvaisier *et al.*, 2005; Devaud *et al.*, 2009; Devaud *et al.*, 2013), lung cancer (Kang *et al.*, 2009; Dokouhaki *et al.*, 2010; Nakajima *et al.*, 2010; Sakamoto *et al.*, 2011), melanoma (Kabelitz *et al.*, 2004; Dudley *et al.*, 2005; Cordova *et al.*, 2012), ovarian cancer (Deniger *et al.*, 2014; Parente-Pereira *et al.*, 2014), pancreatic cancer (Kabelitz *et al.*, 2004; Oberg *et al.*, 2014), prostate cancer (Dieli *et al.*, 2007; Santolaria *et al.*, 2013), renal cell carcinoma (Viey *et al.*, 2005; Kobayashi *et al.*, 2007; Bennouna *et al.*, 2008; Kobayashi *et al.*, 2011; Lang *et al.*, 2011; Kunzmann *et al.*, 2012), skin cancer (Devaud *et al.*, 2009), acute myeloid leukaemia (Kunzmann *et al.*, 2012), chronic myelogenous leukaemia (D'Asaro *et al.*, 2010), Epstein-Barr virus-induced B cell lymphoproliferative disease (Xiang *et al.*, 2014), acute lymphoblastic leukaemia (Deniger *et al.*, 2013), lymphoma (Kunzmann and Wilhelm, 2005) and multiple myeloma (Kunzmann *et al.*, 2000; Abe *et al.*, 2009; Kunzmann *et al.*, 2012).

The direct cytotoxicity of γδ T cells is majorly mediated through the granule exocytosis pathway and the death receptor dependent pathway. Contained within the cytotoxic granules secreted by activated immune effector cells, perforin and granulysin initiate cytotoxicity by creating holes in the membrane of target cancer cells, thereby allowing the entry of granzyme A/B for the induction of caspase-dependent apoptosis. γδ T cells stimulated *via* the TCR by phosphoantigens or through the NK-like receptor DNAM-1 efficiently secrete cytotoxic granules containing perforin and granzyme B for the killing of target cancer cells (Viey *et al.*, 2005; Gertner *et al.*, 2007; Gertner-Dardenne *et al.*, 2012). In addition, γδ T cells activated by cancer cells *via* TCR or NKG2D recognition can also produce TRAIL and/or FasL in soluble and membrane-bound form (Xiang *et al.*, 2014).

Stimulation of Vγ9/Vδ2 T cells with phosphoantigens plus IL-2 and IL-21 efficiently induces the secretion of perforin and granzyme A/B concomitantly with an up-regulation of NKG2D, NKG2A and ILT2 on cell surface, suggesting a possible synergy between NKG2D and TCR in the activation of Vγ9/Vδ2 T cells (Thedrez *et al.*, 2009). However, in a model of TRAIL-mediated lysis of H460 lung cancer cells by γδ T cells upon recognition of ULBP2 *via* NKG2D (Dokouhaki *et al.*, 2013), concomitant NKG2D and TCR triggering did not lead to increased TRAIL secretion, arguing against a synergism between the NKG2D and TCR pathways in this model (Dokouhaki *et al.*, 2013). The question of whether NKG2D acts independently from the TCR in mediating tumour recognition and cytotoxicity, or plays a rather co-stimulatory role likely depends on the context and requires further clarification, especially with regard as to how these pathways can be manipulated for novel therapies (Chen *et al.*, 2013).

Amongst the cytotoxic molecules secreted by γδ T cells, TRAIL was originally identified as a novel γδ T-cell expressed cytotoxic effector molecule, in a set of microarray analyses of human peripheral blood γδ T cells stimulated under different conditions, and which showed that activated γδ T cells displaying a pro-inflammatory profile express substantial levels of TRAIL alongside IFN-γ and TNF-α (Dieli *et al.*, 2007; Vermijlen *et al.*, 2007). Of note, these studies also implied a role for TRAIL *in vivo* in cancer patients receiving intravenous zoledronate in combination with low dose IL-2, whereby improved clinical outcome was associated not only with higher numbers of effector/memory γδ T cells but also with serum levels of TRAIL (Dieli *et al.*, 2007). TRAIL predominantly acts on tumour cells whilst sparing most healthy tissues and is thus a promising candidate for targeted cancer therapy, which is receiving substantial attention for the treatment of colorectal, cervical, pancreatic, liver, lung, breast and ovarian cancer as well as lymphoma and multiple myeloma. In fact, the selective efficacy of certain compounds such as histone deacetylase inhibitors and retinoids against cancer cells involves TRAIL, thus identifying the TRAIL signalling pathway as a major drug-responsive tumour defence system (Nebbioso *et al.*, 2005). Consequently, clinical trials are being conducted using recombinant TRAIL itself or agonistic monoclonal antibodies acting on either TRAIL-R1 or TRAIL-R2, with excellent safety profiles (den Hollander *et al.*, 2013). However, clinical efficacy has so far been comparatively modest, possibly in part due to the relative resistance of many cancer cells to TRAIL-induced apoptosis, and sensitisation strategies are hence being developed to widen the therapeutic potential (Bucur *et al.*, 2006). Of

note, resistance to TRAIL can be overcome by IFN-γ (Taieb *et al.*, 2006), which is produced in high amounts by activated T cells including pro-inflammatory γδ T cells (Dieli *et al.*, 2007; Vermijlen *et al.*, 2007), and which is positively reinforced by signalling *via* TRAIL, and *vice versa* (Chou *et al.*, 2001). Indeed, the combination of an agonistic anti-TRAIL receptor antibody and the induction of IFN-γ producing T cells has been shown to eradicate established tumours in mice (Uno *et al.*, 2006). Other advances include combination therapies of TRAIL-receptor targeting agents with standard chemotherapy or radiotherapy as well as synergistic approaches to specifically interfere with the NF-κB, Akt or MAPK pathways, the proteasome, or key pro- and anti-apoptotic players such as c-FLIP, p53 and Bcl-2 family members (den Hollander *et al.*, 2013). In this context, Piggott *et al*. recently demonstrated that genetic suppression of c-FLIP not only efficiently sensitises breast cancer cells to TRAIL-mediated killing but also selectively eliminates the functional pool of breast cancer stem cells (Piggott *et al.*, 2011). These findings open new avenues for targeted combination therapies specifically directed at the stem cell population to prevent disease recurrence and distant metastases, and ultimately reduce morbidity and mortality.

1.4. Human γδ T cells as professional antigen presenting cells

1.4.1. Antigen presentation

Efficient antigen presentation is the key to successful and potent adaptive immune responses against infection and cancer. Dendritic cells (DCs), macrophages and B cells have been well-characterised as professional antigen-presenting cells (APCs) for their unique ability to stimulate antigen-specific functional differentiation of naïve αβ T cells and to induce rapid responses of memory αβ T cells against infected, stressed and transformed cells expressing cognate antigens. These professional APCs patrol peripheral tissues in homeostasis and are rapidly recruited to sites of infection and inflammation. Apart from the APCs circulating around the body, there is another subset of tissue-resident APCs permanently inhabit in peripherals for immediate sensing of infections and tissue damages. Upon stimulation at inflammatory sites, APCs efficiently process endogenous antigens and acquire exogenous antigens by endocytosis or phagocytosis and process them into peptides of appropriate size for loading onto MHC class I and class II molecules and subsequent presentation to CD8 and CD4 T cells, respectively. In addition, they actively process endogenous antigens for cross-presentation to CD8 T cells through MHC class I. While all nucleated cells express MHC class I and many cells in the body are able to express MHC class II, only professional APCs are unique in providing a second signal through co-stimulatory molecules on their cell surface, *e.g.* B7 family molecules CD80/CD86, CD40, CD70 and CD83, in conjunction with a third signal through secretion of different instructive cytokines polarising T cell differentiation. In addition, APCs are able to acquire a specific chemokine expression profile for homing to secondary lymphoid organs (CCR7) and subsequent priming of naïve T cells in the draining lymph node.

Antigen presentation can be classified into three main categories depending on the origin of antigens and the recipient cell subsets to antigen presentation: (i) presentation of endogenous antigens to CD8 T cells by MHC class I molecules, (ii) presentation of exogenous antigens to CD4 T cells by MHC class II molecules, and (iii) cross-presentation of exogenous antigens to CD8 T cells by MHC class I molecules. The process of antigen presentation and cross-presentation have been extensively described and reviewed (Harding and Boom, 2010; Neefjes *et al.*, 2011; Joffre *et al.*, 2012). For antigen presentation to CD8 T cells (Neefjes *et al.*, 2011), endogenous proteins (including cellular or viral proteins, cancer neoantigens and mis-folded proteins) are fragmented into

small peptides by the proteasome under homeostasis or by the immunoproteasome under inflammatory conditions. Generated peptides in the cytosolic pool are then sampled and modified to appropriate sizes for transportation into the ER via the transporter associated with antigen processing (TAP), followed by assembly with MHC class I molecules. Loaded MHC class I molecules with stable structure are subsequently transported to the cell membrane for presentation to CD8 T cells. In contrast, for antigen presentation to CD4 T cells (Harding and Boom, 2010; Neefjes *et al.*, 2011), exogenous material is taken up by APCs mainly *via* phagocytosis and endocytosis and then degraded into small peptides by proteases in the acidic environment generated during a series of fusions between phagosomes and endosomes with lysosomes. At the same time, MHC class II molecules stabilised by invariant chain are transported from the ER into phagolysosome and endolysosome, where exogenous antigens are properly processed. The invariant chains on MHC class II molecules are then exchanged by antigenic peptides, and mature peptide-MHC class II complexes are delivered to the cell membrane for presentation to CD4 T cells.

Cross-presentation of exogenous material to CD8 T cells is a relatively new concept and not completely understood. However, the observations so far have demonstrated that cross-presentation can proceed *via* two main pathways: the vacuolar pathway and the cytosolic pathway (Joffre *et al.*, 2012). After being taken up by phagocytosis, exogenous antigens in phagosomes may directly enter the vacuolar pathway and become degraded into peptides for assembly with MHC class I molecules in the phagosomes. Otherwise, through cytosolic pathway, exogenous antigens in phagosomes are released into the cytosol from phagosomes, where they are degraded into peptides by the proteasome or immunoproteasome. These peptides are then transported to the ER *via* TAP or back into phagosomes for assembly with MHC class I molecules. Assembled peptide-MHC class I complexes from both vacuolar pathway and cytosolic pathway are eventually transported to the cell surface for presentation to CD8 T cells.

In addition to the classical APCs such as DCs and macrophages, human γδ T cells were recently identified as another cell type capable of acting as professional APC (Brandes *et al.*, 2005; Moser and Eberl, 2007, 2011). In the following sections, I will review the evidences supporting the APC features of γδ T cells in triggering CD4 and CD8 T cell responses through antigen presentation by MHC class II molecules and cross-presentation

by MHC class I molecules, respectively.

1.4.2. Acquisition of APC characteristics by γδ T cells

The first evidence showing the possibility that human γδ T cells, specifically Vγ9/Vδ2 T cells, isolated from peripheral blood of healthy donors can function as APCs came from the observation of their up-regulation of APC-associated markers including antigen presenting molecules, MHC class I and II; co-stimulatory molecules, CD40, CD80/86, CD83, CDw137L (4-1BBL); and adhesion molecules CD11a/b/c and CD54, upon stimulation with HMB-PP, IPP or zoledronate (Brandes *et al.*, 2005; Landmeier *et al.*, 2009; Wu *et al.*, 2009b; Himoudi *et al.*, 2012; Schneiders *et al.*, 2014; Muto *et al.*, 2015). Different from DCs, which constitutively express MHC class II molecules, γδ T cells only start to produce and express MHC class II molecules on their surface when activated (Brandes *et al.*, 2005). Expression or up-regulation of APC-associated markers was also observed in γδ T cells isolated from tonsils (Brandes *et al.*, 2005) and in blood from patients with rheumatoid arthritis (Hu *et al.*, 2012), melanoma (Khan *et al.*, 2014a) and gastric cancer (Mao *et al.*, 2014), with or without *ex vivo* re-stimulations by phosphoantigen, supporting the physiological relevance of the APC function of γδ T cells in different diseases. However, apart from the expression of APC-associated markers, direct evidence of antigen uptake, processing and presentation by γδ T cells is necessary to prove their APC function.

1.4.3. Uptake of exogenous antigens by γδ T cells

The ability of γδ T cells to take up exogenous materials by endocytosis is demonstrated by uptake of soluble BSA (Meuter *et al.*, 2010) and OVA (Muto *et al.*, 2015) conjugated with different fluorochromes. The abrogation of fluorochrome-conjugated BSA uptake by dimethyl amiloride but not cytochalasin D indicates that this uptake of exogenous BSA is specifically mediated by macropinocytosis rather than phagocytosis, which largely involve actin polymerisation and rearrangement (Meuter *et al.*, 2010). This ability to take up extracellular material by macropinocytosis is supported by the observation of dendrite-like formations upon γδ T cell stimulation (Brandes *et al.*, 2005; Wu *et al.*, 2009b), which is a classic morphology of mature DCs functionally contributing to their ability to sample antigens in the surrounding microenvironment. In addition to soluble proteins, γδ T cells have been shown to take up influenza virions and exogenous debris of cells infected by

influenza virus (Meuter *et al.*, 2010) as well as material released by killed tumour cells (Brandes *et al.*, 2005; Wu *et al.*, 2009b). Phagocytosis is one of the main functional characteristics of APCs such as tissue resident DCs and macrophages and non-APC scavenger cells like neutrophils, allowing them to sample pathogenic antigens in peripheral tissues (Rabinovitch, 1995). Wu *et al.* showed that γδ T cells are able to phagocytose *Escherichia coli* bacteria and synthetic latex beads with a size of 1 μm (Wu *et al.*, 2009b), indicating that macropinocytosis as well as phagocytosis may be used for antigen uptake by γδ T cells depending on the size of foreign material. In addition, γδ T cells express the scavenger receptor CD36 (Muto *et al.*, 2015), which is essentially involved in the phagocytosis of apoptotic cells by immature DCs and macrophages (Albert *et al.*, 1998; Greenberg *et al.*, 2006). Furthermore, γδ T cells have been shown to obtain membrane fragments from other cells during the formation of cell-cell contacts by trogocytosis (Poupot *et al.*, 2005; D'Asaro *et al.*, 2010; Himoudi *et al.*, 2012; Mao *et al.*, 2014; Schneiders *et al.*, 2014). These studies clearly demonstrate the ability of γδ T cells to acquire exogenous material from the local microenvironment.

1.4.4. Intracellular trafficking and processing of exogenous antigens in γδ T cells

Direct evidence showing the processing of endocytosed antigens by γδ T cells came from the laboratory of Prof. Bernhard Moser. Meuter *et al.* elegantly elucidated the passage of endocytosed BSA from early to late endosomes/lysosomes in γδ T cells using confocal microscopy by co-staining for markers associated with early endosome, late endosome, lysosome and recycling endosomes (Meuter *et al.*, 2010). Furthermore, by tracing the translocation and retention of BSA conjugated with pH-sensitive or pH-independent fluorochromes in the presence of specific inhibitors of the proteasome, endosomal acidification and serine/cysteine proteases, they demonstrated a delayed lysosomal acidification in γδ T cells that prevents proteolysis and in turn enhances export of antigens from lysoendosomes into the cytosol for further degradation (Meuter *et al.*, 2010). This efficient export into the cytosol was not seen in conventional monocyte-derived DCs serving as control. The treatment of γδ T cells with cytochrome c (cyt c) induced significant apoptosis, indicating the export of exogenous cyt c from endosomes to cytosol, where it functionally triggers apoptosis (Meuter *et al.*, 2010). In addition, the synthesis and translocation of MHC class I molecules from the Golgi complex to the cell membrane were traced in γδ T cells upon stimulation with IPP presented by feeder cells. *De novo*

synthesised MHC class I molecules co-localised with the trans-Golgi network throughout the course of activation, indirectly showing the loading of processed peptides on MHC class I molecules for antigen presentation on the cell surface (Brandes *et al.*, 2009). These results suggest that γδ T cells favour the cytosolic pathway for cross-presentation of exogenous antigens to CD8 T cells. With regard to the processing of antigens for loading onto MHC class II molecules, inhibition of endosomal and lysosomal acidification by chloroquine efficiently abrogated the presentation of tetanus toxoid (TT) and *Mycobacterium tuberculosis*-purified protein derivate (PPD) to CD4 T cells by γδ T cells (Brandes *et al.*, 2005).

1.4.5. Antigen presentation to CD4 T cells by γδ T cells

The professional antigen-presentation function of human Vγ9/Vδ2 T cells was firstly revealed by mixed lymphocyte reactions of CD4 T cells, where IPP-stimulated γδ T cells and LPS-matured DCs as APCs induced similar levels of proliferation of alloreactive CD4 T cells (Brandes *et al.*, 2005). Cross-linking of MHC class II molecules on the surface of APCs with the Vβ2 TCR expressed by subpopulation of CD4 T cells using the superantigen toxic shock syndrome toxin (TSST-1) revealed that both IPP-stimulated γδ T cells and LPS-matured DCs were able to induce the proliferation of naïve $V\beta2^+$ CD4 T cells and their functional differentiation into Th1 and Th2 subsets (Brandes *et al.*, 2005). These findings indicate that the expression of co-stimulatory molecules by activated γδ T cells supports antigen presentation by MHC class II molecules and thus stimulates potent CD4 responses. While expression of MHC class II is a common feature of activated T cells and may play a role in amplifying memory responses (Barnaba *et al.*, 1994), the capacity to prime naive T cell responses has only been reported for Vγ9/Vδ2 T cells so far, indicating that only those γδ T cells may be able to act as true professional APCs.

1.4.6. Antigen-presentation to CD8 T cells by γδ T cells

Mixed lymphocyte reactions also demonstrated that IPP-stimulated γδ T cells could induce proliferation of alloreactive CD8 T cells and their differentiation into cytotoxic effector T cells at similar levels as LPS-matured DCs (Brandes *et al.*, 2005). Following this initial observation, successful presentation of a series of immunodominant peptides of viral (Brandes *et al.*, 2009; Meuter *et al.*, 2010; Altvater *et al.*, 2012) and tumour antigens (Altvater *et al.*, 2012), which are directly loaded onto surface MHC class I molecules,

showed that the surface expression of MHC class I molecules by γδ T cells is functional. Furthermore, transduction of γδ T cells for the expression of Epstein Barr virus latent membrane protein-2 (LMP2) showed that γδ T cells could present endogenous antigens to CD8 T cells and induce their cytotoxicity (Landmeier *et al.*, 2009). As described above, γδ T cells also showed a substantial ability to present exogenous defined antigens such as TT and influenza M1 as well as complex antigens such as PPD for cross-presentation to both naïve and memory CD8 T cells. Indeed, γδ T cells are able to cross-present antigens from exogenous, larger particles antigens such as debris of cells infected by influenza viruses and whole virions (Meuter *et al.*, 2010), and beads coated with Flu M1 in a CD16 (FcγR)-dependent manner (Wu *et al.*, 2009b). The ability of γδ T cells to cross-present Flu M1 from influenza-infected cells (Meuter *et al.*, 2010); and tumour antigens from antibody-opsonised cancer cells (Himoudi *et al.*, 2012) to CD8 T cells indicates the physiological relevance of these findings and suggests an important role in the immune response against infection and cancer.

1.4.7. Antigen-presentation to invariant natural killer T (iNKT) cells by γδ T cells

Set aside from the professional antigen presentation to CD4 and CD8 T cells as discussed in the preceding sections, it was recently shown that upon stimulation by phosphoantigens, γδ T cells can also obtain APC-associated molecules from the membrane of target cells in a process called trogocytosis (Schneiders *et al.*, 2014). This direct acquisition of membrane material from other cells was described earlier for γδ T cells and other cells (Poupot *et al.*, 2005; D'Asaro *et al.*, 2010) and may equip γδ T cells with additional features. Indeed, acquisition of CD1d by trogocytosis allows γδ T cells to present synthetic glycolipid α-galactosylceramide (αGalCer) to iNKT cells (Schneiders *et al.*, 2014).

1.4.8. Homing of γδ T cells for antigen presentation

The expression profile of chemokine receptors that are specific for homeostatic and inflammatory chemokines defines the tissue tropism of immune cells and their migratory potential (Moser *et al.*, 2004). Resting γδ T cells freshly isolated from blood of healthy donors readily express the inflammatory chemokine receptors CCR5, CCR2 and CXCR3, and efficiently migrate *in vitro* toward the corresponding chemokines CCL5/RANTES, CCL2/MCP-1 and CXCL11/I-TAC, respectively. This expression profile indicates that

Vγ9/Vδ2 T cells are likely to patrol through the circulation and are well-equipped to sense and translocate to sites of inflammation (Brandes *et al.*, 2003). The lack of expression for the homeostatic chemokine receptor CCR7, which is pivotal for recruiting naïve and central memory T cells to lymph nodes (Sallusto *et al.*, 1999; Weninger *et al.*, 2001), by circulating Vγ9/Vδ2 T cells prevents them from recirculating through secondary lymphoid organs, which indirectly confirms their tendency to home to inflammatory sites (Brandes *et al.*, 2003). In rapid response to simulation with phosphoantigens *in vitro*, γδ T cells transiently switch off the expression of CCR5 and start to express CCR7 in conjunction with other homeostatic chemokine receptors such as CCR4 and CXCR4. Indeed, IPP-activated γδ T cells migrate efficiently *in vitro* toward the corresponding homeostatic ligands CCL21/SLC, CCL22/MDC and CXCL12/SDF-1, respectively, but not any more toward the inflammatory CCR5 ligand CCL5 (Brandes *et al.*, 2003). This switch in their migratory properties suggests that upon stimulation at inflammatory sites by phosphoantigens, activated γδ T cells are rapidly re-programmed for migration toward secondary lymphoid organ. This is in striking resemblance to DCs, which rapidly up-regulate CCR7 in response to microbial compounds such as LPS, further supporting a role for activated γδ T cells in antigen presentation and priming of naïve CD4 and CD8 T cells responses.

1.5. Animal models: Adoptive transfer of human γδ T cells for targeting human tumour xenografts in immunodeficient mice

Human tumour xenotransplantation models have been established using a range of immunodeficient mice to test the efficacy of human γδ T cell adoptive transfer in controlling development of different types of malignancies including breast cancer (Beck *et al.*, 2010; Benzaid *et al.*, 2011; Capietto *et al.*, 2011), bladder cancer (Yuasa *et al.*, 2009), chronic myelogenous leukaemia (D'Asaro *et al.*, 2010), melanoma (Kabelitz *et al.*, 2004), lung cancer (Dokouhaki *et al.*, 2010), prostate cancer (Santolaria *et al.*, 2013), pancreatic cancer (Kabelitz *et al.*, 2004; Oberg *et al.*, 2014), colon cancer (Devaud *et al.*, 2009; Devaud *et al.*, 2013), skin cancer (Devaud *et al.*, 2009), ovarian cancer (Lai *et al.*, 2012; Deniger *et al.*, 2014; Parente-Pereira *et al.*, 2014), AML (Gertner-Dardenne *et al.*, 2012), Epstein-Barr virus-induced B cell lymphoproliferative disease (Xiang *et al.*, 2014), and leukaemia (Deniger *et al.*, 2013) (Table. 1.5). These models broadly fall into one of two main categories: (*i*) cancer prevention model and (*ii*) therapeutic model. The cancer prevention models were designed to investigate the protective effects of γδ T cell in preventing tumour initiation and development. These models involve reconstitution of immunodeficient mice with human γδ T cells before xenotransplantation of human cancer cells and co-injection of cancer cells with γδ T cells in immunodeficient mice. The therapeutic model on the other hand focus on the control of established tumour by administered γδ T cells. These studies using cancer prevention and therapeutic models demonstrated that expanded γδ T cells, mostly $V\delta2^+$ T cells stimulated with phosphoantigens or nBPs, exhibit potent cytotoxicity to a wide spectrum of cancer cells, albeit with limited efficacy. In particular, single administration of γδ T cells usually has only very limited effects on tumour growth, and hence repeated administrations are necessary to obtain efficient and persistent control of tumour development. Adjuvants sensitising the target cancer cells to γδ T cells, *e.g.* nBPs, monoclonal antibodies against tumour antigens and bispecific chimeric antibodies, are needed to obtain optimal therapeutic effects. Besides, polyclonal γδ T cells genetically engineered to express anti-CD19 CAR showed enhanced cytotoxicity to $CD19^+$ tumours *in vitro* as compared to wild type γδ T cells and the ability to inhibit the growth of $CD19^+$ tumour xenografts in NSG mice (Deniger *et al.*, 2013), suggesting that apart from sensitisation with biological immune modulators, genetic modification of γδ T cells with artificial specificity provides a new approach for controlling tumour development. Other potential sensitising strategies include the use of cytokines other than IL-2 as different combinations of cytokine can

significantly polarise the function of γδ T cells (Vermijlen *et al.*, 2007; Caccamo *et al.*, 2013; Lafont *et al.*, 2014). For example, IL-21, which has been shown to enhance the cytotoxicity and degranulation of γδ T cells (Thedrez *et al.*, 2009), would be a good candidate for enhanced control of tumour growth.

Gertner-Dardenne *et al.*, established an elegant and powerful *in vivo* tracing system studying the homing of γδ T cells and their control of AML development in NOG mice (Gertner-Dardenne *et al.*, 2012). The labelling of γδ T cells with Xenolight DiR and AML with luciferase allows distinguishing and co-localising the effector and target cells in different peripheral tissues. This model will benefit largely our understanding of the migration of γδ T cells *in vivo* and their potential functions and efficacy in control primary tumour and metastases in different tissues.

Table. 1.5. Adoptive transfer of human γδ T cells for targeting human tumour xenografts in immunodeficient mice

Cancer type	γδ T cell subset and expansion	Tumour xenografts, γδ T cell adoptive transfer and sensitising strategies	Efficacy	Reference
Melanoma and pancreatic cancer	**Vγ9/Vδ2 T cells**: 200nM BrHPP or 5 μM alendronate with 100 U/ml IL-2	**5×10^6 MeWo cells/mouse (SCID), *i.p.*** • 2×10^7 γδ T cells, *i.p.*, at day 0 • 2×10^7 γδ T cells, *i.p.*, at day 0 + 10 μg/ml alendronate at day 0, 4, 11, 18, 25, 32 and 39 • 2×10^7 γδ T cells, *i.p.*, at day 0 + 10 μg/ml alendronate and 300 ng IL-2 at day 0, 4, 11, 18, 25, 32 and 39 **5×10^6 MeWo or PancTU-1 cells/mouse (SCID), *i.p.*** 300 ng IL-2 and 10 μg/ml alendronate were given at day 0, 4, 11, 18, 25, 32 and 39 for following groups: • 2×10^7 γδ T cells, *i.p.*, at day 0 + 5×10^6 γδ T cells, *i.p.*, at day 4 • 2×10^7 γδ T cells, *i.p.*, at day 0 + 5×10^6 γδ T cells, *i.p.*, at day 4 + 6×10^6 γδ T cells, *i.p*, at day 10 • 2×10^7 γδ T cells, *i.p.*, at day 0 + 5×10^6 γδ T cells, *i.p.*, at day 4 + 6×10^6 γδ T cells, *i.p*, at day 10 + 10^7 γδ T cells, *i.p.*, at day 20 • 2×10^7 γδ T cells, *i.p.*, at day 0 + 5×10^6 γδ T cells, *i.p.*, at day 4 + 6×10^6 γδ T cells, *i.p*, at day 10 + 10^7 γδ T cells, *i.p.*, at day 20 + 10^7 γδ T cells, *i.p*, at day 30	• Adoptive transfer of γδ T cells alone showed no significant benefits • Supplement of γδ T cells with alendronate significant prolonged the survival of mice with xenotransplantation of MeWo melanoma cells. • Only limited additive effect of IL-2 on prolonging survival of diseased animal was observed • With supplements of IL-2 and alendronate, repeated application of γδ T cells showed enhanced inhibition on tumour growth in both melanoma and pancreatic cancer models. • Administration of γδ T cells decreased the development of metastases and ascites	(Kabelitz *et al.*, 2004)
Bladder cancer	**Vγ9/Vδ2 T cells**: 5 μM ZA with 50 U/ml IL-2	**10^7 UM-UC-3^{Luc} cells/mouse (SCID), *intravesical*** 5 cycles of: • 5 μM ZA, • 10^7 γδ T cells (*intravesical*) or • 10^7 γδ T cells (*intravesical*) + 5 μM ZA daily started from day 3 or from day 8	• Repeated application of ZA had no effect on tumour growth. • Repeated application of γδ T cells inhibited the tumour growth and the therapeutic effect can be enhanced by co-administration with ZA	(Yuasa *et al.*, 2009)

Colon cancer and skin cancer	**$V\delta2^{neg}$ ($V\gamma4/V\delta5$; both clones 4-29 and 4-13) γδ T cells** and **$V\delta2^{+}$ γδ T cell clones** were sorted from PBMCs of children with a neonatal CMV-infection using relevant anti-Vδ chain mAbs and then expanded with 1 μg/ml PHA, irradiated allogeneic PBMCs and 1000 IU/mL IL-2 (Halary *et al.*, 2005)	***Concomitant injection model:*** **5×10^5 HT29 cells/mouse ($Rag^{-/-}\gamma c^{-/-}$), *s.c.*, +** • 2×10^6 $V\delta2^{neg}$ γδ T cells (clone 4-29) + 1000 U/ml IL-2 • 2×10^6 $V\delta2^{neg}$ γδ T cells (clone 4-13) + 1000 U/ml IL-2 **10^5 HT29 cells/mouse ($Rag^{-/-}\gamma c^{-/-}$), *s.c.*, +** • 2×10^6 $V\delta2^{neg}$ γδ T cells (clone 4-29) + 1000 U/ml IL-2 • 2×10^6 $V\delta2^{+}$ γδ T cells + 1000 U/ml IL-2 **Therapy model:** **10^5 HT29 cells/mouse ($Rag^{-/-}\gamma c^{-/-}$), *s.c.*** ***experiment 1*** • Single *i.p.* 2×10^6 $V\delta2^{neg}$ γδ T cells (clone 4-29) at day 0 • 4 cycles of *i.p.* 2×10^6 $V\delta2^{neg}$ γδ T cells (clone 4-29) at day 0, 2, 4 and 7 ***experiment 2*** • 4 cycles of *i.p.* 2×10^6 $V\delta2^{neg}$ γδ T cells (clone 4-29) at day 0, 2, 4 and 7; each injection with 5000 U/ml IL-2 • 4 cycles of *i.p.* 2×10^6 $V\delta2^{neg}$ γδ T cells (clone 4-29) at day 0, 2, 4 and 7; each injection with 100 U/ml IL-2 ***experiment 3*** • 4 cycles of *i.p.* 2×10^6 $V\delta2^{neg}$ γδ T cells (clone 4-29) at day 7, 9, 11 and14 ***experiment 4*** • 4 cycles of *i.p.* 2×10^6 $V\delta2^{+}$ γδ T cells (clone 4-29) at day 0, 2, 4 and 7 **10^5 A431 cells/mouse ($Rag^{-/-}\gamma c^{-/-}$), *s.c.*, +** • 4 cycles of *i.p.* 2×10^6 $V\delta2^{+}$ γδ T cells (clone 4-29) at day 0, 2, 4 and 7	• Cross reactivity of $V\delta2^{neg}$ T cell derived from CMV-infected transplantation patients in killing CMV-infected cells and HT-29 colon cancer cells • Only $V\delta2^{neg}$ γδ T cells but not $V\delta2^{+}$ γδ T cells showed protection to delay initiation and development of colon cancer in concomitant injection model • Repeated administration of $V\delta2^{neg}$ γδ T cells is necessary to reach considerable control of HT29 tumour growth • Supplements with IL-2 in repeated co-injection of $V\delta2^{neg}$ γδ T cells did not show significant improvement on inhibition of HT29 tumour growth • Repeated transfer of $V\delta2^{+}$ γδ T cells did not exhibit any benefit in control of both HT29 and A431 tumour growth	(Devaud *et al.*, 2009)

Chronic myelogenous leukemia	**Vγ9/Vδ2 T cells** expanded from PBMCs of healthy donors and CML patients: 0.5 μM ZA or 1 nM BrHPP with 50 U/ml IL-2	**10^6 MM1 cells/mouse (NOD/SCID), *i.v.*** ***experiment 1*** • *i.p.* 2×10^7 γδ T cells + 2 μg ZA every 14 days from day 1 (at day 1, 15, 29) with 30000 IU IL-2 weekly at day 1, 8, 15, 22, 29 and 36 • γδ T cells + ZA • γδ T cells + IL-2 • ZA + IL2	• The only adoptive transfer model so far using γδ T cells expanded from PBMCs of cancer patients • Repeated applications of γδ T cells with IL-2 or ZA showed no inhibition in development of CML • Repeated applications of γδ T cells with both IL-2 or ZA exhibited effective therapeutic benefits on clearance of CML development	(D'Asaro *et al.*, 2010)
Lung cancer	Pan γδ T cells: γδ T cells were expanded from PBMCs depleted with CD4 and CD8 T cells in the presence of anti-CD3 mAbs (OKT3), 250 U/ml rhIL-2 and 0.1 ng/ml rhIL-4.	**Co-injection of 10^6 H460 cells/mouse (SCID), *s.c., with*** • γδ T cells or • bulk CD8 T cells at E/T ratio of 5:1	• Presence of CD8 T cells in co-injection barely showed any inhibition on tumour development while	(Dokouhaki *et al.*, 2010)
Breast cancer	Pan γδ T cells: 1000 U/ml IFN-γ, 10 U/ml rhIL-12 and 1 – 10 μg/ml α-CD2 mAbs (S5.2) at day 0; 10 ng/ml α-CD3 mAbs (OKT3) and 300 U/ml rhIL-2 at day 1 (Lopez *et al.*, 2000)	**10^6 2LMP/Luc (MDA-MB-231) cells/mouse (nude), *s.c.*** • 2×10^7 γδ T cells, *i.v.* at day 6, 9,13, 16, 20 and 23	• Repeated applications of γδ T cells showed potent therapeutic potential in inhibiting tumour growth	(Beck *et al.*, 2010)

Breast cancer	Vγ9/Vδ2 T cells: 3 μM BrHPP and 300 U/ml IL-2	**2 × 10^6 SK-BR-3 cells/mouse (SCID Beige), *s.c.*** ***experiment 1*** • *i.p.* 10 mg/kg TTZ • *i.v.* 10^7 γδ T cells • *i.v.* 10^7 γδ T cells + *i.p*10 mg/kg TTZ twice a week for two weeks started when tumour size reached around 140 mm^3 at day 56 (exponential growth phase) ***experiment 2*** • Same settings to experiment 1 but with treatments started earlier at day 41 ***experiment 3*** • *i.p.* 10 mg/kg TTZ • *i.v.* 2 × 10^7 γδ T cells • *i.v.* 2 × 10^7 γδ T cells + *i.p.* 10 mg/kg TTZ twice a week for four weeks; start date of treatment was not specified in the paper	• Repeated treatment with γδ T cells alone showed no control in tumour growth • Repeated treatment with TTZ alone exhibited limited benefits in inhibiting tumour growth • Repeated treatment with both γδ T cells and TTZ showed reasonable therapeutic benefits in inhibiting tumour growth and the therapeutic effects can be enhanced by earlier start of treatment, by increased number γδ T cells administrated and by prolonged treatment from two weeks to 4 weeks • Combination with TTZ did not enhance the infiltration of γδ T cells into tumour. The enhancement of γδ T cells in controlling tumour growth was likely due to the opsonisation of tumour cells.	(Capietto *et al.*, 2011)
Breast cancer	Vγ9/Vδ2 T cells: 10 μM ZA and 100 U/ml IL-2 (for use in *in vitro* assays)	**5 × 10^6 B02 or T47D cells/mouse (NOD/SCID), *s.c.*** • 30 μg/kg ZA • 3.5 × 10^7 PBMCs + 100000 U/ml IL-2 • 3.5 × 10^7 PBMCs + 100000 U/ml IL-2 + 30 μg/kg ZA Treatments started from week 4 with single dose of PBMCs. ZA and IL-2 were administrated repeatedly every 2 days for 14 days in the relevant groups.	• No inhibition on tumour growth was observed by any treatment in B02 model • The treatment with PBMCs, IL-2 and ZA blocked the tumour growth since the start of treatment for 2 weeks until the end of experiment	(Benzaid *et al.*, 2011)

Ovarian cancer	Vγ9/Vδ2 T cells: 10 mM MEP and 40 U/ml IL-2	**Co-injection (*s.c.*) of 500 SK-OV-3 sphere cells with 50 γδ T cells into flanks of nude mice in both two sides**	• Co-injection of SK-OV-3 sphere cells with γδ T cells at E/T ratio of 1/10, which is very low, sufficiently reduced the incidence of tumour initiation and inhibited the growth of developed tumour	(Lai *et al.*, 2012)
Acute myeloid leukemic blasts	γδ T cells were expanded with 3 μM BrHPP, 100 U/ml IL-2 and 10 ng/ml IL-15 • Expanded γδ T cells (42% $CD3^+V\delta2^+$) • Purified γδ T cells (98% $CD3^+V\delta2^+$)	***Homing study:*** **(A) 2×10^5 U937 cells/mouse (NSG), *i.v.*** • Single dose of 4×10^7 expanded γδ T cells (*i.v.*) 6 hours after injection of U937 cells at day 0 • Blood, spleen and BM were harvest at day 17 to check the homing of γδ T cells into these tissues • **(B) 2×10^5 U937 cells/mouse (NSG), *i.v.*** • Single dose of labelled 10^7 purified γδ T cells (*i.v.*) at day 14 • Homing of γδ T cells into different tissues were examined by *in vivo* live imaging and imaging at the end of experiment with harvested tissues ***Cancer control study:*** **2×10^5 U937 cells/mouse (NSG), *i.v.*** • Single dose of labelled 10^7 purified γδ T cells (*i.v.*) at day 14	• γδ T cells can home to spleen, liver, lung and BM for the killing of local AML cells and thus prolong the survival of treated mice	(Gertner-Dardenne *et al.*, 2012)

Colon cancer	Vδ1 T cells: Sorted from PBMCs of children with a neonatal CMV-infection using anti-Vδ1 mAbs and then expanded with 1 μg/ml PHA, irradiated allogeneic PBMCs and 1000 IU/mL IL-2 (Halary *et al.*, 2005)	**Co-injection (*s.c.*) of 10^5 HT29 luc cells with 10^7 γδ T cells per mouse** **10^5 HT29 luc cells/mouse (NSG), *orthotopic microinjection in caecum*** • 3 times a week of injection with 4×10^6 γδ T cells (*i.p.*), from day 0 to day 36	• Co-injection of γδ T cells delayed the development of HT29 tumour • Continuous treatment with γδ T cells inhibited orthotopic tumour development and metastases to lung and liver	(Devaud *et al.*, 2013)
Prostate cancer	Vγ9/Vδ2 T cells: 200 μM pamidronate and 60 ng/ml rhIL-2	**10^7 PC3 cells/mouse (NSG), *s.c.*** • 50 μg/kg pamidronate (*i.v.* at day 14) + 10^6 γδ T cells (*i.v.* at day 15) • 50 μg/kg pamidronate (*i.v.* at day 14) + 10^6 γδ T cells (*i.v.* at day 15) followed by 50 μg/kg pamidronate weekly for 3 more cycles (*i.v.* at day 21, 28 and 35) • 50 μg/kg pamidronate (*i.v.* at day 14) + 10^6 γδ T cells (*i.v.* at day 15) followed by 10^6 γδ T cells weekly for 3 more cycles (*i.v.* at day 21, 28 and 35) • Combination of 50 μg/kg pamidronate (*i.v.)* and 10^6 γδ T cells (*i.v.,* one day after pamidronate) weekly from day 14 for 4 cycles	• Single dose of pamidronate with γδ T cells showed limited control of tumour growth • Repeated treatments with both pamidronate with γδ T cells are necessary to enhance and prolong efficacy in controlling tumour growth	(Santolaria *et al.*, 2013)

Acute lymphoblastic leukemia	γδ T cells were isolated from PBMCs transduced with CD19-specific CAR (CD19RCD28) by negative selection and then expanded in co-culture with aAPCs (Singh *et al.*, 2011) in the presence of 50 IU/ml IL-2 and 30 ng/ml IL21.	**10^5 NALM-6-ffLuc-eGFP cells/mouse (NSG), *i.v.*** • 3 administration of 10^7 CAR^+ γδ T cells with 6 $\times 10^4$ U IL-2 at day 1, 8, 15 in supplement with another two injections of 6 $\times 10^4$ U IL-2 at day 2, 9 and 16	• Repeated application of CAR^+ γδ T cells in supplement with IL-2 reduced the dissemination of leukemia and tumour burden in bone marrow, spleen and peripheral blood.	(Deniger *et al.*, 2013)
B cell lymphoproliferative disease	Vγ9/Vδ2 T cells: 200 μM pamidronate and 60 ng/ml rhIL-2	**10^5 GFP-LCL cells/mouse ($Rag2^{-/-}\gamma c^{-/-}$), *s.c.*** • 10^7 Vγ9/Vδ2 T cells (*i.v.)* at day 0, 7, 14 and 21 • 10^7 Vγ9/Vδ2 T cells (*i.v.)* at day 21, 28, 35 and 42 **10^5 GFP-LCL cells/mouse (humanised $Rag2^{-/-}\gamma c^{-/-}$), *s.c.*** • 100 μg pamidronate/mouse (*i.p.)* at day 0, 7, 14, 21 and 28 **100 μg pamidronate/mouse (*i.p.)* at day 0, 7, 14, 21 and 28** • 10^5 GFP-LCL cells/mouse (*s.c.*) in $Rag2^{-/-}\gamma c^{-/-}$ mice humanised with whole human PBMCs • 10^5 GFP-LCL cells/mouse (*s.c.*) in $Rag2^{-/-}\gamma c^{-/-}$ mice humanised with Vγ9/Vδ2 T cell-depleted human PBMCs	• Repeated treatments of Vγ9/Vδ2 T cells from the date of cancer cell challenge efficiently prevent the tumour initiation and inhibited the growth of established tumours • Repeated treatments of established LCL tumours with Vγ9/Vδ2 T cells significantly prolonged the survival of diseased mice, inhibited the tumour growth and even decreased the tumour size • Specific activation of Vγ9/Vδ2 T cells in humanised mice with repeated administration of pamidronate efficiently prolonged survival, decreased tumour incidence and inhibited the growth of tumour in diseased animals	(Xiang *et al.*, 2014)

Pancreatic cancer	Vγ9/Vδ2 T cells: 300 nM BrHPP	**1.5 × 10^6 PancTu-1 cells/mouse (SCID Beige), *s.c.*** • 2.5 ×10^6 γδ T cells (*s.c.* at day 15) + 8 ×10^6 γδ T cells (*s.c.* at day 7) + 4.5 ×10^6 γδ T cells (*s.c.* at day 14) + 2.5 ×10^6 γδ T cells (*s.c.* at day 23) alone and with: o 15 μg/kg (25 × 10^4 U) IL-2 + 2.5 mg/kg ZA or o 15 μg/kg (25 × 10^4 U) IL-2 + 1.25 mg/kg [$(Her2)_2$×Vγ9] bispecific antibodies for each injection of γδ T cells	• Repeated adoptive transfer of γδ T cells with [$(Her2)_2$×Vγ9] bispecific antibodies but not with ZA showed control of tumour growth	(Oberg *et al.*, 2014)
Ovarian cancer	Vγ9/Vδ2 T cells: 1 μg/ml ZA, 100 U/ml IL-2 and 10 ng/ml IL-15	**10^6 SKOV-3-luc cells/mouse (SCID Beige), *i.p.*** • 1 μg ZA (*i.p.* at day 4) +10^7 γδ T cells (*i.p.* at day 5) • 1 μg ZA (*i.p.* at day 6) +10^7 γδ T cells (*i.p.* at day 7) **5 × 10^5 IGROV-luc cells/mouse (SCID Beige), *i.p.*** • 1 μg ZA (*i.p.* at day 17) + 5 μg ZA (*i.p.* at day 18) + 10^7 γδ T cells (*i.p.* at day19) • 30 μg AA (*i.p.* at day 14) + 100 μg AA (*i.p.* at day 15) + 2 × 10^7 γδ T cells (*i.p.* at day 16) • 150 μg AA (*i.v.* at day 9) + 10^7 γδ T cells (*i.p.* at day 10, 12 and 14)	• Strong toxicity of L-ZA • No significant control of tumour growth by γδ T cell with L-ZA • Efficient tumour growth control observed by adoptive transfer of γδ T cells with AA and L-AA as sensitiser • Optimal tumour control observed when mice were given *i.v.* L-AA followed with multiple dose of γδ T cells • Benefit of constituting ZA and AA with liposome in sensitising tumour to γδ T cells	(Parente-Pereira *et al.*, 2014)

Ovarian cancer	γδ T cells were isolated from $CD56^+$ cell-depleted PBMCs by negative selection and then expanded in co-culture with aAPCs (Singh *et al.*, 2011) in the presence of 50 IU/ml IL-2 and 30 ng/ml IL21. **Vδ1 T cells ($Vδ1^+$ $Vδ2^{neg}$)**, **Vδ2 T cells ($Vδ1^{neg}$ $Vδ2^+$) and $Vδ1^{neg}$ $Vδ2^{neg}$ T cells** were isolated from the expansion by FACS for functional assays.	**3×10^6 CAOV3-effLuc-mKate cells/mouse (NSG), *i.p.*** 4 *i.p.* administrations of • Vδ1 T cells, • Vδ2 T cells, • $Vδ1^{neg}$ $Vδ2^{neg}$ T cells or • Polyclonal γδ T cells at day 8 (3×10^6 cells), 15 (6×10^6 cells), 22 (10^7 cells) and 29 (1.5×10^7 cells)	• Repeated treatments of all different types of γδ T cells show potent therapeutic effects in decreasing tumour burden (decreased reporter signal) and prolonging survival.	(Deniger *et al.*, 2014)

aAPC: artificial antigen-presenting cell; MEP: monoethyl phosphate
i.p.: intraperitoneal; *i.v.*: intravenous; *s.c.*: subcutaneous
BLI: bioluminescence
ZA: Zoledronic acid; L-ZA: liposomal zoledronic acid; AA: alendronic acid; L-AA: liposomal alendronic acid

1.6. Hypothesis and aims

Hypothesis:

γδ T cells can function to bridge innate and adaptive immunity specifically against breast CSCs.

Aims:

- To establish a CSC model system available both *in vitro* and *in vivo* for the study of their susceptibility to MHC-restricted and non-MHC-restricted immune cells and for the test of therapeutic efficacy of T cell adoptive transfer in controlling xenografted human breast tumour in immunodeficient mice.
- To identify effective sensitisation strategies in enhancing γδ T cell-mediated immunity targeting breast CSCs.
- To provide *in vivo* experimental evidence showing the APC function of γδ T cells in breast tumour.

Chapter 2. Materials and Methods

2.1. Cell Culture Media and Buffers

2.1.1. Cell culture media

Complete RPMI medium

RPMI-1640 (Invitrogen) medium supplemented with 10% foetal calf serum (FCS; Invitrogen), 50 mg/ml penicillin-streptomycin (Invitrogen), 2 mM L-glutamine (Invitrogen), 1% sodium pyruvate and 100 μM non-essential amino acids (NEAA; Invitrogen).

Complete HMLER medium

DMEM (Invitrogen) and F12 (Invitrogen) medium mixed at 1:1 ratio and supplemented with 10% FCS (Invitrogen), 50 mg/ml penicillin-streptomycin (Invitrogen), 10 μg/ml insulin (Sigma), 10 ng/ml recombinant human EGF (Peprotech), 0.5 μg/ml hydrocortisone (Sigma) and 1 μg/ml puromycin (Sigma).

Mammosphere culture medium

MEBM serum-free epithelial growth medium (Lonza) supplemented with B27 (Life Technologies), 20 ng/ml EGF (Peprotech), 5 μg/ml insulin (Sigma), 0.1 μM β-mercaptoethanol (Sigma), 1 μg/ml hydrocortisone (Sigma) and 20 μg/ml gentamycin (Sigma).

Complete DMEM medium

DMEM medium (Invitrogen) supplemented with 10% FCS (Invitrogen), 50 mg/ml penicillin-streptomycin (Invitrogen), 2 mM L-glutamine (Invitrogen), 1% sodium pyruvate and 100 μM NEAA.

2.1.2. Buffers

Fluorescence activated cell sorting (FACS) buffer

FACS buffer was prepared by adding 2% FCS (Invitrogen) into sterile PBS and passing through 0.22 μm filter.

Magnetic-activated cell sorting (MACS) buffer

MACS buffer was prepared by adding 2% FCS (Invitrogen) and 5 mM EDTA into sterile PBS and passing through 0.22 μm filter.

2.2. Tumour Cells

2.2.1. Transformed mammary epithelial cells

The transformed mammary epithelial cell line HMLER (Elenbaas *et al.*, 2001) was kindly provided by Prof Robert Weinberg (MIT Ludwig Center for Molecular Oncology, Cambridge, MA), and maintained in normal culture with specific HMLER medium at 37°C in 5% CO_2. The CSC-like and non-CSC sublines established from HMLER cells by FACS sorting were maintained as parental HMLER cell line.

2.2.2. Generation and maintenance of CSC-like and non-CSC sublines from HMLER cell line

HMLER cells were harvested by trypsinisation and then stained with FITC-conjugated anti-CD24 mAbs (ML5; BD Biosciences) and PE-Cy7-conjugated anti-CD44 mAbs (G44-26; BD Biosciences) for the separation of $CD44^{hi}/CD24^{lo}$ CSC-like cells and $CD44^{lo}/CD24^{hi}$ non-CSCs by BD FACS Aria III cell sorter (BD Biosciences) to purities >97%. Sorted CSC-like cells and non-CSCs were maintained in adherent culture with complete HMLER medium. CSC-like cells and non-CSCs were further transduced with lentiviral particles for stable expression of influenza M1 or *Gaussia* luciferase with tdTomato as fluorescent reporter (for detail, see section 2.6 and 2.7), and maintained under the same conditions as the parental cells.

2.3. Immune Effector Cells

2.3.1. Isolation of peripheral mononuclear cells (PBMCs)

PBMCs were isolated either from blood bags supplied by the Welsh Blood Service, Velindre, or from venous blood collected locally from healthy volunteers. Blood bags was diluted at 1:1 ratio with PBS, and venous blood was heparinised with anti-coagulant buffer consisting of 20 U/ml heparin and 15 mM EDTA (Fisher Scientific UK Ltd) for subsequent Ficoll-Paque (Axis-Shield) separation. Processed blood was layered on top of Ficoll-Paque and then centrifuged at 1680 rpm (687 xg), at 18°C for 20 minute without break at the end of spin. The mononuclear cells within the buffy coat were collected and washed twice with PBS for the isolation of γδ T cells and monocytes and for the expansion of $CD8^+$ T cells or γδ T cells.

2.3.2. Isolation of γδ T cells from PBMCs

γδ T cells were isolated by MACS (Miltenyi) from PBMCs. PBMCs were incubated with PE-Cy5-conjugated anti-Vγ9 mAbs (Immu360; Beckman Coulter) at 4°C for 20 minute and washed with sterile MACS buffer (PBS supplemented with 2% FCS, 5 mM EDTA), followed by incubation with anti-PE microbeads (Miltenyi) on ice for 20 minutes. Labelled cells were positively selected over two LS columns (Miltenyi). Resulting purities were >98% as determined by flow cytometry.

2.3.3. Isolation of monocytes from PBMCs

Monocytes were purified by MACS (Miltenyi) from Vγ9-depleted PBMCs incubated with anti-CD14 microbeads (Miltenyi) on ice for 20 minutes. Labelled cells were positively selected over two LS columns (Miltenyi) to purities >98% as determined by flow cytometry.

2.3.4. Expansion of Vγ9/Vδ2 T cells from PBMCs

γδ T cells were expanded from PBMCs of healthy donors with 100 U/ml IL-2 (Proleukin; Novartis) and 1 μM zoledronate (Zometa; Novartis) for around 14 days. Zoledronate was added to the culture at the beginning of expansion at day 0, whereas IL-2 was added to the culture every 2-3 days starting from day 5 until the end of expansion. After 14 days, γδ T

cells with purities <90% were enriched further by negative selection using a customised γδ T cell purification kit (Stem Cell Technologies) removing αβ T cells, B cells, NK cells, dendritic cells, stem cells, granulocytes, monocytes without depletion of $CD56^+$ and $CD16^+$ cells, to a final purity > 98% (Figure 2.1).

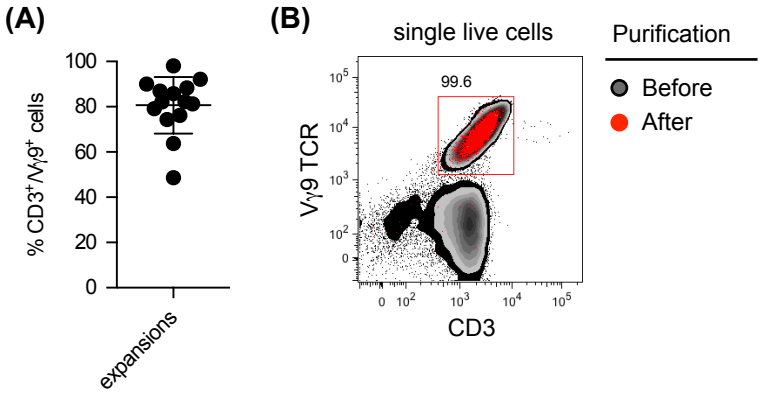

Figure 2.1. Expansion of γδ T cells. **(A)** The purity of expanded γδ T cells was evaluated by staining with fluorochrome-conjugated monoclonal antibodies against CD3 and Vγ9 TCR, and analysed by flow cytometry. **(B)** For γδ T cell lines reaching <90%, γδ T cells were enriched further to a purities >98% using a customised γδ T cell purification kit (Stem Cell Technologies). All analyses were performed by a series of gates on single cells and live cells.

2.3.5. Generation of Vγ9/Vδ2 T cell conditioned supernatants

For the collection of γδ T cell conditioned medium, purified γδ T cells were co-cultured with autologous monocytes for 5 days in the presence of 100 U/ml IL-2 and 10 µM zoledronate. Alternatively, expanded γδ T cells were re-stimulated overnight with 10 nM synthetic HMB-PP (kindly provided by Dr. Hassan Jomaa, University of Giessen, Germany). Supernatants were stored at −80°C until further use.

2.3.6. Expansion of Flu M1- and CMV pp65-specific $CD8^+$ T cells

HLA-A2-restricted $CD8^+$ T cell lines with specificity to Flu M1 p58-66 and to CMV pp65 p495-503, respectively, were established from PBMCs of healthy donors with the help from Dr. Wajid Khan in the laboratory. Flu M1-specific $CD8^+$ T cells were expanded from PBMCs with 20-40 U/ml IL-2, 20 ng/ml IL-15 (Miltenyi) and 0.1 µM Flu M1 p58-66 peptide. Cells attained positive for p58-66 MHC tetramer (kindly provided by Andrew

Thomas in the laboratory) were sorted and further expanded with 1 μg/ml PHA, 100 U/ml IL-2 and 20 ng/ml IL-15 in the presence of irradiated PBMCs as feeder cells (Khan *et al.*, 2014a). At the end of expansion, cells were stained with antibodies against CD3, CD4, CD8 and p58-66 MHC tetramer to make sure the purity of Flu M1-specific $CD8^+$ T cells was > 99% (Figure 2.2). The CMV pp65-specific $CD8^+$ T cells were kindly provided by Dr. Wajid Khan in our laboratory.

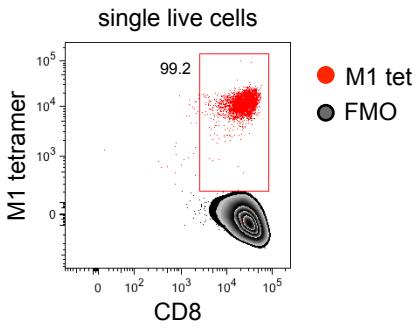

Figure 2.2. Generation of Flu M1-specific $CD8^+$ T cells. The purity of expanded Flu M1-specific $CD8^+$ T cells was evaluated by staining with PE-conjugated MHC tetramers loaded with Flu M1 p58-66 peptide, and analysed by flow cytometry. Analysis was performed by a series of gates on single cells, live cells and $CD3^+/CD8^+$ cells. FMO, Fluorescence Minus One control.

2.4. Flow cytometry

Generally for all flow cytometric measurements, cells were firstly stained with Live/dead fixable Aqua dead cell stain kit (Life Technologies) to distinguish live cells from dead cells and subsequently treated with intravenous immunoglobulin (IvIg) (Kiovig; Baxter) at 1:100 dilution in order to block Fc receptors.

For the staining of cell surface markers, IvIg-blocked cells were incubated for 20 minutes on ice with a panel of monoclonal antibodies conjugated with different fluorochromes. The antibodies used in this study and the appropriate dilutions are summarised in Table 2.1. For intracellular staining, surface stained cells were fixed for 20 minutes at room temperature with fixation buffer (eBioscience) and permeabilised with permeabilisation buffer (eBioscience). Such treated cells were then incubated for 20 minutes at room temperature with fluorochrome-conjugated monoclonal antibodies diluted in permeabilisation buffer. In each case, stained cells were washed with FACS buffer and acquired using a FACS Canto II (BD Biosciences). All analyses of data were performed using FlowJo (version 9.3.2; TreeStar Inc.), by gating on intact cells (FSC-A/SSC-A), single cells (FSC-A/FSC-H), live cells ($Aqua^-$) and expression of markers of interest according to appropriate isotype controls.

Table 2.1. Antibodies used in this study

Antigen	Clone	Conjugate	Dilution (conc.)	Manufacturer	Application
CD3	UCHT1	PB	1/100	BD	Flow cytometry
CD4	SK3	APC-Cy7	1/80	BD	Flow cytometry
CD8	HIT8a	PE	1/50	Pharmingen	Flow cytometry
CD8	SK1	PE-Cy7	1/300	BD	Flow cytometry
CD11c	S-HCL-3	PE	1/25	BD	Flow cytometry
CD14	MOP9	FITC	1/20	BD	Flow cytometry
CD16	3G8	FITC	1/20	Pharmingen	Flow cytometry
CD19	SJ25C1	APC	1/20	eBioscience	Flow cytometry
CD24	ML5	FITC	1/5	BD	Flow cytometry
CD24	ML5	BV421	1/20	BD	Flow cytometry
CD25	M-A251	APC-Cy7	1/20	BD	Flow cytometry
CD27	M-T271	FITC	1/40	Pharmingen	Flow cytometry
CD27	M-T271	PE	1/40	Pharmingen	Flow cytometry
CD40	5C3	PE	1/20	Coulter	Flow cytometry
CD44	G44-26	APC	1/5	BD	Flow cytometry
CD44	G44-26	PE-Cy7	1/40	BD	Flow cytometry
CD44	DF1485	−	1 µg/ml	Santa Cruz	IF
CD45RA	HI100	APC	1/10	eBioscience	Flow cytometry
CD56	B159	PE-Cy7	1/20	Pharmingen	Flow cytometry
CD69	FN50	FITC	1/20	Pharmingen	Flow cytometry
CD80	2D10.4	FITC	1/5	eBioscience	Flow cytometry
CD86	IT2.2	APC	1/10	BioLegend	Flow cytometry
CD107a	H4A3	PE	1/20	BD	Flow cytometry
CD277	103.2	−	10 mg/ml	Dr. Daniel Olive	Neutralisation
HLA-ABC	W6/32	PE	1/10	BioLegend	Flow cytometry
HLA-DR	L243	APC-Cy7	1/40	BD	Flow cytometry
Vγ9 TCR	Immu360	PerCP-Cy5	1/400	Beckman Coulter	Flow cytometry
Vγ9 TCR	7A5	−	10 µg/ml	Biolegend	Neutralisation
GD2	14.G2a	PE	1/20	BD	Flow cytometry
GD2	Hu14.18K322A	−	10 µg/ml	Dr. Fariba Navid	Opsonisation
IFN-γ	B27	FITC	1/100	BD	Flow cytometry
IFN-γ	B27	−	10 µg/ml	Biolegend	Neutralisation

IF: immunofluorescent microscopy; -: purified non-conjugated antibody;

Table 2.1. Antibodies used in this study (continued)

Antigen	Clone	Conjugate	Dilution (conc.)	Manufacturer	Application
NKG2D	1D11	−	10 μg/ml	Biolegend	Neutralisation
α-SMA	1A4	−	1 μg/ml	Santa Cruz	IF
N-cadherin	8C11	−	1 μg/ml	eBioscience	IF
CK14	LL001	−	1 μg/ml	Santa Cruz	IF
CK18	RGE53	−	1 μg/ml	Santa Cruz	IF
EDA-Fibronectin	IST-9	−	1 μg/ml	Santa Cruz	IF
Vimentin	V9	−	1 μg/ml	Santa Cruz	IF

IF: immunofluorescence microscopy; −: purified antibody without any conjugates;

2.5. *In vitro* characterisation of CSC-like cells and non-CSCs

2.5.1. Mammosphere formation assays

For mammosphere cultures, cells were harvested by treatment with 0.05% trypsin and 0.25% EDTA. Dissociated cells were resuspended and plated in ultra-low attachment plates (Corning Life Sciences) at a density of 2.5×10^4 cells/ml in serum-free mammosphere medium. After seven days, mammospheres were collected by centrifugation (400 xg for 5 minutes) and dissociated into single cell suspensions with 0.05% trypsin and 0.25% EDTA. Live cells were identified and counted after trypan blue staining, and re-seeded back into ultra-low attachment plates at the same density of 2.5×10^4 cells/ml for secondary mammosphere formation.

2.5.2. Proliferation analysis

HMLER cells were labelled with CellVue (Sigma-Aldrich) according to the manufacturer's instruction, washed, and maintained under mammosphere-forming conditions for 5 days. Cells were harvested form cultures for live/dead staining cell surface staining for CD44 and CD24, intracellular staining for proliferation markers Ki67, phospho-histone H3 (pHH3) and incorporation of propidium iodide (PI). Stained cells were acquired using a FACS Canto II.

2.5.3. Immunofluorescence (IF) microscopy

Isolated CSC-like cells and non-CSCs were grown in Nunc Lab-Tek cover-slip chamber slides to sub-confluency. The cells were washed twice with PBS prior to fixation in ice-cold acetone/methanol at 1:1 *v*/*v* ratio, and fixed slides were blocked overnight at 4°C with 1% BSA in HBSS buffer (*w*/*v*). The slides were then washed twice with 1% BSA in HBSS buffer and incubated individually with a panel of primary antibodies against CD44, alpha-smooth muscle actin (α-SMA), N-cadherin, cytokeratin-14 (CK14), CK18, extra domain A (EDA)-fibronectin or vimentin for 2 hours at room temperature. The slides were washed twice with 1% BSA in HBSS buffer and then incubated with 1 μg/ml AF-488-cojugated secondary antibodies, followed by counterstaining with DAPI (Sigma) for 10 minutes. Slides were analysed using a Zeiss AxioVert fluorescence microscope (Webber *et al.*, 2010).

2.6. Functional T cell assays

2.6.1. Cytotoxicity assay using mixed target cell populations

For the comparison of their susceptibilities to γδ T cell or $CD8^+$ T cell-mediated cytotoxicity, two different target cell populations were labelled separately with different lipophilic dyes (PKH26, PKH67 or CellVue; all from Sigma-Aldrich), and mixed at 1:1 ratio for the subsequent co-culture with effector T cells at different Effector/Target (E/T) ratios. After 4 hours at 37°C, cultures were harvested, stained by Live/dead® fixable Aqua dead cell stain kit and acquired on a FACS Canto II. As shown in Figure 2.3, the analysis was performed by serial gating on single cells (FSC-A/FSC-H) and distinctively stained targets (for example, $CellVue^+$ $PKH67^-$ or $CellVue^-$ $PKH67^+$), and the proportion of dead cells was determined for each target population. The rate of specific killing was calculated using the formula:

$$\%\ Specific\ killing = \frac{(\%\ dead\ cells\ with\ T\ cells) - (\%\ dead\ cells\ without\ T\ cells)}{100\% - (\%\ dead\ cells\ without\ T\ cells)}\ x\ 100\%$$

For antigen-specific killing by Flu M1- or CMV pp65-specific cytotoxic $CD8^+$ T cells, target cells were transduced with lentiviral vectors expressing specific Flu M1 antigen, or pulsed with 1 μM Flu M1 peptide (p58-66, GILGFVFTL) or 1 μM CMV pp65 peptide (p495-503, NLVPMVATV) (kindly provided by Prof. Per thor Straten, Denmark) prior to the labelling with lipophilic dyes.

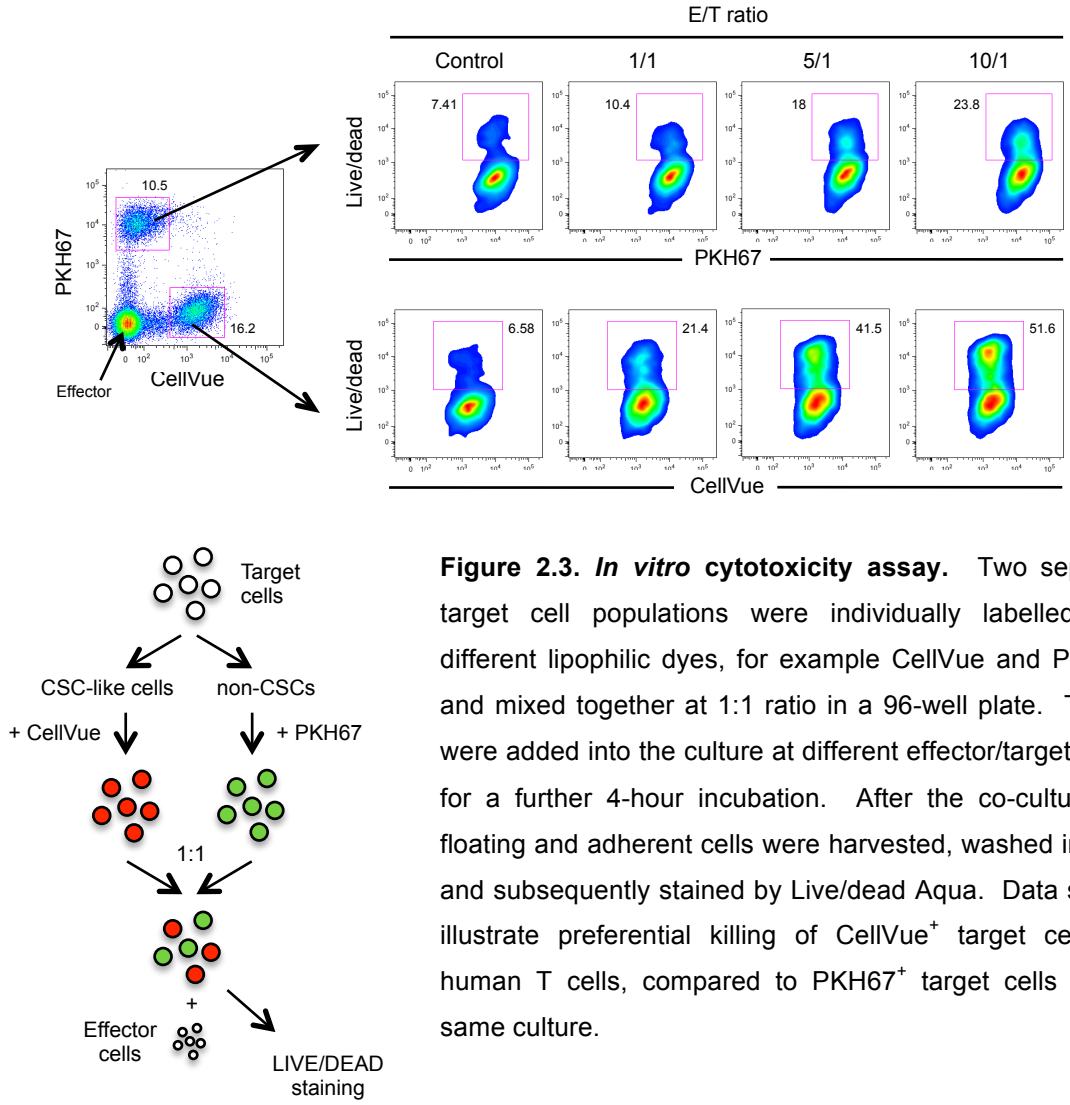

Figure 2.3. *In vitro* cytotoxicity assay. Two separate target cell populations were individually labelled with different lipophilic dyes, for example CellVue and PKH67, and mixed together at 1:1 ratio in a 96-well plate. T cells were added into the culture at different effector/target ratios for a further 4-hour incubation. After the co-culture, all floating and adherent cells were harvested, washed in PBS and subsequently stained by Live/dead Aqua. Data shown illustrate preferential killing of CellVue^{+} target cells by human T cells, compared to PKH67^{+} target cells in the same culture.

2.6.2. CD107a degranulation assay

γδ T cells or CD8^{+} T cells were stimulated under different conditions in the presence of monensin (Golgi-Stop; BD) and PE-conjugated anti-CD107a monoclonal antibodies for 5 hours and stained for cell surface makers to distinguish different cell subsets. 10 nM HMB-PP was used as positive control for the activation of γδ T cells, whereas 100 ng/ml PMA and 100 ng/ml ionomycin were used as positive control for the activation of CD8^{+} T cells.

2.6.3. IFN-γ production

Flow cytometry analysis of intracellular IFN-γ

γδ T cells or $CD8^+$ T cells were stimulated under different conditions in the presence of 5 μg/ml brefeldin A (Biolegend) for 5 hours and stained for cell surface makers to distinguish different cell subsets in co-culture, and then stained intracellularly for their production of IFN-γ as described above.

Enzyme-linked immunosorbent assay (ELISA)

Supernatants from γδ T cell or $CD8^+$ T cell cultures were harvested as indicated in the figure legends, and the level of IFN-γ was measured by ELISA (eBioscience or Biolegend) according to manufacturers' instruction.

2.6.4. Endocytosis assay

Expanded γδ T cells and freshly purified γδ T cells from PBMCs were tested for their ability to uptake fluorescent proteins or fluorochrome-conjugated antigen. Expanded γδ T cells were used in antigen uptake assays directly without further re-stimulation, whereas freshly purified γδ T cells were stimulated with 10 nM HMB-PP and 100 U/ml IL-2 for three days to serve as APCs. γδ T-APCs were incubated with different 10 mg/ml lysate prepared from tdTomato/M1-expressing CSC-like cells, 0.5 mg/ml BSA-DQ (Molecular Probes), or both, either at 4°C or 37°C for 4-5 hours. Pulsed γδ T-APCs were stained with Live/dead Aqua followed by fluorochrome-conjugated antibodies against CD3 and Vγ9, and analysed by flow cytometry.

2.6.5. Antigen cross-presentation assay

Expanded γδ T cells from $HLA\text{-}A2^+$ or $HLA\text{-}A2^-$ donors were cultured overnight with 0.01, 0.1 or 1 μM recombinant Flu M1 protein of Influenza A virus (A/goose/Guangdong/1/1996(H5N1)), which was kindly provided by Andrew Thomas in the laboratory, to serve as APCs. Antigen-treated γδ T-APCs were then washed extensively to remove unbound protein and co-cultured for 5 hours with HLA-A2 restricted, Flu M1 p58-66 specific $CD8^+$ αβ T cell lines at an APC:responder ratio of 1:1, in the presence of 5 μg/ml brefeldin A. Intracellular expression of IFN-γ by $CD8^+$ T cell responders was assessed by flow cytometry.

2.7. Generation of lentiviral vectors expressing tdTomato and Flu M1

2.7.1. Lentiviral vectors and cloning strategies

The lentiviral packaging, envelop and transfer plasmids used in this study are listed in Table 2.2. The lentiviral transfer vector, pELNSxv, was kindly provided by Dr. James Riley (University of Pennsylvania, PA) and used as backbone for the constructs expressing tdTomato together with firefly luciferase, *Gaussia* luciferase or Flu M1 through a T2A-regulated bi-cistronic expressing system. The tdTomato-T2A-firefly luciferase (ffluc) and tdTomato-T2A-*Gaussia* luciferase (Gluc) cassettes were individually cloned into the pELNSxv transfer vector by Dr. John Bridgeman (Cardiff University). Flu M1 of Influenza A virus (A/Puerto Rico/8/34(H1N1)) was then cloned out from pMA_MPT_MATRX_PROTEIN kindly provided by Dr. Mai Ping Tan at Cardiff University, and subsequently put into pELNSxv transfer vector by substituting ffluc from pELNSxv-tdTomato-T2A-ffluc plasmids through a traditional cloning strategy as described in following sections. Although the M1 gene used for this construct was derived from a different strain of Influenza A virus as the recombinant Flu M1 protein used in APC assay, the antigenic peptide region (GILGFVFTL) of M1 proteins is identical in these two strains. The cloning strategy and the sequence of the final tdTomato-T2A-M1 construct are illustrated in Figure 2.4.

Table 2.2. Lentiviral plasmids used in this study

Plasmid	Type	Products	Reference
pELNSxv	Transfer	• tdTomato-T2A-ffluc • tdTomato-T2A-Gluc • tdToamto-T2A-M1	
pMDLg/pRRE	Packaging	Gag and Pol	(Dull *et al.*, 1998)
pRSV-REV	Packaging	Rev	(Dull *et al.*, 1998)
pCMV-VSVG	Envelope	VSVG	(Dull *et al.*, 1998)

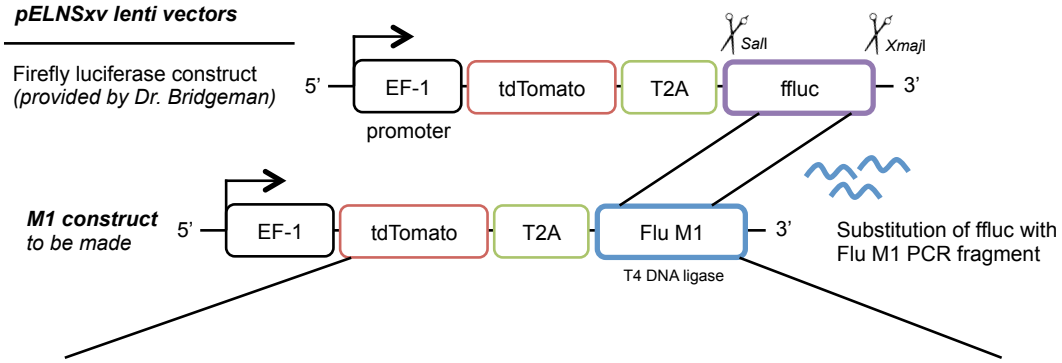

5'-ATGGTGAGCAAGGGCGAGGAGGTCATCAAAGAGTTCATGCGCTTCAAGGTGCGCATGGAGGGCTCCATGAACGGCC
ACGAGTTCGAGATCGAGGGCGAGGGCGAGGGCCGCCCCTACGAGGGCACCCAGACCGCCAAGCTGAAGGTGACCAAGG
GCGGCCCCCTGCCCTTCGCCTGGGACATCCTGTCCCCCCAGTTCATGTACGGCTCCAAGGCGTACGTGAAGCACCCCGCCG
ACATCCCCGATTACAAGAAGCTGTCCTTCCCCGAGGGCTTCAAGTGGGAGCGCGTGATGAACTTCGAGGACGGCGGTCTG
GTGACCGTGACCCAGGACTCCTCCCTGCAGGACGGCACGCTGATCTACAAGGTGAAGATGCGCGGCACCAACTTCCCCCC
CGACGGCCCCGTAATGCAGAAGAAGACCATGGGCTGGGAGGCCTCCACCGAGCGCCTGTACCCCCGCGACGGCGTGCTG
AAGGGCGAGATCCACCAGGCCCTGAAGCTGAAGGACGGCGGCCACTACCTGGTGGAGTTCAAGACCATCTACATGGCCA
AGAAGCCCGTGCAACTGCCCGGCTACTACTACGTGGACACCAAGCTGGACATCACCTCCCACAACGAGGACTACACCATC
GTGGAACAGTACGAGCGCTCCGAGGGCCGCCACCACCTGTTCCTGGGGCATGGCACCGGCAGCACCGGCAGCGGCAGCT
CCGGCACCGCCTCCTCCGAGGACAACAACATGGCCGTCATCAAAGAGTTCATGCGCTTCAAGGTGCGCATGGAGGGCTCC
ATGAACGGCCACGAGTTCGAGATCGAGGGCGAGGGCGAGGGCCGCCCCTACGAGGGCACCCAGACCGCCAAGCTGAAG
GTGACCAAGGGCGGCCCCCTGCCCTTCGCCTGGGACATCCTGTCCCCCCAGTTCATGTACGGCTCCAAGGCGTACGTGAA
GCACCCCGCCGACATCCCCGATTACAAGAAGCTGTCCTTCCCCGAGGGCTTCAAGTGGGAGCGCGTGATGAACTTCGAGG
ACGGCGGTCTGGTGACCGTGACCCAGGACTCCTCCCTGCAGGACGGCACGCTGATCTACAAGGTGAAGATGCGCGGCAC
CAACTTCCCCCCCGACGGCCCCGTAATGCAGAAGAAGACCATGGGCTGGGAGGCCTCCACCGAGCGCCTGTACCCCCGCG
ACGGCGTGCTGAAGGGCGAGATCCACCAGGCCCTGAAGCTGAAGGACGGCGGCCGCTACCTGGTGGAGTTCAAGACCAT
CTACATGGCCAAGAAGCCCGTGCAACTGCCCGGCTACTACTACGTGGACACCAAGCTGGACATCACCTCCCACAACGAGG
ACTACACCATCGTGGAACAGTACGAGCGCTCCGAGGGCCGCCACCACCTGTTCCTGTACGGCATGGACGAGCTGTACAAG
AGATCTGGCAGCGGAGAGGGCAGAGGAAGTCTTCTAACATGCGGTGACGTGGAGGAGAATCCCGGCCCTAGGATGAGC
CTGCTGACCGAGGTGGAGACATACGTGCTGAGCATCATCCCCAGCGGCCCTCTGAAGGCCGAGATCGCCCAGCGGCTGG
AAGATGTGTTCGCCGGCAAGAACACCGACCTGGAAGTGCTGATGGAATGGCTGAAAACCCGGCCCATCCTGAGCCCTCTG
ACTAAGGGGATTTTAGGATTTGTGTTCACGCTCACCGTGCCCTCTGAGCGGGGCCTGCAGCGGAGAAGATTCGTGCAGAA
CGCCCTGAACGGCAACGGCGACCCCAACAACATGGACAAGGCCGTGAAGCTGTACCGGAAGCTGAAGCGGGAGATCAC
CTTCCACGGCGCCAAAGAGATCAGCCTGAGCTACTCTGCCGGCGCTCTGGCCAGCTGCATGGGCCTGATCTACAACCGGA
TGGGCGCCGTGACCACAGAGGTGGCCTTTGGCCTGGTGTGCGCCACATGCGAGCAGATCGCCGACAGCCAGCACCGGTC
CCACAGACAGATGGTGACCACCACCAACCCCCTGATCCGGCACGAGAACCGGATGGTGCTGGCTTCTACCACAGCCAAGG
CCATGGAACAGATGGCCGGCAGCAGCGAACAGGCCGCCGAAGCCATGGAAGTGGCCAGCCAGGCCAGGCAGATGGTGC
AGGCCATGCGGACCATCGGCACCCACCCTAGCAGCAGCGCCGGACTGAAGAACGACCTGCTGGAAAATTTGCAGGCCTA
CCAGAAACGGATGGGCGTGCAGATGCAGCGGTTCAAGTGA-3'

Figure 2.4. Generation of pELNSxv-tdTomato-M1 lentiviral transfer vector. The pELNSxv-tdTomato-T2A-M1 lentiviral transfer vector was constructed by substituting the firefly luciferase (ffluc) gene fragment of pELNSxv-tdTomato-ffluc (constructed by Dr. John Bridgeman) with M1 gene fragment cloned out from the pMA_MPT_MATRX_PROTEIN plasmid (provided by Dr. Mai Ping Tan) by PCR. Both pELNSXv-tdTomato-T2A backbones and M1 PCR fragments were firstly trimmed by restriction enzymes *Sal*I and *Xmaj*I for the following ligation reaction with T4 DNA ligase. As illustrated, the sequence of the final tdTomato-T2A-M1 construct is shown with tdTomato marked in red, T2A in green and M1 in blue.

2.7.2. PCR amplification of M1 gene fragment

PCR reactions were carried out using Phusion High-Fidelity PCR Kit (NEB) according to the manufacturer's instruction with customised primers (Eurofins) for the specific amplification of M1 cDNA from pMA_MPT_MATRX_PROTEIN. The primers were originally designed to amplify M1 fragments to allow both for infusion reactions with an appropriate plasmid backbone and for traditional enzymatic restriction and ligation using sticky ends. The sequences of both forward and reverse primers are listed below, with the enzymatic restriction sites (*Xamj*I in forward primer and *Sal*I in reverse primer) marked in blue.

Forward: GAATCCCGGCCCTAGGATGAGCCTGCTGACCGAGGT

Reverse: GAGGTTGATTGTCGACTCACTTGAACCGCTGCATCT

PCR reactions were carried out for 30 cycles as followed:

- Initial denaturation: 98°C for 30 seconds
- Denaturation: 98°C for 10 seconds
- Annealing: 60°C for 30 seconds
- Extension: 72°C for 30 seconds
- Final extension: 72°C for 10 minutes

The final PCR product with a size of 791 bps was separated from the PCR reaction by gel electrophoresis and extracted using the NucleoSpin Gel and PCR Clean-up kit (Macherey-Nagel) according to the manufacturer's instructions. The purified M1 inserts were then examined quantitatively and qualitatively using a NanoDrop ND1000 (Thermo Scientific) for DNA concentration and purity (ratios of OD at wavelength of 230, 260 and 280 nm).

2.7.3. Digestion of M1 gene fragments and ligation into pELNSxv

The purified M1 inserts and pELNSxv-tdToamto-T2A-ffluc plasmids were digested by FastDigest *Sal*I and *Xmaj*I (Life Technologies) in Green buffer (Life Technologies) at 37°C for 40 minutes. The digested products were then separated from unwanted fragments in the reaction mixtures by gel electrophoresis and extracted from the gel using the NucleoSpin Gel and PCR Clean-up kit. The purified M1 inserts and vector backbones

were examined quantitatively and qualitatively using a NanoDrop ND1000. Ligation reactions were performed by incubating 200 ng of the *Sal*I/*Xmaj*I-digested pELNSxv-tdTomato-T2A vector with *Sal*I/*Xmaj*I-digested M1 inserts at vector:insert molecule ratios of 1:5 and 1:10 in the presence of T4 DNA ligase (NEB) overnight at 16°C.

2.7.4. Transformation and identification of positive clones

The product of the ligation reaction was used for transformation of XL10-Gold Ultracompetent Cells (Agilent Technologies) by heat shock. Briefly, the ligated product was added into 100 μl XL10-Gold Ultracompetent Cells and incubated on ice for 1 hour. The plasmid/competent cell mixture was then placed on a heat block for 45 seconds at 42°C followed immediately by a 5-minute recovery on ice. After the recovery, 200 μl SOC medium (Invitrogen) were added and the mixture was cultured in an Orbi-Safe New Orbit incubator (Sanyo) at 37°C for 1 hour with shaking at a speed of 220 rpm. The bacterial cell culture was then spread and grown on a LB plate supplemented with 100 μg/ml carbenicillin for the selection of transformed cells at 37°C for overnight.

Resulting colonies were picked and cultured overnight at 37°C in 5 ml LB broth supplemented with 100 μg/ml carbenicillin. 3 ml bacterial cultures were then sampled for preparation of plasmids using the Zyppy™ Plasmid Miniprep Kit (Zymo Research) according to the manufacturer's instructions. The purified plasmids were examined by NanoDrop ND1000 for their DNA concentration and quality. To check if the M1 insert incorporated correctly into the vector, the purified plasmids were digested by FastDigest *Sal*I and *Xba*I (Life Technologies) in Green buffer (Life Technologies) for 20 minutes at 37°C and analysed by gel electrophoresis.

2.7.5. DNA sequencing of construct region

The plasmids of five positive clones that passed the selection procedures described above were sequenced at the M1 region to make sure the construct was correct without any point mutation. Plasmids of each clone were sequenced starting from each end of the M1 gene with the forward or reverse primers used for the PCR reaction to make sure the sequence of M1 at the primer binding regions were correct. The plasmids were mixed with 2 pM

forward or reverse primers and sent to Eurofins for sequencing. The resulting sequences were analysed by using CLC Genomics Workbench 5 (CLC Bio).

2.7.6. Maxi-prep of plasmids

250 µl bacterial culture of a positive clone with correct sequence being confirmed were expanded in 250 ml LB broth (MP Biomedicals) supplemented with 100 µg/ml carbenicillin (Sigma) at 37°C for overnight at a shaking speed of 220 rpm. Plasmids were extracted from bacterial cultures using the PureLink HiPure Plasmid Filter Maxiprep Kit (Invitrogen) according to the manufacturer's instructions. The purified pELNSxv-tdTomato-T2A-M1 plasmids were examined by NanoDrop ND1000 for DNA concentration and quality and stored at −20°C for later use.

2.7.7. Packaging of lentiviral particles

For the production of lentiviral particles containing pELNSxv-tdToamto-T2A-M1 or pELNSxv-tdToamto-T2A-Gluc vectors, 293T cells were seeded overnight in T175 flasks at a density of 15-20 × 10^6 cells/flask before transient transfection with lentiviral packaging, envelop and transfer plasmids (Table 2.2) by $CaCl_2$ precipitation. All four lentiviral plasmids – 15 µg pELNSxv containing genes of interest, 18 µg pMDLg/pRRE, 18 µg pRSV-PEV and 7 µg pCMV-VSVg – were mixed evenly with 50 µM $CaCl_2$ in 3ml DMEM supplemented with 10 mM HEPES (pH adjusted to 7.1) for 30 minutes. The spent medium of the 293T culture was replaced with 12 ml fresh DMEM medium supplemented with 10% FCS and 10 mM HEPES (pH 7.9) before the plasmid mixtures were added. The 293T cells were cultured overnight at 37°C, before replacing the medium with fresh complete DMEM medium. Lentiviral particles were collected 48 hours and 72 hours post-transfection, and pooled. All collected lentiviral particles were then spun at 1200 rpm for 5 minutes to remove debris of 293T cells, clear supernatants containing lentiviral particles were passed through 0.45 µm filters. The filtered supernatants with lentiviral particles were centrifuged in polyallomer tubes at a speed of 26,000 × *g* for 2 hours at 4°C using an Optima™ L-100 XP Ultracentrifuge (Beckman Coulter) with SW28 rotor and corresponding buckets. The pellets of lentiviral particles were resuspended in 1 ml complete RPMI and stored at −80°C.

2.7.8. Infection of CSC-like cells and non-CSCs with lentiviral particles

For the transfection with lentiviral particles, CSC-like cells and non-CSCs were seeded overnight into 24-well plate at a density of 1×10^5 cells/well. The lentiviral suspension was mixed with fresh complete HMLER medium at a 1:1 ratio. Polybrene was then added into lentiviral supernatant at a final concentration of 4 μg/ml. The spent HMLER medium in cultures of CSC-like cells and non-CSCs was then replaced by the lentiviral particle and polybrene mixture, and the cells were incubated overnight at 37°C. On the next day, 500 ml fresh HMLER medium were added to the cell cultures, and the cells were eventually harvested 48 hours post-infection and analysed by flow cytometry.

2.7.9. Identification and selection of transduced CSC-like cells and non-CSCs

Transduced cells with the highest expression levels of tdTomato upon transfection with lentiviral particles were sorted using a FACS Aria III cell sorter (BD Biosciences) to purities >98%, based on their tdTomato expression. The sorted cells were regularly monitored throughout passages to ensure the stability of the tdTomato expression, their CD44/CD24 expression profiles and their general morphology.

Sorted M1-expressing CSC-like cells and non-CSCs were assessed for their M1 expression by intracellular staining using purified mouse anti-M1 mAbs (clone GA2B, Abcam) followed by FITC-conjugated goat anti-mouse IgG secondary Abs (DAKO).

Gluc-expressing CSC-like cells and non-CSCs were lysed by 5 freeze/thaw cycles using liquid nitrogen and a 37°C water bath. Expression of *Gaussia* luciferase in the cell protein lysate was examined using the Biolux™ *Gaussia* Luciferase Assay Kit (NEB) according to the manufacturer's instruction. Optical densities were measured on a Dynex MRX II reader (Dynex Technologies).

2.8. Establishment of breast cancer model in immunodeficient mice

2.8.1. Tumour development induced by CSC-like cells and non-CSCs in NSG mice

Transduced CSC-like cells and non-CSCs co-expressing Flu M1 and tdTomato were resuspended in a 1:1 mixture of DMEM/F12 medium and Matrigel Matrix to doses of 2×10^6 and 10^3 cells/100 µl. The cell suspensions were xenotransplanted *s.c.* into the mammary fat pads of 6-8 week old NSG mice (Charles River), with each group consisting of 6 mice. Tumour growth was monitored by weekly live imaging of tdTomato using a Kodak Fx-Pro imager (Kodak) and by biweekly caliper measurements of the tumour size, for up to 182 days after injection. The volume of palpable tumour nodules was calculated using the formula, tumour volume (mm^3) = $0.52 \times a \times b^2$, where a is the major tumour diameter (in mm) and b is the minor diameter perpendicular to the major one (in mm) (O'Reilly *et al.*, 1997). Fluorescence signals were analysed using the Carestream Molecular Imaging software (Carestream Health, Inc.). Animals were sacrificed when the tumours reached 1000 mm^3, in accordance with Home Office regulations (PPL 30/2891 and PIL 30/9936). The tumours and organs (draining and non-draining lymph nodes, liver, lung, brain) were taken out and imaged separately using the Kodak Fx-Pro to detect micro-metastases. The harvested tumours were cut into three pieces with two each being preserved in 4% paraformaldehyde (Fisher) or OCT embedding matrix (CellPath), respectively, for histological analyses, and one piece dissociated immediately into single cell suspensions for immunophenotyping by flow cytometry. The remaining dissociated cell suspensions from each tumour were aliquoted and frozen in liquid nitrogen.

2.8.2. Cross-presentation of Flu M1 antigen by γδ T-APCs in tumour-bearing NSG mice

Transduced CSC-like cells co-expressing tdTomato with either Flu M1 or Gluc were xenotransplanted into the mammary fat pads of 6-8 week old NSG mice (Charles River) at a dose of 2×10^6 cells/mouse with Matrigel. Tumour growth was monitored by live imaging and caliper measurements, and the resulting tumours were used as targets for γδ T-APCs when their diameter reached 0.5 cm (around 65 mm^3). The tumours were sensitised by intravenous (*i.v.*) injection with 1 mg/kg zoledronate or with saline as control (kindly performed by Dr. Garry Dolton), and 24 hours later 5×10^6 expanded γδ T-APCs (suspended in 50 µl saline) were injected directly into the tumours. 18-20 hours after the

injection with γδ T-APCs, the tumours were harvested and dissociated into single cell suspensions by cutting thoroughly with a scalpel and careful passing through 0.7 μm and 0.4 μm cell strainers using the rubber plunge of a syringe. The resulting single cell suspensions were then stained using the Live/dead Aqua dead cell stain kit, followed by surface staining of CD3 and Vγ9 TCR. Live γδ T-APCs were analysed for their expression of tdTomato by flow cytometry, or isolated by BD FACS Aria III cell sorter for functional assays. Sorted γδ T-APCs were then co-cultured with M1-specific $CD8^+$ responder T cells in the presence of brefeldin A for 5 hours. After the co-culture, the cells were stained with Live/dead Aqua and stained for surface expression of CD3, Vγ9 TCR and $CD8^+$; and intracellularly for IFN-γ. Antigen cross-presentation assays using *in vitro* generated γδ T-APCs (see section 2.6.5) were performed in parallel as internal controls for these *ex vivo* experiments.

2.9. Statistical analysis

Statistical analysis was carried out by the use of GraphPad Prism 6 software (GraphPad Software, Inc., CA, USA). Column statistics were performed at the first place to check the distribution of each data set and to determine whether datasets were parametric or non-parametric. Student's *t* test (parametric data), Mann-Whitney U test (non-parametric data) and Wilcoxon matched-pairs signed rank test (paired non-parametric data) were used to compare two variables, whereas ordinary one-way ANOVA and RM one-way ANOVA were performed for the comparison of multiple variables within the parametric and non-parametric data sets, respectively. Two-way ANOVA was performed to compare multiple variables within two different groups. Cumulative survival curves were generated using the Kaplan-Meier approach. Descriptive statistics are expressed as means ± standard deviation of the mean (SD) in all figures. All statistical tests were performed as two-tailed tests, and the resulting statistical significances of difference indicated in the figures and tables as *, $p < 0.05$; **, $p < 0.01$; ***, $p < 0.001$.

Chapter 3. Functional and Phenotypical Characterisation of Breast Cancer Stem-like Cells

3.1. Introduction

Cancer stem cells (CSCs) comprise a minor cell population responsible for the initiation and relapse of tumours due to (*i*) their potential to self-renew and differentiate (Reya *et al.*, 2001; Pardal *et al.*, 2003), (*ii*) their resistance to chemotherapy (Dean *et al.*, 2005) and radiation (Rich, 2007), and (*iii*) their ability to escape from immunosurveillance (Schatton *et al.*, 2010a). In this study, I aimed to develop an appropriate experimental model for the investigation of therapeutic strategies targeting CSCs efficiently and specifically *in vitro* and *in vivo* by harnessing γδ T cells with or without prior sensitisation or adjuvants. To achieve this aim, I first sought to establish a well-defined cellular model, which allows a reliable phenotypical distinction of CSC-like cells and non-CSCs. This work took advantage of a well-established cell line originally described by Prof. Robert Weinberg's laboratory at the Whitehead Institute for Biomedical Research, Cambridge, MA.

To study how mammary epithelial cells transform and become malignant during carcinogenesis of breast cancer, the Weinberg laboratory isolated primary human mammary epithelial (HMLE) cells from a patient undergoing breast reduction surgery and immortalised these cells by transduction with human telomerase reverse transcriptase (hTERT) and co-expression of simian virus 40 (SV40) large T (LT) and small T (ST) antigens, which inhibit the p53 and retinoblastoma protein (pRB) signalling pathways (Elenbaas *et al.*, 2001). The tumourigenicity of HMLE cells in immunodeficient mice was very limited but could be enhanced by additional transformation with an oncogenic H-RasV12 mutant (Elenbaas *et al.*, 2001). Although being artificially generated, this experimental model allowed to study the malignant transformation of residual mammary stem cells originally sat within the isolated mammary epithelial cells after *ras* transformation. CSCs were firstly identified and isolated in breast cancer with a $CD44^{hi}$ $CD24^{-/lo}$ ESA^{+} phenotype while lacking lineage markers (lin^{-}) (Al-Hajj *et al.*, 2003). Of note, both non-tumourigenic HMLE and tumourigenic HMLER cells constitute an intra-tumour heterogeneity with a predominantly $CD44^{lo}$ $CD24^{hi}$ phenotype and features of differentiated cells, and a minor but stable and distinct population of $CD44^{hi}$ $CD24^{lo}$ cells with putative CSC-like nature that typically comprises 0.4-2% of all cells when cultured under normal adherent conditions (Mani *et al.*, 2008). Interestingly, induction of epithelial-to-mesenchymal transition (EMT) by treatment with TGF-β (Mani *et al.*, 2008;

Morel *et al.*, 2008) or by over-expressing the transcription factors snail, twist (Mani *et al.*, 2008) or slug alone or in combination with FoxC2 (Hollier *et al.*, 2013) trigger a phenotypic and morphological change from a $CD44^{lo}$ $CD24^{hi}$ epithelial-like phenotype to a $CD44^{hi}$ $CD24^{lo}$ mesenchymal-like phenotype concomitantly with the acquisition of CSC-like properties. The tight link between EMT and stemness led to a conceptual hypothesis that the induction of EMT by environmental cues, *e.g.* by oxidative stress, growth factors and cytokines, may elicit disease progression and metastasis (May *et al.*, 2011; Velasco-Velazquez *et al.*, 2011; Tsai and Yang, 2013). The acquisition of enhanced mobility and invasiveness upon EMT could contribute to the systemic dissemination of malignant cells that enter from the primary tumour site into the vasculature and later extravasate from the circulation to distant sites. Thus, the generation of an easy-to-use and reliable CSC-like model derived from HMLER cells might allow investigations into the control of tumour progression at different disease stages by immune cells.

In this chapter, I aimed to establish a cellular CSC-like model by sorting $CD44^{lo}$ $CD24^{hi}$ and $CD44^{hi}$ $CD24^{lo}$ cells from the original HMLER cell line. The isolated $CD44^{lo}$ $CD24^{hi}$ and $CD44^{hi}$ $CD24^{lo}$ cells were characterised (*i*) for their long-term stability in cell culture; (*ii*) phenotypically for their expression of CSC-associated and EMT markers; (*iii*) morphologically for their epithelial- or mesenchymal- like appearance under different culture conditions; (*iv*) functionally for their self-renewal and plasticity *in vitro* using a mammosphere formation assay (Dontu and Wicha, 2005; Liao *et al.*, 2007); and (*v*) for their ability to initiate heterogeneous tumours in immunodeficient mice *in vivo*. In addition, HMLER-derived CSC-like cells and non-CSCs were further transformed to express luciferase and/or tdTomato fluorescent reporters (Winnard *et al.*, 2006) in order to facilitate *in vivo* imaging for future adoptive transfer studies using human T cells.

3.2. Aim

- To validate and establish a cellular model, which mimics most features typically associated with CSCs, and which can be manipulated easily both *in vitro* and *in vivo*, to study their interaction with human T cells.

3.3. Phenotypical and functional characterisation of $CD44^{hi}/CD24^{lo}$ and $CD44^{lo}/CD24^{hi}$ HMLER cells

3.3.1. Characterisation of HMLER subpopulations with differential expression of classical CSC markers

A panel of well-characterised CSC-associated markers including CD44 and CD24 (Al-Hajj *et al.*, 2003; Mani *et al.*, 2008) and GD2 (Battula *et al.*, 2012) was used to characterise the parental HMLER cell line by flow cytometry. Figure 3.1 shows that the HMLER cell line comprises two distinct cell subpopulations, with the majority (~99%) displaying a $CD44^{lo}/CD24^{hi}$ phenotype and the remainder (~1%) a $CD44^{hi}/CD24^{lo}$ phenotype (Figure 3.1). Expression of GD2 was restricted to cells with a $CD44^{hi}/CD24^{lo}$ phenotype and was absent on cells with a $CD44^{lo}/CD24^{hi}$ phenotype (Figure 3.1). To further dissect the nature of these two $CD44^{lo}/CD24^{hi}$ and $CD44^{hi}/CD24^{lo}$ cell populations, a series of *in vitro* functional analyses was performed, as described in the following sections.

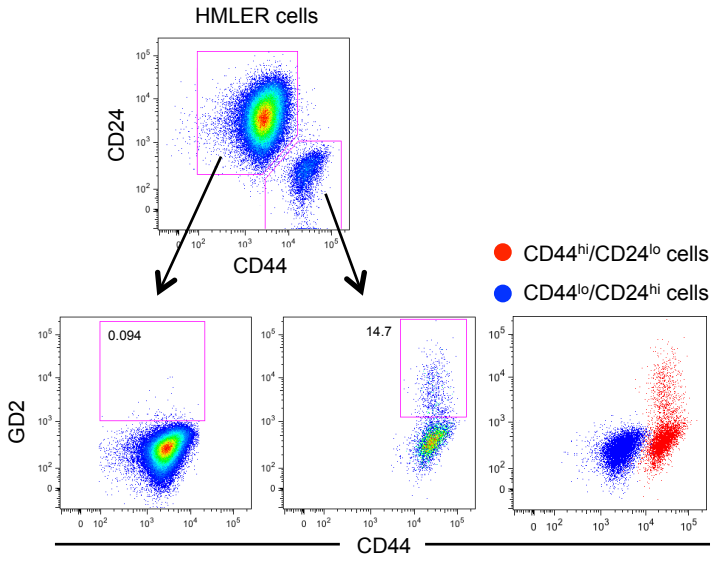

Figure 3.1. Expression of CSC markers by HMLER cells cultured under normal, adherent conditions. HMLER cells were examined for their expression of CD44, CD24 and GD2 by flow cytometry analysis.

3.3.2. Enrichment of $CD44^{hi}/CD24^{lo}$ cells in mammosphere cultures

Mammosphere culture has been well established and widely used as surrogate assay to examine the self-renewal of breast cancer cells (Dontu and Wicha, 2005; Liao *et al.*, 2007). To define the actual self-renewing cell population within the parental HMLER cell line, we cultured the cells in an anchorage-independent manner in mammosphere medium in the absence of FCS. After seven days, mammospheres were collected and dissociated into single cell suspensions and stained for CD44 and CD24 expression on the cell surface. Under these culture conditions, the $CD44^{hi}/CD24^{lo}$ cell population was significantly enriched, increasing from 0.4-2% of total live cells within parental HMLER cells to 20-50% after primary culture under mammosphere-forming conditions, and to > 70% after secondary culture (Figure 3.2). Accordingly, the proportion of $CD44^{lo}/CD24^{hi}$ cells within HMLER cells dropped significantly along extended passages under mammosphere-forming conditions. Of note, a population of cells with an unusual $CD44^{hi}/CD24^{hi}$ phenotype emerged in mammosphere cultures. Whether this population was in transition (differentiation or de-differentiation) between $CD44^{hi}/CD24^{lo}$ and $CD44^{lo}/CD24^{hi}$ cells is currently unknown. The origin of this population and the direction of cell transition both need further examination.

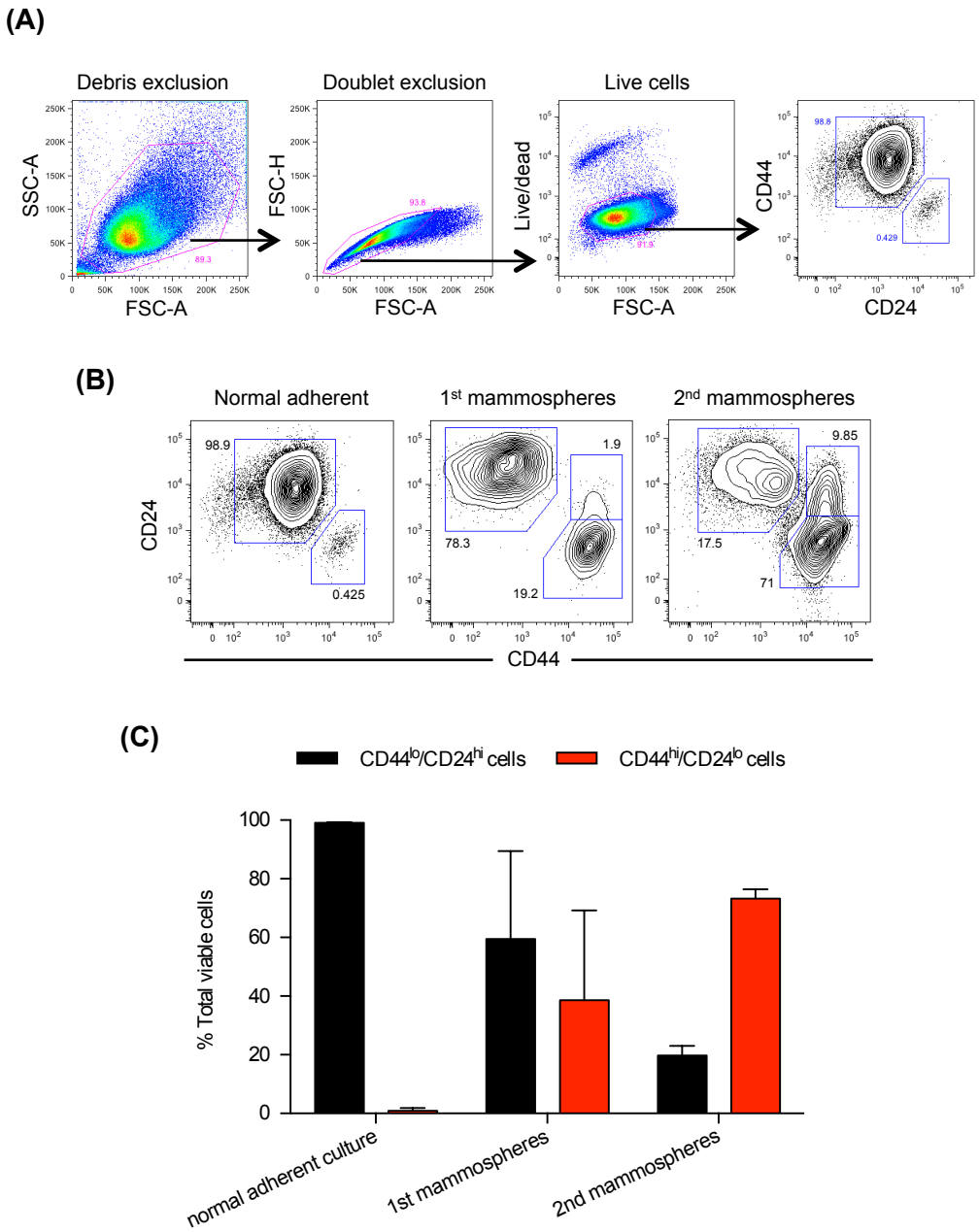

Figure 3.2. Enrichment of CD44^{hi}/CD24^{lo} HMLER cells cultured under mammosphere-forming conditions. HMLER cells maintained in normal adherent culture, or from primary or secondary mammosphere cultures were examined for the proportion of CD44^{hi}/CD24^{lo} and CD44^{lo}/CD24^{hi} cells. **(A)** For analysis, gates were sequentially set on intact, single and live cells. Representative FACS plots for the expression of CD44 and CD24 by HMLER cells under each culture condition are shown in **(B)**. Data collected from three independent cultures were shown as mean ± SD in **(C)**.

3.3.3. Survival and proliferation of CD44^{hi}/CD24^{lo} cells but not CD44^{lo}/CD24^{hi} cells in mammosphere cultures

To further dissect how CD44^{hi}/CD24^{lo} cells became enriched under mammosphere-forming conditions, the viability and proliferation of CD44^{hi}/CD24^{lo} and CD44^{lo}/CD24^{hi} cells were examined after seven days in culture.

CD44^{hi}/CD24^{lo} cells adapted well to mammosphere-forming conditions with no significant reduction of viability. In contrast, the viability of CD44^{lo}/CD24^{hi} cells dropped significantly from 96% under normal adherent conditions to 42% in mammosphere cultures (Figure 3.3).

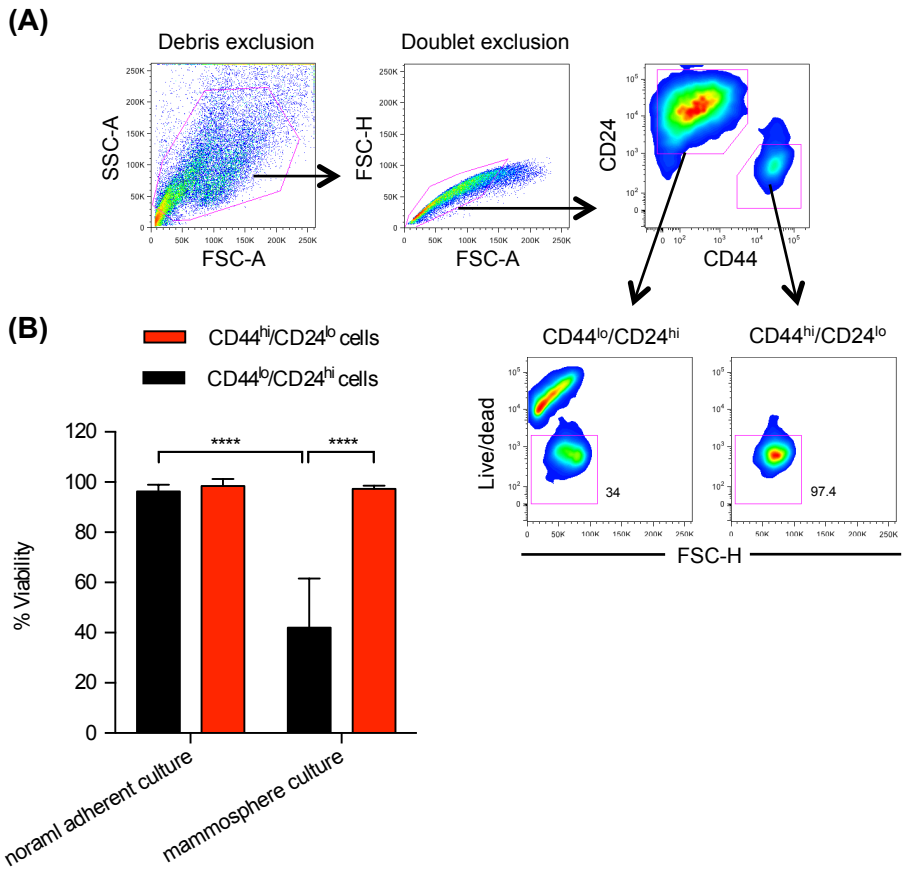

Figure 3.3. Differential viability of CD44^{hi}/CD24^{lo} cells and CD44^{lo}/CD24^{hi} cells in mammosphere cultures of HMLER cells. (A) For analysis, gates were sequentially set on intact and single cells. **(B)** Data are pooled from four independent experiments and are shown as mean ± SD. The significance of difference was analysed by Ordinary two-way ANOVA (****$p \leq 0.0001$).

Two complementary assays were carried out to identify the cell population(s) that actually proliferate and expand in mammosphere cultures. HMLER cells were labelled with CellVue to track the cell divisions of $CD44^{hi}/CD24^{lo}$ and $CD44^{lo}/CD24^{hi}$ cells. As shown in Figure 3.4A, $CD44^{hi}$ cells proliferated as confirmed by dilution of their surface labelling, whereas $CD44^{lo}$ cells did not proliferate and retained their original labelling. Staining for the cell proliferation markers Ki67 and phospho-histone H3 (pHH3) showed that in mammosphere culture only $CD44^{hi}/CD24^{lo}$ but not $CD44^{lo}/CD24^{hi}$ cells proliferated (Figure 3.4B).

These results show that within HMLER cells, only $CD44^{hi}/CD24^{lo}$ cells but not $CD44^{lo}/CD24^{hi}$ cells exhibit CSC-like properties including the capacity to self-renew and differentiate in an anchorage-independent manner.

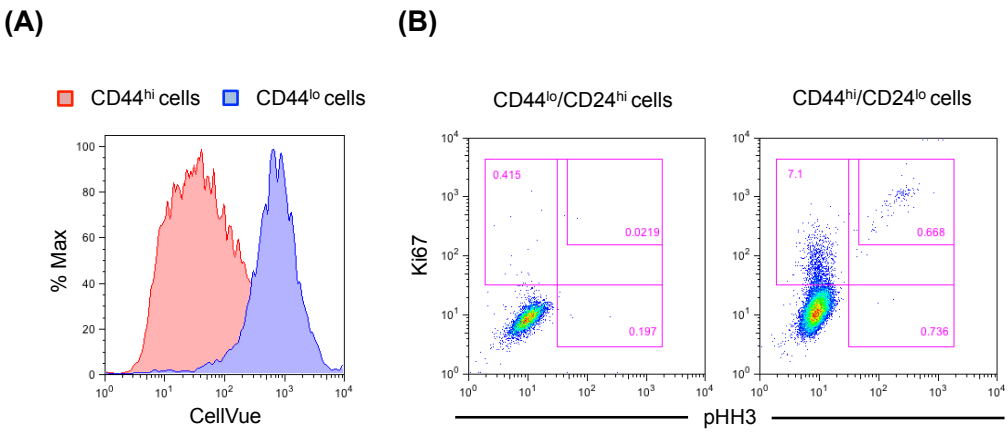

Figure 3.4. Proliferation of $CD44^{hi}/CD24^{lo}$ cells but not $CD44^{lo}/CD24^{hi}$ cells in mammosphere cultures of HMLER cells. The proliferation of $CD44^{hi}/CD24^{lo}$ and $CD44^{lo}/CD24^{hi}$ cells within HMLER cells maintained in normal adherent culture or from primary mammospheres were examined by (**A**) dilution of CellVue labelling and (**B**) Ki67 and pHH3 expression. Representative FACS plots of two independent experiments are shown.

3.4. Isolation and maintenance of $CD44^{hi}/CD24^{lo}$ and $CD44^{lo}/CD24^{hi}$ cells from the parental HMLER cell line

3.4.1. Phenotypical characteristics of CSC-like and non-CSC sublines

To investigate the nature of $CD44^{hi}/CD24^{lo}$ and $CD44^{lo}/CD24^{hi}$ cells within the HMLER cell line further, these two cell populations were purified by FACS (Figure 3.5A). In long-term culture under normal adherent conditions, both $CD44^{hi}/CD24^{lo}$ and $CD44^{lo}/CD24^{hi}$ cells stably retained their phenotype over at least 32 days (Figure 3.5B). However, a minor population of sorted $CD44^{hi}/CD24^{lo}$ CSC-like cells showed signs of CD24 up-regulation, giving rise to $CD44^{hi}/CD24^{+}$ cells as observed in mammosphere cultures. Similarly, long-term culture of $CD44^{lo}/CD24^{hi}$ non-CSCs revealed the presence of a minor contamination with $CD44^{hi}/CD24^{lo}$ CSC-like cells (~0.05%). In accordance with the expression profile of parental HMLER cell line (Figure 3.1), GD2 expression was restricted to sorted CSC-like cells and was not found on sorted non-CSCs (Figure 3.5C).

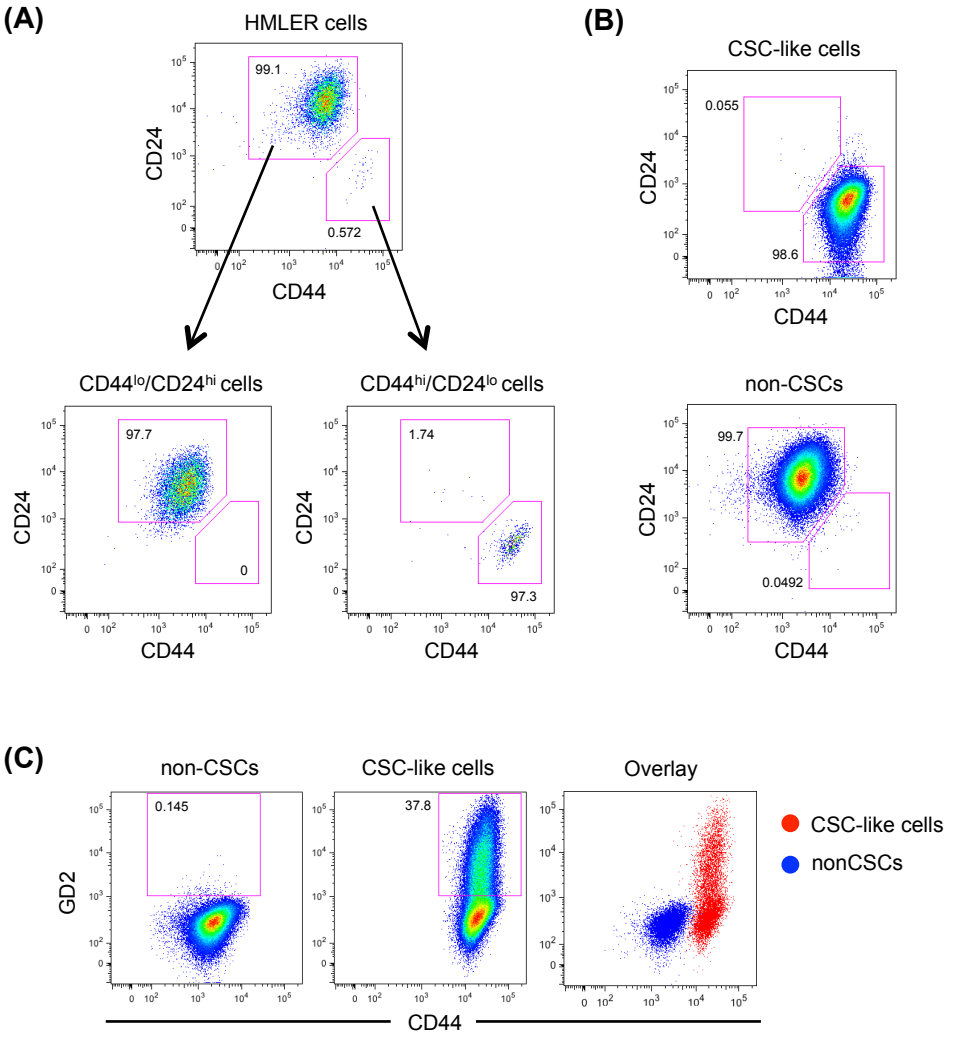

Figure 3.5. Isolation of CD44^{hi}/CD24^{lo} CSC-like cells and CD44^{lo}/CD24^{hi} non-CSCs from the parental HMLER cell line by FACS. HMLER cells were labelled with PE-Cy7-conjugated anti-CD44 mAbs and FITC-conjugated anti-CD24 mAbs and then sorted using a BD FACS Aria cell sorter. CD44/CD24 expression profiles of the sorted cell populations were determined **(A)** right after the sort and **(B)** after culturing them for 32 days under normal adherent culture conditions. **(C)** GD2 expression of both cell populations maintained in normal adherent culture as examined by flow cytometry

3.4.2. Morphological and epithelial-mesenchymal transition (EMT) characteristics of CSC and non-CSC sublines

Sorted $CD44^{hi}/CD24^{lo}$ and $CD44^{lo}/CD24^{hi}$ cells were cultured in normal HMLER medium or with mammosphere medium, which lack of FCS supplement, to examine their potential to differentiate *in vitro* depending on the culture conditions. As shown in Figure 3.6, sorted $CD44^{hi}/CD24^{lo}$ and $CD44^{lo}/CD24^{hi}$ cells exhibited distinct mesenchymal-like and epithelial-like morphologies, respectively, in adherent culture with normal HMLER medium. Surprisingly, neither $CD44^{hi}/CD24^{lo}$ nor $CD44^{lo}/CD24^{hi}$ cells showed signs of differentiation and maintained their characteristic morphology and CD44/CD24 phenotype stably over a period of at least 14 days (Figure 3.6) and up to 32 days (Figure 3.5B) in this culture condition. In contrast to the morphological and phenotypical stability of both cell populations in standard culture, sorted $CD44^{hi}/CD24^{lo}$ CSC-like cells gradually gave rise to a population with $CD44^{lo}/CD24^{hi}$ phenotype and formed epithelial-like patches when cultured in mammosphere medium. Strikingly, $CD44^{lo}/CD24^{hi}$ non-CSCs failed to expand and eventually died under these culture conditions.

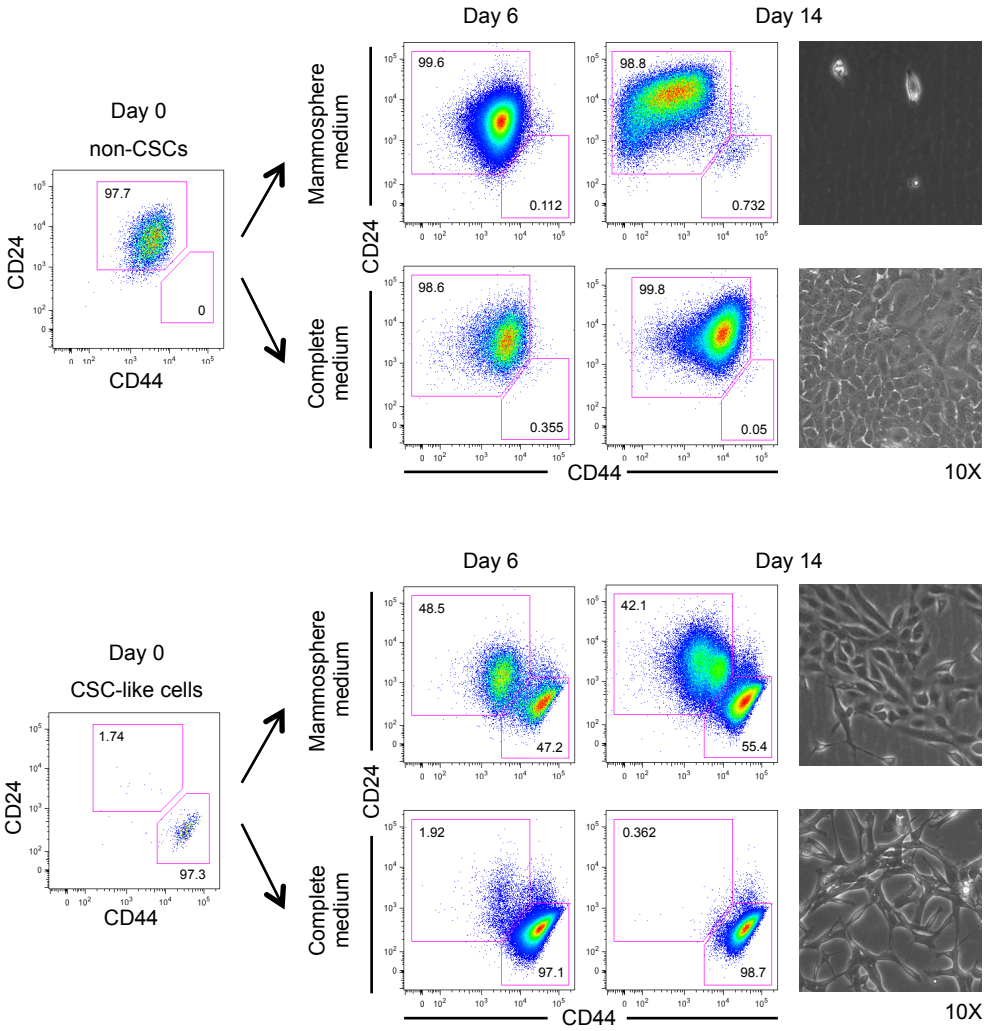

Figure 3.6. Differentiation of CD44^{hi}/CD24^{lo} CSC-like cells but not CD44^{lo}/CD24^{hi} non-CSCs dependent on the culture conditions. Sorted cells were maintained in adherent cultures with complete HMLER medium or with mammosphere culture medium for up to 14 days and examined by flow cytometry.

In the HMLE/HMLER model, induction of EMT triggers the acquisition of CSC-like properties (Mani *et al.*, 2008; Morel *et al.*, 2008; Hollier *et al.*, 2013). As sorted $CD44^{hi}/CD24^{lo}$ and $CD44^{lo}/CD24^{hi}$ cells exhibited distinct mesenchymal-like and epithelial-like morphologies in adherent culture, I next examined their expression of EMT-associated markers by immunofluorescence microscopy. As shown in Figure 3.7, CSC-like cells stained positively for the mesenchymal markers vimentin and (albeit less prominently) for fibronectin extra domain A (EDA fibronectin) while only a small fraction of non-CSCs expressed these markers. Although this small fraction of the non-CSCs was stained positive for these makers, these cells exhibited an epithelial-like morphology rather than mesenchymal-like morphology. Of note, there is about 0.05% contaminant $CD44^{hi}/CD24^{lo}$ cells sitting in the culture of non-CSCs. Thus, the possibility that these cells are actually contaminant residual $CD44^{hi}/CD24^{lo}$ cells with an epithelial-like morphology still cannot be excluded. For the expression of epithelial markers cytokeratin-14 (CK-14) as marker for basal/myoepithelial lineage and cytokeratin-18 (CK-18) as marker for luminal lineage, CSC-like cells showed no expression of CK-14 and only intermediate levels of CK-18, whereas non-CSCs expressed comparatively higher level of CK-14 and CK-18, suggesting a more differentiated states of non-CSCs. Both CSC-like and non-CSCs stained negative for N-cadherin and α-smooth muscle actin (α-SMA). In summary, the phenotype and morphology of non-CSCs is consistent with epithelial characteristics, whereas CSC-like cells shows signs of an incomplete EMT with predominantly mesenchymal characteristics.

These findings suggest that under certain culture condition without sufficient supply of nutrients and growth factors, differentiation could only be induced in $CD44^{hi}/CD24^{lo}$ but not in $CD44^{lo}/CD24^{hi}$ cells. Mammosphere forming assays were thus carried out to further functionally characterise the self-renewal and pluripotency of these two cell populations.

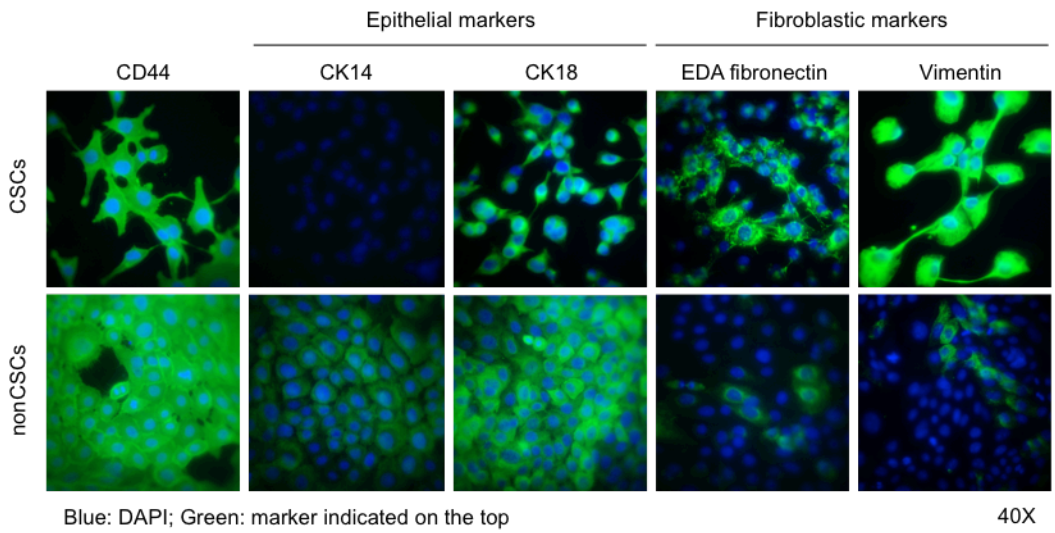

Figure 3.7. Expression of epithelial- and mesenchymal-associated markers by CD44^{hi}/CD24^{lo} CSC-like cells and CD44^{lo}/CD24^{hi} non-CSCs. The isolated CSC-like cells and non-CSCs were seeded on cover-slip chamber slides and labelled with purified antibodies against CD44, epithelial markers CK14 and CK18, and fibroblastic markers EDA fibronectin and vimentin. AF-488-conjugated secondary antibodies were used to visualise stained cells by fluorescent microscopy.

3.5. Functional characteristics of CSC-like and non-CSC sublines *in vitro*

3.5.1. Self-renewal of CSC-like and non-CSC sublines *in vitro*

The self-renewal capacity of CSC-like cells and non-CSCs was judged from their ability to survive and proliferate under mammosphere-forming conditions. As shown in Figure 3.8, CSC-like cells were far superior quantitatively and qualitatively in forming mammospheres as compared to their non-CSC counterparts. Quantitatively, CSC-like cells contained a greater number of mammosphere-forming cells as compared to non-CSCs, and this difference increased further upon passaging cells into secondary mammosphere cultures. Qualitatively, CSC-like cells consistently gave rise to substantial, round and compact mammospheres, whereas the mammospheres derived from non-CSCs were small and loose with aberrant shapes (deformity). Of note, mammospheres derived from sorted CSC-like cells were larger and better differentiated than mammospheres derived from the parental HMLER cell line, indicating that the mammosphere-forming potential of HMLER cells resides within the $CD44^{hi}/CD24^{lo}$ CSC-like subpopulation.

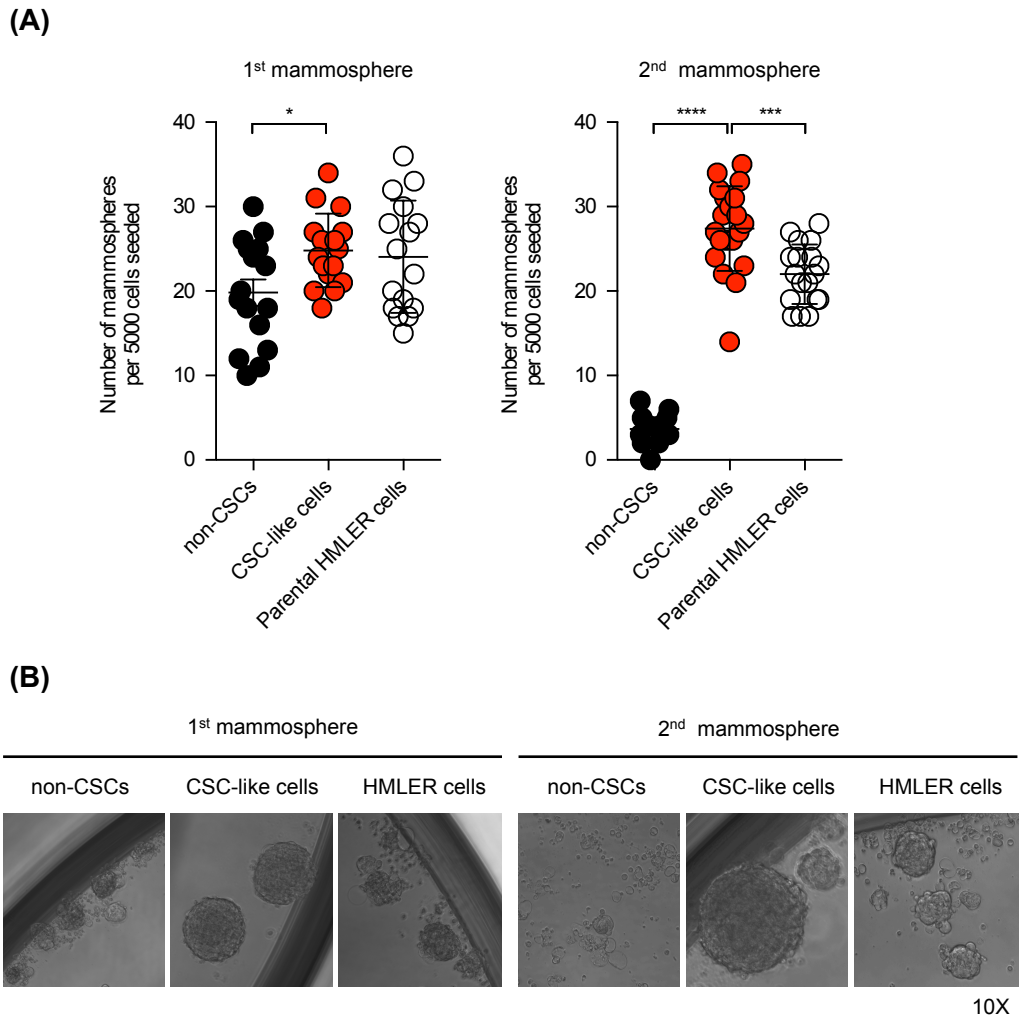

Figure 3.8. Self-renewal of CD44^{hi}/CD24^{lo} CSC-like cells and CD44^{lo}/CD24^{hi} non-CSCs. Sorted CSC-like cells and non-CSCs were seeded in ultralow-attachment 96-well plate at a density of 5000 cells/well in mammosphere medium for 7 days. **(A)** The mammospheres generated under these conditions were counted. **(B)** The results and pictures shown are representative for three independent experiments taken at a 10X magnification. Data are shown as mean ± SD and analysed with Ordinary one-way ANOVA (*$p \leq 0.05$; ***$p \leq 0.001$; ****$p \leq 0.0001$).

During repeated passaging of non-CSCs under mammosphere-forming conditions, the proportion of $CD44^{hi}/CD24^{lo}$ cells gradually increased (Figure 3.9). Further analysis showed that under these culture conditions, regardless of their origin from CSC-like cells of non-CSCs, only $CD44^{hi}/CD24^{lo}$ but not $CD44^{lo}/CD24^{hi}$ cells survived (Figure 3.10). This selective outgrowth of $CD44^{hi}/CD24^{lo}$ cells from non-CSC cultures is likely due to preferential survival and proliferation of minor contaminations of non-CSC with CSC-like cells due to insufficient purities from the cell sorting. However, this increase of $CD44^{hi}/CD24^{lo}$ cells may also reflect reversion/dedifferentiation of non-CSCs back to CSCs as a result of phenotypical plasticity, which needs further investigation with cell lineage tracking (Chaffer *et al.*, 2011). In contrast to non-CSCs, CSC-like cells were very stable in mammosphere culture and only gave rise to a very small population of $CD44^{lo}/CD24^{hi}$ cells, indicative of the potential of CSC-like cells to differentiate *in vitro* and give rise to non-CSCs. Moreover, only CSC-like cells but not non-CSCs proliferated and expanded in mammosphere culture during the two passages examined (Figure 3.11).

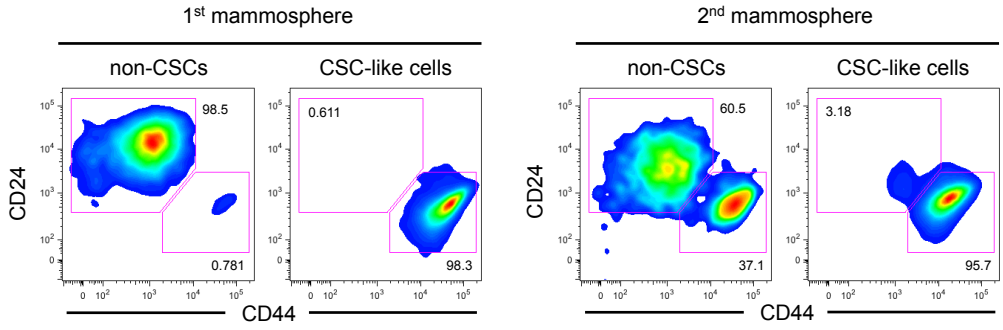

Figure 3.9. Distribution of $CD44^{hi}/CD24^{lo}$ and $CD44^{lo}/CD24^{hi}$ cells in mammosphere cultures of CSC-like cells and non-CSCs. Sorted CSC-like cells and non-CSCs were maintained in mammosphere culture over two passages, and their phenotype was examined by flow cytometry. . The results shown are representative for three independent experiments.

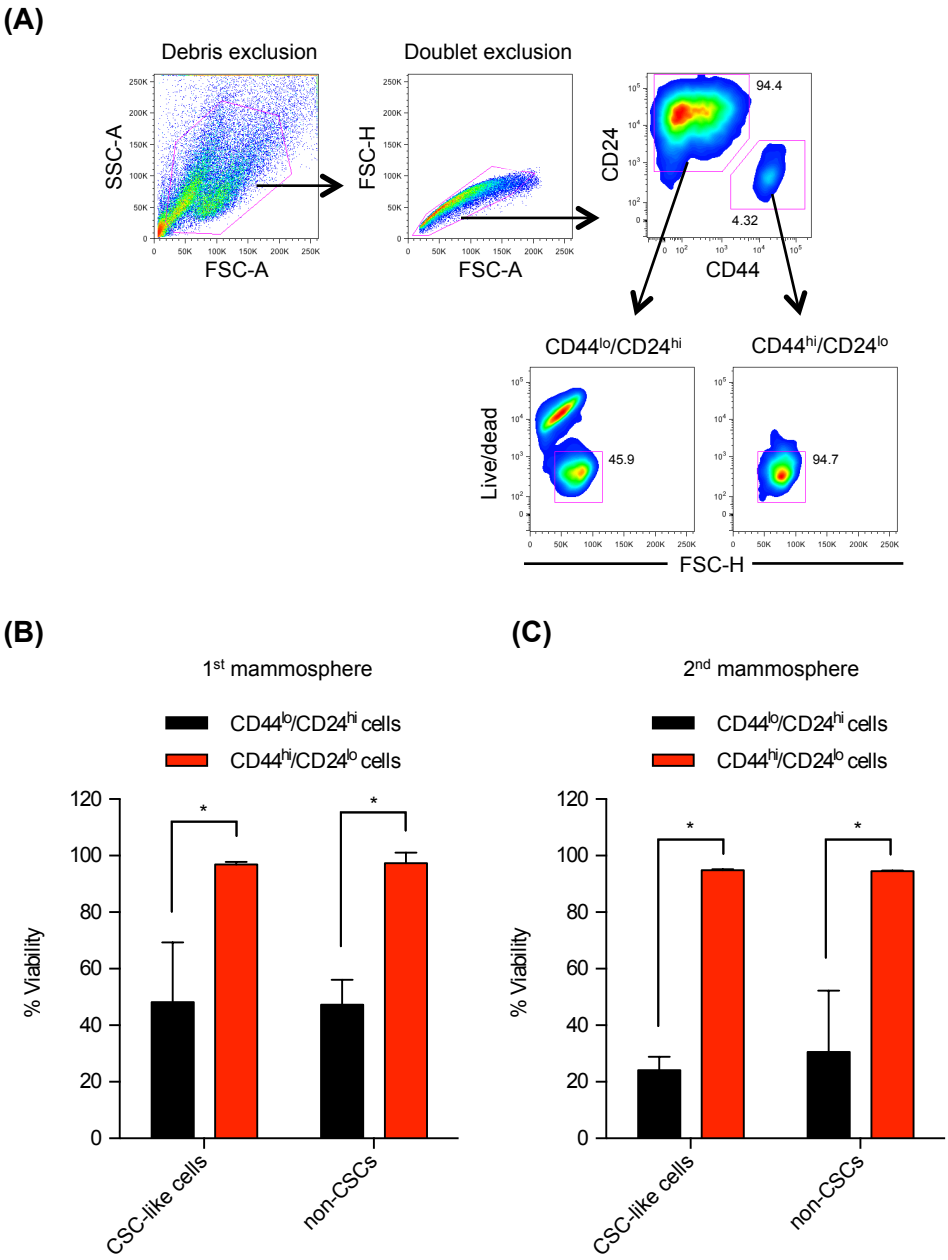

Figure 3.10. Survival of CD44^{hi}/CD24^{lo} CSC-like cells but not CD44^{lo}/CD24^{hi} non-CSCs in mammosphere culture. Sorted CSC-like cells and non-CSCs were maintained in mammosphere culture over two passages, and their phenotype was examined using Live/dead fixable Aqua staining and analysed by flow cytometry. Representative FACS plots for two independent experiments are shown in **(A)**. Data shown were pooled from two independent **(B)** 1st and **(C)** 2nd mammosphere cultures and shown as mean ± SD. Ordinary two-way ANOVA was applied for the analysis of differences between each group (*$p \leq 0.05$).

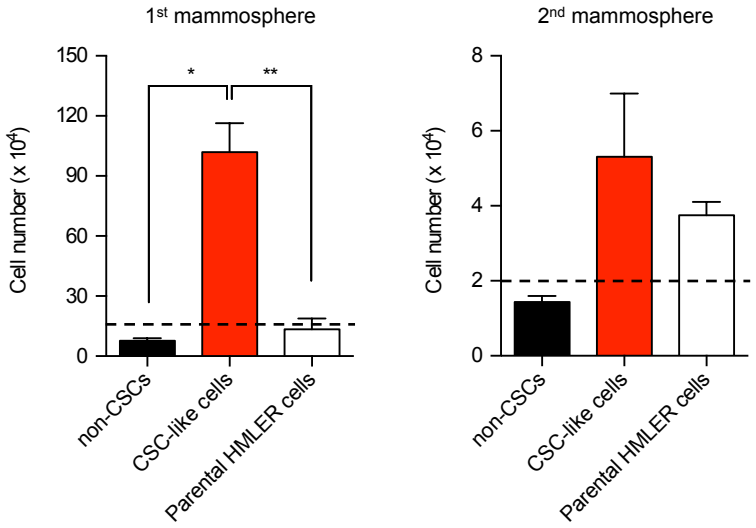

Figure 3.11. Proliferation of CD44^{hi}/CD24^{lo} CSC-like cells but not CD44^{lo}/CD24^{hi} non-CSCs in mammosphere culture. Sorted CSC-like cells and non-CSCs were maintained in mammosphere culture over two passages, and their proliferation was examined by counting the live cells harvested from the culture under haemocytometer in the presence of trypan blue for the distinguish and exclusion of dead cell from counting. The results shown are pooled from two independent experiments and shown as mean ± SD. RM one-way ANOVA was applied for the analysis of differences between each group (*$p \leq 0.05$; **$p \leq 0.01$). The dash line shows the number of cells seeded in the beginning of culture.

3.5.2. Differentiation of purified GD2$^+$ CSC-like cells in culture

It has been documented that GD2 expression distinguishes a population of cells with CSC-like characteristics from a panel of breast cancer cell lines including HMLER cells and from biopsies of breast cancer patients (Battula *et al.*, 2012; Liang *et al.*, 2013). As shown in Figures 3.1 and 3.5C, consistent with the report, only a proportion of (i) CD44^{hi}/CD24^{lo} cells within HMLER cells and (ii) HMLER-derived CSC-like cells expressed the CSC-associated marker GD2. In order to test whether GD2 expression identifies further true CSCs within the CSC-like cell line, GD2$^+$ cells were sorted from CSC-like cells to a purity of 99.9% and then maintained in normal adherent culture. GD2 expression by the sorted cells was checked by flow cytometry every three days. As shown in Figure 3.12, expression of GD2 by sorted GD2$^+$ cells was gradually lost and dropped to approximately 40% at the end of the experiment, which was comparable to the GD2 expression level of the parental CD44^{hi}/CD24^{lo} CSC-like cells. These results indicate that potentially the true CSCs are harboured exclusively within CSC-like cells but not within non-CSCs.

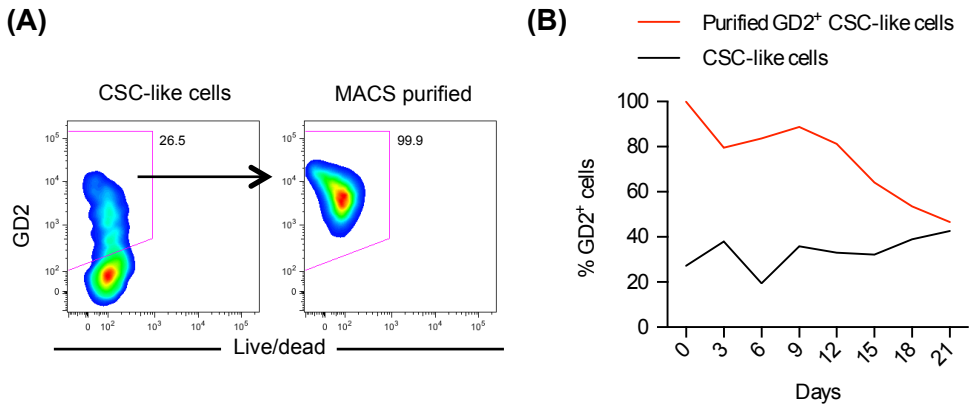

Figure 3.12. GD2 expression by sorted GD2$^+$ cells and parental CD44^{hi}/CD24^{lo} CSC-like cells over extended culture periods. **(A)** GD2$^+$ cells were isolated from CSC-like cells by MACS. **(B)** GD2 expression by GD2$^+$ cells and parental CSC-like cells over 21 days in culture as analysed by flow cytometry. The results shown are representative for two independent experiments.

3.6. Functional characteristics of CSC-like and non-CSC sublines *in vivo*

3.6.1. Generation of CSC-like cells and non-CSCs co-expressing red fluorescent protein reporter and a viral model antigen

To further examine the tumourigenicity of CSC-like cells and non-CSCs *in vivo*, we transduced these two cell sublines with lentiviral particles delivering a T2A gene cassette bicistronically expressing tdTomato as a fluorescent reporter for repeated and non-invasive *in vivo* live imaging and influenza virus matrix protein M1 (Flu M1) as surrogate tumour-specific antigen for subsequent cellular adoptive transfer studies. As internal control for expression of an irrelevant antigen, *Gaussia* luciferase (Gluc) was used instead of Flu M1.

CSC-like cells and non-CSCs transduced with the tdTomato-T2A-Gluc control gene cassette were isolated by FACS sorting twice according to their high expression level of tdTomato to purities >99% (Figure 3.13A). The CD44/CD24 phenotype of transduced CSC-like cells (CSC-tdTomato-T2A-Gluc, or in short CSC-Gluc) and non-CSCs (non-CSC-tdTomato-T2A-Gluc, or in short non-CSC-Gluc) remained stable in culture, as assessed by flow cytometry (Figure 3.13B). The transduced Gluc protein was functionally expressed in both CSC-Gluc cells and non-CSC-Gluc cells as confirmed using the Biolux^{TM} Gaussia Luciferase Assay Kit (NEB) (Figure 3.13C).

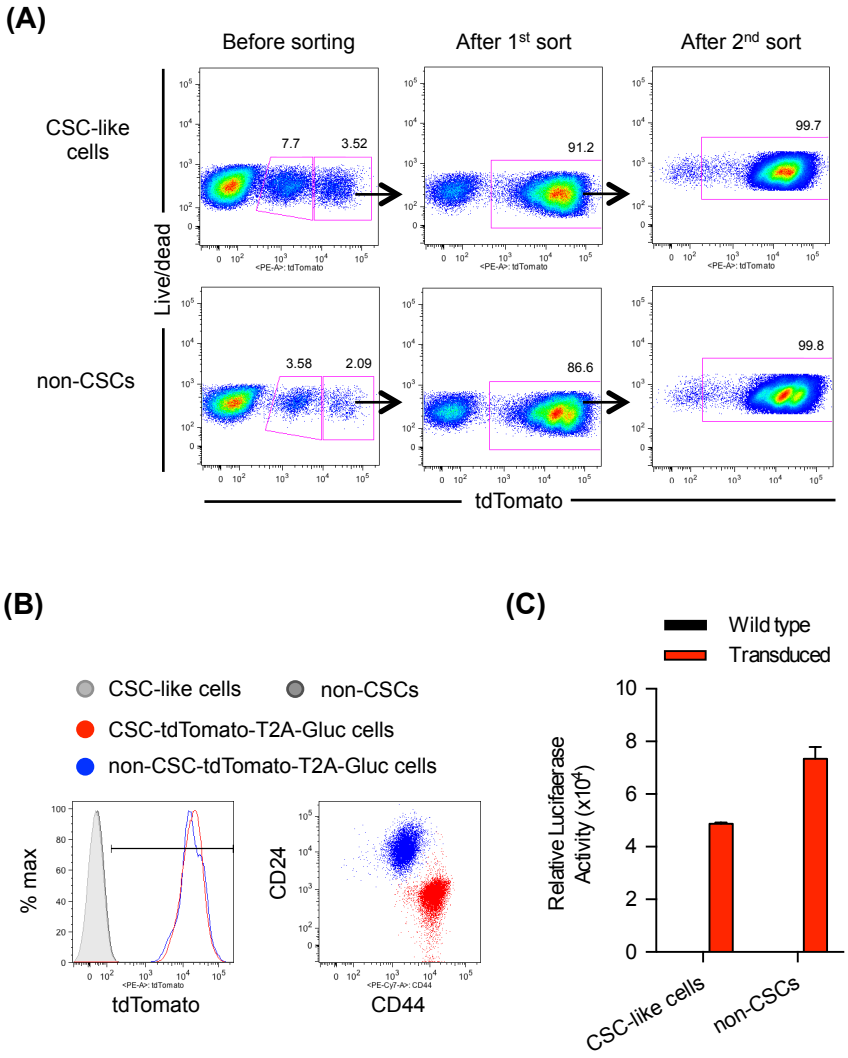

Figure 3.13. Generation of CD44^{hi}/CD24^{lo} CSC-like cells and CD44^{lo}/CD24^{hi} non-CSCs co-expressing tdTomato fluorescent reporter and *Gaussian* luciferase. **(A)** CSC-like cells and non-CSCs were transduced with lentiviral particles delivering bicistronic tdTomato-T2A-Gluc gene cassette. Successfully transduced tdTomato^{hi} cells were sorted twice to reach purities higher than 99% by FACS. **(B)** tdTomato expression and CD44/CD24 phenotype of purified transduced CSC-like cells and non-CSCs as assessed by flow cytometry. **(C)** Luciferase activity within the lysate of CSC-like cells and non-CSCs with or without transduction. Data are shown as mean ± SD.

Similarly, CSC-like cells and non-CSCs were transduced with lentiviral particles delivering a tdTomato-T2A-M1 gene cassette. Successfully transduced cells were sorted to purities >99% according to their high expression levels of tdTomato (Figure 3.14A). As already seen for CSC-Gluc and non-CSC-Gluc cells, the CD44/CD24 phenotype of M1-transduced CSC-like cells (CSC-tdTomato-T2A-M1, or in short CSC-M1 cells) and non-CSCs (non-CSC-tdTomato-T2A-M1, in short non-CSC-M1 cells) remained stable in culture as assessed by flow cytometry (Figure 3.14B). As shown in Figure 3.14C, the positive staining of both CSC-M1 cells and non-CSC-M1 cells with M1-specific antibodies for intracellular M1 confirmed successful expression of the viral antigen in these transduced lines. Staining with appropriate isotype control antibodies as well as with parental (*i.e.* M1-deficient) CSC-like cells was included as negative controls for the flow cytometry analysis.

Importantly, these lentivirally transduced CSC-like cells and non-CSCs were indistinguishable from the corresponding non-transduced parental cell lines with respect to phenotype, morphology and long-term stability in culture, demonstrating that co-expression of Flu M1 and tdTomato, or Gluc and tdTomato, did not affect their viability nor behaviour in cell culture. The CSC-M1 cells and non-CSC-M1 cells were consequently used for orthotopic xenotransplantation in immunodeficient NSG mice.

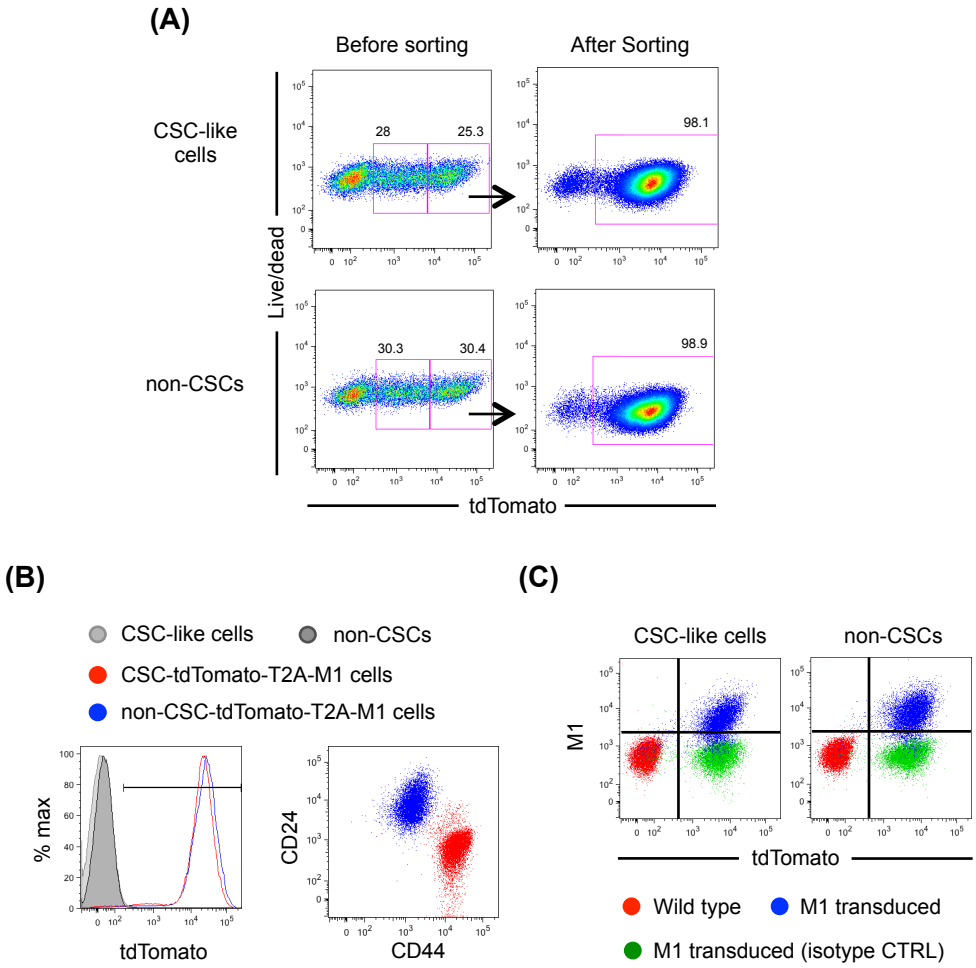

Figure 3.14. Generation of CD44^{hi}/CD24^{lo} CSC-like cells and CD44^{lo}/CD24^{hi} non-CSCs expressing tdTomato fluorescent reporter and M1. **(A)** CSC-like cells and non-CSCs were transduced with lentiviral particles delivering a bicistronic tdTomato-T2A-M1 gene cassette. Successfully transduced tdTomato^{hi} cells were sorted to purities >99% by FACS. **(B)** tdTomato expression and CD44/CD24 phenotype of transduced CSC-like cells and non-CSCs as assessed by flow cytometry. **(C) I**ntracellular expression of M1 by transduced CSC-like cells and non-CSCs as assessed by flow cytometry.

3.6.2. Tumourigenicity of CSC-like cells and non-CSCs in immunodeficient NSG mice

CSC-M1 cells and non-CSC-M1 cells were orthotopically implanted into immunodeficient NSG mice by injecting a high (2×10^6 cells/mouse) or low dose (10^3 cells/mouse) of either cell type subcutaneously (*s.c.*) into mammary fat pad in the presence of matrigel. Each group consisted of 6 mice. The development of tumours arising from each injection was monitored closely by live imaging of tdTomato reporter using a Kodak Fx-Pro imager (representative images as shown in Figure 3.15; and measurements as shown in Figure 3.16A) and by measurement of palpable tumours using calipers (Figure 3.16B). In accordance with Home Office regulations, mice were sacrificed by Schedule 1 method before tumours reached 1.5 cm in the longest dimension (maximum size permitted in the license is 1.7 cm in diameter) or when any signs of (*i*) discharge, (*ii*) redness of skin surrounding lesion or (*iii*) development of a crater-like appearance (indicative of erosion of deeper layers of the skin) at the site of the lesion were observed.

For survival analyses, development of tumours was as positive when any dimension of the tumour reached 1 cm in length (Figure 3.17). All six NSG mice receiving 2×10^6 CSC-M1 cells developed tumours while only one of six mice (16.7%) receiving 2×10^6 non-CSC-M1 cells developed a tumour. The tumours derived from injections of 2×10^6 CSC-M1 cells grew rapidly, with the fastest one reaching a size of >1 cm as early as day 46 and the slowest one reaching that size at day 63. With a much slower growth rate, the only tumour derived from injection of 2×10^6 non-CSC-M1 cells reached a size of >1 cm at day 91, *i.e.* 1-2 months later than the CSC-M1-derived tumours.

In contrast to the rapid development of tumours in NSG mice receiving CSC-M1 cells at a high dose, injection of CSC-M1 cells at a low dose of 10^3 cells per animal only reached tumour sizes of >1 cm at much later time points, ranging from day 95 to day 154. Despite the bigger variation as compared to the injection with CSC-M1 cells at a high dose, tumours developed in all six treated mice, demonstrating the striking tumour-forming potential of HMLER-derived CSC-like cells *in vivo*. Of note, the first tumour developing upon injection of 10^3 CSC-M1 cells reached >1 cm in size at day 95, which is very close to the time point when the only tumour derived from injection of 2×10^6 non-CSC-M1 cells developed, indicating the potential that this tumour may actually derived from the very minor contamination of non-CSCs with CSC-like cells (< 0.1% of all live cells as

determined by flow cytometry analysis; Figure 3.5 and 3.6) rather than non-CSCs. However, the actual origin of the tumour derived from the injection of 2×10^6 non-CSC-M1 cells remains unclear at this stage. Finally, no palpable tumour had developed in any of the six NSG mice receiving10^3 non-CSC-M1 cells by day 183, *i.e.* one month after the last tumour derived from low dose CSC-M1 cells was confirmed.

The tumourigenicity of CSC-like cells was further confirmed by similar results obtained in a second, independent experiment assessing tumour development upon orthotopic injection of 2×10^6 CSC-M1 or CSC-Gluc cells into NSG mice (data not shown).

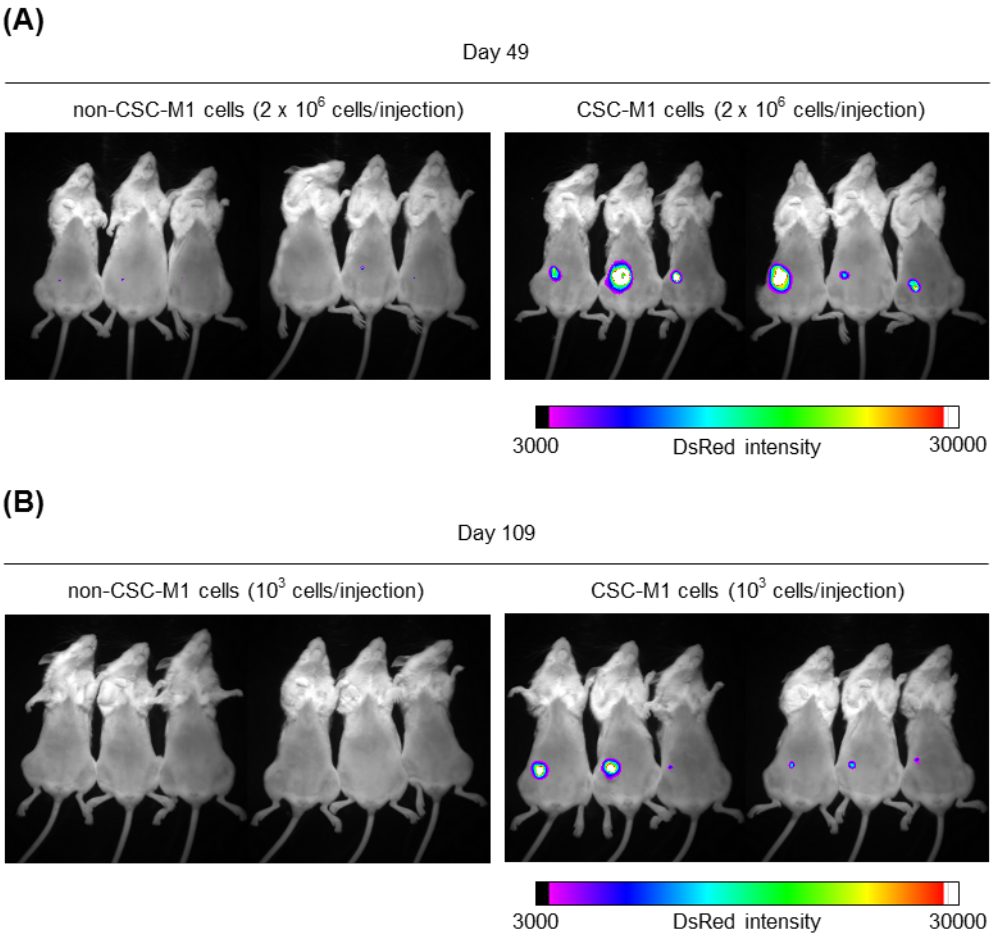

Figure 3.15. Representative live imaging pictures of tumours using the Kodak Fx-Pro system. Mice receiving injections of CSCs or non-CSCs at **(A)** high or **(B)** low dose were monitored twice a week using a Kodak Fx-Pro imager detecting expression of the reporter tdTomato. Mice were anaesthetised using isoflurane, shaved on the abdomen to reduce background autofluorescence, and examined under both white light (emission filter at 700 nm for 0.5 seconds) and DsRed (excitation filter at 550 nm and emission filter at 600 nm for 20 seconds) settings. Pictures were taken under both settings and overlaid by using the Carestream Molecular Imaging software.

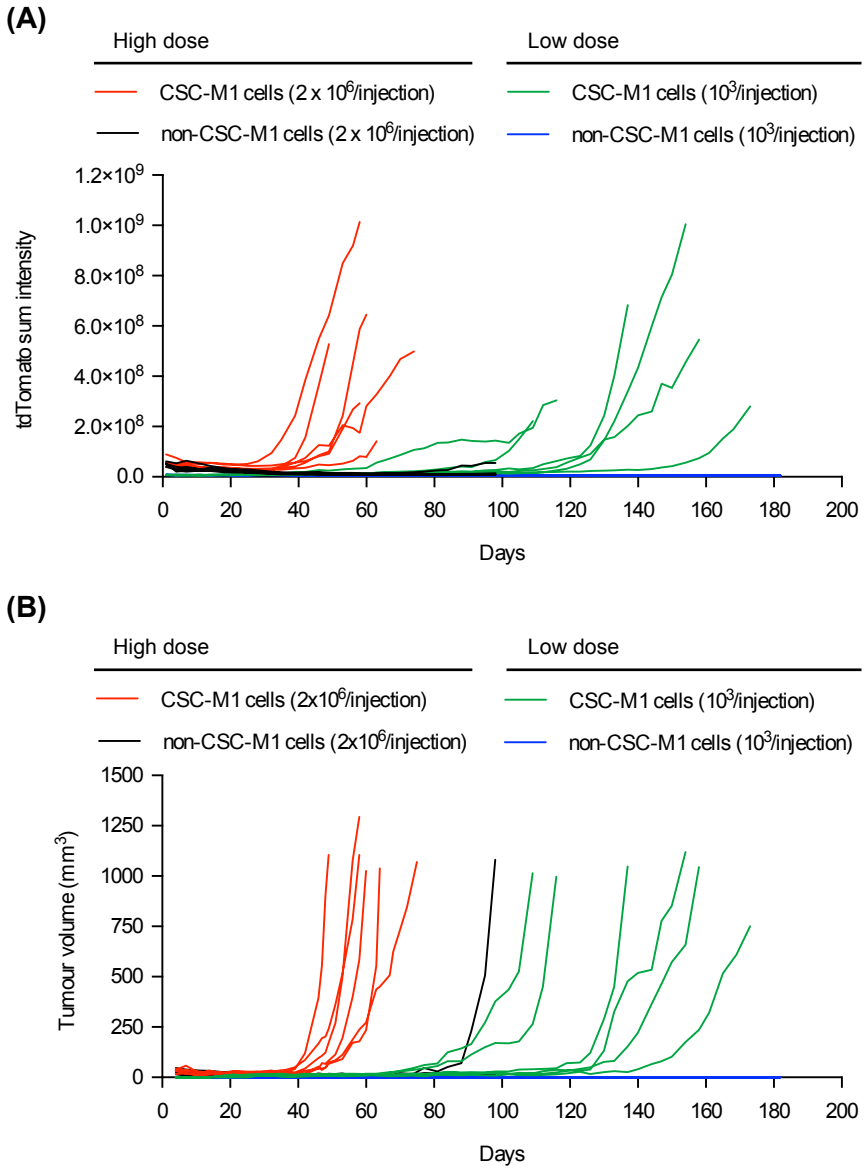

Figure 3.16. Development of tumours derived from CSC-like cells and non-CSCs expressing tdTomato fluorescent reporter and Flu M1. CSC-like cells or non-CSCs were xenotransplanted with matrigel into the mammary fat pad of NSG mice at two different doses; at a high dose with 2 × 10^6 cells/mouse and at a low dose with 10^3 cells/mouse (n=6 per group). Tumour development and growth were monitored **(A)** by live imaging of tdTomato using then Kodak Fx-Pro system and **(B)** by caliper measurements.

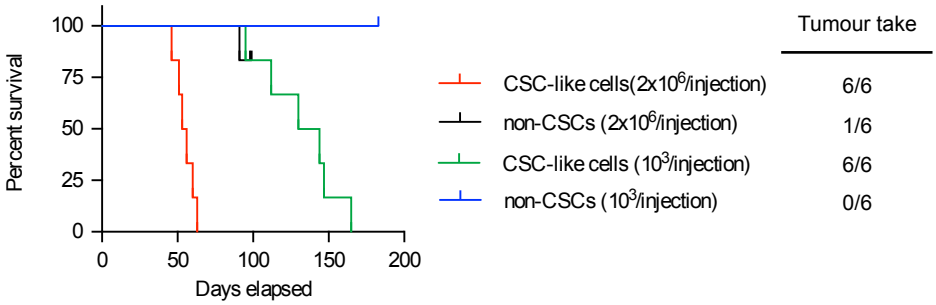

Figure 3.17. Tumour take of mice upon injection of CSC-like or non-CSCs at high and low dose. Mice receiving low doses of CSCs or non-CSCs were monitored for up to 98 days after injection, while mice receiving high doses of CSCs or non-CSCs were monitored for up to 180 days after injection. The end point of monitoring was determined as no further increase in the tdTomato signal over at least two weeks. Disease was defined as tumour with longest diameter reaching 1 cm. The disease-free survival curves were plotted using the Kaplan-Meier method.

Of note, quantification of the tdTomato reporter signal acquired by *in vivo* live imaging resulted in similar growth curves as the caliper measurements, yet with larger variation (Figure 3.15B). Despite this variability between the two methods, linear regression analysis showed that the caliper measurements and live imaging data were highly correlated and comparable in all tumours regardless of the cell type or dose (Figure 3.18).

In conclusion, the CSC-M1 cells exhibited significantly stronger ability to initiate and develop tumours in NSG mice compared to their non-CSC-M1 counterparts.

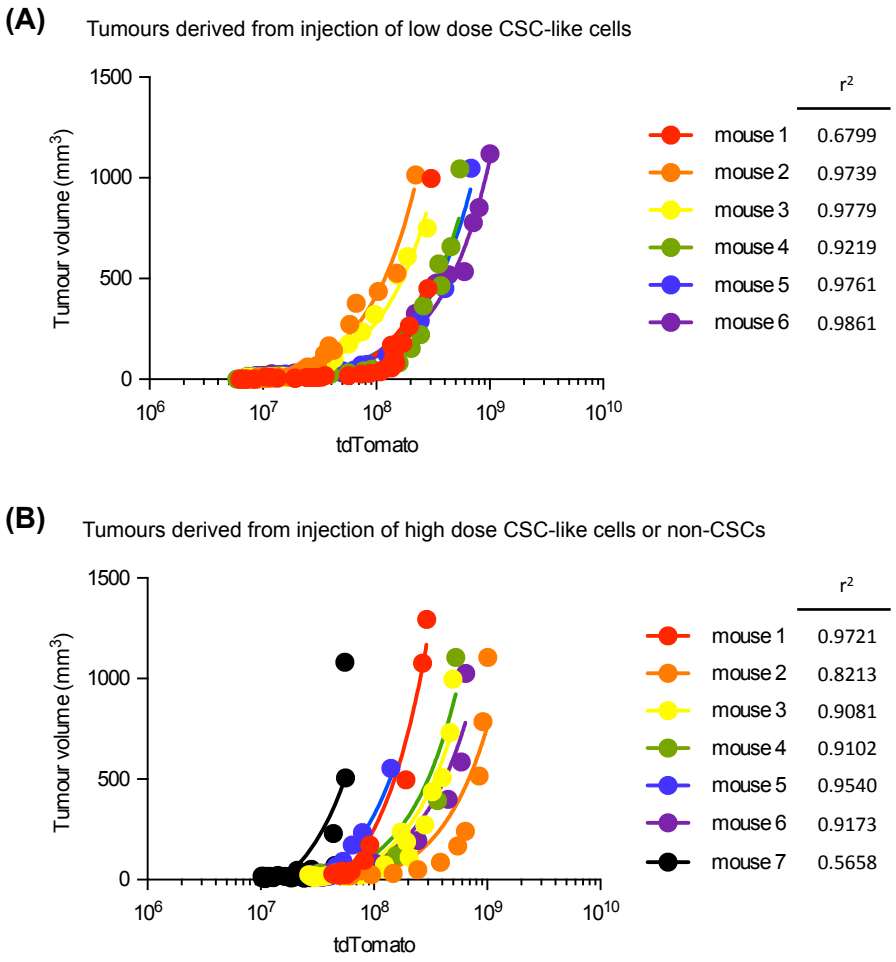

Figure 3.18. Correlation of caliper measurements with tdTomato imaging data. The results of the two approaches to monitor the growth of tumours derived from injections of **(A)** low dose CSCs or **(B)** high dose CSC-like cells or non-CSCs were compared by linear regression correlation. In **(B)**, mice 1 to 6 were injected with CSCs, whereas mouse 7 was the only mouse developing a tumour upon injection of non-CSCs.

3.6.3. Metastases derived from CSC-like cells and non-CSCs in immunodeficient NSG mice

To determine the metastatic potential of CSC-like cells and non-CSCs, all mice sacrificed were examined thoroughly for signs of macro-metastasis by autopsy or for micro-metastasis by imaging of tdTomato from the harvested organs including draining and non-draining lymph nodes (dLNs), spleen, liver, lung and brain (Figure 3.19A and B). In agreement with their poor ability to generate tumours in NSG mice as observed in the previous section, there was no metastasis found in any mouse receiving either high dose or low dose non-CSCs-M1 cells. In striking contrast, reporter tdTomato signal was detected in 4 of 6 (66.7%) dLNs harvested from mice receiving high doses of CSC-M1 cells, and 2 of 5 (40%) dLNs harvested from mice receiving low dose CSC-M1 cells. Distant metastases to the lung were detected in 1 of 6 (16.7%) mice receiving high dose CSC-M1 cells as well as in 1 of 6 (16.7%) mice receiving low dose CSC-M1 cells. Interesting, the spleens of mice with injection of CSC-like cells were observed to be significantly larger then those of mice with injection of non-CSCs, indicating stronger inflammation and immune responses in correspondence to more advanced disease, *e.g.* possibly systemic dissemination, in the mice with injection of CSC-like cells (Figure 3.19C). In conclusion, the CSC-like cells exhibited a stronger metastatic potential compared to their non-CSC counterparts.

(A)

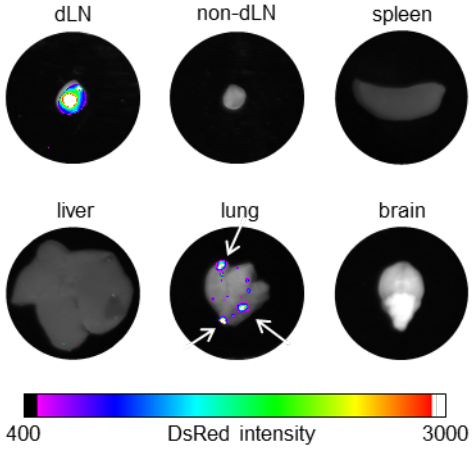

(C)

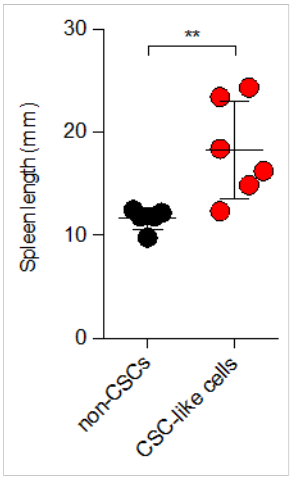

(B)

	Metastasis observed			Metastasis observed	
High dose	lung	dLN	Low dose	lung	dLN
CSC-like cells	1/6*	4/6	CSC-like cells	1/6	2/5
non-CSCs	0/6	0/6	non-CSCs	0/6	0/6

*number of mice with metastasis observed at site of indication/number of mice per group;
dLN: draining lymph node

Figure 3.19. Metastasis status of mice upon xenotransplantation of CSCs or non-CSCs. (A) Representative live imaging pictures of organs including draining and non-draining lymph nodes, spleen, liver, lung and brain, which were harvested from one of the CSC tumour-bearing mice. **(B)** Summary of the status of tumour metastasis to lung and to draining lymph nodes in each group of mice. **(C)** The spleens of mice receiving low dose CSCs or non-CSCs were harvested at the end of the experiment and measured for their length. Significance of difference was calculated by Mann-Whitney test (**$p \leq 0.01$).

3.6.4. Differentiation of CSC-like cells and non-CSCs *in vivo*

To investigate whether CSC-like cells have the ability to differentiate into non-CSCs *in vivo*, and *vice versa*, the primary tumours generated in the preceding section were subjected to a phenotypical analysis of CD44 and CD24 expression by flow cytometry and to histological and pathological examinations. In total, 13 tumours (six each derived upon injection of 2×10^6 and 10^3 CSCs, respectively, and one derived upon injection of 2×10^6 non-CSCs) were dissociated into single cell suspensions and analysed by flow cytometry.

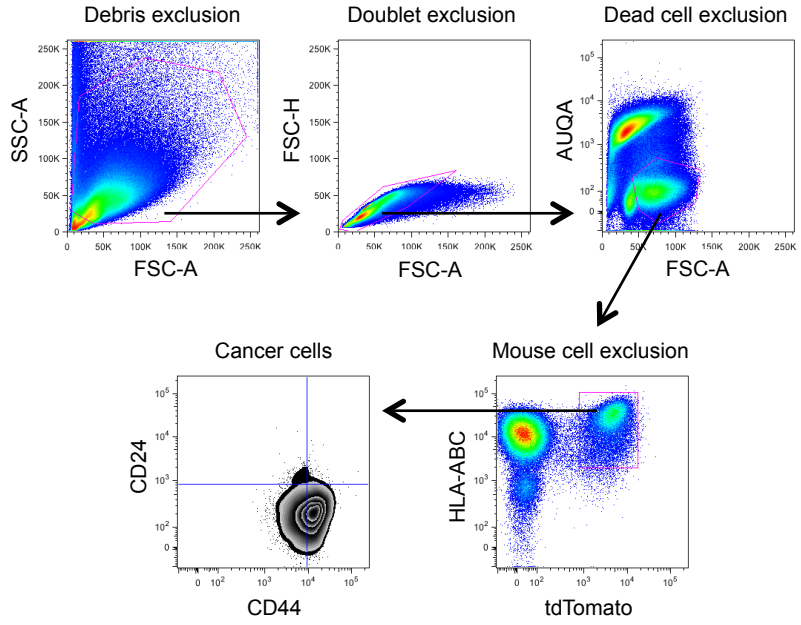

Figure 3.20. Gating strategy for the analysis of CD44/CD24 expression by dissociated CSC-M1 and non-CSC-M1 tumours. The tumours derived from injection of CSC-M1 or non-CSC-M1 cells were harvested and dissociated into single cell suspension for flow cytometry analysis. The dissociated tumour cells were stained with Live/dead Aqua and fluorochrome-conjugated antibodies against CD44, CD24 and HLA class I. Analysis was conducted by setting sequential gates on intact cells (FSC-A/SSC-A), single cells (FSC-A/FSC-H), live cells ($Aqua^-$) and engrafted human cells ($tdTomato^{hi}$ $HLA\text{-}ABC^+$).

The initial analysis was conducted according to the gating strategy as shown in Figure 3.20 with a series of gates excluding cell debris, dead cells and murine cells to determine the CD44 and CD24 expression profile of live human tumour cells defined by their $Aqua^{-}$ $HLA\text{-}ABC^{+}$ $tdTomato^{hi}$ phenotype. Although the results showed minimal differentiation of original CSCs during the development of tumours derived upon injection of 2×10^6 CSC-M1 cells, an intermediate cell population with lower CD44 expression and marginally higher CD24 expression could be observed in two out of six tumours examined (Figures 3.21A). However, this apparent down-regulation of CD44 expression and up-regulation of CD24 by dissociated tumour cells did not reach statistical significance (Figure 3.21B), indicating only marginal differentiation of injected CSC-like cells *in vivo*. As opposed to this marginal differentiation of CSCs into non-CSCs *in vivo*, the only one tumour derived upon injection of 2×10^6 non-CSC-M1 cells showed signs of a possible de-differentiation *in vivo*, with the appearance of a distinct $CD44^{hi}/CD24^{dim}$ population and a minor population (~10%) with an actual $CD44^{hi}/CD24^{lo}$ CSC-like phenotype (Figure 3.21C). However, it is not clear from these data whether the non-CSCs did indeed de-differentiate *in vivo* and gave rise to CSCs, or whether this was due to outgrowth of a minor contamination of CSC-like cells present in the original non-CSC preparation.

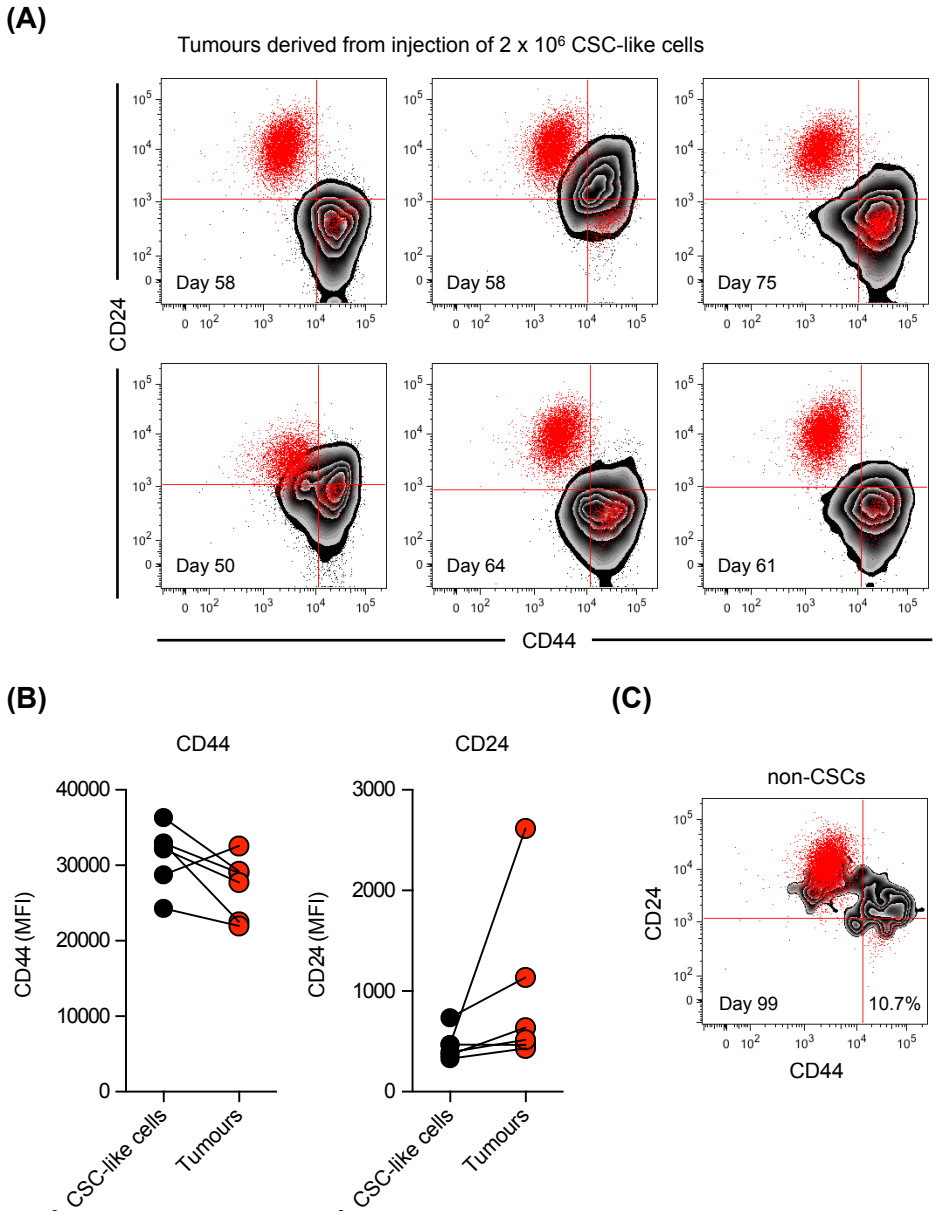

Figure 3.21. CD44 and CD24 expression by dissociated tumours derived from injection of high dose CSC-M1 or non-CSC-M1 cells. Tumours derived from injection of 2 × 10^6 **(A)** CSC-M1 or **(C)** non-CSC-M1 cells were harvested for analysis of their CD44/CD24 phenotype when their sizes reached 1000 mm^3 at the time points indicated in the lower left corner of each plot. The CD44/CD24 expression profile of each tumour was shown as zebra plots, whereas the CD44/CD24 expression profile of parental HMLER cells in culture was shown as red dots as internal control. **(B)** The expression levels of CD44 and CD24 by dissociated tumour cells were compared with cultured $CD44^{hi}/CD24^{lo}$ CSC-like cells within the parental HMLER cell line serving as control. Data shown are mean fluorescence intensities for each tumour cell preparation and cells in culture. Data were analysed by Wilcoxon matched-pairs signed rank test.

Even clearer evidence of an apparent transition *in vivo* was obtained from the phenotyping of tumours derived upon injection of 1×10^3 CSC-M1 cells (Figure 3.22A), with the difference in CD44 expression reaching statistical significance (Figure 3.22B). Of note, these tumours generated by injections of low dose CSC-like cells were harvested at much later time points (81 days longer on average) compared to the tumours derived upon injection of high dose CSC-like cells. These results indicate that CSC-like cells injected at a low dose may have differentiated more, possibly due to the longer growth period *in vivo*.

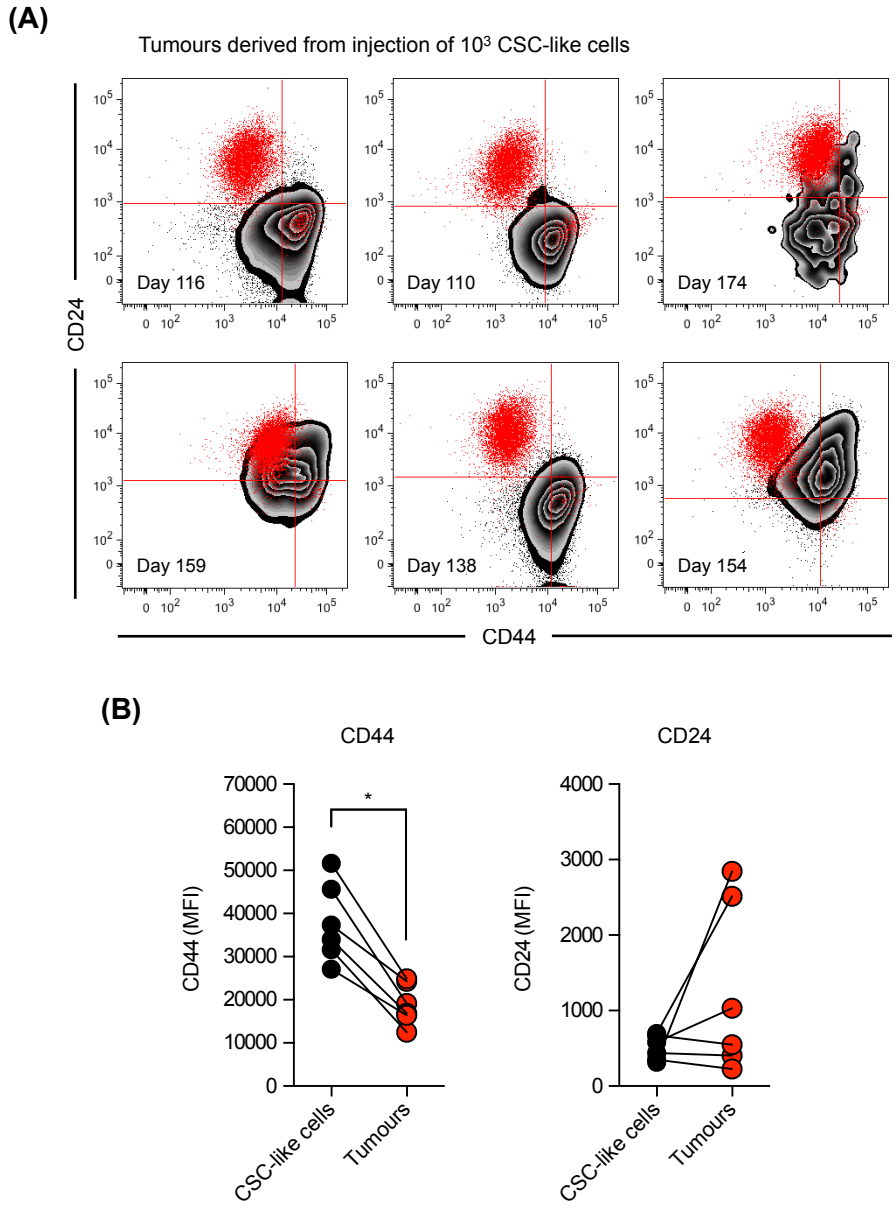

Figure 3.22. CD44 and CD24 expression by dissociated tumours derived from injection of low dose CSC-M1 cells. Tumours derived from injection of 1 × 10^3 **(A)** CSC-M1 cells were harvested for analysis of their CD44/CD24 phenotype when their sizes reached 1000 mm^3 at the time points indicated in the lower left corner of each plot. The CD44/CD24 expression profile of each tumour was shown as zebra plots, whereas the CD44/CD24 expression profile of parental HMLER cells in culture was shown as red dots as internal control. **(B)** The expression levels of CD44 and CD24 by dissociated tumour cells were compared with cultured $CD44^{hi}/CD24^{lo}$ CSC-like cells within the parental HMLER cell line serving as control. Data shown are mean fluorescence intensities for each tumour cell preparation and cells in culture. Data were analysed by Wilcoxon matched-pairs signed rank test.

Of note, the loss in fluorescence of transduced tumour cells expressing reporter proteins such as tdTomato and GFP is a useful indicator of cell death (Steff *et al.*, 2001). In agreement, I discovered that the live/dead gating excluded a considerable fraction of cells, which were still positive for tdTomato but at a reduced level. As revealed by back gating, non-CSCs were much more fragile and exhibited substantial cell death during experimental procedures such as FACS sorting (data not shown) and in this case, mechanical dissociation (Figure 3.23A) as compared to CSC-like cells. Within dissociated non-CSCs tumour, $CD44^{hi}/CD24^{lo}$ cells showed a $tdTomato^{hi}$ $Aqua^{-}$ phenotype, whereas $CD44^{lo}/CD24^{hi}$ cells showed a decreased tdTomato expression and were positive for Aqua (Figure 3.23A). As the overall viability of the cells was low (in average 10.6% live cells of total dissociated single cells with the majority of the cells being positive for Aqua; Figure 3.20), live/dead may actually exclude a considerable fraction of cells with decreased tdTomato expression but that are not yet dead (Figure 3.23B), and may thus mask the true composition of tumours by CSC-like cells and non-CSCs. I therefore introduced an alternative gating strategy for the analysis of the phenotyping data as outlined in Figure 3.23C.

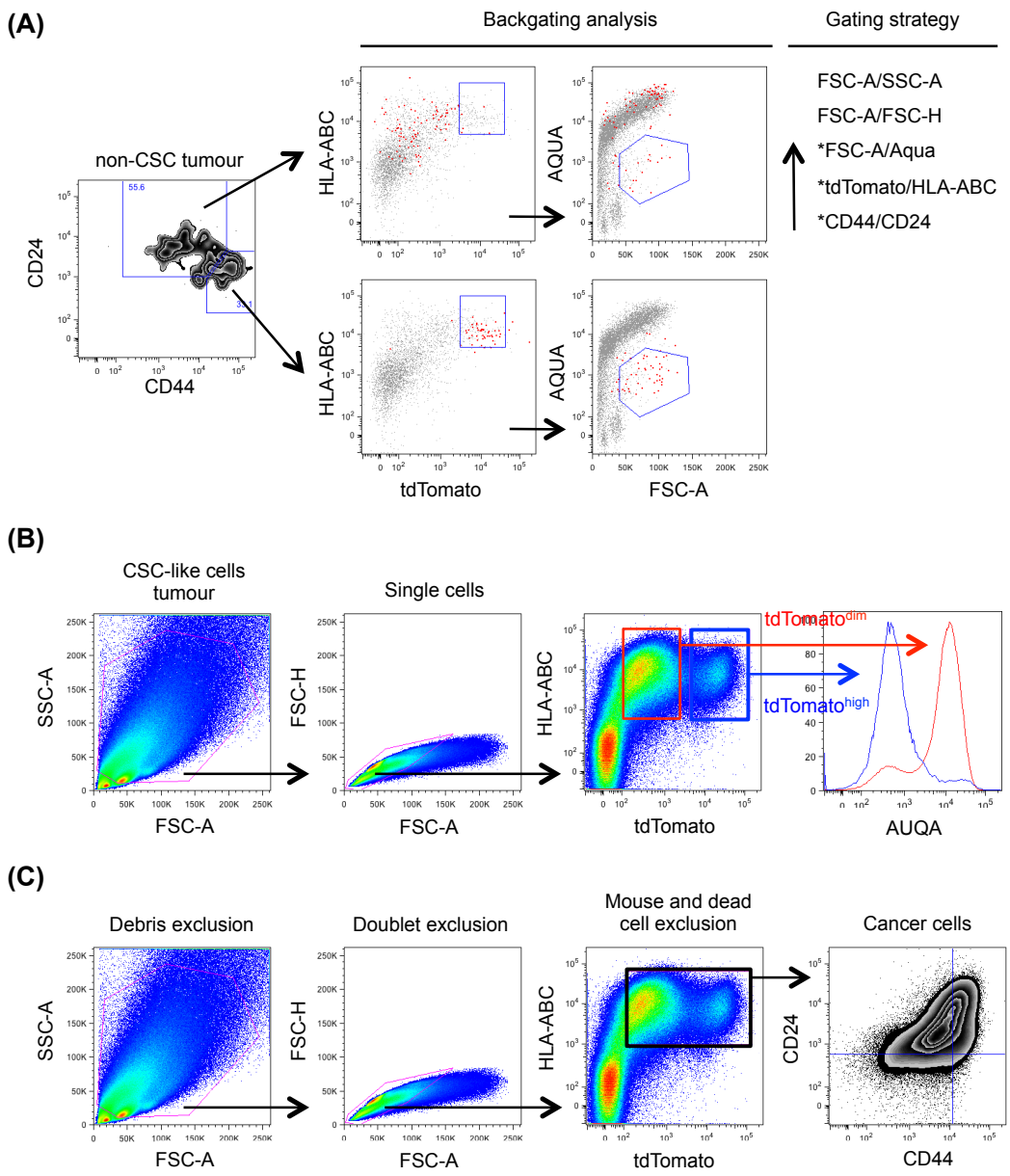

Figure 3.23. Alternative gating strategy for the analysis of CD44/CD24 expression by dissociated CSCs. **(A)** The tdTomato expression and Aqua staining of $CD44^{hi}/CD24^{lo}$ and $CD44^{lo}/CD24^{hi}$ cells derived from tumours established upon injection of non-CSCs-M1 cells were analysed by backgating. Red dots represent for $CD44^{hi}/CD24^{lo}$ (lower panel) and $CD44^{lo}/CD24^{hi}$ (upper panel) cells and grey dots shown as background stand for total cells within previous gate. The serial gates are showed on the right while arrows show the direction of backgating. **(B)** Cells with different levels of tdTomato expression ($tdTomato^{hi}$ in red and $tdTomato^{dim}$ in blue) were analysed for their viability using Aqua. **(C)** The new analysis for dissociated tumours was conducted by setting sequential gates set on intact cells (FSC-A/SSC-A), single cells (FSC-A/FSC-H), and engrafted human cells ($tdTomato^{+}$ $HLA\text{-}ABC^{+}$; including both $tdTomato^{hi}$ and $tdTomato^{dim}$ cells) for their CD44/CD24 expression profile, while disregarding the live/dead staining.

Using this alternative gating strategy, the CD44/CD24 expression profiles were re-determined for all HLA-ABC^{+} tdTomato^{+} cells, irrespective of the tdTomato expression levels and their live/dead staining, to account for the fact that non-CSCs may have rapidly undergone apoptosis during the experimental procedure. As shown in Figures 3.24 and 3.25, the tumours analysed with this modified gating strategy derived from injections of 2 × 10^6 or 10^3 CSCs showed much clearer signs of differentiation into non-CSCs as compared to the observations in the previous section. A distinct CD44^{lo}/CD24^{hi} cell population could be identified in 2 out of 6 high dose CSC tumours and in 5 out of 6 low dose CSC tumours. In summary, HMLER-derived CSCs showed a strong ability to initiate tumours *in vivo* as well as some degree of plasticity to differentiate and give rise to non-CSCs, especially in the case of low starting cell numbers and long tumour growth periods, which most likely provided the most favourable conditions for tumour cell growth and differentiation.

Of note, and distinct from what was found using the original gating strategy (Figure 3.21), the single tumour derived upon injection of 2 × 10^6 non-CSCs showed a nearly homogenous CD44^{lo}/CD24^{hi} non-CSC phenotype but with a very limited number of CD44^{hi}/CD24^{lo} cells (~0.02%) (Figure 3.24B). This phenotype is nearly identical to the phenotype of sorted non-CSCs-M1 in culture, which included a tiny population (~0.05%) of contaminating CD44^{hi}/CD24^{lo} cells. Intriguingly, the growth of the tumour derived upon injection of 2 × 10^6 non-CSCs (which therefore can be estimated to have contained approximately 1 × 10^3 contaminating CD44^{hi}/CD24^{lo} CSC-like cells), was very similar to the growth curve of tumours derived upon injection of 1 × 10^3 CSC-like cells, supporting the notion that this tumour may have derived in fact from the small contamination of highly tumourigenic CSC-like cells and not from the non-tumourigenic non-CSC population. However, the CD44/CD24 phenotype of the cells harvested from this non-CSC-derived tumour was clearly distinct from the tumours derived from low dose CSC-like cells. While it is unclear whether the differentiation status of CSC-like cells might be affected by the presence of excess non-CSCs, these observations lead to the general conclusion that non-CSCs have a very limited ability to initiate tumours *in vivo*.

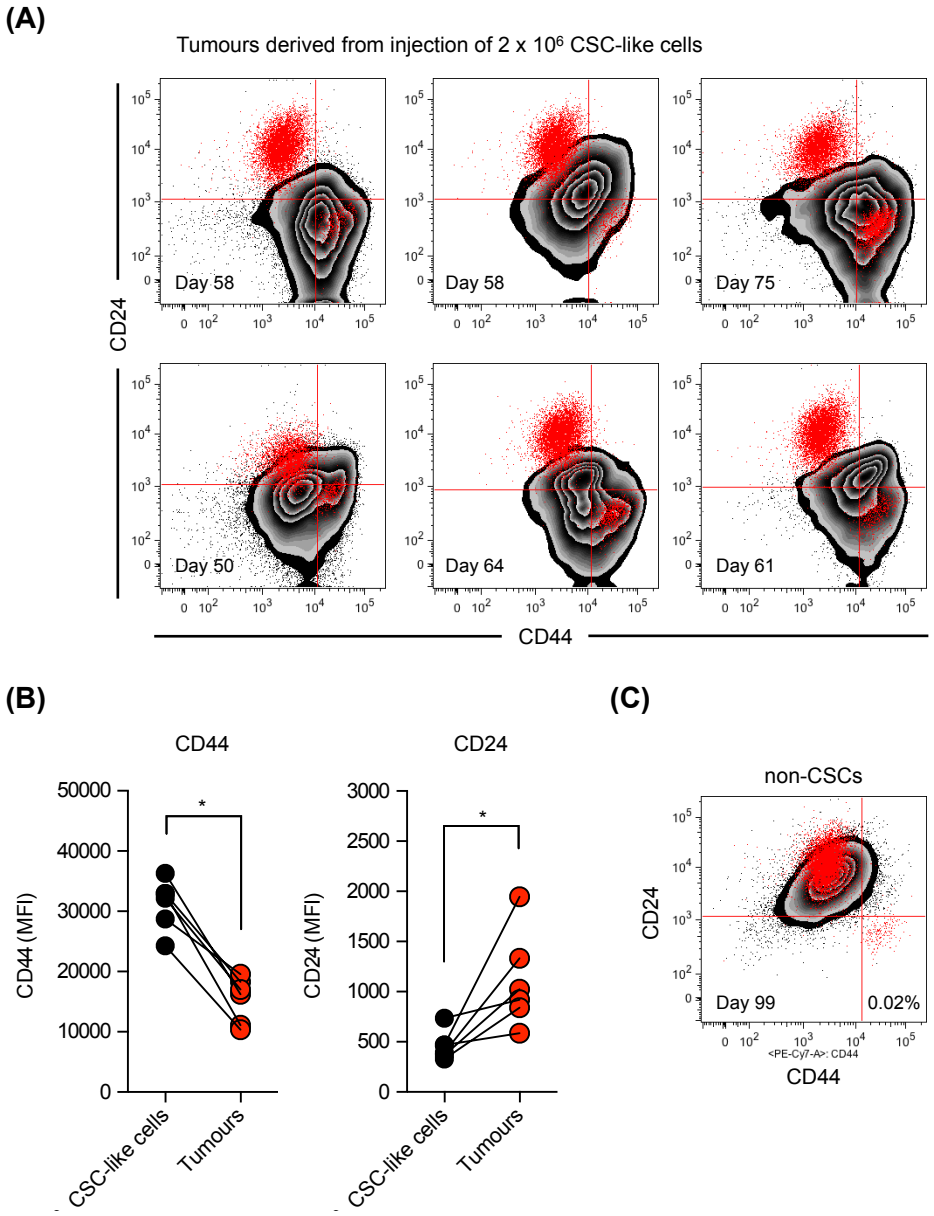

Figure 3.24. CD44 and CD24 expression by dissociated tumours derived from injection of high dose CSC-M1 and non-CSC-M1 cells. Tumours derived from injection of 2 × 10^6 **(A)** CSC-M1 or **(C)** non-CSC-M1 cells were harvested for analysis of their CD44/CD24 phenotype when their sizes reached 1000 mm^3 at the time points indicated in the lower left corner of each plot. The CD44/CD24 expression profile of each tumour was shown as zebra plots, whereas the CD44/CD24 expression profile of parental HMLER cells in culture was shown as red dots as internal control. **(B)** The expression levels of CD44 and CD24 by dissociated tumour cells were compared with cultured $CD44^{hi}/CD24^{lo}$ CSC-like cells within the parental HMLER cell line serving as control. Data shown are mean fluorescence intensities for each tumour cell preparation and cells in culture. Data were analysed by Wilcoxon matched-pairs signed rank test.

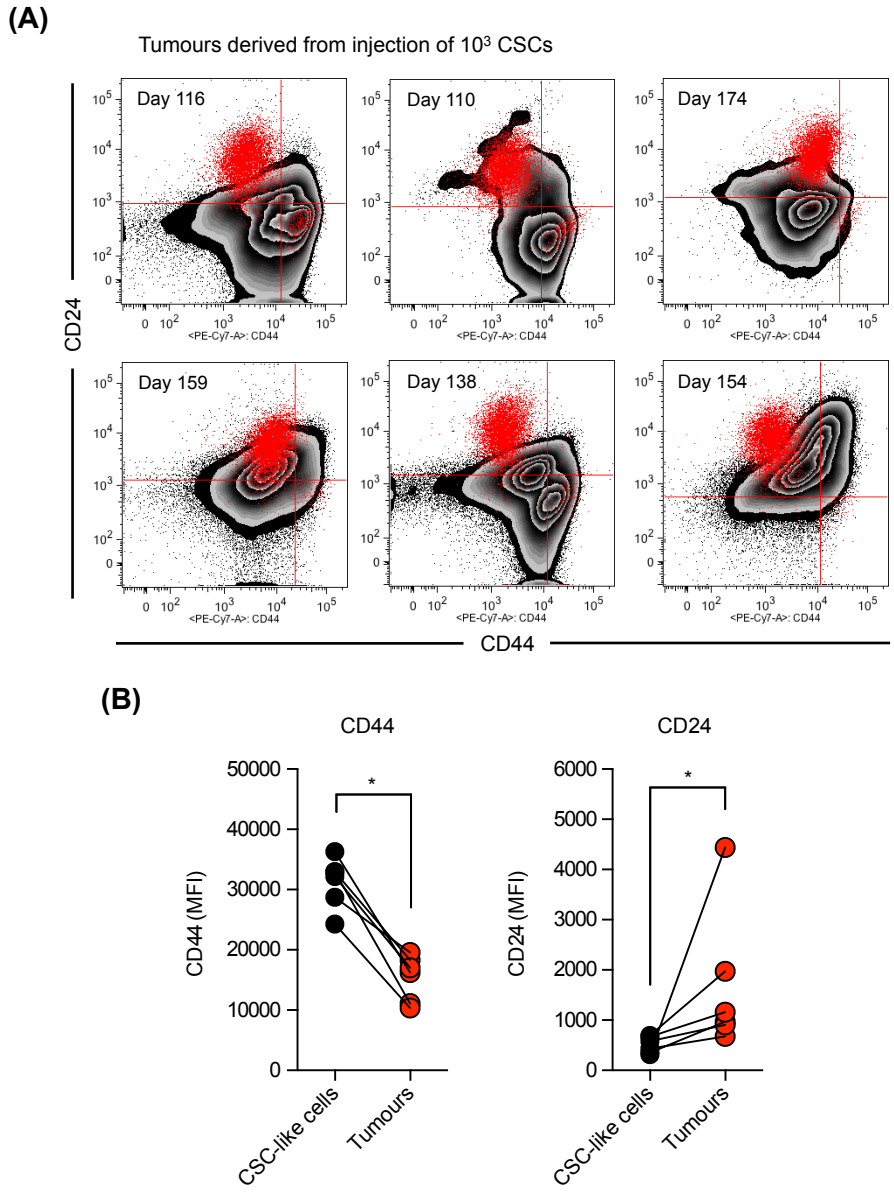

Figure 3.25. CD44 and CD24 expression by dissociated tumours derived from injection of low dose CSC-M1 cells. Tumours derived from injection of 1 × 10^3 **(A)** CSC-M1 cells were harvested for analysis of their CD44/CD24 phenotype when their sizes reached 1000 mm^3 at the time points indicated in the lower left corner of each plot. The CD44/CD24 expression profile of each tumour was shown as zebra plots, whereas the CD44/CD24 expression profile of parental HMLER cells in culture was shown as red dots as internal control. **(B)** The expression levels of CD44 and CD24 by dissociated tumour cells were compared with cultured $CD44^{hi}/CD24^{lo}$ CSC-like cells within the parental HMLER cell line serving as control. Data shown are mean fluorescence intensities for each tumour cell preparation and cells in culture. Data were analysed by Wilcoxon matched-pairs signed rank test.

3.7. Discussion

In this Chapter, I have shown that within the transformed mammary epithelial cell line HMLER a minor but distinct population of cells with a $CD44^{hi}$ $CD24^{lo}$ phenotype could be identified while the majority of HMLER cells showed a $CD44^{lo}$ $CD24^{hi}$ phenotype. Whereas $CD44^{lo}$ $CD24^{hi}$ HMLER cells died under non-adherent mammosphere-forming conditions, $CD44^{hi}$ $CD24^{lo}$ cells displayed a significant ability to self-renew, proliferate and generate mammospheres with heterogeneous cell composition when cultured in suspension. This Chapter demonstrates that the two cell subsets could be isolated from parental HMLER cells by FACS and maintained in culture with their original $CD44^{hi}$ $CD24^{lo}$ and $CD44^{lo}$ $CD24^{hi}$ phenotypes remaining stable at least a month. In the absence of FCS, only $CD44^{hi}$ $CD24^{lo}$ CSC-like cells but not $CD44^{lo}$ $CD24^{hi}$ non-CSCs had the ability to differentiate and give rise to both cell subsets, indicating that only CSC-like cells but not non-CSCs possessed cellular plasticity. Phenotypically, only CSC-like cells expressed the novel CSC-associated marker GD2 on the cell surface, and further isolation of $GD2^{+}$ cells from the pool of CSC-like cells showed the capacity of these purified $GD2^{+}$ cells to differentiate into $GD2^{-}$ cells. This loss of GD2 expression by $GD2^{+}$ $CD44^{hi}$ $CD24^{lo}$ cells in culture indicated that GD2 may serve as a more precise marker for the identification of breast CSCs and confirmed that CSC-like cells may in fact contaminated with non-CSCs to certain degree, which allows the maintenance of their phenotype under self-sufficient nutrient supply and balance by the co-existence and cross-talk of CSCs and non-CSCs as seen in parental HMLER cells. However, these observations were restricted by the use of CD44, CD24 and GD2 as phenotypic markers, and it is unclear whether HMLER-derived CSC-like cells or non-CSCs may give rise to other cell populations not being revealed by the characterisation with these markers. Morphologically, CSC-like cells showed a mesenchymal-like appearance with expression of markers including EDA-fibronectin and vimentin in adherent culture, whereas non-CSCs had a epithelial morphology and expressed CK14 and CK18 indicative of a combination of basal and luminal features.

In vivo, CSC-like cells showed a strong capacity to initiate tumours in NSG mice at a dose as low as 1,000 cells per mouse as opposed to their non-CSC counterparts, which showed very limited tumourigenicity with only 16.7% (1/6) mice developing a tumour at a high dose of 2×10^6 cells/mouse. Of note, the tumours developing upon injection of CSC-like

cells recapitulated a heterogeneous cellular composition with both $CD44^{hi}$ $CD24^{lo}$ and $CD44^{lo}$ $CD24^{hi}$ cells present in the tumour mass. In contrast, the single tumour developing upon injection of non-CSCs showed a homogenous $CD44^{lo}$ $CD24^{hi}$ phenotype comparable to non-CSCs in culture, indicating a differentiation of CSC-like cells but not non-CSCs *in vivo*. Moreover, only CSC-like cells but not non-CSCs exhibited the ability to develop distant metastases in the lung, further supporting the CSC-like nature of HMLER-derived $CD44^{hi}$ $CD24^{lo}$ cells.

However, I have not been able to address the descendant ability of tumour-derived $CD44^{hi}$ $CD24^{lo}$ cells to seed new tumours during serial passages in mice, which marks one of the pivotal criteria defining true CSCs (Al-Hajj *et al.*, 2003; Kreso and Dick, 2014), thus leaving certain doubts regarding the real stemness of HMLER-derived $CD44^{hi}$ $CD24^{lo}$ cells. Nevertheless, the present study establishes HMLER-derived CSC-like cells as a valid experimental model that fulfils most (albeit not all) features of *bona fide* CSCs and that can be manipulated easily *in vitro* and *in vivo* to (*i*) study the differential susceptibilities of CSCs and non-CSCs to T cell mediated killing and possibly other treatment including chemotherapy and radiation therapy, and (*ii*) identify molecular targets and pathways specifically present in CSCs for novel therapies specifically targeting the cells responsible for tumour initiation and progression. Any findings obtained using this initial model can then be validated using primary CSCs from breast cancer biopsies defined by appropriate markers such as ALDHA1 (Ginestier *et al.*, 2007) and GD2 (Battula *et al.*, 2012), alone or in combination with CD44 and CD24.

The observation that the HMLER-derived CSC-like and non-CSC populations described in this Chapter could be maintained stably in culture offered an opportunity to manipulate and modify their antigenicity by lentiviral transduction to study possible interactions of CSCs and non-CSCs with different immune cells, in particular with MHC-restricted antigen-specific $CD8^{+}$ T cells. Transduction with reporter proteins such as tdTomato or luciferase allowed to establish a convenient, sensitive and non-invasive *in vivo* imaging system in NSG mice, and also provided a useful tool to identify micro-metastases in distant organs such as the lung.

In summary, although compromised in some aspects, we conclude that these CSC-like cells and non-CSCs therefore represent a powerful experimental model system for initial attempts on the targeting of true CSCs by human T cells both *in vitro* and *in vivo*.

Chapter 4. Synergistic Targeting of Breast Cancer Cells by γδ T cells and Cytotoxic $CD8^+$ T Cells

4.1. Introduction

Cancer stem cells (CSCs) comprise a minor cell population responsible for the initiation and relapse of tumours due to their potential to self-renew and differentiate (Reya *et al.*, 2001) and their intrinsic resistance to currently used cancer treatments such as chemotherapy drugs (Dean *et al.*, 2005) and radiation (Rich, 2007), as well as their ability to escape from the immunosurveillance by both MHC-restricted and non-MHC-restricted immune cells (Kawasaki and Farrar, 2008; Schatton and Frank, 2009; Chouaib *et al.*, 2014). We previously demonstrated that genetic suppression of c-FLIP, followed by treatment with TRAIL, a potent effector molecule produced by activated effector cells including human γδ T cells (Dieli *et al.*, 2007; Vermijlen *et al.*, 2007), selectively diminishes the functional breast CSC pool *in vitro* and *in vivo* (Piggott *et al.*, 2011). It is therefore interesting to evaluate whether γδ T cells can specifically recognise and kill CSCs efficiently, which may inform novel γδ T cell-based immunotherapies to efficiently eradicate CSCs and prevent cancer relapse. This may involve direct killing of CSCs by γδ T cells, or else require a strategy that can sensitise CSCs to γδ T cell-mediated cytotoxicity. As an innate-like effector, γδ T cells are activated and expand rapidly upon stimulation, and are believed to infiltrate inflammatory sites including sites of infection and tumours. Onsite, they serve as a major early source of pro-inflammatory cytokines such as IFN-γ and IL-17A, which may modulate the αβ T cell response and subsequently lead to tumour control (Gao *et al.*, 2003; Ma *et al.*, 2011). In this aspect, it is intriguing to investigate how non-MHC-restricted γδ T cells cooperate with MHC-restricted cytotoxic $CD8^+$ T cells to eradicate CSCs in a synergistic manner relying on the recognition of different ligands by these two cytotoxic effector populations.

In this chapter, I aimed to develop strategies harnessing both innate-like γδ T cells and adaptive cytotoxic $CD8^+$ T cells to target efficiently and specifically breast CSCs by the use of the model established in Chapter 3.

4.2. Aims

- To examine the susceptibility of CSCs and non-CSCs to killing by MHC-restricted cytotoxic $CD8^+$ T cells and by non-MHC-restricted γδ T cells.

- To show that γδ T cells can kill CSC-like cells and non-CSCs sensitised by zoledronate and modulate the immunogenicity of surviving target cells to cytotoxic $CD8^+$ T cell-mediated killing.

- To explore the underlying mechanism of the synergistic effects between γδ T cells and cytotoxic $CD8^+$ T cells in the inhibition of tumour growth by targeting CSC-like cells and non-CSCs.

4.3. *Ex vivo* expansion of Vγ9/Vδ2 T cells

4.3.1. Characterisation of *ex vivo* expanded γδ T cells

γδ T cells were expanded from PBMCs of healthy donors with zoledronate in the presence of IL-2 to 83.95±9.44% of total live cells (n=11). As shown in Figure 4.1, the activation marker CD69 was strongly expressed by expanded γδ T cells at day 14, whereas expression of CD25 was not detectable. As CD25 expression by γδ T cells is rapidly up-regulated during the first few days of expansion but gradually down-modulated afterwards (data not shown) (Lafont *et al.*, 2001), these results indicate that at this stage the expanded γδ T cells were not fully activated any more and had become less responsive to IL-2 due to lack of CD25 (IL-2R) expression.

It has been shown that γδ T cells can be activated by cancer cells opsonised with humanised antibodies *via* CD16 (Fcγ receptor) expression (Gertner-Dardenne *et al.*, 2009; Capietto *et al.*, 2011; Himoudi *et al.*, 2012). However, in our hands the expression of CD16 by expanded γδ T cells is low and largely fluctuated between individual donors from 5.82% to 73.7% with around 70% of expanded γδ T cells tests having expression level <25% (Figure 4.1). The expression of CD56, which defines the lineage of cytotoxic γδ T cells (Alexander *et al.*, 2008; Urban *et al.*, 2009), as well varied predominantly in expanded γδ T cells (Figure 4.1).

For functional experiments, expanded γδ T cells were further enriched to purities >97% using a custom-made modified γδ T cell negative selection kit (StemCell Technologies; proprietary information part of a non-disclosure agreement) that depletes red blood cells, platelets, B cells, αβ T cells, NK cells, dendritic cells, hematopoietic stem cells, granulocytes, and monocytes. As expression levels of CD16, CD25 and CD56 on activated and expanded γδ T cells vary between donors (Figure 4.1), antibodies against these makers were excluded from the antibody cocktail used for negative selection of γδ T cells. The expanded and enriched cells were aliquoted and preserved in liquid nitrogen for later use in functional assays.

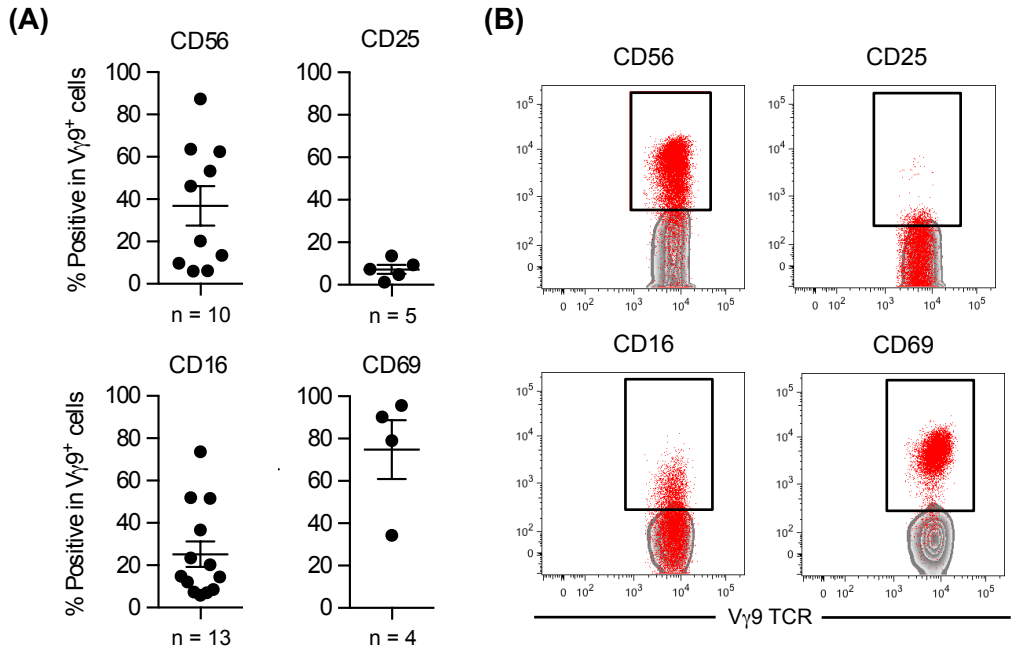

Figure 4.1. Phenotypic characterisation of expanded γδ T cells. **(A)** Expression of CD56, CD16 and activation markers CD25 and CD69 by γδ T cells were measured by FACS after 14 days of expansion from PBMCs with zoledronate and IL-2 (n = number of donors used for γδ T cell expansion). **(B)** Representative density plots of different cell surface makers expressed by expanded γδ T cells. Isotype controls are shown as grey zebra and the stained markers are shown as red dots with the name of maker on top of plot.

The memory status of the expanded γδ T cells was examined next, to check the potential persistency and efficacy of these cells after adoptive transfer. As shown in Figure 4.2, the majority of expanded γδ T cells showed a $CD45RA^{-}/CD27^{-}$ effector memory phenotype as described firstly by (Dieli *et al.*, 2003). All cultures showed very limited number of residual T_{naive} ($CD45RA^{+}/CD27^{+}$) cells and only one expansion included a small proportion (~10%) of T_{CM} ($CD45RA^{-}/CD27^{+}$) cells.

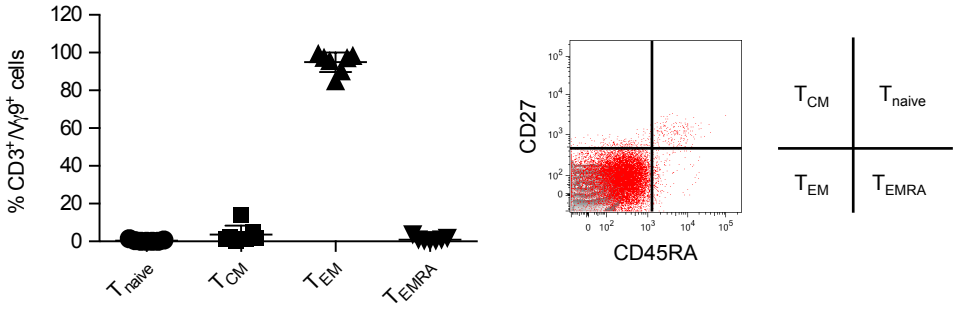

Figure 4.2. Memory status of expanded γδ T cells. The proportion of T_{naive} ($CD45RA^{+}/CD27^{+}$), T_{CM} ($CD45RA^{-}/CD27^{+}$), T_{EM} ($CD45RA^{-}/CD27^{-}$) and T_{EMRA} ($CD45RA^{+}/CD27^{-}$) cells was examined by FACS analysis. Data shown were derived from independently expanded γδ T cell populations derived from seven healthy individuals. A representative density plot of one γδ T cell lines shown on the right, with the isotype control shown as grey zebra plot and the stained sample shown as red dots.

4.3.2. Re-stimulation of expanded γδ T cells

Expanded γδ T cells were treated with HMB-PP to examine their responsiveness to re-stimulation and to increase their cytolytic potential. As shown in Figure 4.3, treatment of expanded γδ T cells with HMB-PP induced significant levels of degranulation and IFN-γ secretion. These results indicate that expanded γδ T cells retain the ability to respond to re-stimulation via the T cell receptor and thus can potentially serve as potent effectors in targeting cancer cells, especially those with aberrant accumulation of intracellular IPP upon sensitisation with zoledronate.

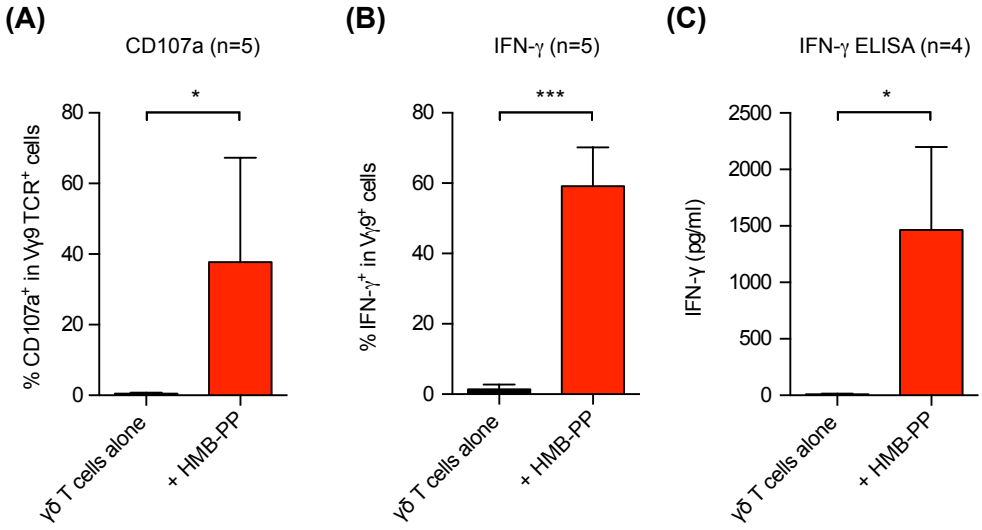

Figure 4.3. Responsiveness of expanded γδ T cells to re-stimulation with HMB-PP. (A) Expanded γδ T cells were re-stimulated with 10 nM HMB-PP in the presence GolgiSTOP and PE-conjugated antibodies against CD107a for 5 hours, followed by Live/dead staining and surface staining for CD3 and Vγ9 TCR. **(B)** Expanded γδ T cells were re-stimulated with 10 nM HMB-PP in the presence brefeldin A for 5 hours and followed by Live/dead staining, surface staining for CD3 and Vγ9 TCR and intracellular staining of IFN-γ. **(C)** Expanded γδ T cells were re-stimulated with 10 nM HMB-PP overnight, and the amount of IFN-γ in the culture supernatants was assessed by ELISA. Statistical significances were determined using paired Student's t tests (*$p < 0.05$; ***$p < 0.001$)

4.4. Non-MHC-restricted killing of CSC-like cells and non-CSCs by γδ T cells

4.4.1. Sensitisation of CSC-like cells and non-CSCs to γδ T cell-mediated cytotoxicity by zoledronate

Human γδ T cells are increasingly appreciated as promising effectors for novel immunotherapy strategies (Tyler *et al.*, 2015), not least due to their ability to recognise stress-induced changes in transformed cells, including breast cancer cells, in a non-MHC-restricted manner (Bonneville *et al.*, 2010; Fisher *et al.*, 2014; Lo Presti *et al.*, 2014). Thus, I next examined the susceptibility of CSC-like cells and non-CSCs to γδ T cell-mediated cytotoxicity. As shown in Figure 4.4, both CSC-like cells and non-CSCs exhibited strong resistance to γδ T cell-mediated killing, even at effector/target (E/T) ratios as high as 20/1.

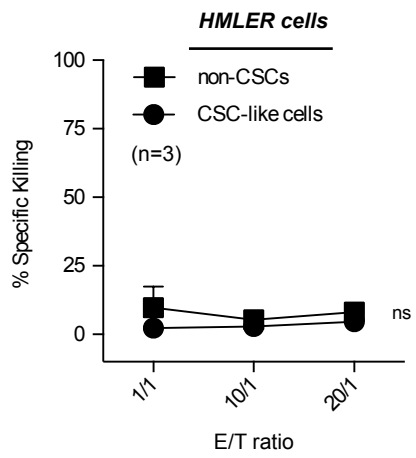

Figure 4.4. Cytotoxicity of HMLER-derived CSC-like cells and non-CSCs established by γδ T cells. CSC-like cells and non-CSCs were labelled with CellVue and PKH26 membrane dyes, respectively, and then mixed at 1:1 ratio as targets for γδ T cell-mediated killing. Data were pooled from two independent experiments with γδ T cells expanded from PBMCs of three healthy individuals. Significance of differences was calculated by non-parametric two-way ANOVA.

4.4.2. Sensitisation of CSC-like cells and non-CSCs to γδ T cell-mediated cytotoxicity by zoledronate

I next sought to establish strategies that could efficiently activate γδ T cells to harness them against CSC-like cells. It has been shown that cancer cells in general (Beck *et al.*, 2010; Meraviglia *et al.*, 2010; Benzaid *et al.*, 2011; Capietto *et al.*, 2011) and even CSCs of colon cancer (Todaro *et al.*, 2009) can be sensitised to γδ T cell-mediated killing by zoledronate, which stimulates γδ T cells *via* induction of intracellular accumulation of IPP (Monkkonen *et al.*, 2007; Roelofs *et al.*, 2009; Benzaid *et al.*, 2011) and binding to BTN3A1 (Wang *et al.*, 2013; Hsiao *et al.*, 2014; Sandstrom *et al.*, 2014; Rhodes *et al.*, 2015). Consistently, overnight treatment of both CSC-like cells and non-CSCs with

zoledronate significantly enhanced their susceptibility to γδ T cell-mediated killing (Figure 4.5). Treatment of both CSC-like cells and non-CSCs with zoledronate also enhanced the activation of γδ T cells in co-culture as judged by mobilisation of CD107a (Figure 4.6) and by their secretion of IFN-γ (Figure 4.7). Taken together, these findings show that treatment of CSC-like cells and non-CSCs with zoledronate enhances the activation of γδ T cells and leads to better killing of sensitised targets.

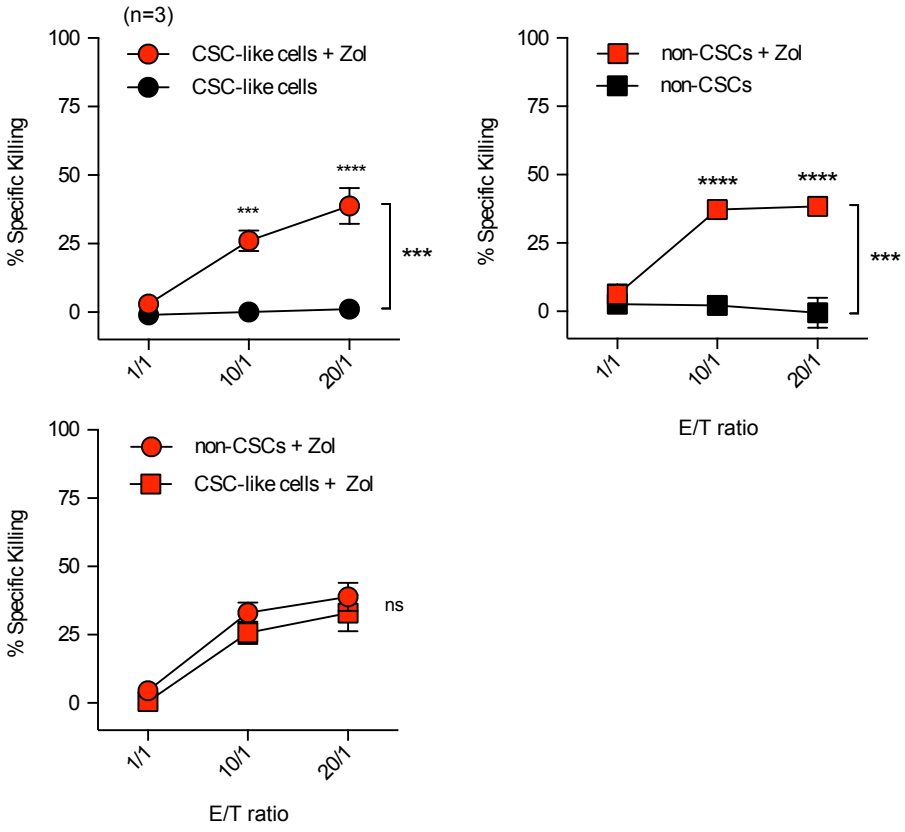

Figure 4.5. Sensitisation of CSC-like cells and non-CSCs to γδ T cell-mediated killing by pretreatment with zoledronate. CSC-like cells and non-CSCs were sensitised overnight with 10 mM zoledronate and then mixed 1:1 with their untreated counterparts, respectively, for the analysis of their susceptibilities to γδ T cell-mediated killing. Mixtures of sensitised CSC-like cells and non-CSCs (1:1) were analysed as control for possible interactions between CSC-like cells and non-CSCs. Data were pooled from two independent experiments with γδ T cells expanded from PBMCs of three healthy individuals. Significance of differences was calculated by two-way ANOVA. (***$p \leq 0.001$; ****$p \leq 0.0001$)

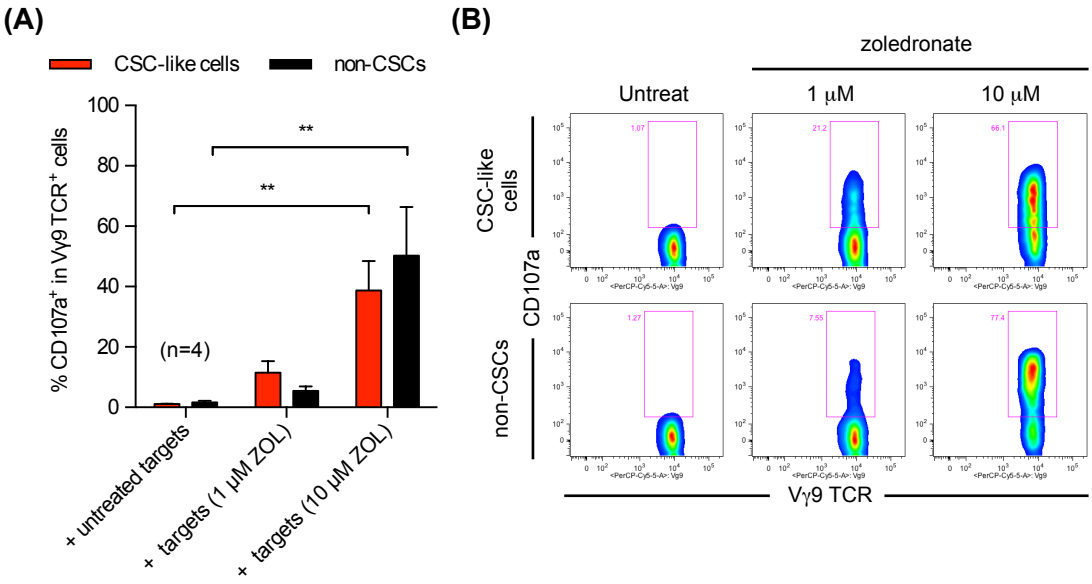

Figure 4.6. Degranulation of γδ T cells in response to CSC-like cells and non-CSCs sensitised with zoledronate. **(A)** CSC-like cells and non-CSCs were pretreated overnight with or without zoledronate and co-cultured with γδ T cells for a further 5 hours, in the presence of GolgiSTOP and PE-conjugated antibodies against CD107a. Representative FACS plots of CD107a expression are shown in **(B)**.

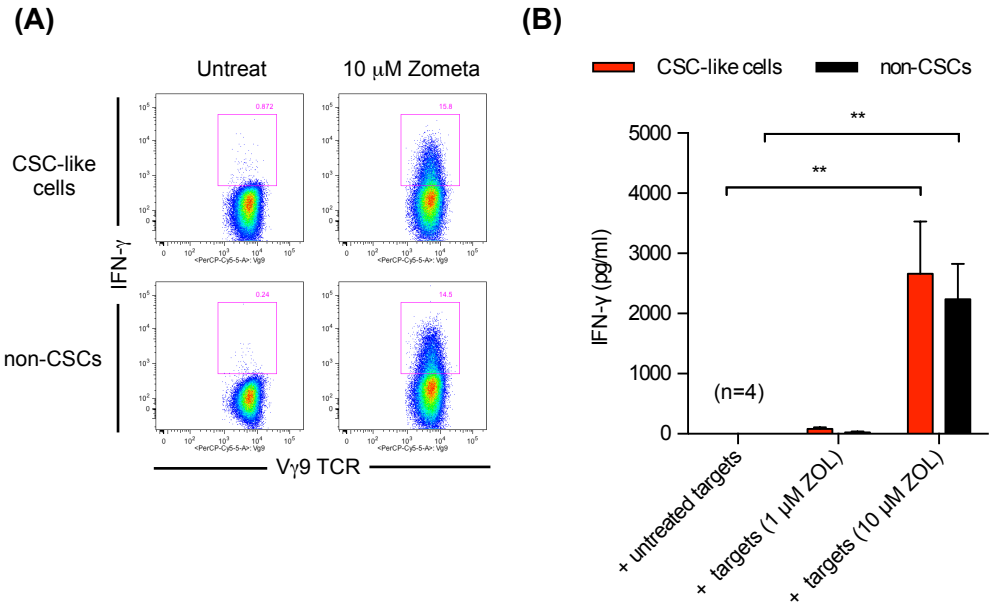

Figure 4.7. IFN-γ secretion of γδ T cells in co-culture with CSCs and non-CSCs sensitised with zoledronate. **(A)** CSC-like cells and non-CSCs were pretreated overnight with or without zoledronate and co-cultured with γδ T cells for a further 5 hours, in the presence of brefeldin A. The intracellular IFN-γ expression by γδ T cells was analysed by flow cytometry. **(B)** Secretion of IFN-γ by activated γδ T cells in different co-culture conditions for 24 hours was examined by ELISA.

4.4.3. Sensitisation of CSC-like cells and non-CSCs to γδ T cell-mediated cytotoxicity by shRNA targeting farnesyl pyrophosphate synthase

To mimic the action of zoledronate in inducing γδ T cell activation, both CSC-like cells and non-CSCs were transduced with lentiviral vectors delivering a specific shRNA targeting farnesyl pyrophosphate synthase (FPPS), together with eGFP as reporter. The successful transduction with FUTG-SR22 vector established a doxycycline-inducible, FPPS-specific shRNA expression system under control of the *tet* repressor protein (Figure 4.8) (Li *et al.*, 2009). All transduced CSC-like cells and non-CSCs were enriched by FACS sorting according to their eGFP expression to purities >98% (Figure 4.9A). Examination of CD44, CD24 and GD2 expression levels by transduced CSC-like cells and non-CSCs confirmed the stability of their phenotypical features upon transduction (Figure 4.9B). As shown in Figure 4.10, under the pretreatment with doxycycline, induction of FPPS-specific shRNA in both CSC-like cells and non-CSCs transduced with FUTG-SR22 expressing vector enhanced their susceptibility to γδ T cell-mediated killing as compared to their counterparts transduced with control FUTG-INSR vector. These results indicate that similar to the action of zoledronate, knock down of FPPS can sensitise both CSC-like cells and non-CSCs to γδ T cell-mediated killing, possibly as well through the intracellular accumulation of down-stream metabolite IPP.

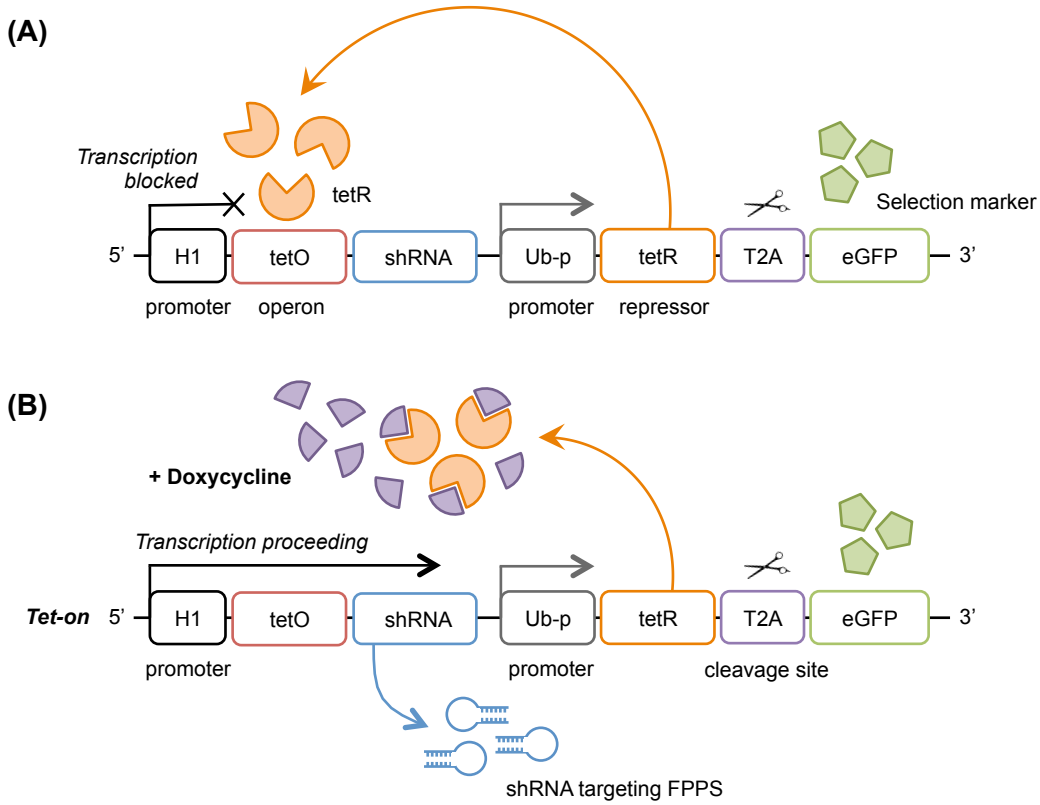

Figure 4.8. Generation of CSC-like cells and non-CSCs with inducible FPPS knockdown controlled by the *tet* operon. CSC-like cells and non-CSCs were transduced with lentiviral particles delivering the FH1tUTG vector (Li *et al.*, 2009), which contains two cassettes for the establishment of an inducible shRNA expressing system controlled by the presence of doxycycline. The FUTG-SR22 vector contains one gene cassette expressing a shRNA targeting FPPS located downstream the *tet* operon (*tet*O) under the control of the H1 promoter, and a second bicistronic cassette expressing *tet* repressor (*tet*R) in conjunction with eGFP under the control of the ubiquitin C promoter (Ub-p). *Tet*R and eGFP sequences are linked by the self-splicing 2A cleaving site of Thosea asigna virus (T2A). **(A)** In the absence of doxycycline, *tet*R is constitutively expressed by the second cassette and binds to *tet*O in the first cassette, thereby blocking the transcription of the downstream shRNA. **(B)** In the presence of doxycycline, *tet*R preferentially binds to doxycycline and is released from *tet*O, thus facilitating the onset of shRNA expression. Of note, under either condition, with or without doxycycline present, the eGFP reporter gene is expressed constitutively at the same level as *tet*R due to its linkage by T2A as a self-cleavage site.

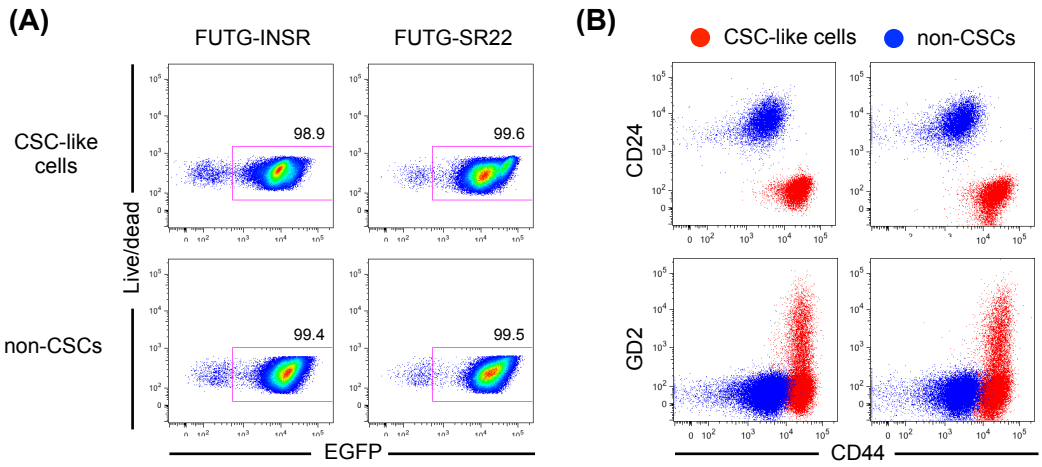

Figure 4.9. Generation of CSC-like cells and non-CSCs with regulatory FPPS knockdown. CSC-like cells and non-CSCs were transduced with lentiviral particles delivering control FUTG-INSR control vectors or FUTG-SR22 vector targeting FPPS with shRNA under control of the *tet* operon. **(A)** The transduced cells were sorted to purities >98% according to their expression of eGFP. **(B)** The transduced cells were examined for their expression of CD44, CD24 and GD2 by flow cytometry.

Note: Vector construction and cell transduction was carried out by Prof. Thomas Herrmann and his team at the University of Würzburg, Germany. Sorting of $eGFP^+$ cells and their phenotypical characterisation was performed by myself in Cardiff.

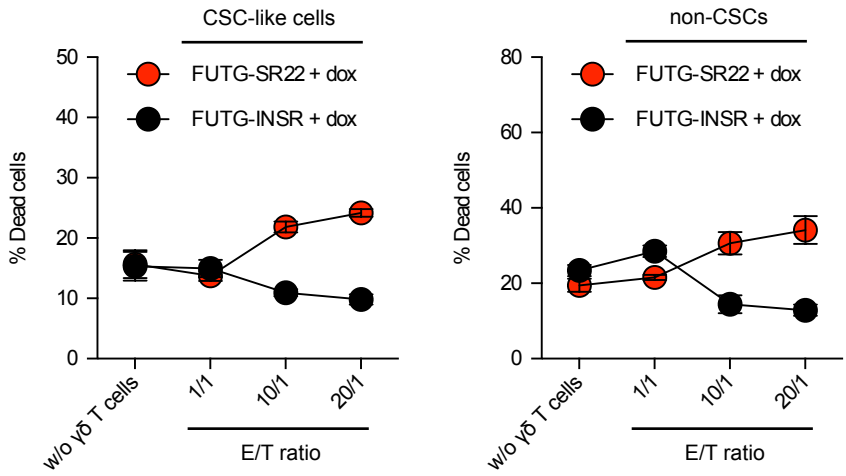

Figure 4.10. Sensitisation of CSC-like cells and non-CSCs to γδ T cell-mediated killing by FPPS knockdown. CSC-like cells and non-CSCs transduced with FUTG-INSR control vector or FUTG-SR22 vector were pretreated overnight with 0.1 mg/ml doxycycline to induce the expression of shRNA targeting FPPS in cells with FUTG-SR22 expression. After overnight pretreatment, CSC-like cells transduced with FUTG-INSR or FUTG-SR22 vector were mixed at 1:1 ratio as targets for the comparison of their susceptibility to γδ T cell-mediated killing. In parallel, non-CSCs similarly transduced with FUTG-INSR or FUTG-SR22 vector were mixed at 1:1 ratio as targets to examine the preferential killing of these two populations by γδ T cells. Results shown are from a duplicate experiment.

4.4.4. Mechanism underlying the sensitisation of CSC-like cells and non-CSCs to γδ T cell-mediated cytotoxicity by zoledronate

To confirm the involvement of γδ T cell receptor and/or other activating receptor(s) in the recognition of zoledronate-sensitised CSC-like cells and non-CSCs by γδ T cells, I next explored the possible mechanism using a panel of blocking antibodies. As shown in Figure 4.11, degranulation of γδ T cells in response to zoledronate-pretreated CSC-like cells and non-CSCs could readily be blocked by treatment of γδ T cells with neutralising antibodies against Vγ9 TCR or by treatment of target cancer cells with neutralising antibodies against BTN3A. Treatment of γδ T cells with neutralising antibodies against NKG2D showed only partial blocking effect on the activation of γδ T cells in response to zoledronate sensitised CSC-like cells and non-CSCs. Similar results were observed in experiments using IFN-γ secretion instead of CD107a translocation as readout of γδ T cell activation (Figure 4.12). These data are in line with previous findings (Thedrez *et al.*, 2007; Li *et al.*, 2009; Riganti *et al.*, 2012; Rhodes *et al.*, 2015) and confirm that zoledronate-treated target cells are predominantly recognised *via* the TCR-BTN3A axis, with NKG2D playing only a minor role.

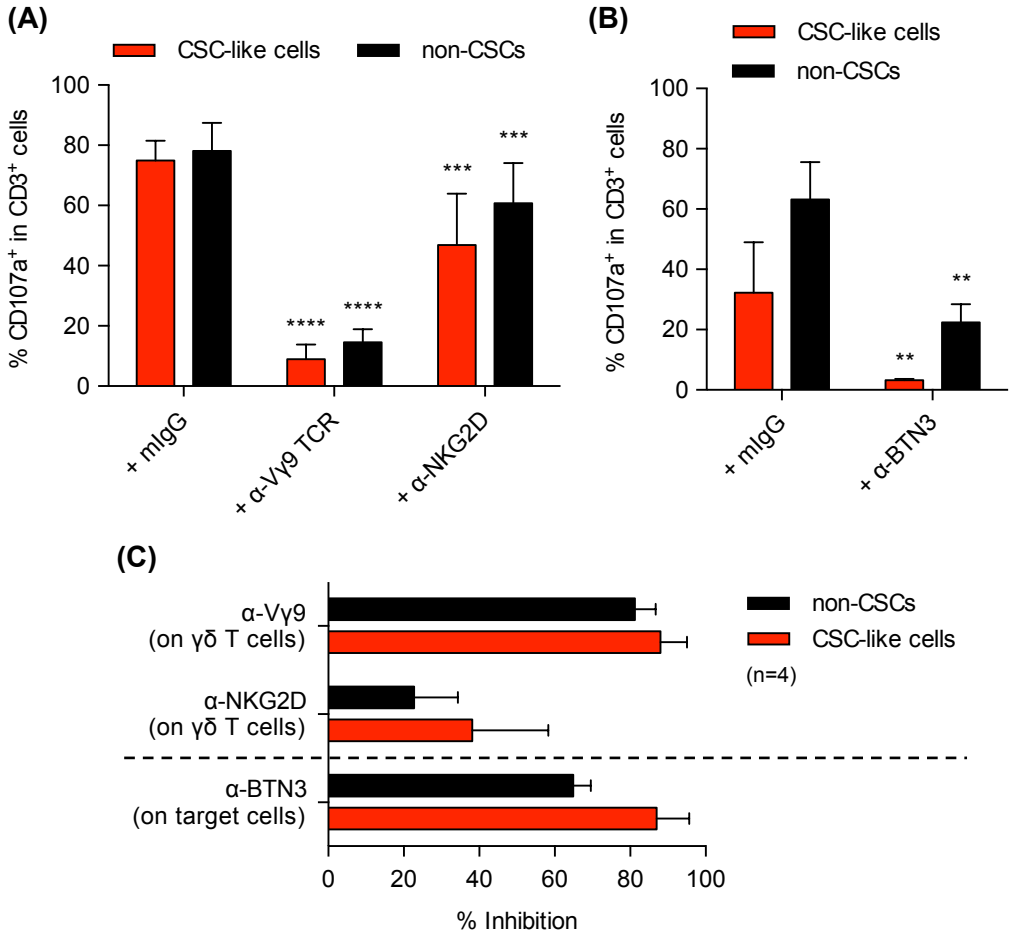

Figure 4.11. Blocking the degranulation of γδ T cells. CSC-like cells and non-CSCs were sensitised overnight with 10 μM zoledronate and co-cultured with γδ T cells. **(A)** Degranulation of γδ T cells was assessed by co-culturing target cells with γδ T cells in the presence of GolgiSTOP, PE-conjugated antibodies against CD107a and blocking antibodies against Vγ9 TCR, NKG2D or an irrelevant isotype control (mIgG) for 5 hours. **(B)** For the blocking of BTN3, cancer cells were incubated with blocking BTN3 antibodies for one hour and then washed before co-culturing them with γδ T cells. Significance of differences was calculated by two-way ANOVA. (**$p \leq 0.01$; ***$p \leq 0.001$; ****$p \leq 0.0001$). **(C)** Relative inhibition by each blocking antibody as compared with isotype controls

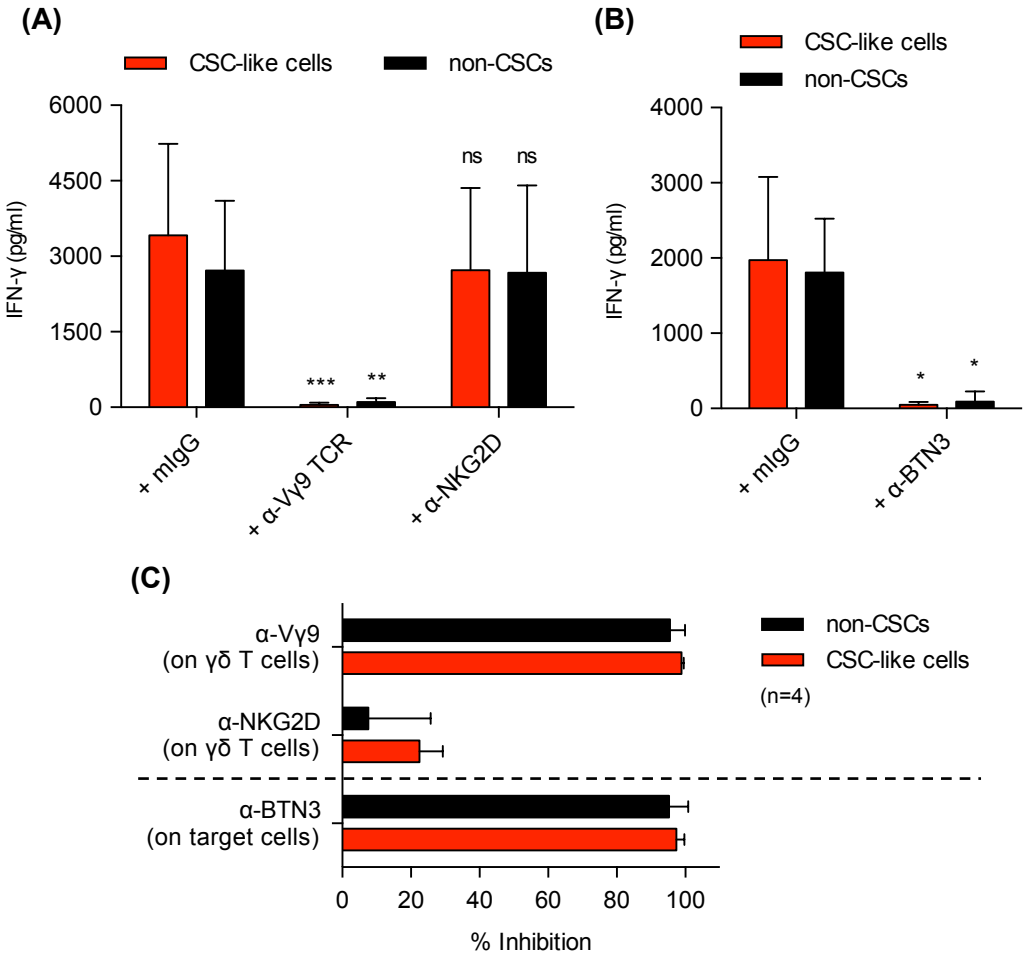

Figure 4.12. Blocking the IFN-γ secretion of γδ T cells. CSC-like cells and non-CSCs were sensitised overnight with 10 μM zoledronate and co-cultured with γδ T cells. **(A)** IFN-γ secretion by γδ T cells was assessed by co-culturing target cells with γδ T cells overnight in the presence of blocking antibodies against Vγ9 TCR, NKG2D or an irrelevant isotype control (mIgG). The amount of IFN-γ in the culture supernatants was assessed by ELISA. **(B)** For the blocking of BTN3, cancer cells were incubated with blocking BTN3 antibodies for one hour and then washed before co-culturing them with γδ T cells. Significance of differences was calculated by two-way ANOVA. (*$p \leq 0.05$; **$p \leq 0.01$; ***$p \leq 0.001$). **(C)** Relative inhibition by each blocking antibody as compared with isotype controls.

4.4.5. Sensitisation of CSC-like cells and non-CSCs to Vγ9/Vδ2 T cell-mediated cytotoxicity by humanised anti-GD2 antibodies

Besides recognition *via* the TCR and/or NKG2D (Wrobel *et al.*, 2007), Vγ9/Vδ2 T cells have also been shown to target tumour cells including breast cancer cells upon antibody opsonisation and engagement of CD16, the low affinity IgG receptor III (FcγRIII) (Gertner-Dardenne *et al.*, 2009; Capietto *et al.*, 2011; Seidel *et al.*, 2014). In line with the expression of GD2 by CSC-like cells (Figure. 3.5C), I therefore tested whether the humanised anti-GD2 antibody hu14.18K322A could confer Vγ9/Vδ2 T cells the ability to recognise and lyse CSC-like cells in the absence of zoledronate treatment. As shown in Figure 4.13, treatment with humanised anti-GD2 antibody induced a relatively small but significant enhancement of Vγ9/Vδ2 T cell activation as judged by CD107a mobilisation and IFN-γ secretion in response to hu14.18K322A-treated CSC-like cells but not to treated non-CSCs. These findings provided proof-of-concept that a specific sensitisation of cancer stem cells by monoclonal antibodies to attacks by human T cells is feasible.

In summary, these data demonstrate that resistant CSC-like cells can be sensitised to recognition by human Vγ9/Vδ2 T cells through inhibition of FPPS *via* zoledronate treatment or using shRNA, and through the use of CSC-specific opsonising antibodies.

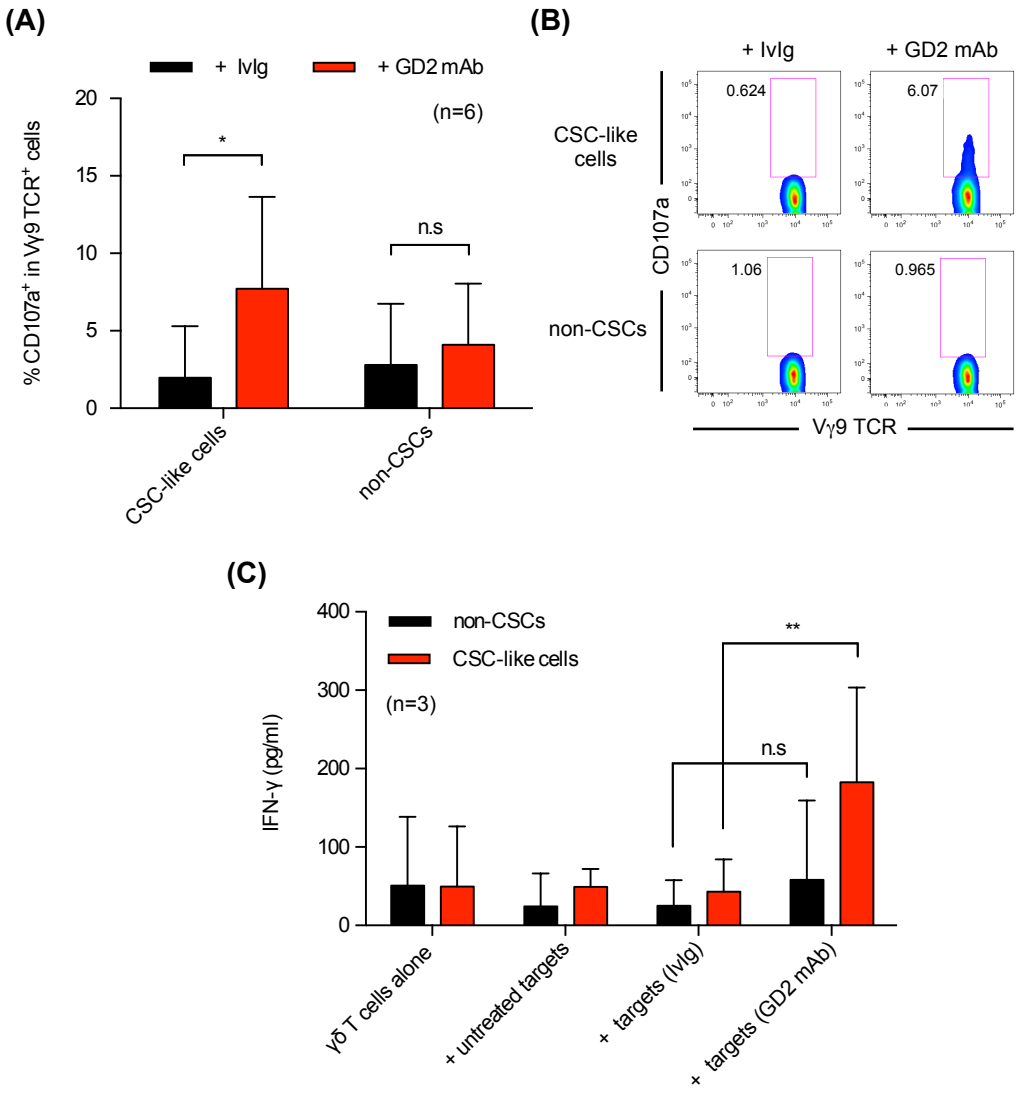

Figure 4.13. Specific targeting of CSC-like cells but not non-CSCs to γδ T cell-mediated immunity *via* opsonising antibodies. CSC-like cells or non-CSCs were individually co-cultured with expanded γδ T cells in the presence of 10 μg/ml humanised anti-GD2 monoclonal antibodies or 10 μg/ml human Ivlg as control. **(A)** Degranulation of to co-cultures of γδ T cells after five hours of co-culture in the presence of anti-CD107a antibodies and GolgiSTOP. Representative FACS plots of results are shown in **(B)**. **(C)** IFN-γ secretion by γδ T cells co-cultured overnight with CSC-like cells or non-CSCs. Significance of differences was calculated by two-way ANOVA. (*$p \leq 0.05$).

4.5. MHC-restricted killing of CSCs by antigen-specific CD8$^+$ T cells

4.5.1. Killing of CSC-like cells and non-CSCs pulsed with specific peptides by corresponding antigen-specific CD8$^+$ T cells

Apart from the non-MHC-restricted killing mediated by γδ T cells, I next investigated the recognition of HMLER-derived CSC-like cells and non-CSCs by MHC-restricted CD8$^+$ αβ T cells using two well-characterised peptides as surrogate antigens, namely the immunodominant epitopes of Flu M1, p58-66 (GILGFVFTL), and of the human cytomegalovirus (CMV) lower matrix phosphoprotein UL83/pp65, p495-503 (NLVPMVATV). As shown in Figure 4.14A, CSC-like cells and non-CSCs pulsed with Flu M1 (p58-66) were readily targeted by Flu M1-specific CD8$^+$ T cells but not by pp65-specific CD8$^+$ T cells as antigen-mismatched negative control. Similarly, CSC-like cells and non-CSCs pulsed with CMV pp65 (p495-503) were only lysed by pp65-specific CD8$^+$ T cells but not by Flu M1-specific CD8$^+$ T cells, demonstrating the specificity of the experimental system (Figure 4.14B). Of note, while epitope-specific CD8$^+$ T cells were able to kill both CSC-like cells and non-CSCs when pulsed with the cognate peptides, CSC-like cells were significantly more resistant to killing than their non-CSC counterparts (Figure 4.14A and Figure 4.14B, left panels).

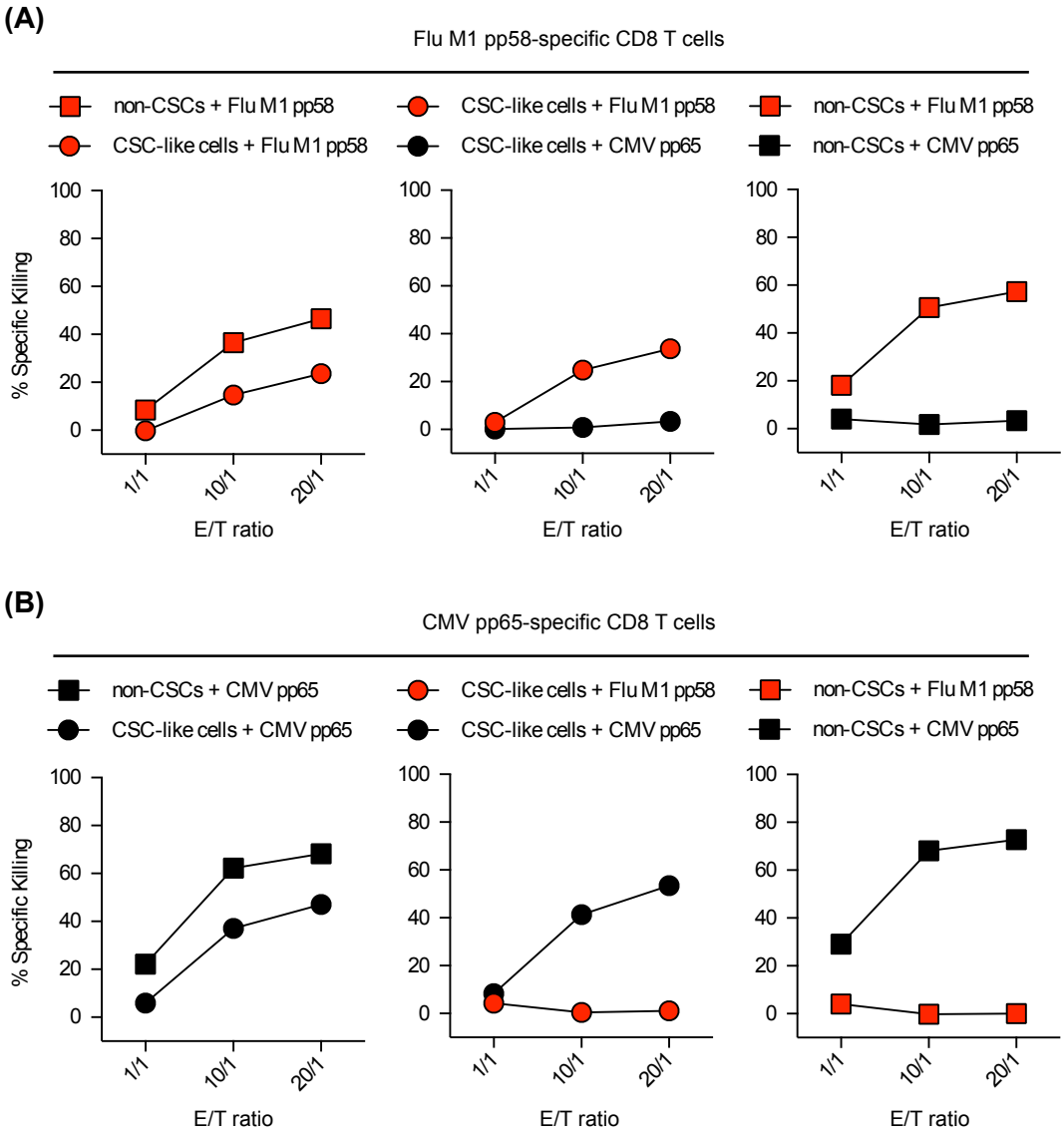

Figure 4.14. Increased resistance of CSC-like cells to MHC-restricted cytotoxic CD8$^+$ T cells. CSC-like cells and non-CSCs were pulsed with Flu M1 p58-66 peptides or CMV pp65 p495-503 peptides, labelled with CellVue or PKH26 and mixed at 1:1 ratios to prepare different target combinations as shown in the figure. These different target combinations were then co-cultured with **(A)** Flu M1- or **(B)** CMV pp65-specific CD8$^+$ T cells for 4 hours. Specific killing of target cells by CD8$^+$ T cells was revealed by Live/dead Aqua staining and analysed by flow cytometry. Data shown are from a duplicate experiment representative for two independent experiments.

4.5.2. Killing of CSC-like cells and non-CSCs with endogenous Flu M1 expression by Flu M1-specific $CD8^+$ T cells

I next translated the observations with peptide-pulsed CSC-like cells and non-CSCs to CSC-like cells and non-CSCs that had been lentivirally transduced to express Flu M1 endogenously (for generation of CSC-M1 and non-CSC-M1 cells, see section 3.6.1). As expected, Flu M1-specific $CD8^+$ T cells targeted only CSC-M1 and non-CSC-M1 cells but not their non-transduced or Gluc-expressing counterparts, which both lacked endogenous Flu M1 expression (Figure 4.15A). Notably however, in co-culture with mixtures of both CSC-M1 and non-CSC-M1 cells, Flu M1-specific $CD8^+$ T cells preferentially killed non-CSC-M1 cells compared to CSC-M1 cells (Figure 4.15B).

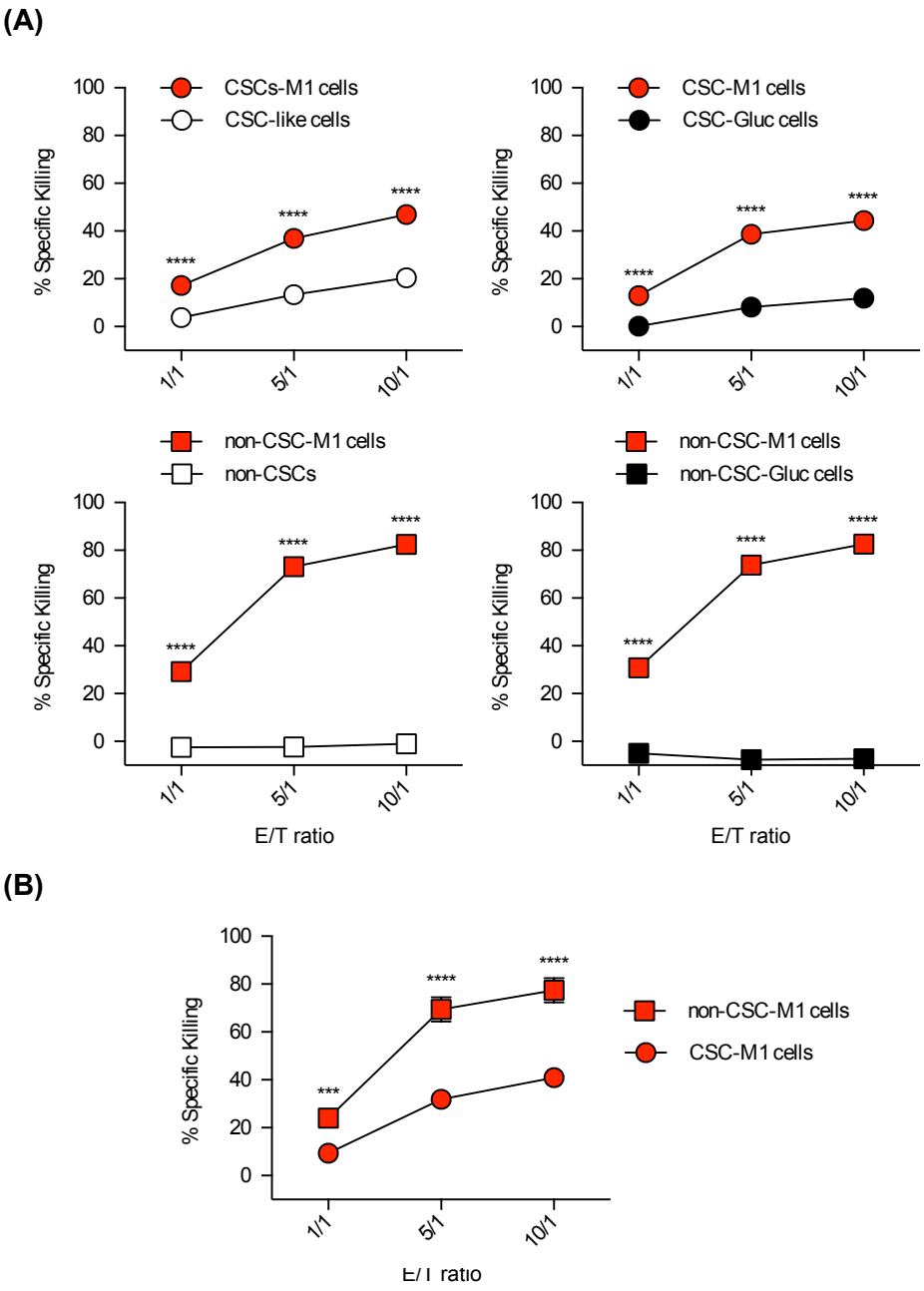

Figure 4.15. Relative resistance of CSC-M1 cells against antigen-specific cytotoxicity by CD8$^+$ T cells, compared to non-CSC-M1 cells. **(A)** CSC-M1 and non-CSC-M1 cells were mixed with their non-transduced or Gluc-expressing counterparts at 1:1 ratios and used as targets for killing by Flu M1-specific CD8$^+$ T cells. **(B)** CSC-M1 and non-CSC-M1 cells were mixed at 1:1 ratios and used as targets for killing by Flu M1-specific CD8$^+$ T cells. Data shown are from a triplicate experiment representative for two independent experiments. Significance of differences was calculated by two-way ANOVA. (***$p \leq 0.001$; ****$p \leq 0.0001$).

4.5.3. Degranulation and IFN-γ secretion by cytotoxic CD8$^+$ T cells in targeting CSC-like cells and non-CSCs

I next investigated the possible mechanism underlying the relative resistance of CSC-M1 cells to antigen-specific killing by CD8$^+$ T cells. As shown in Figure 4.16A, both non-CSC-M1 and CSC-M1 cells strongly triggered degranulation of Flu M1-specific CD8$^+$ T cells using CD107a translocation to the cell surface as experimental readout. Of note, there was a trend towards reduced degranulation in response to CSC-like cells compared to non-CSCs. This trend was substantiated by data on the cytokine secretion of activated CD8$^+$ T cells, where Flu M1-specific CD8$^+$ T cells co-cultured overnight with non-CSC-M1 cells produced considerably more IFN-γ than those co-cultured with CSC-M1 cells (Figure 4.16B). Taken together, these results show that compared to their non-CSC counterparts, CSC-like cells evade better from CD8$^+$ T cell-mediated cytotoxicity by inducing lower degree of T cell activation. Whether the CSC-like cells also acquire intrinsic resistance to cytotoxic molecules secreted by T cells such as TRAIL (Dieli *et al.*, 2007; Piggott *et al.*, 2011; Chen *et al.*, 2013) remains unclear at this stage and needs further investigation.

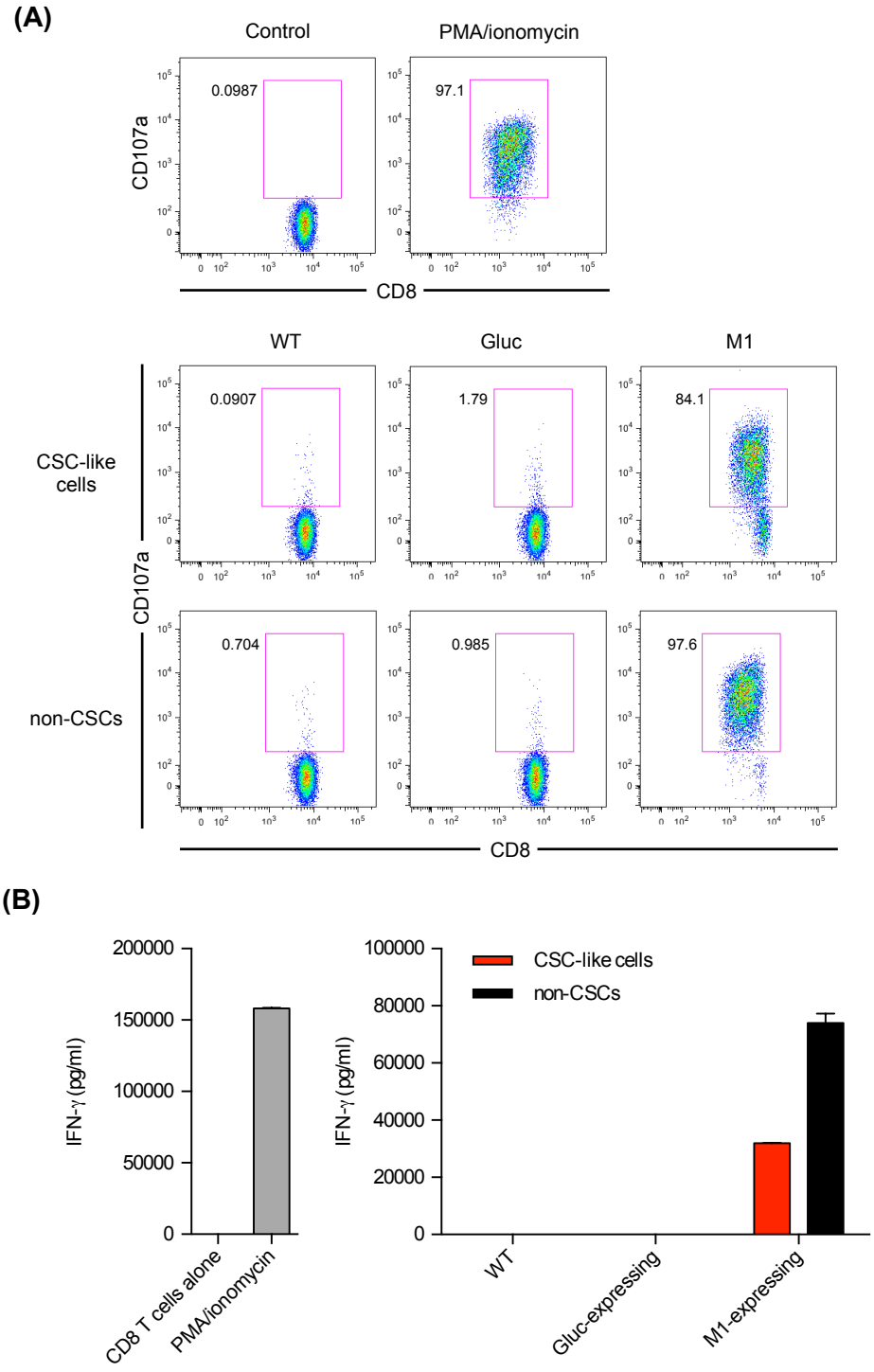

Figure 4.16. Activation of Flu M1-specific CD8$^+$ T cells by CSC-M1 and non-CSC-M1 cells. **(A)** Flu M1-specific CD8$^+$ T cells were co-cultured separately for five hours with CSC-M1 or non-CSC-M1 cells at an E/T ratio of 1:1 in the presence of GolgiSTOP and PE-conjugated mAbs against CD107a, and then analysed by flow cytometry. (**B**) Flu M1-specific CD8$^+$ T cells were co-cultured overnight with CSC-M1 or non-CSC-M1 cells at an E/T ratio of 1:1 for. Culture supernatants were collected and the amount of IFN-γ within was measured by ELISA. Data shown are from a triplicate experiment.

4.6. Sensitisation of CSC-like cells and non-CSCs to $CD8^+$ T cell-mediated killing by IFN-γ

Down-modulation of cell adhesion molecules involved in cell-cell contact and of MHC molecules and other proteins involved in antigen presentation and target cell recognition are widely used by many tumour cells as part of effective immune evasion strategies (Vesely *et al.*, 2011). Indeed, within the parental HMLER cell line, $CD44^{hi}/CD24^{lo}$ cells expressed lower levels of MHC class I (HLA-ABC) and of CD54 (ICAM-1) on the cell surface as compared to $CD44^{hi}/CD24^{lo}$ cells (Figure 4.17). Consistently, HMLER-derived CSC-like cells showed lower expression levels of both MHC class I and of CD54 as compared to their non-CSC counterparts (Figure 4.17). Interestingly, the down-regulation of CD54 in CSC-like cells increased after the isolation and maintenance as a separated line.

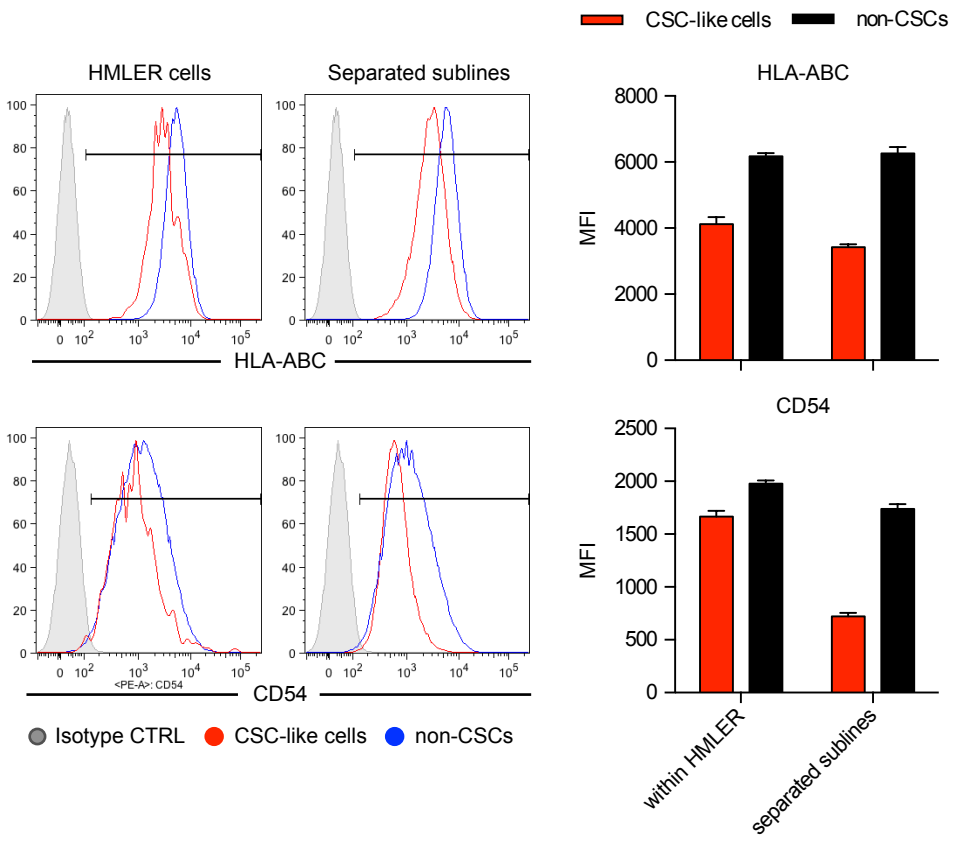

Figure 4.17. Reduced levels of MHC class I and CD54 expression on CSC-like cells compared to non-CSCs. Parental HMLER cells and HMLER-derived CSC-like cells and non-CSCs were stained with mAbs against CD44, CD24, HLA-ABC and CD54 and analysed by flow cytometry. For parental HMLER cells, the expression of HLA-ABC and CD54 was analysed by gating separately on $CD44^{hi}/CD24^{lo}$ CSC-like cells and $CD44^{lo}/CD24^{hi}$ non-CSCs. The histogram shown is representative of 3 individual stainings, the bar diagrams show means + SD from 3 independent experiments.

Treatment of parental HMLER cells with recombinant IFN-γ readily up-regulated the expression of MHC class I and CD54 by $CD44^{hi}/CD24^{lo}$ CSC-like cells and $CD44^{lo}/CD24^{hi}$ non-CSCs to similar levels (Figure 4.18A). These findings were replicated using sorted HMLER-derived CSC-like cells and non-CSCs. While recombinant IFN-γ induced similar levels of MHC class I expression on CSC-like cells and non-CSCs, the levels of IFN-γ induced CD54 expression remained lower than those induced on non-CSCs (Figure 4.18B). These findings demonstrate that the down-modulation of MHC class I and CD54 expression in CSC-like cells was regulatory rather than due to non-reversible defect at genetic level caused lost-of-function mutation.

I next tested the functional implications of the IFN-γ induced up-regulation of MHC class I and CD54 on tumour cells for their recognition by $CD8^+$ T cells. Using the peptide-loading model with Flu M1 or CMV pp65 as antigen, treatment of CSC-like cells and non-CSCs with recombinant IFN-γ led to a significantly improved killing by Flu M1-specific $CD8^+$ T cells (Figure 4.19) or by CMV pp65-specific $CD8^+$ T cells (Figure 4.20). Indeed, treatment of CSC-M1 and non-CSC-M1 cells with recombinant IFN-γ significantly increased their susceptibility to killing by Flu M1-specific $CD8^+$ T cells (Figure 4.21). Taken together, these findings indicate that the relative resistance of CSC-like cells toward $CD8^+$ T cell-mediated killing is significantly due to their reduced levels of MHC class I and CD54 expression.

The fact that IFN-γ, a cytokine that is abundantly secreted by activated γδ T cells, could effectively sensitise resistant CSC-like cells to killing by tumour antigen-specific T cells prompted me to investigate the potential of using γδ T cells as modulator for adaptive $CD8^+$ T cell responses.

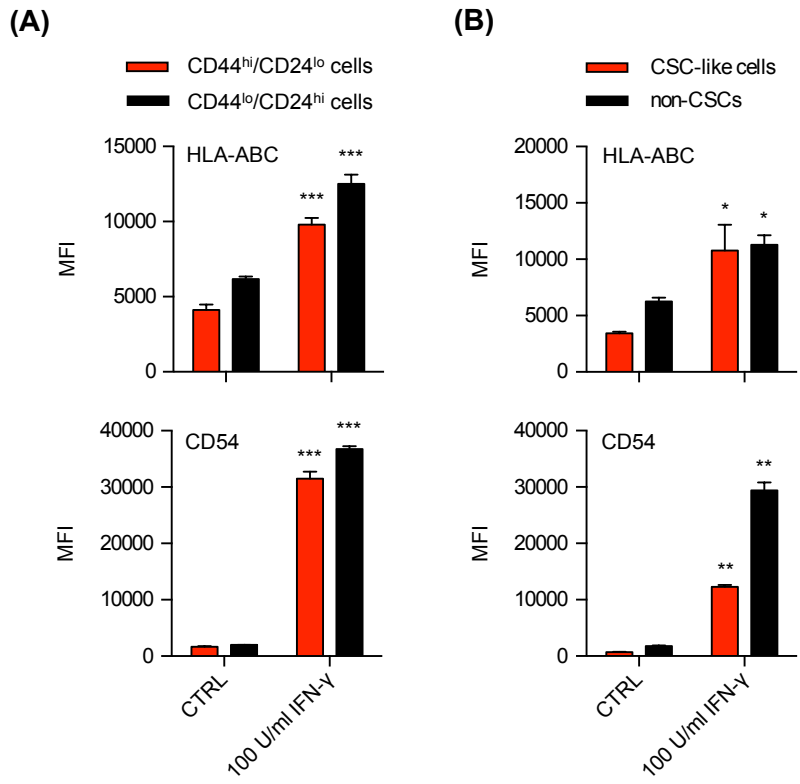

Figure 4.18. Up-regulation of MHC class I and CD54 expression on CSC-like cells and non-CSCs by IFN-γ. Parental HMLER cells and HMLER-derived CSC-like cells and non-CSCs were sensitised overnight with 100 U/ml recombinant human IFN-γ and stained with mAbs against CD44, CD24, HLA-ABC and CD54 and analysed by flow cytometry. **(A)** For parental HMLER cells treated with or without IFN-γ, the expression of HLA-ABC and CD54 was analysed by gating individually on $CD44^{hi}/CD24^{lo}$ CSC-like cells and $CD44^{lo}/CD24^{hi}$ non-CSCs. **(B)** Sorted CSC-like cells and non-CSCs were analysed for their expression of HLA-ABC and CD54 upon IFN-γ treatment as performed with parental HMLER cells. The histogram shown is representative of 3 individual staining, the bar diagrams show means + SD from 3 independent experiments. Significance of differences was calculated by non-parametric two-way ANOVA (*$p \leq 0.05$; **$p \leq 0.01$; ***$p \leq 0.001$). Asterisks indicate the significance of difference between untreated control group and group with IFN-γ treatment for CSC-like cells or non-CSCs.

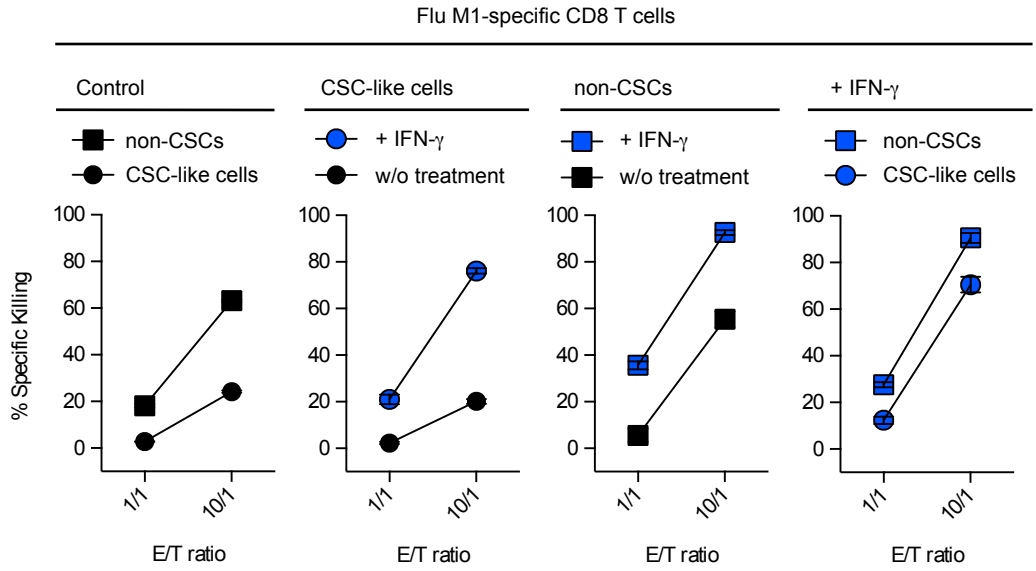

Figure 4.19. Sensitisation of CSC-like cells and non-CSCs to killing by Flu M1-specific CD8$^+$ T cells. CSC-like cells and non-CSCs were sensitised overnight with or without 100 U/ml recombinant human IFN-γ and then pulsed with Flu M1 pp58-66 peptides. Different target cell populations loaded with peptides were then labelled with CellVue or PKH26, and mixed at 1:1 ratio to generate the target cell mixtures shown in the figure for co-cultures with Flu M1-specific CD8$^+$ T cells. The killing of different targets in co-culture with Flu M1-specific CD8$^+$ T cells was analysed by flow cytometry by gating on CellVue$^+$ and PKH26$^+$ cells. Data shown are results of an experiment with triplicates.

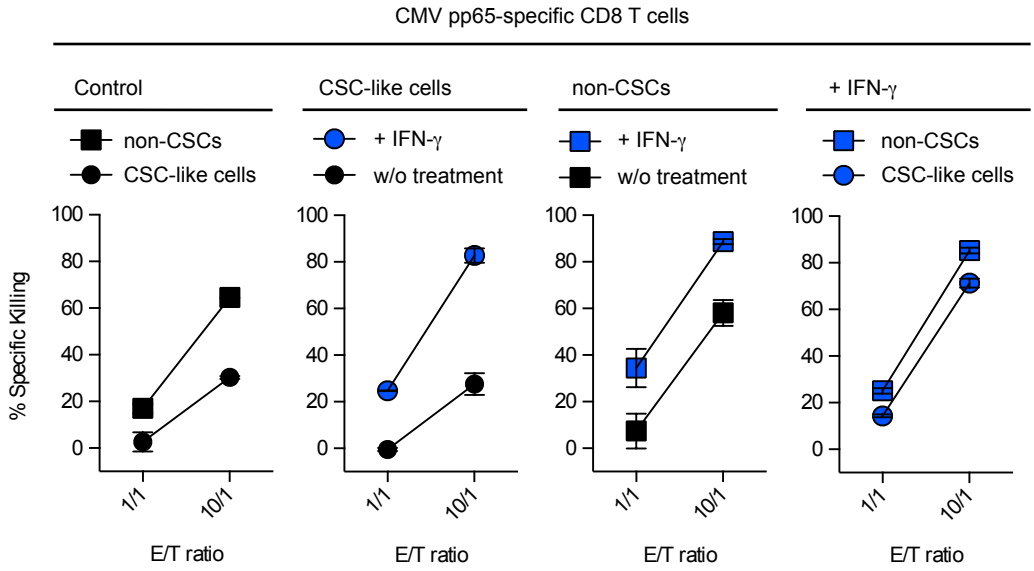

Figure 4.20. Sensitisation of CSC-like cells and non-CSCs to killing by CMV pp65-specific CD8$^+$ T cells. CSC-like cells and non-CSCs were sensitised with or without 100 U/ml recombinant human IFN-γ for overnight and then pulsed with CMV pp65 p495-503 peptides. Target cells loaded with peptides were then mixed at 1:1 ratio to make the pairs as shown in the figure for the following co-culture with CMV pp65-specific CD8$^+$ T cells. Data shown are results of an experiment with triplicates.

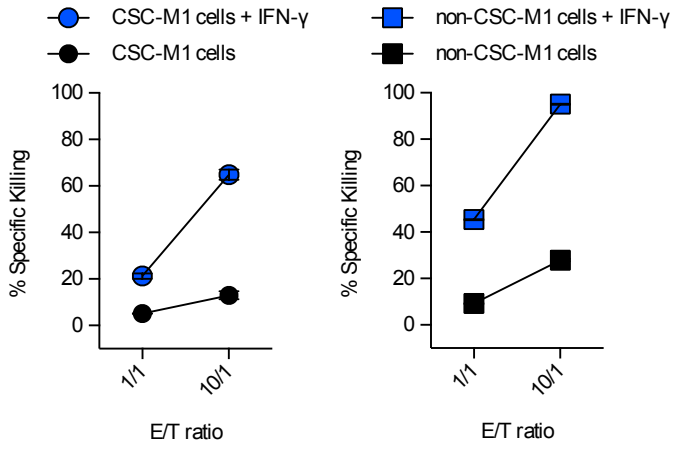

Figure 4.21. Sensitisation of CSC-M1 cells and non-CSC-M1 cells to killing by Flu M1-specific CD8$^+$ T cells. CSC-M1 cells and non-CSC-M1 cells were sensitised overnight with or without 100 U/ml recombinant human IFN-γ. Different target cell populations were then labelled with CellVue or PKH26, and mixed at 1:1 ratio to generate the target cell mixtures shown in the figure for co-cultures with Flu M1-specific CD8$^+$ T cells. The killing of different targets in co-culture with Flu M1-specific CD8$^+$ T cells was analysed by flow cytometry by gating on CellVue$^+$ and PKH26$^+$ cells. Data shown are results of experiment with triplicates.

4.7. Sensitisation of CSC-like cells and non-CSCs to cytotoxic $CD8^+$ T cells by Vγ9/Vδ2 T cell conditioned supernatant

Having shown that both CSC-like cells and non-CSCs can be sensitised to killing by either human αβ T cells and γδ T cells, we next addressed the potential synergy of these types of T cells in targeting resistant tumour cells, especially CSC-like cells, by combining the antigen-specific nature of cytotoxic $CD8^+$ T cells and the innate killer function of non-MHC restricted γδ T cells. Given earlier reports showing that IFN-γ increases immunogenicity of CSCs in head and neck cancer cell lines to cytotoxic $CD8^+$ T cells (Liao *et al.*, 2013) and my own observation that recombinant IFN-γ had a striking effect on sensitising CSC-like cells to cytotoxic $CD8^+$ T cells (Figure 4.19, 20 and 21), I next explored the possibility to manipulate γδ T cells as physiological source of IFN-γ in order to boost the targeting of CSCs by cytotoxic $CD8^+$ T cells. For these experiments I generated conditioned medium by treating expanded γδ T cells overnight with HMB-PP, based on the earlier observation that stimulation of expanded γδ T cells with HMB-PP could induce section of IFN-γ (Figure 4.3). Alternatively, I generated conditioned medium by treating co-cultures of primary γδ T cells and autologous monocytes overnight with zoledronate. Treatment of CSC-like cells and non-CSCs with supernatant of HMB-PP stimulated expanded γδ T cells significantly increased their expression of MHC class I and CD54 (Figure 4.22). A similar up-regulation was observed when treating CSC-like cells and non-CSCs with conditioned medium of zoledronate-treated co-cultures of freshly isolated γδ T cells and monocytes, which mimics the activation of γδ T cells by zoledronate-sensitised tumour cells (Figure 4.23).

In order to confirm the crucial role of γδ T cell-derived IFN-γ in mediating these phenotypical changes, I used neutralising monoclonal antibodies against IFN-γ. As shown in Figure 4.24, the γδ T cell-induced up-regulation of MHC class I and CD54 expression by CSC-like cells and non-CSCs could be blocked completely with anti- IFN-γ antibodies, identifying IFN-γ as the major modulator secreted by γδ T cells enhancing target immunogenicity to cytotoxic $CD8^+$ T cells.

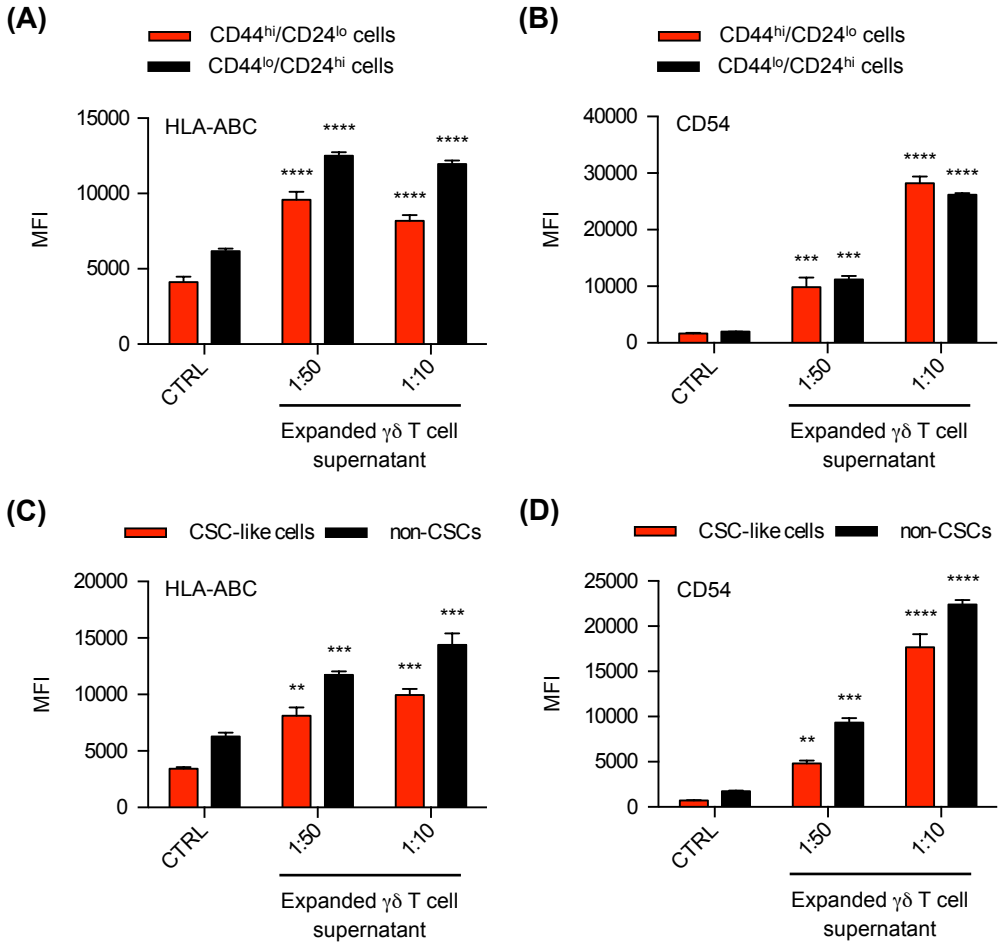

Figure 4.22. Up-regulation of MHC class I and CD54 expression on CSC-like cells and non-CSCs by HMB-PP stimulated primary γδ T cells. HMLER cells were treated overnight with conditioned medium of HMB-PP stimulated γδ T cells at 1:10 and 1:50 dilutions and analysed for their expression of **(A)** MHC class I and **(B)** CD54 by flow cytometry. Data shown are pooled from experiments using γδ T cell supernatants collected from 3 different donors. Significance of differences was calculated by non-parametric two-way ANOVA (**$p \leq 0.01$; ***$p \leq 0.001$; ****$p \leq 0.0001$). For both CSC-like cells and non-CSCs, asterisks indicate the significance of difference between untreated control group and groups treated with γδ T cell supernatants at 1:10 or 1:50 dilution.

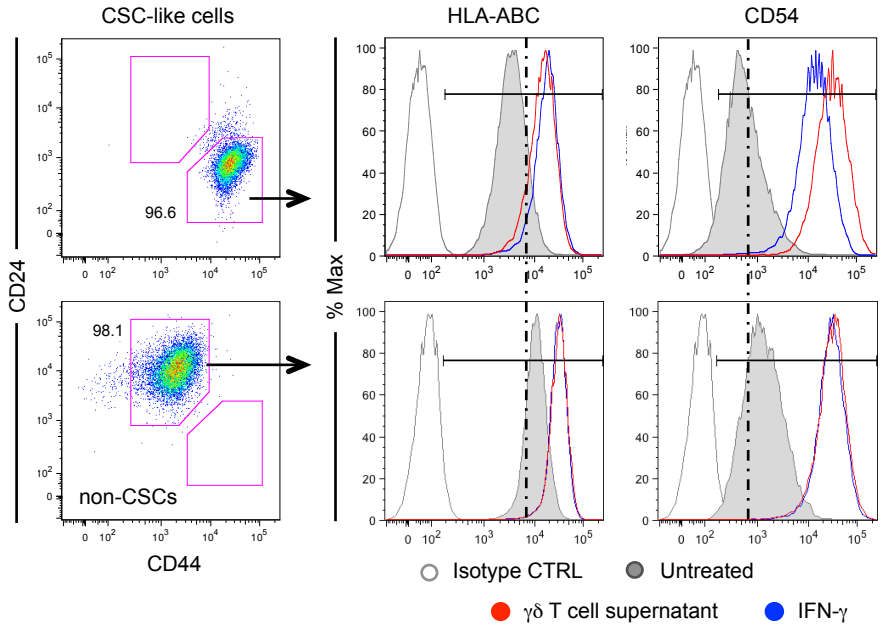

Figure 4.23. Up-regulation of MHC class I and CD54 expression on CSC-like cells and non-CSCs by zoledronate-stimulated expanded γδ T cells. CSC-like cells and non-CSCs were treated overnight with conditioned medium of zoledronate-stimulated co-cultures of γδ T cells and monocytes, and analysed for their expression of MHC class I and CD54 by flow cytometry. Data shown are representative for two independent experiments

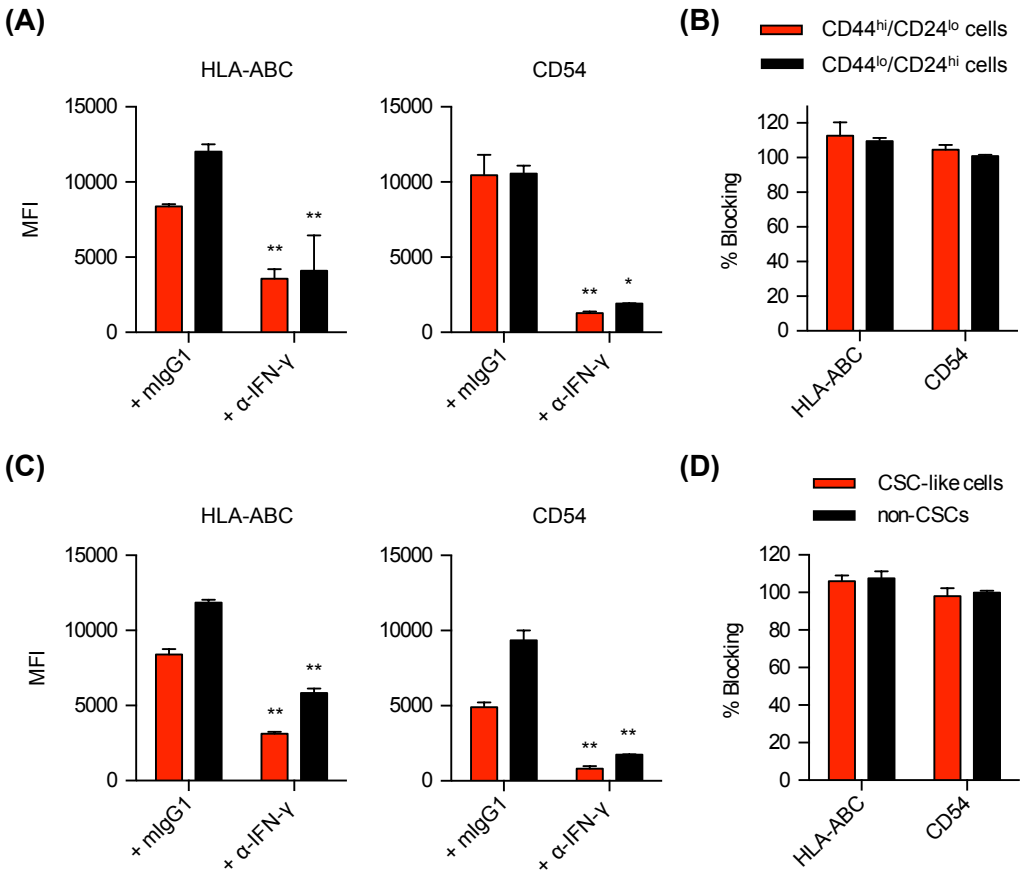

Figure 4.24. Abrogation of expanded γδ T cell-mediated MHC class I and CD54 up-regulation on CSC-like cells and non-CSCs by IFN-γ neutralising antibodies. HMLER cells **(A, B)** or HMLER-derived CSC-like cells and non-CSCs **(C, D)** were treated overnight with γδ T cell conditioned medium in the presence of IFN-γ neutralising antibodies or isotype antibodies, and analysed for their expression of **(A, C)** MHC class I and CD54 by flow cytometry. The % blocking was calculated and shown in **(B, D)**. Data shown are pooled from experiments using γδ T cell supernatants collected from 3 different donors. Significance of differences was calculated by non-parametric two-way ANOVA (*$p \leq 0.05$; **$p \leq 0.01$). For both CSC-like cells and non-CSCs, asterisks indicate the significance of difference between untreated control group and group treated with γδ T cell supernatants at 1:10 dilution.

These findings indicate that γδ T cells can enhance antigen presentation by CSC-like cells and non-CSCs to $CD8^+$ T cells, thus potentially leading to improved immunosurveillance by $CD8^+$ T cells. Indeed, using the peptide pulsing as assay described before (Figures 4.14, 4.19 and 4.20), treatment of both CSC-like cells and non-CSCs with conditional medium of activated primary γδ T cells by zoledronate in the presence of monocytes as APCs led to better killing by cytotoxic $CD8^+$ T cells specific for Flu M1 (Figure 4.25) or to CMV pp65 (Figure 4.26). Consistently, treatment of both CSC-M1 and non-CSC-M1 cells with culture supernatants obtained from HMB-PP stimulated γδ T cells also significantly enhanced their susceptibility to killing by Flu M1-specific $CD8^+$ T cells (Figure 4.27). Neutralisation of IFN-γ in the γδ T cell supernatants effectively abrogated the enhanced killing of both CSC-M1 and non-CSC-M1 by Flu M1-specific $CD8^+$ T cells (Figure 4.28).

Taken together, these results indicate that IFN-γ secreted by activated γδ T cells enhance the susceptibility of CSC-like cells and non-CSCs to cytotoxic $CD8^+$ T cell-mediated killing *via* up-regulating their expression of HLA class I and CD54, thereby enabling better antigen presentation and cell-cell contact with $CD8^+$ T cells.

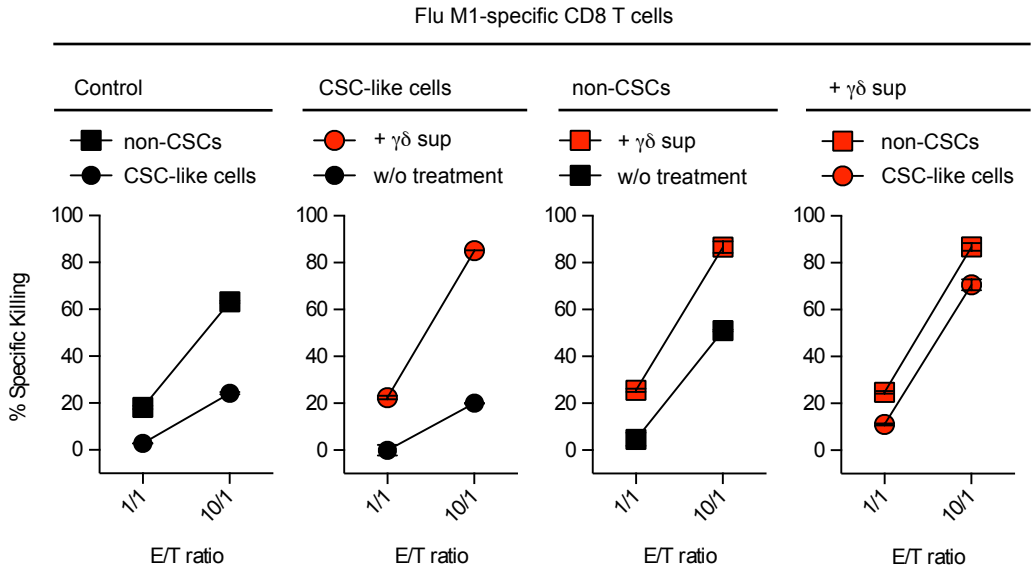

Figure 4.25. Sensitisation of CSC-like cells and non-CSCs to Flu M1-specific CD8$^+$ T cell killing by γδ T cells. CSC-like cells and non-CSCs were treated overnight with conditioned medium of zoledronate-stimulated co-cultures of γδ T cells and monocytes, and pulsed with Flu M1 p58-66 peptides for the analysis of their susceptibility to Flu M1-specific CD8$^+$ T cells. Data shown are results of an experiment with triplicates.

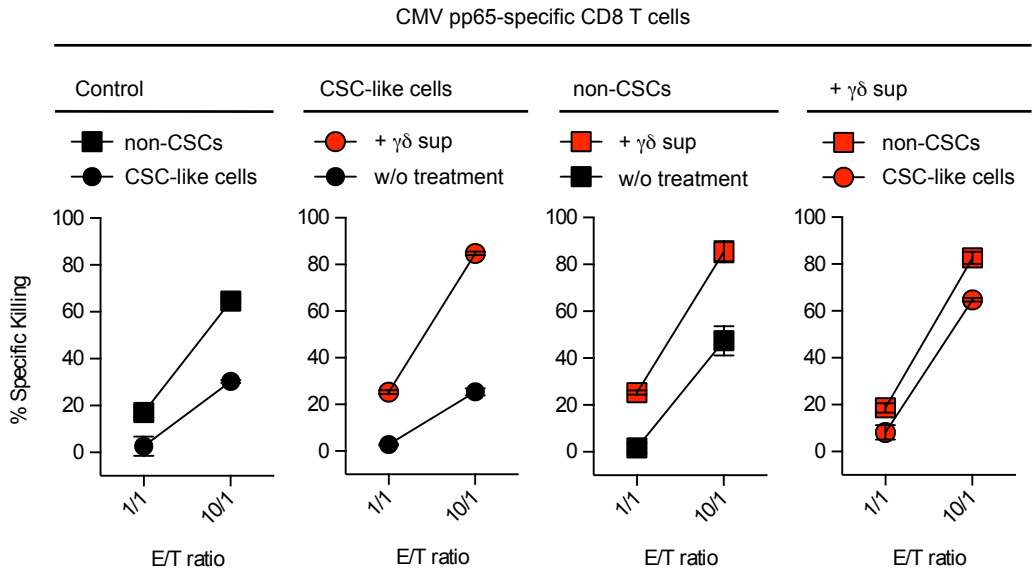

Figure 4.26. Sensitisation of CSC-like cells and non-CSCs to CMV pp65-specific CD8$^+$ T cell killing by γδ T cells using CMV pp65 p495-503 pulsing model. CSC-like cells and non-CSCs were treated for overnight with conditioned medium of zoledronate-stimulated co-cultures of γδ T cells and monocytes, and the pulsed with CMV pp65 p495-503 peptides for the analysis of their susceptibility to CMV pp65-specific CD8$^+$ T cells. Data shown are results of an experiment with triplicates.

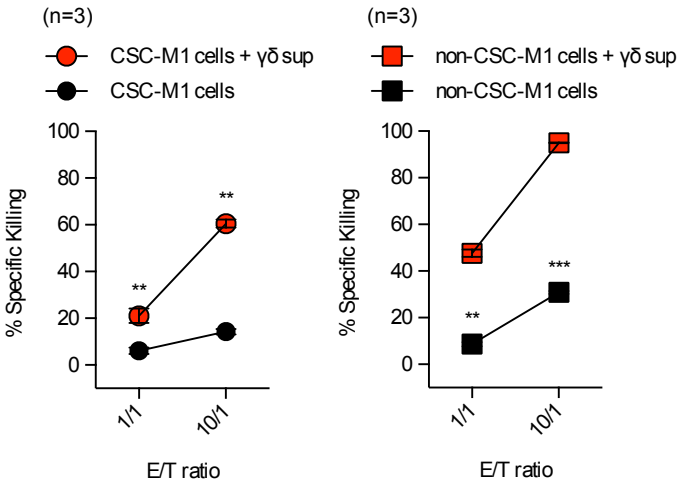

Figure 4.27. Sensitisation of CSC-M1 and non-CSC-M1 cells to Flu M1-specific CD8$^+$ T cell killing by γδ T cells. CSC-M1 and non-CSC-M1 cells were treated overnight with conditioned medium of expanded γδ T cells stimulated with HMB-PP for the analysis of their susceptibility to Flu M1-specific CD8$^+$ T cells. Data shown are pooled from experiments using γδ T cell supernatants collected from 3 different donors. Significance of differences was calculated by non-parametric two-way ANOVA (**$p \leq 0.01$; ***$p \leq 0.001$).

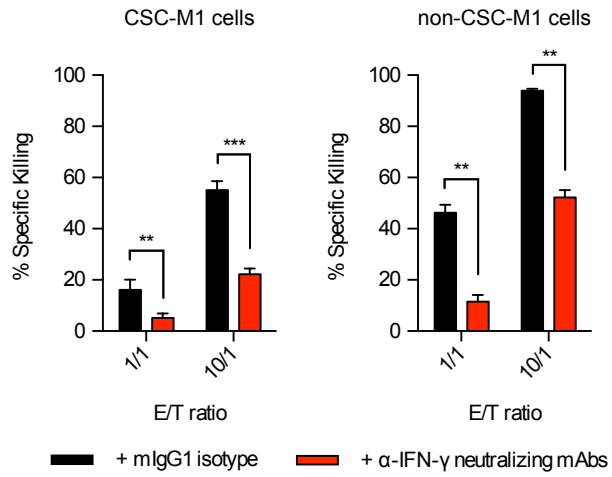

Figure 4.28. Abrogation of γδ T cell-mediated sensitisation of CSC-like cells and non-CSCs to CD8$^+$ T cell killing by IFN-γ neutralising antibodies. CSC-M1 and non-CSC-M1 cells were treated overnight with conditioned medium of HMB-PP stimulated γδ T cells in the presence of anti-IFN-γ neutralising antibodies or mouse IgG1 isotype control antibodies for the analysis of their susceptibility to Flu M1-specific CD8$^+$ T cells. Data shown are pooled from experiments using γδ T cell supernatants collected from 3 different donors. Significance of differences was calculated by non-parametric two-way ANOVA (**$p \leq 0.01$; ***$p \leq 0.001$).

4.8. Discussion

In this chapter, I firstly show that Vγ9/Vδ2 T cells could be expanded from healthy donor PBMCs with zoledronate and IL-2 in long-term culture over a period of 14 days. Over 14 days of expansion, Vγ9/Vδ2 T cells uniformly differentiated into T_{EM} status with a $CD45RA^{-}$ $CD27^{-}$ phenotype (Figure 4.2), which has been characterised as the main population functionally responsible for release of IFN-γ upon stimulation with phosphoantigens through TCR recognition (Dieli *et al.*, 2003). Angelini *et al.* showed that CD16 expression specifically discriminates a population of T_{EMRA} cells that exhibits strong cytotoxicity through the perforin pathway but lacks the capacity to secrete IFN-γ (Angelini *et al.*, 2004). My results show that expanded Vγ9/Vδ2 T cells expressed CD16 generally at a relatively low level with large variability between different donors (Figure 4.1). Expanded Vγ9/Vδ2 T cells maintained their responsiveness to stimulation with exogenous HMB-PP and with zoledronate-treated cancer cells, and were able to both secrete IFN-γ and kill (in terms of degranulation and cytotoxicity) efficiently (Figure 4.3 and 4.5-7). These functional analyses confirm the expansion of a mixture of secretory T_{EM} and cytotoxic T_{EMRA} cells, and that T_{EM} within the expanded populations may retain the plasticity to differentiate further into T_{EMRA} cells. The functional differentiation of Vγ9/Vδ2 T cells into memory subsets and their subsequent maintenance has been shown essential and critical for competent disease control and clinical outcome of end-stage prostate and breast cancer patients treated with zoledronate and IL-2 (Dieli *et al.*, 2003; Dieli *et al.*, 2007; Meraviglia *et al.*, 2010). A phase I trial on metastatic hormone-refractory prostate cancer showed that expansion of effector memory Vγ9/Vδ2 T cells by administration of zoledronate and low-dose IL-2 was correlated with beneficial clinical outcomes with remission or stable disease in several treated patients (Dieli *et al.*, 2007). Similarly, another trial with 10 patients with advanced metastatic breast cancer showed that treatment of these patients with zoledronate and low-dose IL-2 was safely tolerated and successfully promoted the effector maturation of Vγ9/Vδ2 T cells. The sustained maintenance of Vγ9/Vδ2 T cell responses in three patients may have contributed to partial remission and stable disease in these individuals (Meraviglia *et al.*, 2010). These findings strongly suggest that treatment of cancer patients with zoledronate and IL-2 is safe and feasible. Expansion of Vγ9/Vδ2 T cells with nBPs *in vitro* has been reported by the use of PBMCs collected from patients with melanoma (Khan *et al.*, 2014a), chronic myelogenous leukaemia (D'Asaro *et al.*, 2010) and others, suggesting *ex vivo* expansion of autologous Vγ9/Vδ2 T cells from patients for personalised adoptive transfer is feasible.

Taken together, adjuvant therapy by continuous administration of zoledronate and IL-2 may benefit the efficacy of adoptive transfers of *ex vivo* expanded effector γδ T cells in cancer patients (Dieli *et al.*, 2007; Santini *et al.*, 2009; Meraviglia *et al.*, 2010; Welton *et al.*, 2013a). These encouraging observations prompt us to investigate further the possibility of using *ex vivo* expanded Vγ9/Vδ2 T cells as effector cells for targeting CSCs.

Both CSC-like cells and non-CSCs isolated from the HMLER cell line (Chapter 3) were resistant to killing by Vγ9/Vδ2 T cells but could be sensitised efficiently by pretreatment with zoledronate (Figure 4.4 and 4.5). In co-culture with CSC-like or non-CSCs, there no activation of Vγ9/Vδ2 T cells was observed in terms of degranulation and IFN-γ secretion, suggesting that both CSC-like and non-CSCs were invisible for the recognition by Vγ9/Vδ2 T cells. This invisibility could be due to suboptimal concentrations of intracellular IPP, and the lack of expression of ligands such as MICA/B and ULBP1-4 for the recognition by Vγ9/Vδ2 TCR and NKG2D, respectively (Rey *et al.*, 2009; Chen *et al.*, 2013). The fact that both zoledronate-sensitised CSC-like cells and non-CSCs could be killed efficiently by Vγ9/Vδ2 T cells (Figure 4.5 and 4.10) and nearly 100% by cytotoxic $CD8^+$ T cells (Figure 4.19-21 and 4.25-27) showed that these cells possessed no intrinsic resistance to apoptosis induced by cytotoxic molecules such as TRAIL, FasL, granulysin, granzyme and perforin released by activated immune effector cells including both Vγ9/Vδ2 T cells and cytotoxic $CD8^+$ T cells. By mimicking the action of zoledronate through specific knock-down of FPPS, a similar sensitisation effect to Vγ9/Vδ2 T cell-mediated cytotoxicity was observed, confirming the role of IPP accumulation in activating Vγ9/Vδ2 T cells (Figure 4.10). Ginestier *et al.*, showed by gene expression profiling that mammospheres derived from basal-like cancer cell lines exhibited a hyperactivated mevalonate pathway as compared to their counterparts cultured in adherent conditions and that protein geranylgeranylation downstream geranylgeranyl-PP (Figure 1.1) is critical for the maintenance of breast CSCs (Ginestier *et al.*, 2012). These findings may partially explain why CSC-like cells are resistant to Vγ9/Vδ2 T cells, assuming that IPP does not accumulate inside the cells due to rapid turnover and strong downstream geranylgeranyl transferase activity. This also indicates that the mevalonate pathway is a critical candidate for targeting CSCs due to its pivotal role in both essential metabolism of CSCs and in stimulating effector functions of Vγ9/Vδ2 T cells

The stimulation of Vγ9/Vδ2 T cells by both zoledronate-sensitised CSC-like cells and non-CSCs could almost totally be abrogated by neutralisation of the TCR (but not NKG2D) on Vγ9/Vδ2 T cells and by neutralisation of BTN3 on target cells (Figure 4.11 and12). These results suggest that the zoledronate-mediated sensitisation was majorly through the Vγ9/Vδ2 TCR recognition of intracellularly accumulated phosphoantigens, most likely IPP. Consistently, Dhar *et al*., showed that treatment with zoledronate and pamidronate efficiently sensitised the breast cancer cell line MCF-7 to Vγ9/Vδ2 T cell-mediated killing majorly through TCR recognition and downstream perforin cytotoxic pathway (Dhar and Chiplunkar, 2010). Although recognition through NKG2D alone without engagement on Vγ9/Vδ2 TCR is sufficient for the activation of Vγ9/Vδ2 T cells (Rincon-Orozco *et al.*, 2005; Lanca *et al.*, 2010), concomitant recognition of MICA/B *via* NKG2D may enhance the effector function of Vγ9/Vδ2 T cells activated *via* Vγ9/Vδ2 TCR engagement (Das *et al.*, 2001; Nedellec *et al.*, 2010b). Nevertheless, it remains unclear whether treatment of CSC-like cells and non-CSCs with zoledronate modulate their expression of ligands for NKG2D and NCRs. A comprehensive screening for the expression of ligands in CSC-like cells and non-CSCs with and without zoledronate pretreatment should be done in the future.

Todaro *et al.* recently demonstrated the feasibility of such a combined approach, by showing that low concentrations of the chemotherapeutic agents 5-fluorouracil and doxorubicin successfully sensitise colon cancer-initiating cells to γδ T-cell-mediated cytotoxicity, which is dependent on the recognition of target cells by NKG2D and the interaction between TRAIL and TRAIL-R2 (Todaro *et al.*, 2013). Of note, the same population of colon cancer-initiating cells could also be sensitised to γδ T-cell-mediated cytotoxicity by pretreatment with zoledronate, leading to increased recognition by the TCR and killing *via* perforin and granzyme (Todaro *et al.*, 2009). It is therefore conceivable that in instances in which TCR ligand expression by tumour cells is below the threshold required for efficient recognition by γδ T cells, especially in CSCs, target recognition may occur predominantly through NKG2D (Figure 4.29). Forced accumulation of IPP in zoledronate-treated cells may then favour TCR-mediated killing. In contrast, chemotherapy or other treatments enhancing expression of NKG2D ligands may boost NKG2D-mediated killing. As consequence, appropriate manipulation of anti-apoptotic and pro-apoptotic pathways will effectively sensitise tumour cells to either perforin/granzyme or TRAIL, or both.

Consistently, Nishio *et al*. showed that neuroblastoma cells maintained in both sphere culture and adherent culture were resistant to Vγ9/Vδ2 T cell-mediated killing but could be efficiently sensitised by treatment with zoledronate (Nishio *et al.*, 2012). In contrary, Lai *et al.* showed that spheres of SKOV3 ovarian cancer cells were endogenously susceptible to Vγ9/Vδ2 T cell killing (Lai *et al.*, 2012), reinforcing the notion that Vγ9/Vδ2 T cells are indeed an important candidate for targeting CSCs. Of note, these studies used sphere cultures to enrich CSCs from the bulk population of tumour cells. However, long-term culture in sphere culture may potentially change the nature of both CSCs and non-CSCs with respect to differentiation, dedifferentiation or environmental stresses. Taking advantage of the stability of HMLER-derived CSC-like and non-CSC cells as described in this Thesis, my experimental model provides a powerful approach by maintaining both subsets under identical culture conditions for direct comparison of their susceptibility to Vγ9/Vδ2 T cells.

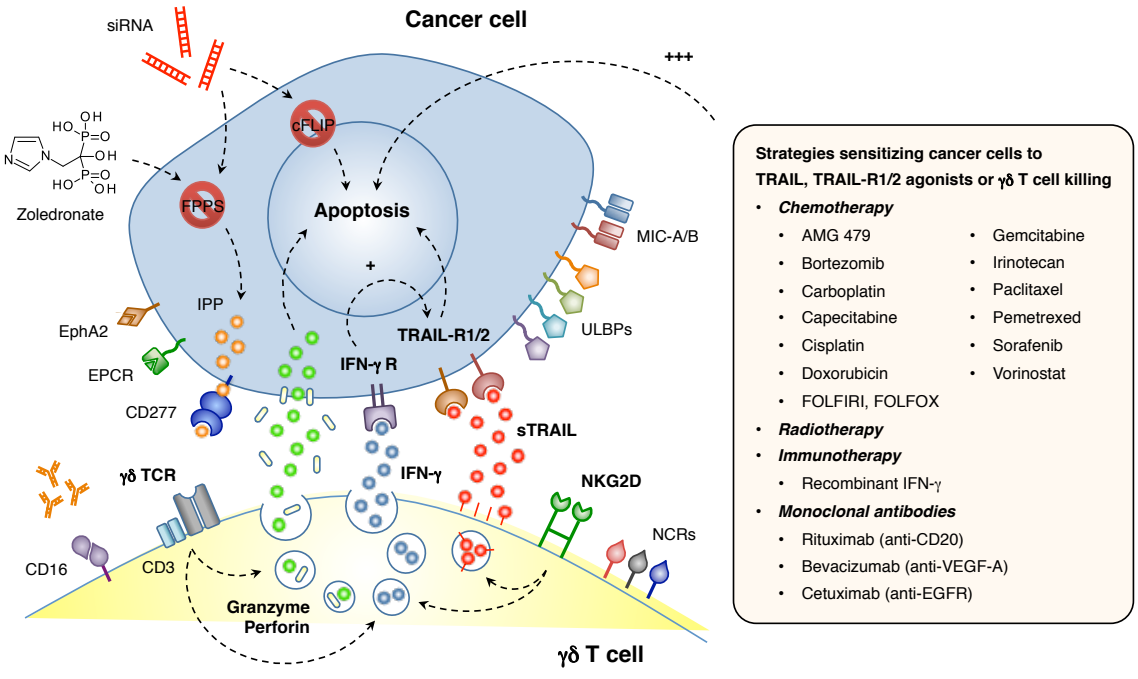

Figure 4.29. Human γδ T-cell mediated killing of tumour cells (Chen *et al.*, 2013). Different targets are recognised through expression of NKG2D ligands such as MICA/B or members of the ULBP family, or by expression of γδ T-cell receptor (TCR) ligands such as butyrophilin-3A1 (CD277), endothelial protein C receptor (EPCR) or ephrin receptor A2 (EphA2), ultimately inducing local secretion of effector molecules including IFN-γ, TRAIL, perforin and granzymes. Other pathway such as triggering of natural cytotoxicity receptors (NCRs) or induction of antibody-

dependent cellular cytotoxicity (ADCC) via CD16 may contribute to this response. TRAIL induces apoptosis in target cells via binding to TRAIL-R1 and/or TRAIL-R2. In the case of Vδ2$^+$ T cells, tumour cells can be specifically sensitised by inhibition of farnesyl pyrophosphate synthase (FPPS) through zoledronate and related aminobisphosphonates, or through siRNA-mediated knockdown, leading to intracellular accumulation of IPP and 'presentation' by BTN3/CD277. Other strategies to sensitise refractory cells to TRAIL mediated killing involve a wide range of approaches, including targeted inhibition of c-FLIP.

In addition to sensitisation with zoledronate, I showed that treatment with humanised anti-GD2 antibodies (hu14.18K322A) could selectively direct Vγ9/Vδ2 T cell against CSCs but not non-CSCs (Figure 4.13). However, the effect of this opsonisation-dependent sensitisation was limited. This is possibly due to the fact that only about 30% of CSC-like express GD2 on their surface. An attempt to sensitise purified GD2$^+$ CSCs failed as these cells quickly differentiated and lost their expression of GD2. Although the effect of sensitisation is therefore limited in my hands, similar strategies have widely been employed for treating neuroblastoma by efficiently inducing NK-mediated ADCC (Ahmed and Cheung, 2014; Navid *et al.*, 2014), and for facilitating cross-presentation of tumour cell-released antigens by Vγ9/Vδ2 T cells to CD8$^+$ T cells (Himoudi *et al.*, 2012). Besides GD2, other markers could potentially be targeted for directing Vγ9/Vδ2 T cells specifically against breast CSCs. In this respect, it has been shown that Her2 is critical in regulating the self-renewal of ALDH$^+$ mammary stem/progenitor cells and subsequently drives tumourigenesis and disease progression in Her2$^+$ breast cancers and also in luminal breast cancers, which normally lack Her2 expression (Korkaya *et al.*, 2008; Korkaya *et al.*, 2009; Ithimakin *et al.*, 2013; Korkaya and Wicha, 2013). These findings indicate that Her2 is a promising candidate for targeting CSCs in different subtypes of breast cancer. Indeed, Capietto *et al.* showed that monoclonal trastuzumab specifically against Her2 efficiently opsonised human breast cancer xenografts and induced significant therapeutic benefit by enhancing the ability of γδ T cells to control tumour progression (Capietto *et al.*, 2011).

CD44 represents another option for targeting breast CSCs. Apart from the standard form of CD44, an alternative splicing isoform, CD44v6, was recently identified to be a potent CSC markers for colon cancer (Todaro *et al.*, 2014). Humanised monoclonal antibodies against CD44 and certain variant isoforms, *e.g.* CD44v6, may thus efficiently label breast

CSCs as targets for Vγ9/Vδ2 T cells. Jin *et al.* showed that anti-CD44 monoclonal antibodies, H90, selectively eradicate CSCs of AML by blocking their trafficking to the supportive microenvironment that is essential for their survival in a NOD/SCID mouse model (Jin *et al.*, 2006). Young *et al.* described that treatment with humanised anti-CD44 monoclonal antibodies, H460-16-2, significantly inhibited the growth of human BxPC3 pancreatic cancer xenografts and increase the survival of mice with AML engrafts by targeting on $CD34^+$ $CD38^-$ CSCs (Young D. Patent WO2007098571, 2007; Arius Research Inc.). In conclusion, targeting breast CSCs with humanised monoclonal antibodies represents an efficient sensitisation strategy not only enhancing the specificity of treatment with effector γδ T cells and γδ T-APCs but also potentially modulating the tumour microenvironment to control tumour initiation and progression.

I next examined the susceptibility of CSC-like cells and non-CSCs to cytotoxic $CD8^+$ T cells using peptide pulsing and endogenous antigen expression models. I found that as compared to non-CSCs, CSC-like cells expressed lower levels of MHC class I and CD54 molecules on their cell surface and thus were more resistant to $CD8^+$ T cell-mediated killing. Importantly, IFN-γ secreted by γδ T cells enhanced MHC class I and CD54 expression by CSC-like cells non-CSCs, and enhanced their clearance by cytotoxic CD8 T cells (Figure 4.30).

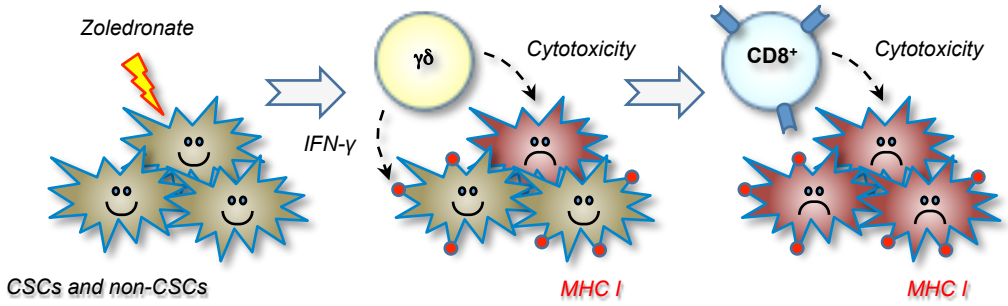

Figure 4.30. Proposed synergism between γδ T cells and cytotoxic $CD8^+$ T cells in effective tumour killing. Non-MHC-restricted γδ T cells kill a proportion of tumour cells sensitised by zoledronate and secrete IFN-γ to up-regulate the expression of MHC class I and CD54 on the surface of surviving tumour cells for better recognition by MHC-restricted cytotoxic $CD8^+$ T cells. Subsequently, this immunomodulatory effect leads to the clearance of residual targets by cytotoxic $CD8^+$ T cells.

As opposed to their intrinsic resistance to chemotherapeutic drugs, my results show that the resistance of CSC-like cells to cytotoxic $CD8^+$ T cells is majorly due to the down-regulation of antigen presenting molecules (MHC class I) and cell-cell adhesion molecules (CD54), which are both essential for successful recognition by $CD8^+$ effector T cells. These observations provide great hope in targeting CSCs efficiently by immune effector cells in combination with different biological immune modulators. A similar down-regulation of MHC class I was noticed before in CSCs of different primary tumours and metastasis (Di Tomaso *et al.*, 2010; Schatton *et al.*, 2010b; Chen *et al.*, 2011; Tallerico *et al.*, 2013). Schatton *et al.* showed that tumourigenic $ABCB5^+$ malignant melanoma TICs display lower levels of MHC class I as compared with their $ABCB5^-$ counterpart, and were able to inhibit IL-2-dependent activation of effector T cells through induction of $CD4^+$ $CD25^+$ $FoxP3^+$ Treg cells (Schatton *et al.*, 2010b). Similarly, Di Tomaso *et al.* showed that glioblastoma CSCs are only weakly positive for MHC class I and II as well as NKG2D ligands, and carry defects in their antigen-processing machinery (Di Tomaso *et al.*, 2010). Similar to my own observation in breast CSC-like cells, the down-regulation of MHC class I by glioblastoma CSCs could be rescued by the treatment with IFN-γ (Di Tomaso *et al.*, 2010). Consistently, Chen *et al.* showed that within a unique cell line established from the lymph node metastasis of a patient with unknown primary tumour, CSCs were majorly harboured in spheroids/floating aggregates under normal adherent culture condition and exhibited a $CD44^{hi}$ $CD24^{lo}$ phenotype accompanied by down-regulation of MHC class I expression that could be rescued by IFN-γ treatment (Chen *et al.*, 2011). The susceptibility of CSC-like cells to IFN-γ-mediated up-regulation of MHC class I expression indicates that the depressed expression of MHC class I in CSC-like cells does not represent a non-reversible loss and can readily be overcome. However, the underlying mechanism of MHC class I down-regulation is currently unclear apart from limited insight into the defective antigen-processing machinery (Di Tomaso *et al.*, 2010). In contrast to total loss of MHC class I expression by structural defective mutations (Chang and Ferrone, 2006; Hsieh *et al.*, 2009), down-regulation of the molecules might be a better strategy to escape from both cytotoxic $CD8^+$ T cells and innate-like NK and γδ T cell-mediated immunosurveillance, since the thresholds for MHC class I expression levels to activate CTLs and NK cells may be different (Figure 4.31).

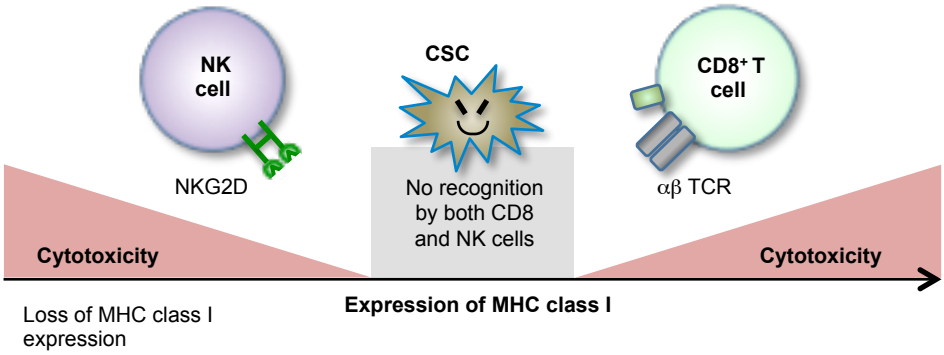

Figure 4.31. Proposed regulation of MHC class I expression by CSCs to escape killing by both MHC-restricted and innate-like effector cells. Through partial down-regulation of MHC class I expression to a certain degree CSCs may successfully escape from the surveillance of both MHC-restricted and innate-like effector cells.

Of note, down-regulation of MHC class I does not occur in all CSCs. Using a Flu M1 and CMV pp65 surrogate antigen model similar to the one utilised in this Thesis, Brown *et al.* showed no difference between $CD133^+$ brain tumour initiating cells (BTSCs) enriched in sphere culture and their differentiated $CD133^-$ counterparts in the expression of MHC class I and CD54 (Brown *et al.*, 2009). Both BTSCs and differentiated cells induced similar levels of cytotoxic $CD8^+$ T cell responses in terms of degranulation and cytokine production, and most importantly, were equally sensitive to killing by cytotoxic $CD8^+$ T cells both *in vitro* and *in vivo* in a NOD/SCID model of human glioma (Brown *et al.*, 2009). Liao *et al.* showed that $ALDH^{hi}$ cells derived from sphere culture of CaSki and UM-SCC11B cell lines were more sensitive to killing by alloantigen-specific $CD8^+$ T cells as compared to their $ALDH^{lo}$ counterparts (Liao *et al.*, 2013). Visus *et al.* identified ALDH1A1, an isoform of ALDH that actively distinguishes $ALDH^{hi}$ CSCs in the ALDEFLOUR assay (Ginestier *et al.*, 2007), as a novel CSC-specific tumour antigen for cytotoxic $CD8^+$ T cells in squamous cell carcinoma of head and neck cancer (SCCHN) (Visus *et al.*, 2007). The recognition by cytotoxic $CD8^+$ T cells is HLA-A2-restricted and specific for the p88-96 peptide of ALDH1A1 (Visus *et al.*, 2007). Later, Visus *et al.* showed that *in vitro* $ALDH^{hi}$ CSCs in SCCHN, breast and pancreatic cell lines, in SCCHN xenografts and in surgical removed lesion could be efficiently recognised by ALDH1A1 p88-96-specific $CD8^+$ T cells. Encouragingly, adoptive transfer of these *ex vivo* expanded ALDH1A1 p88-96-specific $CD8^+$ T cells efficiently inhibited the growth of orthotopic SCCHN xenografts and the development of pulmonary metastasis by MDA-MB-231

breast cancer cells in immunodeficient mice. These ALDH1A1 p88-96-specific $CD8^+$ T cells were found by tetramer staining in the circulation of SCCHN patients at rates of 1/500-1/2000, suggesting their important physiological relevance in patients (Visus *et al.*, 2011).

Indeed, the present approach using viral surrogate antigens for studying the efficacy of CSC targeting by cytotoxic $CD8^+$ T cells needs to be further translated into CSC-specific antigens like ALDH1A1 and general tumour-associated antigens such as Muc1, 5T4, NY-ESO, MART-1 and MAGE-3, which are potential targets for cytotoxic $CD8^+$ T cell-based immunotherapies. In conclusion, my findings provide promising proof-of-concept evidence that the efficacy of cytotoxic $CD8^+$ T cell-based immunotherapies could be significantly potentiated by the synergism with innate-like γδ T cells, which provides a different spectrum of target recognition and killing and modulation of immunogenicity of those originally resistant to $CD8^+$ T cell-mediated killing.

Chapter 5. Cross-Presentation of Tumour-Expressed Proteins to Antigen-Specific Cytotoxic CD8$^+$ T Cells by γδ T Cells

5.1. Introduction

The functional plasticity of γδ T cells is an intriguing topic in the field (Vantourout and Hayday, 2013; Lafont *et al.*, 2014; Tyler *et al.*, 2015). Apart from their well-characterised cytotoxic effector functions against malignant cells and their ability to boost adaptive αβ T cell responses by modulating the immunogenicity of transformed cells *via* the secretion of pro-inflammatory cytokines such as IFN-γ and TNF-α (Chapter 4), human Vδ9/Vδ2 T cells possess a unique ability to function as APCs upon stimulation with phosphoantigens, *e.g.* HMB-PP and IPP. The characterisation of the APC function of human Vδ9/Vδ2 T cells was first conducted in our laboratory (Brandes *et al.*, 2005; Brandes *et al.*, 2009; Meuter *et al.*, 2010; Khan *et al.*, 2014a) but was subsequently confirmed by others (Landmeier *et al.*, 2009; Wu *et al.*, 2009b; Altvater *et al.*, 2012; Himoudi *et al.*, 2012; Schneiders *et al.*, 2014; Muto *et al.*, 2015). In particular, the processes involved in cross-presentation of exogenous antigens by both short-term activated primary γδ T cells and long-term expanded γδ T cells to CD8$^+$ T cells in an antigen-specific manner have been characterised (Brandes *et al.*, 2009; Meuter *et al.*, 2010; Khan *et al.*, 2014a). In an attempt to address the physiological relevance of those findings, Himoudi *et al.* established an *in vitro* co-culture system of cancer cells with both γδ T cells as APCs and antigen-specific CD8$^+$ T cells as responders, and showed that opsonisation of target cells with humanised antibodies may be required to "license" antigen cross-presentation by γδ T cells to antigen-specific CD8$^+$ T cells (Himoudi *et al.*, 2012). In their study, Vγ9/Vδ2 T cells acquired an APC phenotype (as judged by expression of APC-associated markers) upon co-culture with non-opsonised cancer cells but were only fully functional with regard to cross-presentation of tumour antigens to CD8$^+$ T cells when co-cultured with cancer cells that had been opsonised by humanised antibodies, suggesting that a secondary signal, particularly through CD16-dependent phagocytosis of foreign antigens, is important to induce the potent cross-presentation by γδ T cells (Wu *et al.*, 2009b; Himoudi *et al.*, 2012). These results suggest that γδ T cells may function concomitantly as killer cells and APCs upon appropriate stimulation under the control of the TCR and CD16 triggered two signalling pathways. Whether other signalling pathway(s) under the control of additional activating receptors, *e.g.* NKG2D and NCRs, are involved in the regulation of killer and APC function of γδ T cells is not clear (Chen *et al.*, 2013) and merits further investigations.

Whether and how γδ T cells function as killer cells and APCs in a sequential dynamic is still unclear. In particular, it is not known whether γδ T cells acquire different functions concomitantly and hence become multiple-functional upon activation, or acquire different functions at different stages of activation reflecting the requirement of different signals in the local environment of infection and tumour. It is also thinkable that cytotoxic γδ T cells and γδ T-APCs are mutually exclusive subsets and are induced as different lineages upon different activatory signals and regulations during infection and inflammation.

In this chapter, I aimed to link the cytotoxicity and APC function of γδ T cells and to illustrate that killing of target cells (including CSCs and non-CSCs), uptake of exogenous antigens released from lysed cancer cells, and cross-presentation of tumour-derived antigens are sequential functional events mediated by γδ T cells. In addition, an attempt was made to establish an *ex vivo* antigen-cross presentation assay to investigate how γδ T cells kill, obtain and cross-present tumour-associated antigens to cytotoxic $CD8^+$ T cells *in vivo* using a human tumour xenograft model in immunodeficient NSG mice.

5.2. Aim

- To show that γδ T cells have the ability to take up tumour cell expressed antigens from lysed CSC-like cells and non-CSCs upon sensitisation with zoledronate, and subsequently cross-present those antigens to antigen-specific cytotoxic $CD8^+$ T cells *in vitro* and *in vivo*.

5.3. *Ex vivo* expansion of γδ T-APCs

5.3.1. Expression of effector and APC markers by expanded γδ T cells

The APC function of both primary and expanded human γδ T cells including their (*i*) expression of cellular makers associated with antigen presentation, (*ii*) ability to take up exogenous antigens by endocytosis, and (*iii*) capacity to cross-present exogenous antigens to CD8 T cells, has been well characterised in our lab (Brandes *et al.*, 2005; Brandes *et al.*, 2009; Meuter *et al.*, 2010; Khan *et al.*, 2014a).

In order to generate sufficient numbers of γδ T-APCs for adoptive transfer studies in animal models, γδ T cells were here expanded from PBMCs of healthy donors in the presence of zoledronate and IL-2, and their APCs characteristics were examined at day 14 in culture. As shown in Figure 5.1, expanded γδ T cells expressed the antigen-presenting molecules MHC class I and II and the co-stimulatory molecules CD80 and CD86 at intermediate to high levels, whereas another co-stimulatory molecule, CD40, was only expressed at low levels. Low levels of CD11c expression distinguished the expanded γδ T cells from monocyte-derived and inflammatory DCs, which express high level of CD11c (Segura and Amigorena, 2013; Segura *et al.*, 2013). Of note, as described in Figure 4.1, the strong expression of CD69 by expanded γδ T cells indicated their activation status at that stage.

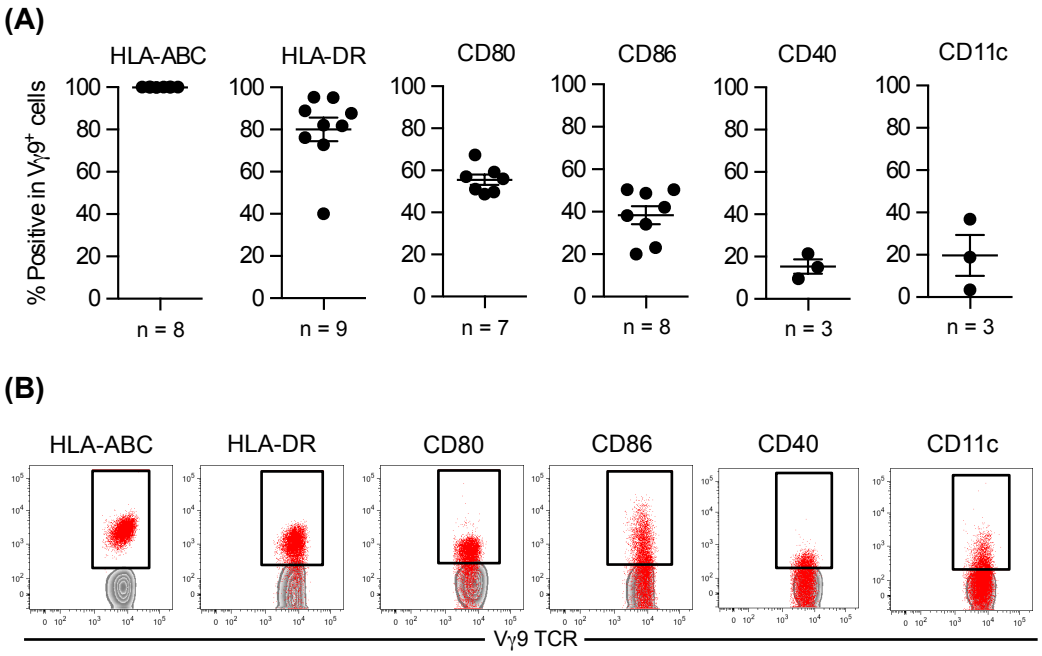

Figure 5.1. Phenotypic characterisation of expanded γδ T cells. **(A)** Expression of APC markers including CD11c, CD40, CD80, CD86, MHC class I and MHC class II by γδ T cells were measured by FACS after 14 days of expansion from PBMCs with zoledronate and IL-2 (n = number of donors used for γδ T cell expansion). Representative FACS plots of different cell surface markers expressed by expanded γδ T cells are shown in **(B)**. Isotype controls are shown as grey zebra plots and the stained markers are shown as red dots.

5.3.2. Re-stimulation of expanded γδ T cells to enhance APC characteristics

Given the relatively low expression levels of some APC markers by expanded γδ T cells as in semi-resting status after around 14 days in culture and the fact that *de novo* cross-presentation by DCs requires activation for up-regulation of their antigen presenting molecules, I next determined whether γδ T cells expanded by the treatment of zoledronate can be re-stimulated again for further enhancement of their APC features by specific TCR-mediated stimulation. Expanded γδ T cells were re-stimulated with HMB-PP and assayed for their expression of APC-associated markers. As shown in Figure 5.2, HMB-PP stimulated γδ T cells significantly up-regulated their expression of APC-associated markers including MHC class I, MHC class II and CD80. A small increase in the expression of CD86 by HMB-PP stimulated γδ T cells was observed in 3 of 4 donors examined (Figure 5.2). However, the increase was not significant statistically, which may have been in part due to the small number of experiments conducted.

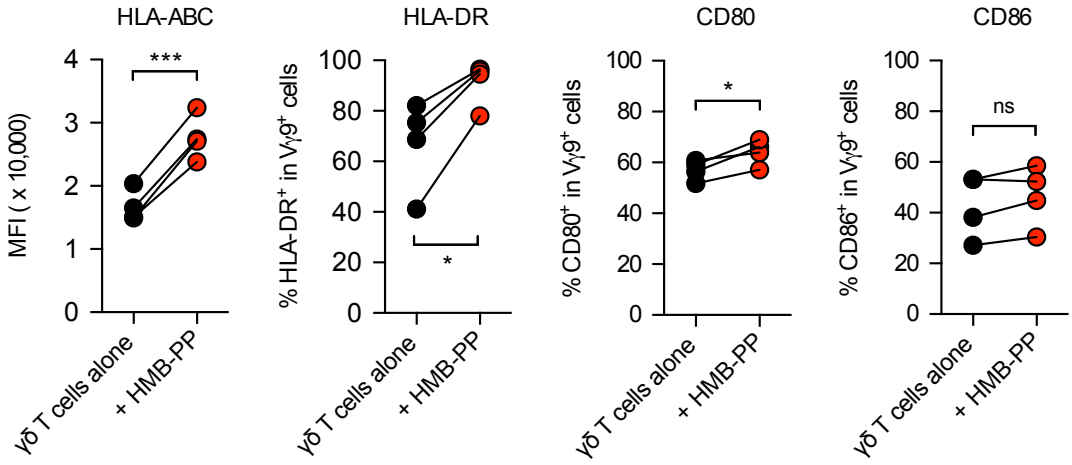

Figure 5.2. Enhanced APC phenotype of expanded γδ T cells upon re-stimulation with HMB-PP. Expression of APC markers including CD80, CD86, HLA class I and HLA class by γδ T cells cultured for 24 hours in the presence or absence of 10 nM HMB-PP were measured by FACS. Data were pooled from experiments with expanded γδ T cells derived from four healthy individuals. Significance of differences was calculated using paired Student's t test (*$p \leq 0.05$; ***$p \leq 0.001$).

5.3.3. Cross-presentation of recombinant Flu M1 protein by expanded γδ T cells *in vitro*

In order to confirm the APC characteristics of expanded γδ T cells on the functional level, their ability to take up and cross-present exogenous antigens to cytotoxic $CD8^+$ T cells was examined in more detail. As described in previous publications from our laboratory (Brandes *et al.*, 2009; Meuter *et al.*, 2010; Khan *et al.*, 2014a), expanded γδ T cells were cultured overnight in the presence of 0.01, 0.1 or 1 μM recombinant Flu M1 protein serving as model antigen. Using this well-established experimental system, I investigated the potential of expanded γδ T cells to take up and process exogenous M1 protein and load the immunodominant peptide p58-66 onto MHC I molecules for presentation to HLA-A2-restricted cytotoxic $CD8^+$ T cells with specificity to M1 p58-66 (as described in Chapter 4). As shown in Figure 5.3, MHC-matched γδ T-APCs (HLA-$A2^{+ve}$) exhibited a strong ability to cross-present M1 antigen and induce robust cytotoxic $CD8^+$ T cell responses in a dose-dependent manner (M1 concentration during preparation of γδ T-APCs), as determined by intracellular IFN-γ staining of $CD8^+$ T cell responders. As negative control, MHC-mismatched γδ T-APCs (HLA-$A2^{-ve}$) pulsed with recombinant M1 protein failed to induce such $CD8^+$ T cell responses, and no activation of $CD8^+$ T cells was observed in the absence of M1 regardless of the MHC haplotype of the γδ T-APCs, confirming the antigen specificity of the experimental system. Treatment of $CD8^+$ T cell responders with universal non-specific mitogen PMA and ionomycin served as positive control. In conclusion, consistent with the observation on short-term activated γδ T cells (Brandes *et al.*, 2009; Meuter *et al.*, 2010) and long-term expanded γδ T cells with zoledronate, IL-2 and IL-15 (Khan *et al.*, 2014a), here I showed that γδ T cells expanded with zoledronate and IL-2 for 14 days retain the potential to respond to HMB-PP and act as APC that can uptake, process and cross-present exogenous antigen to cytotoxic $CD8^+$ T cells.

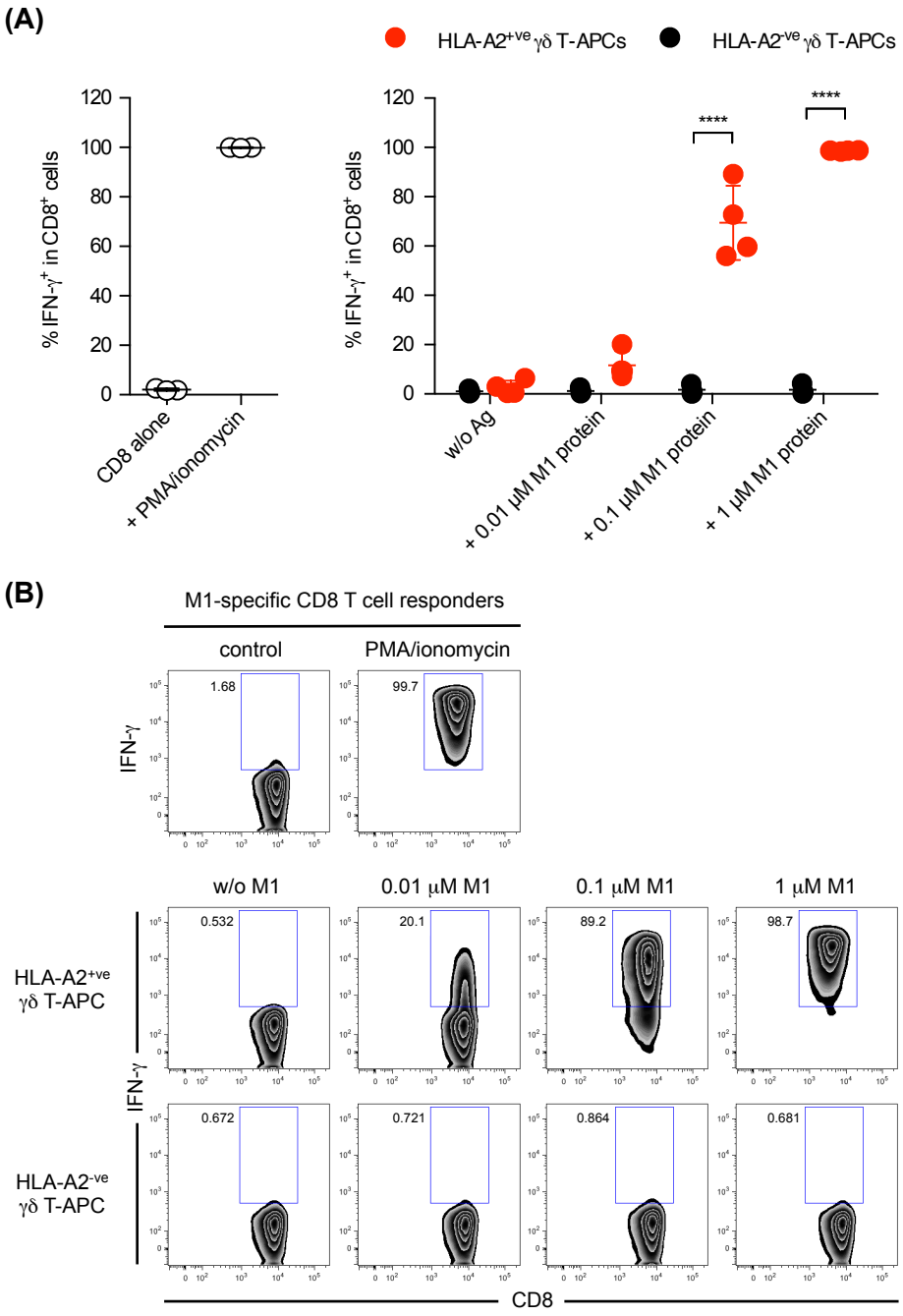

Figure 5.3. Cross-presentation of recombinant influenza M1 model antigen by γδ T cells *in vitro*. **(A)** γδ T cells expanded from PBMCs with IL-2 and zoledronate were cultured overnight in the presence of recombinant influenza M1 protein at various concentrations and then used as APCs for cross-presentation to M1-specific $CD8^+$ T cell responders. The activation of $CD8^+$ T cell responders in co-cultures with γδ T-APCs was measured by intracellular staining of IFN-γ and analysed by FACS. Data were pooled from experiments with expanded γδ T cells derived from PBMCs of three $HLA\text{-}A2^{+ve}$ and three $HLA\text{-}A2^{-ve}$ healthy donors. Significance of differences was calculated by non-parametric two-way ANOVA (****$p \leq 0.0001$). Representative FACS plots of intracellular IFN-γ staining are shown in **(B)**.

5.4. Cross-presentation of tumour cell-expressed Flu M1 by γδ T cells *in vitro*

5.4.1. Induction of APC characteristics in expanded γδ T cells by sensitised CSC-like cells and non-CSCs *in vitro*

Although it is clear that γδ T cells can function both as cytotoxic effectors in targeting various types of cancer cells and as APCs, there is only very limited evidence showing that γδ T cells can obtain antigens from the cancer cells they lyse and cross-present them to $CD8^+$ T cells (Himoudi *et al.*, 2012). Here, I assessed whether γδ T cells can be activated in co-culture with cancer cells and show APC features, taking advantage of the CSC-like cell model established in Chapter 3. As shown in Figure 5.4A, expanded γδ T cells co-cultured with zoledronate-sensitised CSC-like cells up-regulated MHC class I, II and CD86 expression as compared to baseline levels observed in co-cultures with their non-sensitised CSC-like counterparts. A similar, or even better, activation of expanded γδ T cells was observed in co-culture with zoledronate-sensitised non-CSCs (Figure 5.4B). These results demonstrate that the APC characteristics of expanded γδ T cells can be induced further not only upon exposure to soluble HMB-PP but also upon co-culture with zoledronate-treated tumour cells, suggesting that a similar induction of APC features may take place in patients receiving intravenous zoledronate.

Furthermore, these results also indicate that upon activation induced by zoledronate-sensitised CSC-like cells and non-CSCs, γδ T cells seem to concomitantly acquire APC feature along with cytotoxicity. However, whether the activation of γδ T cells through TCR recognition leads to induction of these two functionally distinct subsets or to acquisition of both cytotoxicity and APC features by every single γδ T cells still remain unclear.

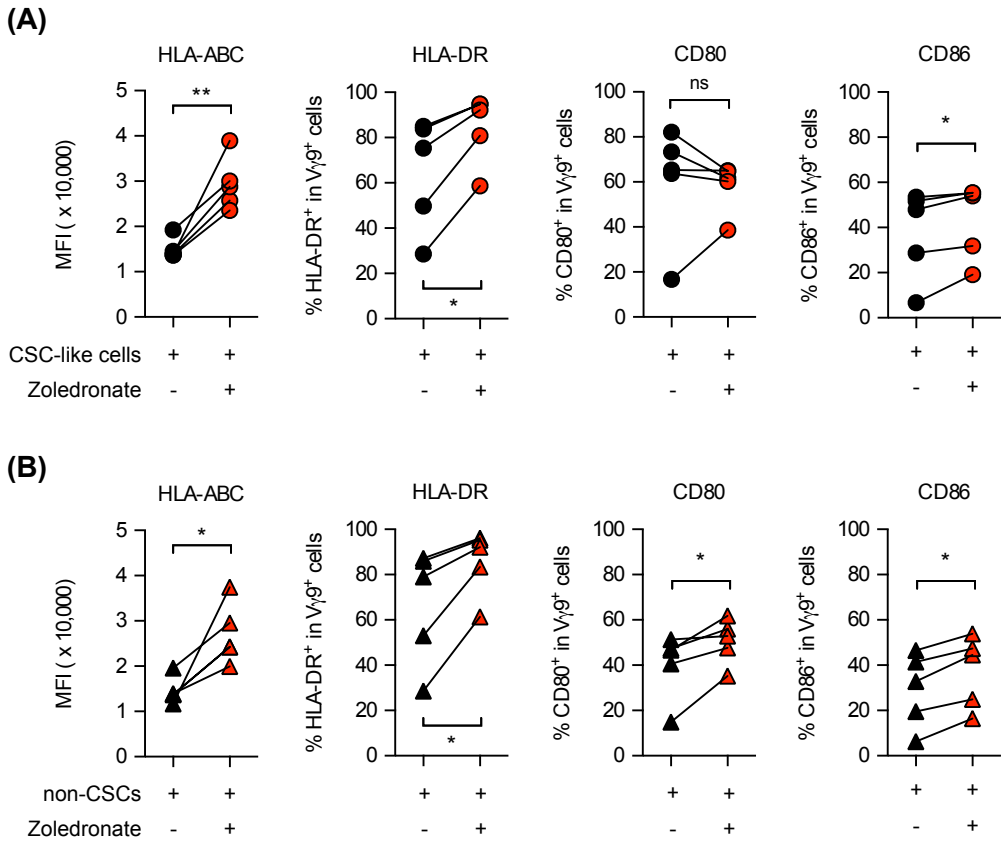

Figure 5.4. Sensitisation of CSC-like cells and non-CSCs with zoledronate enhanced the APC phenotype of expanded γδ T cells in co-culture. Expression of the APC markers CD80, CD86, MHC class I and MHC class II by γδ T cells in co-culture with CSC-like cells **(A)** or non-CSCs **(B)** pretreated with or without 10 μM zoledronate was measured by FACS. Data were pooled from two experiments with expanded γδ T cells derived from five healthy individuals. Significance of differences was calculated by paired Student's t test (*$p \leq 0.05$; **$p \leq 0.01$).

5.4.2. Cross-presentation of Flu M1 expressed in transduced CSC-like cells and non-CSCs by expanded γδ T cells *in vitro*

Having shown that γδ T cells can lyse zoledronate-treated cancer cells and at the same time up-regulate the expression of APC markers, I next examined whether γδ T cells can cross-present tumour cell-expressed antigens released from the lysed targets to CD8 T cells. M1-expressing CSC-like cells and non-CSCs were sensitised overnight with zoledronate and served both as stimulus for γδ T cell activation and as cellular source of M1 protein. Gluc-expressing CSC-like cells and non-CSCs were used as negative control for antigen specificity. Untreated CSC-M1 cells and non-CSC-M1 cells were used as negative controls for activation and cytotoxicity of γδ T cells and for subsequent cross-presentation as lack of antigen release from healthy targets. As shown in Figure 5.5A, γδ T-APCs were isolated by FACS to purities >95% from the co-culture of expanded γδ T cells with CSC-like cells or non-CSCs. The sorted γδ T-APCs were then co-cultured with M1-specific $CD8^+$ T cells and the activation of the responder cells was judged from their IFN-γ production. Unexpectedly, all types of γδ T-APCs prepared failed to induce significant $CD8^+$ T cell responses, irrespective of the culture conditions used to generate such γδ T-APCs (Figure 5.5B). As almost 100% killing of sensitised CSC-like cells and non-CSCs by γδ T cells was observed during the preparation of γδ T-APCs (determined by the observation that no adherent CSC-like cells or non-CSCs were left after overnight co-culture with γδ T cells; data not shown), it is conceivable that the amount of M1 antigen released from lysed cells was not sufficient for potent cross-presentation by γδ T cells. In agreement, no tdTomato signal was detected in γδ T-APCs isolated from co-cultures with sensitised CSC-like or non-CSC targets (data not shown), further suggesting that the uptake of exogenous antigens released from lysed target cells by activated γδ T cells under those experimental conditions was suboptimal. Besides the generally limited concentrations of M1 and tdTomato produced by the tumour cells and hence available for uptake by γδ T cells, it is thinkable that at least a proportion of these two proteins were already degraded during cell apoptosis before being released into the culture.

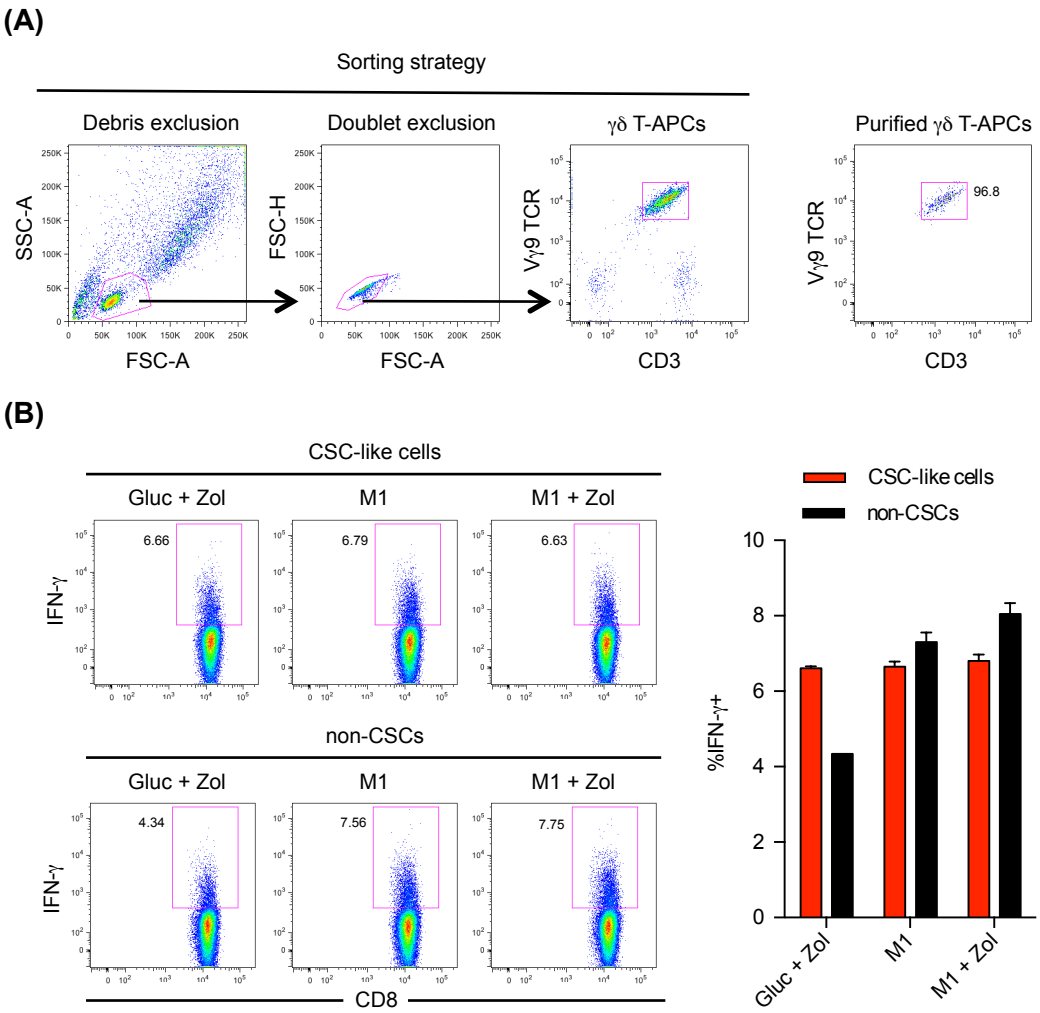

Figure 5.5. *In vitro* cross-presentation of Flu M1 by expanded γδ T cells in co-culture with M1-expressing CSC-like and non-CSC targets. M1-expressing CSC-like cells and non-CSCs were sensitised overnight with 10 μM zoledronate and then mixed with expanded γδ T cells at 1:1 ratio for overnight, allowing γδ T cells to kill and uptake antigens from lysed target cells. γδ T cells were then isolated from co-culture by FACS sorting and served as APCs for M1-specific $CD8^+$ T cell responders. Intracellular IFN-γ expression was used as readout for $CD8^+$ T cell activation. The gating strategy used for isolation of γδ T cells from co-cultures is shown in **(A)**. Results shown were representative for two independent experiments. Error bars shown in the figures were representative for SD.

5.4.3. *In vitro* antigen uptake by γδ T cells

To further investigate the uptake of exogenous antigens, γδ T cells were pulsed with (*i*) protein extract of CSC-M1 cells with expression of tdTomato as fluorescent reporter protein and/or (*ii*) BSA tagged with DQ, which is resistant to degradation in lysosome, as fluorescent label (Meuter *et al.*, 2010) for the visualisation of antigen uptake, and analysed by flow cytometry. As short-term activated γδ T cells (MACS-purified primary γδ T cells stimulated with HMB-PP and IL-2 for 3 days) have been shown for their good capacity to uptake soluble antigens in cultures (Meuter *et al.*, 2010), we first used short-term activated γδ T cells to test whether the experimental model is optimal to reveal the uptake of tdTomato from extract of CSC-M1 cells by γδ T cells in the presence of BSA-DQ as internal positive control for antigen uptake. When pulsed with BSA-DQ at 37°C, short-term activated γδ T cells showed a strong ability to endocytose this exogenous fluorescence-tagged protein (Figure 5.6A). Serving as negative control, γδ T cells incubated with BSA-DQ at 4°C showed no such antigen uptake. Next, short-term activated γδ T cells were pulsed with BSA-DQ together with soluble extracts of CSC-M1 cells co-expressing tdTomato as fluorescent reporter protein for the visualisation of antigen uptake. Although only a very small proportion of γδ T cells became positive for tdTomato under these conditions, all tdTomato$^+$ γδ T cells were also positive for BSA-DQ indicative of a real uptake of tdTomato protein (Figure 5.6B). In order to translate these findings with primary γδ T cells to long-term cultures and determined whether expanded γδ T cells can pick up specific antigen from the mixed protein pool released form lysed cells for cross-presentation, expanded γδ T cells were incubated with a soluble extract of M1-expressing CSC-like cells for a longer 4 hours period allowing both antigen uptake and subsequent processing. Consistent with the results obtained using short-term activated γδ T cells, limited tdTomato uptake was observed in expanded γδ T cells (Figure 5.7). These results confirmed the ability of γδ T cells to uptake exogenous antigens from culture. However, these findings also supported the possibility that the concentration of tumour-expressed proteins present in soluble cell extracts may be too low to demonstrate efficient uptake and cross-presentation by γδ T-APCs.

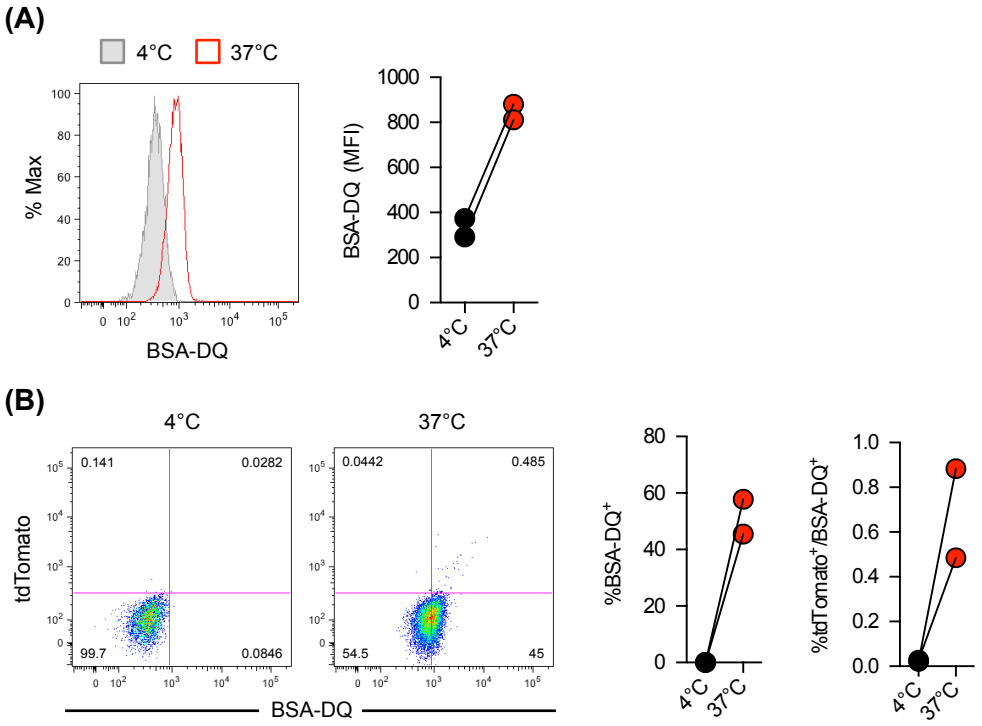

Figure 5.6. ***In vitro*** **antigen uptake by primary γδ T-APCs.** γδ T cells were purified by MACS sorting and then activated in culture with 10 nM HMB-PP and 100 U/ml IL-2 for three days to serve as APCs. Generated gd T-APCs were incubated with 0.5 mg/ml BSA-DQ alone **(A)** or with both 0.5 mg/ml BSA-DQ and 10 mg/ml protein extract of M1-expressing CSC-like cells **(B)** at 4°C or 37°C for one hour. The uptake of BSA-DQ and tdTomato fluorescent reporter in the extract of M1-expressing CSC-like cells by γδ T-APCs was analysed by FACS. Figures shown were pooled results with use of γδ T cells isolated from two healthy donors.

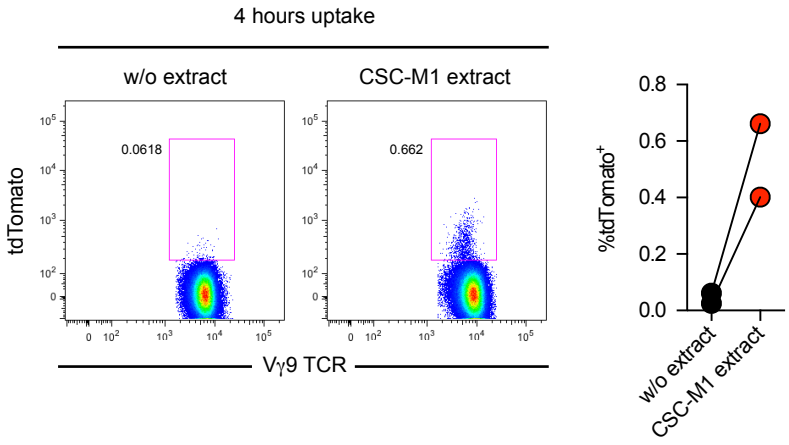

Figure 5.7. *In vitro* antigen uptake by expanded γδ T-APCs. γδ T cells were expanded from PBMCs in the presence of zoledronate and IL-2 for 14 days to serve as APCs. Expanded γδ T-APCs were incubated with 10 mg/ml protein extract of M1-expressing CSC-like cells at 37°C for four hours. The uptake of tdTomato fluorescent reporter in the extract of M1-expressing CSC-like cells by γδ T-APCs was analysed by FACS. Figures shown were pooled results with use of γδ T cells isolated from two healthy donors.

5.4.4. Cross-presentation of FluM1 within the protein extract of transduced CSC-like cells by expanded γδ T cells *in vitro*

Having demonstrated limited yet detectable uptake of tumour-expressed proteins, I next examined the capacity of γδ T-APCs to cross-present tumour cell-expressed M1 present in the soluble extract prepared from CSC-M1 cells. Expanded γδ T cells were incubated with 1 or 10 mg/ml cell extract of M1-expressing CSC-like cells for 6 hours and then washed to serve as γδ T-APCs for the induction of M1-specific $CD8^+$ T cell responses. γδ T-APCs incubated with a cell extract prepared from Gluc-expressing CSC-like cells and thus presenting an irrelevant antigen were used as negative control. In addition, HLA-$A2^{-ve}$ γδ T-APCs were used as MHC-mismatched negative control to identify any non-specific activation of $CD8^+$ responder cells by γδ T-APCs. γδ T-APCs prepared with 10 mg/ml soluble extract of CSC-M1 cells induced a slightly increased IFN-γ production by $CD8^+$ responder cells, compared to γδ T-APCs prepared without antigens and γδ T-APCs prepared with 1 mg/ml soluble extracts of CSC-M1 cells (Figure 5.8). The better $CD8^+$ T cell response induced by M1-presenting γδ T-APCs as compared to Gluc-presenting γδ T-APCs suggested a certain degree of cross-presentation by γδ T-APCs. However, there was no difference between MHC-matched HLA-$A2^{+ve}$ γδ T-APCs and MHC-mismatched HLA-$A2^{-ve}$ γδ T-APCs in inducing IFN-γ production by $CD8^+$ responder cells, indicating that the activation of $CD8^+$ T cells observed was non-specific rather than actual cross-presentation of M1 by γδ T-APCs.

Taken together, the present attempt to show cross-presentation of tumour cell-expressed M1 from CSC-like cells by γδ T-APCs failed, most likely because of the insufficient supply of antigen to γδ T-APCs in our *in vitro* co-culture system. The fact that only less than 1% of cells were actually positive for tdTomato uptake after incubation with cell extract suggests that our experimental system is not sensitive enough to observe efficient cross-presentation by γδ T-APCs. However, the results did confirm that γδ T cells can function to kill CSC-like cells and non-CSCs sensitised with zoledronate and take up exogenous antigens from the lysed cancer cells.

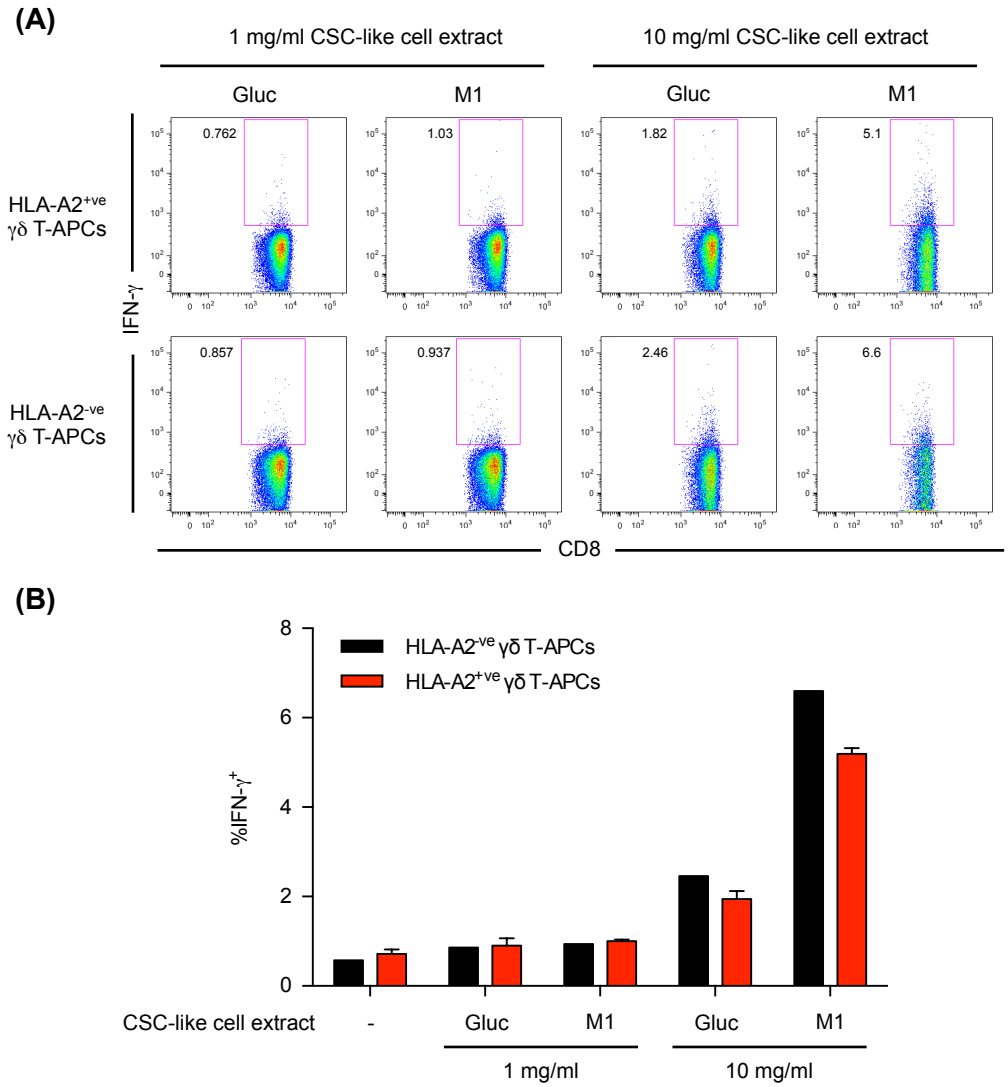

Figure 5.8. *In vitro* cross-presentation by expanded γδ T-APCs. γδ T cells were expanded from PBMCs in the presence of zoledronate and IL-2 for 14 days to serve as APCs. Expanded γδ T-APCs were incubated with 1 or 10 mg/ml protein extract of M1- or Gluc-expressing CSC-like cells at 37°C for six hours, washed extensively and then co-cultured with M1-specific $CD8^+$ T cell responders for 5 hours in the presence of Brefeldin A. The activation of M1-specific $CD8^+$ T cell responders was analysed by FACS using intracellular IFN-γ expression as readout. Results shown were experiment pooled with use of HLA-$A2^{+ve}$ γδ T cells from two healthy donors and HLA-$A2^{-ve}$ γδ T cells from one healthy donor. Error bars shown in the figures were representative for SD.

5.5. Cross-presentation of tumour cell-expressed Flu M1 by γδ T cells *in vivo*

5.5.1. Generation of Flu M1-expressing tumours in NSG mice

In order to increase the local amount and concentration of exogenous M1 antigen available for γδ T-APCs to take up, we sought to utilise an *in vivo* M1-expressing tumour model, which is likely to provide a better microenvironment with respect to tighter contacts for the formation of stable immune synapses between γδ T-APCs and cancer cell targets, and the presence of a more condensed antigen pool for γδ T-APCs to obtain appropriate antigens from the immune synapses. Of note, if successful, these experiments would be the first ever demonstration that human γδ T cells indeed act as APCs *in vivo*. In order to achieve this, we used mice bearing tumours that co-expressed M1 and tdTomato by orthotopic xenotransplantation of M1-expressing CSC-like cells in NSG mice (see Chapter 3). Mice with tumours co-expressing tdTomato and Gluc as irrelevant antigen were used as antigen-mismatched negative control. When the tumours reached sizes of 0.5 cm in the longest dimension, they were sensitised with zoledronate (or saline as negative control) through *i.v.* injection (Figure 5.9A). Expanded γδ T cells were injected directly into the tumours on the next day and harvested again from the tumours 24 hours later by FACS sorting to purities of approx. 85% with contaminants majorly consisted of tumour cells and cell debris as distinguished by their sizes (FSC/SSC) and tdTomato expression (Figure 5.9B).

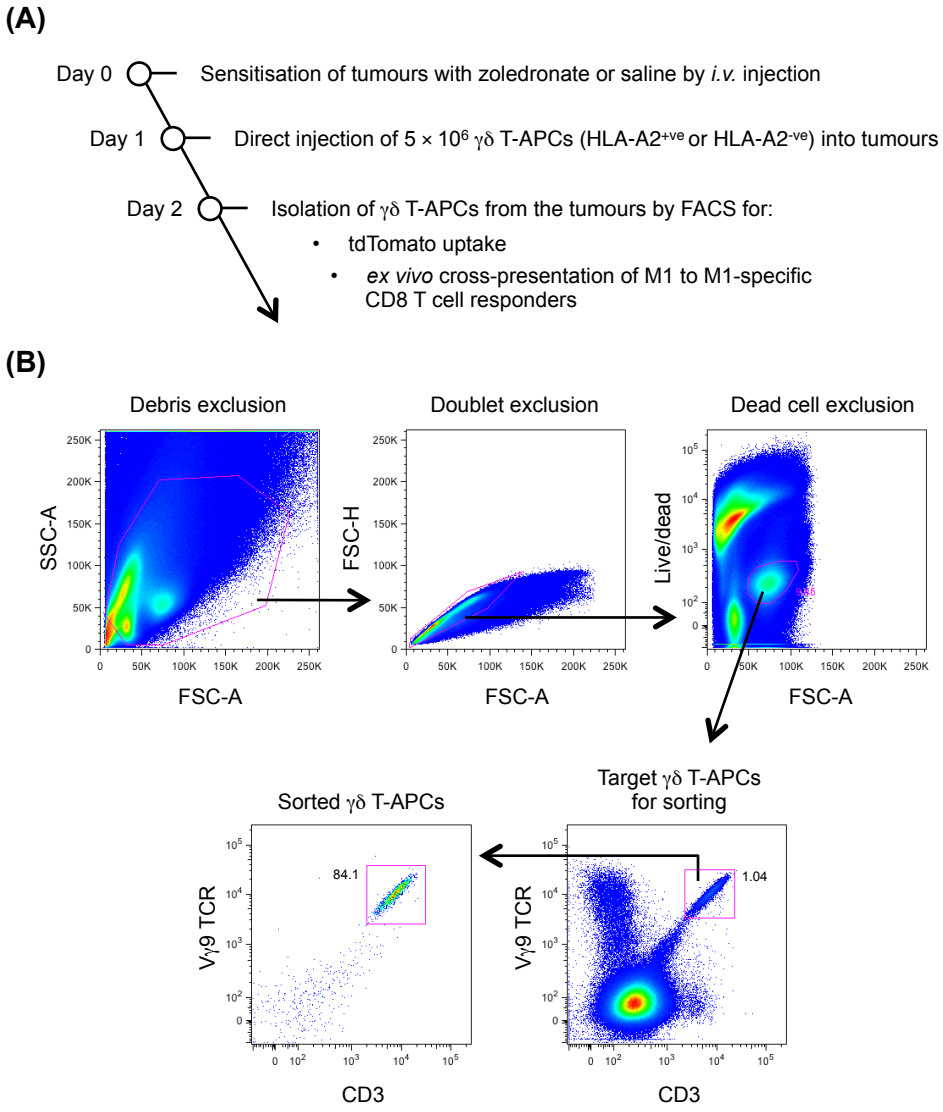

Figure 5.9. FACS isolation of γδ T-APCs from tumours derived from M1- or Gluc-expressing CSC-like cells. γδ T cells were expanded from PBMCs in the presence of zoledronate and IL-2 for 14 days to serve as APCs. Tumours were established in NSG mice by *s.c.* injecting 2 × 10^6 M1- or Gluc-expressing CSC-like cells into the mammary gland. The developed tumours were used as targets for gd T-APCs when the size of tumour reaches > 0.5 cm in longest dimension. Tumours were sensitised with 50 μg/kg zoledronate or PBS given intravenously in a total volume of 100 μl one day before 5 × 10^6 γδ T-APCs (HLA-A2^{+ve} or HLA-A2^{-ve}) were given directly into each tumours in 50 μl saline. 24 hours later, tumours were harvested, dissociated by chopping thoroughly with a scalpel, and then filtered through 70 μm and 40 μm cell strainers to release γδ T-APCs into single cell suspensions. These mixed cell suspensions were then stained with fixable AQUA live/dead followed by surface staining for CD3 and Vγ9 TCR before FACS sorting. γδ T-APCs were sorted to purities of approx. 85% according to sequential gating on intact, single and live CD3$^+$/Vγ9$^+$ cells.

5.5.2. APC phenotype of *in vivo* antigen-primed γδ T-APCs isolated from M1-expressing tumours

To investigate whether γδ T cells could be activated and obtain APC-associated features *in vivo*, γδ T-APCs were isolated from M1- or Gluc-expressing tumours that had been sensitised or not with zoledronate, and were analysed by flow cytometry for their expression of MHC class II. These experiments demonstrated that γδ T-APCs isolated from non-sensitised M1-expressing tumours, zoledronate-sensitised M1-expressing and Gluc-expressing tumours all showed marginal up-regulation of MHC class II expression compared to γδ T-APCs in cell culture (Figure 5.10), indicating that the γδ T cells in the tumours maintained (and in some cases even enhanced) their APC features *in vivo*.

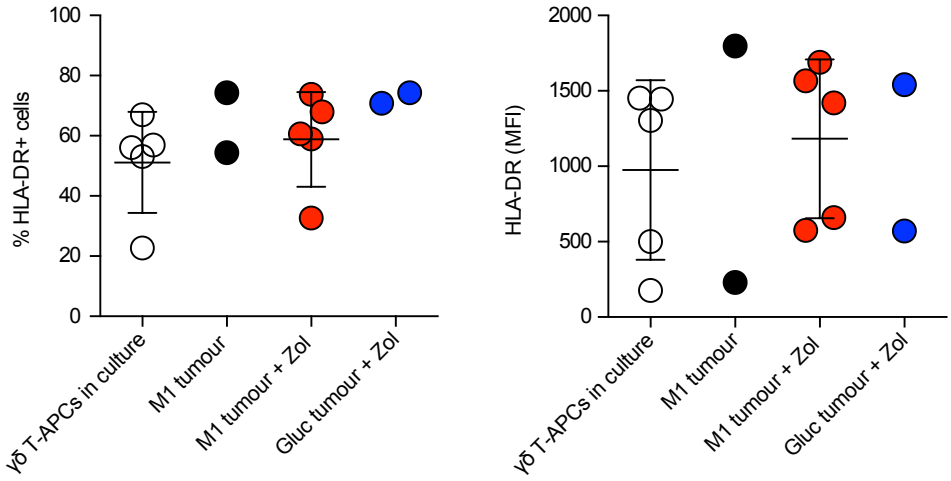

Figure 5.10. Modulation of APC phenotype of expanded γδ T-APCs in tumours. γδ T-APCs isolated from M1-expressing or Gluc-expressing tumours with or without Zoledronate sensitisation were examined for their expression of HLA-DR by flow cytometry. Results shown were three experiments pooled with use of HLA-A2^{+ve} γδ T cells from three healthy donors and HLA-A2^{-ve} γδ T cells from two healthy donors. Error bars shown in the figures were representative for SD.

5.5.3. Uptake of tdTomato by *in vivo* primed γδ T-APCs in tumours

In addition to HLA-DR expression, uptake of the fluorescent reporter tdTomato from the tumour cells by expanded γδ T cells was assessed by flow cytometry. As shown in Figure 5.11, γδ T cells harvested from M1-expressing tumours sensitised with zoledronate exhibited significant uptake of tdTomato with respect to both the proportion of tdTomato$^+$ γδ T cells and the MFI of the tdTomato signal. Uptake of tdTomato by γδ T cells isolated from non-sensitised M1-expressing tumours and from sensitised Gluc-expressing tumours was less pronounced but nevertheless detectable. The lower level of tdTomato uptake by γδ T cells in zoledronate-sensitised Gluc tumours compared to M1 tumours was likely due to generally lower expression levels of tdTomato in CSC-Gluc cells compared to CSC-M1 cells (data not shown). In conclusion, these findings demonstrate that γδ T cells have the ability to take up antigen released by tumour cells *in vivo*.

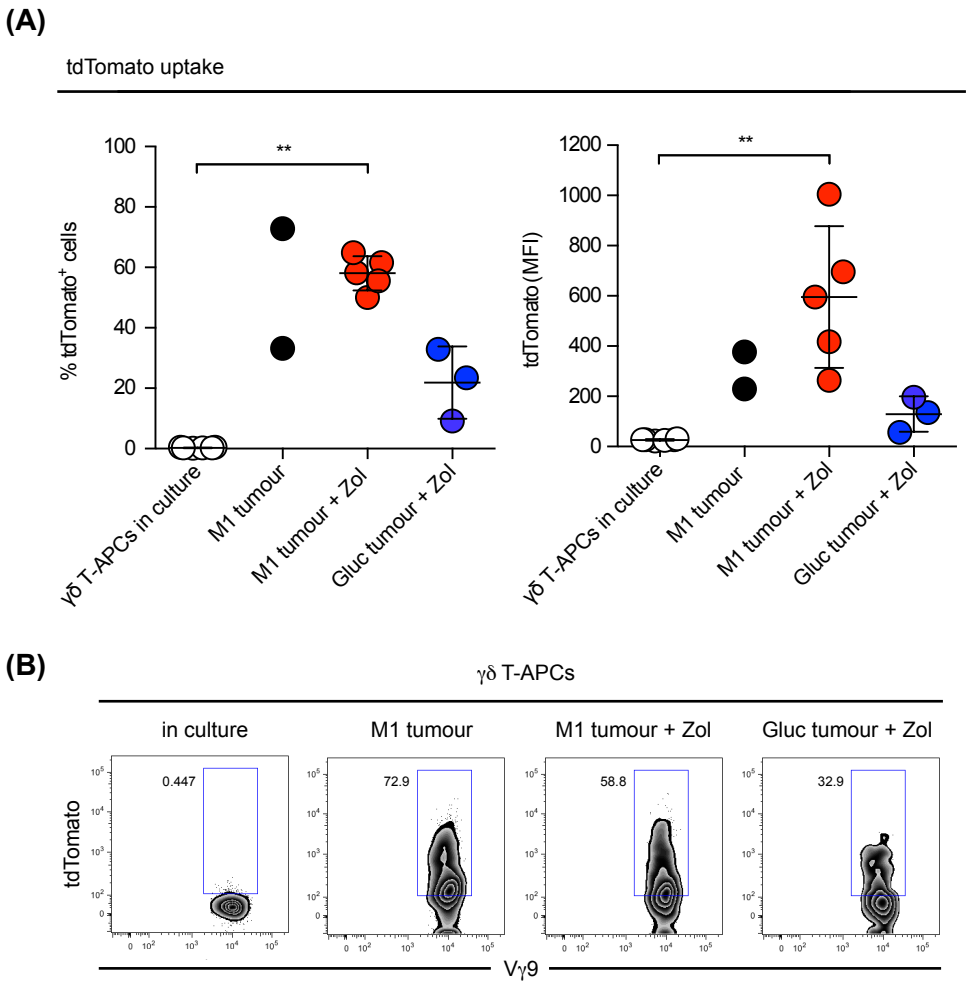

Figure 5.11. Uptake of tdTomato by expanded γδ T-APCs in tumours. (A) γδ T-APCs isolated from M1-expressing or Gluc-expressing tumours with or without prior zoledronate sensitisation were examined for their expression of tdTomato. Representative zebra plots showing tdTomato uptake by antigen-primed γδ T-APCs under different conditions *in vivo* were shown in **(B)**. Results shown were three experiments pooled with use of HLA-A2^{+ve} γδ T cells from three healthy donors and HLA-A2^{-ve} γδ T cells from two healthy donors. Error bars shown in the figures were representative for SD. Significance of differences was calculated by Kruskal-Wallis tests. (**$p \leq 0.01$)

5.5.4. *Ex vivo* cross-presentation of M1 by *in vivo* primed γδ T-APCs isolated from M1-expressing tumours

Finally, γδ T cells isolated from the tumours were used as γδ T-APCs in co-culture with M1-specific $CD8^+$ T cells to examine their ability to cross-present model antigens from the tumour. Cross-presentation of M1 by these *in vivo* primed γδ T-APCs was assessed by intracellular staining of $CD8^+$ responder cells for IFN-γ as before, and analysed by flow cytometry. As shown in Figure 5.12, M1-specific $CD8^+$ T cells in co-culture with γδ T-APCs isolated from either zoledronate-sensitised or non-sensitised M1 tumours showed substantial production of IFN-γ, whereas $CD8^+$ T cells in co-culture with γδ T-APCs isolated from Gluc tumour failed to produce IFN-γ, confirming the antigen specificity of the experimental system. However, IFN-γ production was observed in M1-specific $CD8^+$ T cells in co-culture with both HLA-$A2^{+ve}$ (MHC-matched) and HLA-$A2^{-ve}$ (MHC-mismatched) γδ T-APCs isolated from zoledronate-sensitised M1 tumours (Figure 5.13). These results showed that the antigen-specific activation of M1-specific $CD8^+$ T cells in co-culture with γδ T-APCs was likely due to the presence of residual HLA-$A2^{+ve}$ M1-expressing tumour cells (up to 15%; Figure 5.9B) being present as contaminants in the γδ T-APC preparations, thereby masking any potential effect by γδ T-APCs.

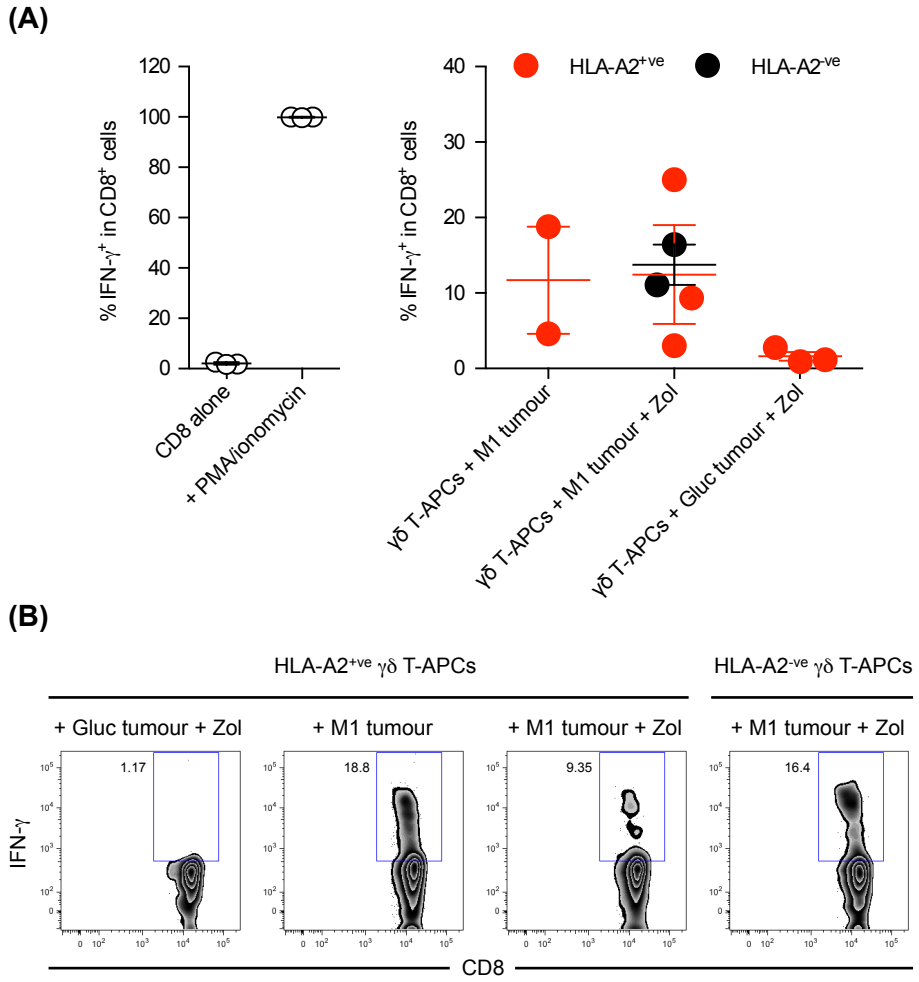

Figure 5.12. *Ex vivo* cross-presentation of M1 by γδ T-APCs isolated from tumours. (A) γδ T-APCs isolated from M1-expressing or Gluc-expressing tumours with or without Zoledronate sensitisation were examined for their ability to cross-present M1 to $CD8^+$ T cells. Representative zebra plots showing IFN-γ production by M1-specific $CD8^+$ T cell responders in co-culture with γδ T-APCs generated under different conditions *in vivo* were shown in **(B)**. Results shown were three experiments pooled with use of HLA-$A2^{+ve}$ γδ T cells from three healthy donors and HLA-$A2^{-ve}$ γδ T cells from two healthy donors. Error bars shown in the figures were representative for SD.

5.6. Discussion

In this chapter, firstly I showed that re-stimulation of expanded γδ T cells with soluble HMB-PP or by co-culture with zoledronate-sensitised CSCs-like cells and non-CSCs enhanced their expression of MHC and co-stimulatory molecules, indicating the successful acquisition of APC features through activating signals *via* the γδ TCR (Himoudi *et al.*, 2012). However, the observation that *in vitro* expanded γδ T cells were readily able to cross-present exogenous Flu M1 to antigen-specific $CD8^+$ T cells indicates that a secondary signal *via* FcγR postulated earlier (Wu *et al.*, 2009b; Himoudi *et al.*, 2012) may play an additive or synergistic role but is not required for the induction of a potent $CD8^+$ T responses by γδ T-APCs. This was confirmed by similar phenomeon observed using γδ T-APCs that had been expanded by zoledronate in the presence of IL-2 and IL-15 (Khan *et al.*, 2014a). As the triple co-culture system of γδ T-APCs, $CD8^+$ responder cells and target cancer cells established by Himoudi *et al.*, 2012 is very complex and may hinder some potential cross-talks in between each cell populations that could affect the activation of $CD8^+$ T cell responders, I tried to establish a simpler and "cleaner" co-culture system by isolating pure γδ T-APCs from co-cultures with zoledronate-sensitised tumour targets. These purified γδ T-APCs were then used to test their ability to cross-present tumour cell-expressed Flu M1 to $CD8^+$ T cells. However, no activation of $CD8^+$ T cell responders was observed by the use of these γδ T-APCs, indicating that the experimental conditions may not have been optimal. As γδ T-APCs are very efficient in presenting soluble proteins to antigen-specific $CD8^+$ T cells and were substantially activated in co-cultures with sensitised targets, it can be speculated that the supply of tumour cell-released soluble M1 in these co-culture was insufficient, possibly due to degradation of the transduced Flu M1 protein during apoptosis. While Meuter *et al.* showed that short-term activated γδ T-APCs can cross-present M1 from debris of influenza-infected cells (Meuter *et al.*, 2010), my own experiments attempted to induce $CD8^+$ T cell responses by loading γδ T-APCs with lysates of M1-expressing cells failed. The most likely explanation for this apparent failure to detect antigen-specific $CD8^+$ T cell responses under these conditions is the fact that in contrast to a productive viral infection, the Flu M1 protein in the transduced HMLER-derived cell lines used here may only constitute a very minor proportion of the whole cell lysate. In fact, uptake of tdTomato by γδ T cells incubated with protein lysate of Flu M1/tdTomato-expressing cells was also only observed at very low levels, supporting the notion that concentrations of defined proteins were very limited in the tumour cell lysates, even though expression of Flu M1 and tdTomato was under the

control of strong EF-1 promoters. Further experiments are required to determine the exact proportion and amount of Flu M1 in these lysates by Western blotting and compare the cross-presentation efficiency of recombinant Flu M1 with endogenously expressed Flu M1.

In order to overcome these experimental hurdles in a physiologically more relevant microenvironment, γδ T cells were injected directly into established Flu M1-expressing tumours that had been pre-conditioned overnight by *i.v.* zoledronate treatment. As CSC-like cells are resistant to γδ T cell-mediated killing *in vitro*, tumours without prior sensitisation by zoledronate were used as negative control for *in vivo* killing and subsequent antigen uptake and cross-presentation. In these studies, γδ T cells acquired similar levels of tdTomato *in vivo* as indicator of antigen uptake from tumours, irrespective of prior zoledronate sensitisation. In addition, no significant up-regulation of HLA-DR was observed in γδ T-cells *in vivo* as compared to γδ T-APCs maintained in cell culture *in vitro*. These results suggested that γδ T cells did not become fully activated *in vivo* even in zoledronate-treated animals, which prompted us to query whether *i.v.* sensitisation with zoledronate was actually effective enough to activate γδ T-APCs in the tumour. In collaboration with Dr. Emmanuel Scotet at the University of Nantes, France, we therefore looked into the effect of zoledronate in sensitising CSC-M1 tumours *in vivo* using different injection routes. The results obtained by the team of Dr. Scotet showed that only sensitisation *via s.c.* injection near the tumour successfully induced *ex vivo* activation of γδ T cells (Figure 5.13) but not injections that were given *i.p.* or *i.v.*, which may explain why in our *in vivo* γδ T-APC model, γδ T cells were not fully activated and were unable to cross-present tumour-released Flu M1.

So far, I have not yet able to determine the exact intracellular location of tdTomato acquired by intratumoural γδ T-APCs *in vivo*. In particular, it needs to be tested whether the tdTomato signal detectable in γδ T-APCs residing in the tumours was due to membrane exchange with cell debris or apoptotic bodies by trogocytosis (Poupot *et al.*, 2005; D'Asaro *et al.*, 2010; Himoudi *et al.*, 2012; Mao *et al.*, 2014; Schneiders *et al.*, 2014) or whether it was true endocytosis. The disappearance of the tdTomato signal in γδ T-APCs after 5 hours of co-culture with $CD8^+$ responder T cells suggests that the antigens were actually internalised and processed for cross-presentation. However, only rigorous examinations such as visualisation of intracellular tdTomato and Flu M1 in γδ T-APCs isolated from tumours by IF confocal microscopy, and/or by Western blotting of tdTomato

and/or M1 within cytosolic and membrane protein extracts of γδ T-APCs isolated from tumour would provide solid evidence of actual antigen uptake by γδ T-APCs *in vivo*.

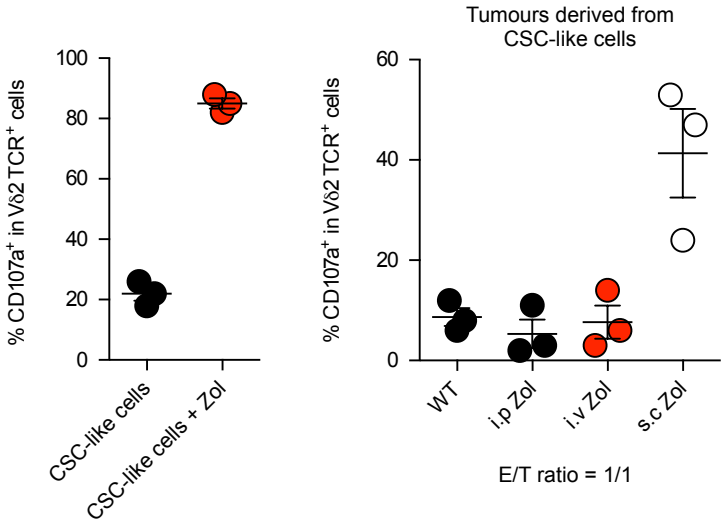

Figure 5.13. Effect of zoledronate sensitisation in tumour-bearing mice through different routes. Tumours derived from CSC-like cells were sensitised *in vivo* by administering zoledronate via different injection routes including *i.p.*, *i.v.* and *s.c.* near the tumour. Tumours were harvested on the next day and dissociated into single cells for co-cultures with γδ T cells. The activation of γδ T cells was examined by their degranulation (data kindly provided by Drs Emmanuel Scotet and Ulrich Jarry at the University of Nantes, France).

The observation of large areas of necrosis in tumours derived from CSC-like by histology (data not shown) indicates that the tdTomato signal acquired by γδ T-APCs *in vivo* may have been due to uptake of material released from tumour cells undergoing necrosis rather than originating from tumour cells killed by γδ T cells. This poses an interesting question as to which kind of cell death, *i.e.* apoptosis and necrosis, is more suitable for antigen uptake and cross-presentation by local APCs. In this respect, it has been shown that DCs can efficiently cross-present antigens from apoptotic cells to cytotoxic $CD8^+$ T cells and prime an immune response (Heath and Carbone, 2001; Steinman *et al.*, 2003). γδ T cells exhibit their cytotoxicity by inducing apoptosis of target cells through secretion of cytotoxic molecules including TRAIL, TNF, FasL, perforin, granzymes and granulysin (Chen *et al.*, 2013). The γδ T cell-induced apoptosis of cancer cells may thus create an ideal scenario for optimal cross-presentation of tumour antigens to $CD8^+$ T cells.

Moreover, apoptosis of tumour cells induced by chemotherapy, specifically doxorubicin, showed strong immunogenicity and elicited phagocytosis by DCs and protective $CD8^+$ T cells responses against established tumours in mice (Casares *et al.*, 2005; Ma *et al.*, 2011). Todaro *et al.* recently showed that treatment of colon cancer initiating cells with chemotherapeutic agents, 5-fluorouracyl and doxorubicin, enhanced their expression of NKG2D ligands and death receptor 5 (TRAIL-R2), which modulated their susceptibility to killing by γδ T cells through the secretion of TRAIL (Todaro *et al.*, 2013). Taken together, these results suggest that sensitisation of tumours, especially CSC-like cells, may significantly enhance killing by γδ T cells and cross-presentation of tumour-specific antigens to $CD8^+$ T cells for the induction of potent adaptive immunity against CSCs eventually contributing to tumour control.

While substantial $CD8^+$ T cell responses were observed in co-culture with γδ T-APCs isolated from tumours, both HLA-$A2^+$ and HLA-$A2^-$ γδ T-APCs induced similar levels of $CD8^+$ T cell responses, indicating that any true cross-presentation by γδ T-APCs, even if only minor, was likely to have been masked by contaminant HLA-$A2^+$ tumour cells remaining after FACS sorting.

Despite the failure to demonstrate cross-presentation by γδ T-APCs *in vivo*, the findings in this Chapter give important clues as to how to optimise the experimental model further. Firstly, *s.c.* injection of zoledronate near the established tumour has been identified as the most effective sensitisation route for activation of γδ T-cells. Secondly, my findings show that humanised anti-GD2 can specifically sensitise CSC-like cells to induce cytotoxicity (Figure 4.13) and possibly APC features (data not shown); future studies should therefore explore a combined sensitisation approach using both zoledronate and anti-GD2. Thirdly, in preliminary work I have already generated another Flu M1-expressing model using the HLA-$A2^-$ breast cancer cell line SKBR3 (data not shown), to overcome the inherent limitations of FACS sorting of intratumoural γδ T-cells to sufficient purities for functional assays. Experiments assessing the tumour take of these SKBR3-M1 cells in NSG mice are ongoing. Fourthly, it might be feasible to knock out HLA-A2 specifically in CSC-M1 cells using the novel CRISPR/Cas9 technology and use HLA-$A2^-$ tumour cells as targets for cross-presentation assays *in vivo*.

Chapter 6. General Discussion

6.1. Summary

In this thesis, I generated stable CSC-like and non-CSC sublines from the HMLER cell line (Elenbaas *et al.*, 2001; Mani *et al.*, 2008) with distinct phenotypical and functional characteristics confirmed *in vitro* and *in vivo* in NSG mice to study the interaction between CSC-like cells/non-CSCs and anti-tumour effector T cells. By the use of this model, I observed a powerful synergism between non-MHC-restricted γδ T cells and MHC-restricted cytotoxic $CD8^+$ T in targeting CSC-like cells. By sensitising CSC-like cells and non-CSCs with zoledronate or farnesyl diphosphate synthase (FPPS)-targeting shRNA, γδ T cells showed enhanced cytotoxicity and IFN-γ secretion. The secretion of IFN-γ by activated γδ T cells efficiently sensitised surviving CSC-like cells and non-CSCs to cytotoxic $CD8^+$ T cell-mediated killing through up-regulating the surface expression of MHC class I and CD54 on sensitised cancer cells. As alternative sensitisation strategy, the humanised anti-GD2 monoclonal antibody, (Navid *et al.*, 2014), directed γδ T cell responses including cytotoxicity and APC properties against opsonised CSC-like cells but not non-CSCs.

With regard to the APC characteristic of γδ T cells, I have shown *in vitro* that γδ T cells are able to take up exogenous antigens and cross-present them to antigen-specific cytotoxic $CD8^+$ T cells. By establishing a breast cancer model in NSG mice with transduced CSCs-like cells, which stably express tdTomato as fluorescent reporter and Flu M1 as surrogate for yet-to-be-discovered CSC-associated antigens, my data demonstrate that γδ T cells readily obtain tumour-associated antigen (tdTomato) for processing. The potential *ex vivo* cross-presentation of tumour-associated antigen (Flu M1) however was masked by technical limitations for sorting intra-tumoural γδ T-APCs to purities that are sufficient for these challenging functional studies.

In summary, the experimental model established during my PhD studies provide proof-of-principle results for CSC-targeting immunotherapies by γδ T cells with special emphasis on novel immunotherapies that might benefit from a two-pronged approach combining γδ T cell and $CD8^+$ T cell targeting strategies that triggers effective innate-like and tumour-specific adaptive responses (Figure 6.1).

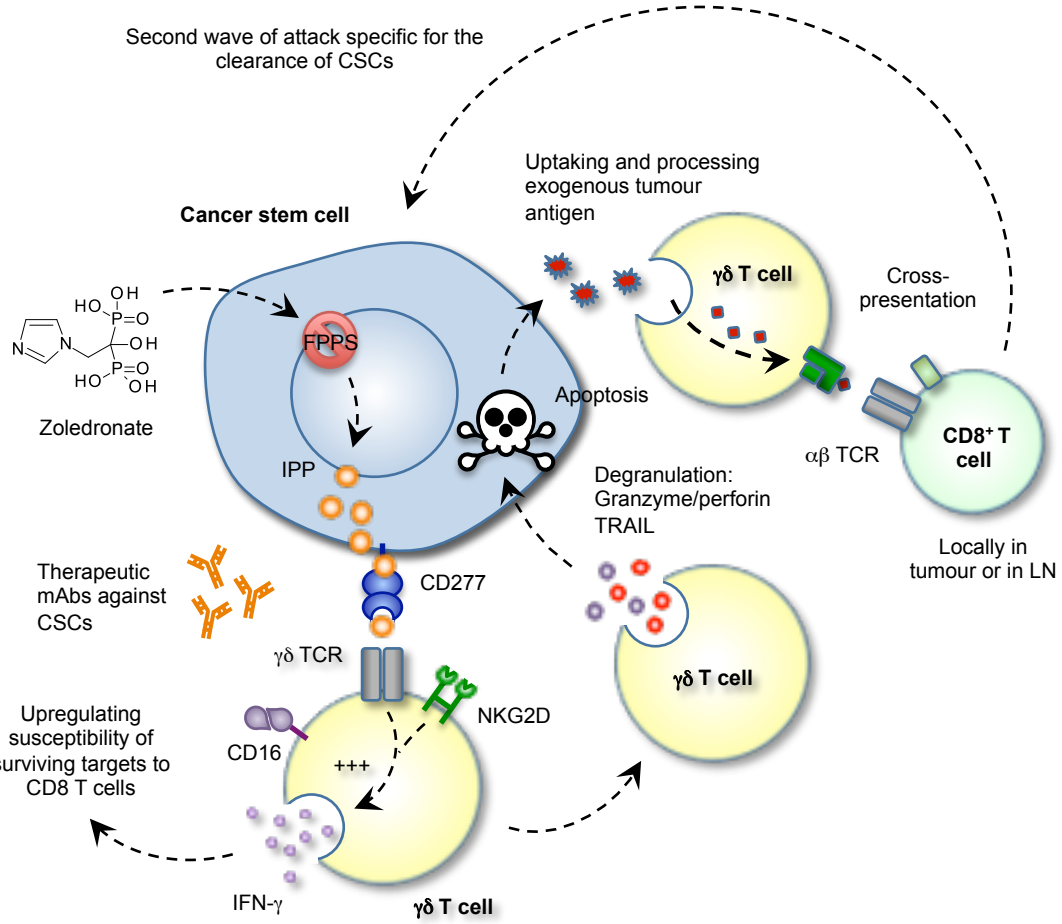

Figure 6.1. Synergistic targeting of breast CSCs by innate-like non-MHC-restricted γδ T cells and MHC-restricted cytotoxic CD8$^+$ T cells. Within a tumour, both CSCs and non-CSCs can be sensitised by zoledronate efficiently through increased presentation of IPP by BTN3 to γδ T cells. Sensitisation with therapeutic monoclonal antibodies against CSC-specific antigens, *e.g.* GD2, CD44 and Her2, may enhance the specificity of γδ T cell responses to CSCs. Upon activation, γδ T cells will kill a proportion of CSCs and concomitantly secrete IFN-γ to modulate the susceptibility of surviving CSCs to cytotoxic CD8$^+$ T cell-mediated killing. Moreover, γδ T cells may function as APCs to take up CSC-specific antigens such as ALDH1A1, released from dead CSCs into the microenvironment for cross-presentation to induce local cytotoxic CD8$^+$ T cell immunity. Activated γδ T-APCs switch their chemotactic properties by up-regulating CCR7 expression and down-regulating CCR5 expression for migration from the tumour to draining lymph nodes, where they may cross-present CSC-specific antigens and induce the maturation of naïve/central memory CD8$^+$ T cells. Mature cytotoxic CD8$^+$ T cells with specificity against CSCs will expand clonally and establish a second wave of attack for infiltrating into the tumour and subsequent eradication of residual CSCs. The re-establishment of comprehensive innate and adaptive immunity against CSCs in combination with other therapies, *e.g.* hormone therapy, chemotherapeutic drugs and radiation eradicating non-CSCs, might eventually shrink the tumour mass and prevent disease progression and relapse by the newly established balance between effective immunosurveillance and immune evasion.

6.2. γδ T cell-based immunotherapy for breast cancer

An overall survival benefit of zoledronate treatment in breast cancer patients was recently demonstrated by comprehensive meta-analyses of clinical trials on using zoledronate as an adjuvant therapy (Huang *et al.*, 2012; Valachis *et al.*, 2013). Although these studies failed to elucidate the biological mechanism underlying the anti-tumour role of zoledronate, the clinical benefit may at least in part be mediated by Vγ9/Vδ2 T-cells (Kunzmann and Wilhelm, 2011; Welton *et al.*, 2013a). In fact, targeted γδ T cell-based immunotherapies have successfully been tested in early clinical trials against various types of cancer. The design of these trials mainly relied on the cytotoxic nature of γδ T cells against cancer cells with two main approaches, namely (*i*) direct activation and expansion of γδ T cells in patients *in vivo* by administration of nBPs or synthetic phosphoantigens (Dieli *et al.*, 2007; Gertner-Dardenne *et al.*, 2009; Meraviglia *et al.*, 2010; Lang *et al.*, 2011; Kunzmann *et al.*, 2012), and (*ii*) adoptive transfer of γδ T cells expanded *ex vivo* with phosphoantigens or nBPs with or without co-administration of nBPs and IL-2 (Kobayashi *et al.*, 2007; Bennouna *et al.*, 2008; Abe *et al.*, 2009; Nakajima *et al.*, 2010; Kobayashi *et al.*, 2011; Nicol *et al.*, 2011; Sakamoto *et al.*, 2011). Fisher *et al.* as well concluded from 12 clinical trials with information on 157 patient who had received γδ T cell-based immunotherapies that γδ T cell-based immunotherapy is generally well-tolerated, safe and potentially superior to current second-line therapies such as prednisolone + docetaxel and everolimus for advanced prostate cancer and renal cell carcinoma, respectively (Fisher *et al.*, 2014). These results support the great potential of utilising Vγ9/Vδ2 T cell-cased immunotherapy as adjuvant to conventional therapies for cancer patients with advanced or refractory disease. However, besides these encouraging results suggesting the benefit of harnessing γδ T cells for treatment of cancer patient, the situation in breast cancer remains challenging. Distinct from melanoma, where tumour mass infiltration of γδ T cells, especially $V\delta2^+$ T cells is positively correlated with better prognosis (Bialasiewicz *et al.*, 1999; Cordova *et al.*, 2012), infiltration of γδ T cells in breast cancer is oppositely correlated with poor prognosis (Ma *et al.*, 2012). Specifically, Ma *et al.* showed that high numbers of tumour-infiltrating γδ T cells as determined by high magnification microscopy was positively correlated with advanced tumour stage, Her2 expression levels and lymph node metastasis, and negatively correlated with the survival of patients (Ma *et al.*, 2012). Although such retrospective studies cannot identify causal relationships and determine whether tumour-infiltrating γδ T cells actually promote or control disease progression, these findings indicate that γδ T cells play an important role in the tumour

microenvironment and progression of breast cancer. Indeed, given the striking functional plasticity of γδ T cells and distinct specificities of different subsets, γδ T cells might become distinctly polarised by the tumour microenvironment depending on the type of cancer and the disease stage, and subsequently modulate intra-tumoural responses by secretion of different sets of cytokines (Lo Presti *et al.*, 2014). Although the anti-tumour activity of γδ T cells has been well characterised by their cytotoxicity against a wide spectrum of different tumour types and their abundant IFN-γ secretion, certain γδ T cell subsets have been reported to oppositely exhibit pro-tumour activity, mainly through their production of IL-17, in various murine cancer models and in human colorectal cancer (Silva-Santos *et al.*, 2015). Murine $V\gamma4^+$ T cells in breast cancer (Coffelt *et al.*, 2015) and haptocellular carcinoma (Ma *et al.*, 2014), and $V\gamma6^+$ T cells in ovarian cancer (Rei *et al.*, 2014) were identified as the major source of IL-17, which facilitated the recruitment and function of immunesuppressive cells such as myeloid-derived suppressor cells (MDSCs), macrophages and inducible regulatory T cells. In particular, as revealed by the use of a spontaneous murine breast cancer model, secretion of IL-17 by $V\gamma4^+$ T cells contributed to the systemic polarisation and expansion of $CD11b^+Ly6G^+$ neutrophils that suppressed the $CD8^+$ T cells responses (Coffelt *et al.*, 2015). The dysregulation of protective $CD8^+$ T cell immunity subsequently led to enhanced tumour metastases to lung and lymph nodes (Coffelt *et al.*, 2015). Apart from murine γδ T cells, the pro-tumour activity of IL-17-producing γδ T cells was also reported recently in human colorectal cancer. Wu *et al.* showed that in addition to being the main source of IL-17 in the tumour microenvironment, $V\delta1^+$ T cells also secret significant level of IL-8, TNF-α and GM-CSF, which facilitate recruitment of MDSCs into the tumour microenvironment for onsite expansion, and therefore sustained the chronic pro-tumour inflammation in colorectal cancer (Wu *et al.*, 2014). In fact, the regulatory and pro-tumour activity of certain γδ T cell populations was reported majorly in breast cancer (Peng *et al.*, 2007; Ye *et al.*, 2013; Wesch *et al.*, 2014). Peng *et al.* were first to show that $V\delta1^+$ T cells within breast tumours inhibited the activation of both $CD4^+$ and $CD8^+$ T cells and abrogated the maturation of DCs possibly through a TLR8 signalling-dependent mechanism (Peng *et al.*, 2007). Later, results from the same group showed that CXCL10 secreted by breast cancer cells recruits $V\delta1^+$ T cells to the tumour microenvironment where they function as regulatory cells that induce the transition of local T cells and DCs to an immunosuppressive status (Ye *et al.*, 2013). Although these observations were on $V\delta1^+$ T cells rather than $V\delta2^+$ T cells, which exhibit distinct specificity to antigens and functions, it is important to keep in mind that

the overall tumour microenvironment in breast cancer might be uniquely immunosuppressive. The manipulation of γδ T cell responses for targeting breast cancer should therefore be carefully designed with appropriate sensitisation strategies overcoming inhibitory signals and aim to create a new anti-cancer microenvironment. Check-point inhibition of two major suppressive pathways, PD1/PD-L1 and CTLA-4/B7, might significantly help tilt the balance toward pro-inflammatory, cytotoxic T cell responses anti-cancer status to polarise γδ T cells to initiate favourable new αβ T cell response by their APC function.

Besides harnessing γδ T cells as cytotoxic killer in immunotherapy for breast cancer, their function as APC makes them a promising candidate for cancer vaccines (Moser and Eberl, 2007, 2011; Khan *et al.*, 2014b). DCs as traditional APCs have widely been used in clinical trials, albeit with disappointing results with regard to improving clinical outcomes (Palucka and Banchereau, 2012). Recently, CSCs have been used as target for the making of DC vaccines and showed substantial efficacy in targeting breast cancer (Sharma *et al.*, 2012), melanoma (Ning *et al.*, 2012), prostate cancer (Jachetti *et al.*, 2013), pancreatic cancer (Yin *et al.*, 2014), and glioma (Xu *et al.*, 2009b; Hua *et al.*, 2011). Specifically for targeting breast CSCs, Sharma *et al.* showed that administration of a Her2 DC vaccine to patients suffering from Her2-overexpressing ductal carcinoma *in situ* (DCIS) is safe and well-tolerated. The vaccination significantly induced the decline and/or eradication of Her2 expression in these patients (Sharma *et al.*, 2012). Ning *et al.* showed that as compared to vaccination with DCs pulsed with bulk cancer cells, vaccination of DCs pulsed with $ALDH^+$ CSCs isolated from melanoma or squamous tumours augmented CSC-specific antibody responses, primed CSC-specific cytotoxic $CD8^+$ T cell responses, and ultimately led to reduced lung metastasis. These findings suggest that vaccines specifically targeting CSCs may have true clinical impact. Meuter *et al.* showed that γδ T cells process antigens in a way distinctly from DCs and generate different peptide fragments from the same antigen for cross-presentation (Brandes *et al.*, 2009; Meuter *et al.*, 2010), suggesting that the APC function of γδ T cells is non-redundant and may be important to broaden the spectrum of adaptive αβ T cell immunity. Indeed, which types of antigens are preferentially presented by γδ T cells or DCs (which utilise different proteasomes for antigen processing) requires further investigation. In addition, the detailed mechanism of how γδ T cells process antigens needs to be defined better to ultimately inform the design of a γδ T cell-based vaccine that boost anti-tumour αβ T cell

responses. In conclusion, taking advantage of the dual innate-like cytotoxicity and antigen-presentation function of γδ T cells and their rapid and substantial expansion *ex vivo*, preparation of a γδ T cell vaccine is feasible and can thus establish potent and persistent anti-cancer immunity by *in situ* killing of cancer cell and induction of αβ T cell immunity (Moser and Eberl, 2011; Khan *et al.*, 2014b).

References

Abe, Y., Muto, M., Nieda, M., Nakagawa, Y., Nicol, A.*, et al.* (2009). Clinical and immunological evaluation of zoledronate-activated Vγ9 γδ T-cell-based immunotherapy for patients with multiple myeloma. ***Exp Hematol*** *37*, 956-968.

Abeler-Dorner, L., Swamy, M., Williams, G., Hayday, A.C., and Bas, A. (2012). Butyrophilins: an emerging family of immune regulators. ***Trends Immunol*** *33*, 34-41.

Adams, E.J., Gu, S., and Luoma, A.M. (2015). Human γδ T cells: evolution and ligand recognition. ***Cell Immunol*** *296*, 31-40.

Ahmed, M., and Cheung, N.K. (2014). Engineering anti-GD2 monoclonal antibodies for cancer immunotherapy. ***FEBS Lett*** *588*, 288-297.

Al-Hajj, M., Wicha, M.S., Benito-Hernandez, A., Morrison, S.J., and Clarke, M.F. (2003). Prospective identification of tumorigenic breast cancer cells. ***Proc Natl Acad Sci U S A*** *100*, 3983-3988.

Albert, M.L., Pearce, S.F., Francisco, L.M., Sauter, B., Roy, P.*, et al.* (1998). Immature dendritic cells phagocytose apoptotic cells *via* αvβ5 and CD36, and cross-present antigens to cytotoxic T lymphocytes. ***J Exp Med*** *188*, 1359-1368.

Alexander, A.A., Maniar, A., Cummings, J.S., Hebbeler, A.M., Schulze, D.H.*, et al.* (2008). Isopentenyl pyrophosphate-activated $CD56^+$ γδ T lymphocytes display potent antitumor activity toward human squamous cell carcinoma. ***Clin Cancer Res*** *14*, 4232-4240.

Altvater, B., Pscherer, S., Landmeier, S., Kailayangiri, S., Savoldo, B.*, et al.* (2012). Activated human γδ T cells induce peptide-specific $CD8^+$ T-cell responses to tumor-associated self-antigens. ***Cancer Immunol Immunother*** *61*, 385-396.

Angelini, D.F., Borsellino, G., Poupot, M., Diamantini, A., Poupot, R.*, et al.* (2004). FcγRIII discriminates between 2 subsets of Vγ9Vδ2 effector cells with different responses and activation pathways. ***Blood*** *104*, 1801-1807.

Arnett, H.A., and Viney, J.L. (2014). Immune modulation by butyrophilins. ***Nat Rev Immunol*** *14*, 559-569.

Asslan, R., Pradines, A., Pratx, C., Allal, C., Favre, G.*, et al.* (1999). Epidermal growth factor stimulates 3-hydroxy-3-methylglutaryl-coenzyme A reductase expression *via* the ErbB-2 pathway in human breast adenocarcinoma cells. ***Biochem Biophys Res Commun*** *260*, 699-706.

Bai, L., Picard, D., Anderson, B., Chaudhary, V., Luoma, A., *et al.* (2012). The majority of CD1d-sulfatide-specific T cells in human blood use a semiinvariant Vδ1 TCR. ***Eur J Immunol*** *42*, 2505-2510.

Bao, S., Wu, Q., McLendon, R.E., Hao, Y., Shi, Q., *et al.* (2006). Glioma stem cells promote radioresistance by preferential activation of the DNA damage response. ***Nature*** *444*, 756-760.

Barnaba, V., Watts, C., de Boer, M., Lane, P., and Lanzavecchia, A. (1994). Professional presentation of antigen by activated human T cells. ***Eur J Immunol*** *24*, 71-75.

Battistini, L., Caccamo, N., Borsellino, G., Meraviglia, S., Angelini, D.F., *et al.* (2005). Homing and memory patterns of human γδ T cells in physiopathological situations. ***Microbes Infect*** *7*, 510-517.

Battula, V.L., Shi, Y., Evans, K.W., Wang, R.Y., Spaeth, E.L., *et al.* (2012). Ganglioside GD2 identifies breast cancer stem cells and promotes tumorigenesis. ***J Clin Invest*** *122*, 2066-2078.

Beck, B., and Blanpain, C. (2013). Unravelling cancer stem cell potential. ***Nat Rev Cancer*** *13*, 727-738.

Beck, B.H., Kim, H.G., Kim, H., Samuel, S., Liu, Z., *et al.* (2010). Adoptively transferred *ex vivo* expanded γδ-T cells mediate *in vivo* antitumor activity in preclinical mouse models of breast cancer. ***Breast Cancer Res Treat*** *122*, 135-144.

Bennouna, J., Bompas, E., Neidhardt, E.M., Rolland, F., Philip, I., *et al.* (2008). Phase-I study of Innacell γδ, an autologous cell-therapy product highly enriched in γ9δ2 T lymphocytes, in combination with IL-2, in patients with metastatic renal cell carcinoma. ***Cancer Immunol Immunother*** *57*, 1599-1609.

Benzaid, I., Monkkonen, H., Stresing, V., Bonnelye, E., Green, J., *et al.* (2011). High phosphoantigen levels in bisphosphonate-treated human breast tumors promote Vγ9Vδ2 T-cell chemotaxis and cytotoxicity *in vivo*. ***Cancer Res*** *71*, 4562-4572.

Bessoles, S., Ni, M., Garcia-Jimenez, S., Sanchez, F., and Lafont, V. (2011). Role of NKG2D and its ligands in the anti-infectious activity of Vγ9Vδ2 T cells against intracellular bacteria. ***Eur J Immunol*** *41*, 1619-1628.

Bialasiewicz, A.A., Ma, J.X., and Richard, G. (1999). α/β and γ/δ TCR^+ lymphocyte infiltration in necrotising choroidal melanomas. ***Brit J Ophthalmol*** *83*, 1069-1073.

Biddle, A., Liang, X., Gammon, L., Fazil, B., Harper, L.J.*, et al.* (2011). Cancer stem cells in squamous cell carcinoma switch between two distinct phenotypes that are preferentially migratory or proliferative. ***Cancer Res*** *71*, 5317-5326.

Bombonati, A., and Sgroi, D.C. (2011). The molecular pathology of breast cancer progression. ***J Pathol*** *223*, 307-317.

Bonnet, D., and Dick, J.E. (1997). Human acute myeloid leukemia is organized as a hierarchy that originates from a primitive hematopoietic cell. ***Nat Med*** *3*, 730-737.

Bonneville, M., O'Brien, R.L., and Born, W.K. (2010). γδ T cell effector functions: a blend of innate programming and acquired plasticity. ***Nat Rev Immunol*** *10*, 467-478.

Born, W.K., Vollmer, M., Reardon, C., Matsuura, E., Voelker, D.R.*, et al.* (2003). Hybridomas expressing γδ T-cell receptors respond to cardiolipin and β2-glycoprotein 1 (apolipoprotein H). ***Scand J Immunol*** *58*, 374-381.

Borst, J., Vroom, T.M., Bos, J.D., and Van Dongen, J.J. (1991). Tissue distribution and repertoire selection of human γδ T cells: comparison with the murine system. ***Curr Top Microbiol Immunol*** *173*, 41-46.

Borst, J., Wicherink, A., Van Dongen, J.J., De Vries, E., Comans-Bitter, W.M.*, et al.* (1989). Non-random expression of T cell receptor γ and δ variable gene segments in functional T lymphocyte clones from human peripheral blood. ***Eur J Immunol*** *19*, 1559-1568.

Brandes, M., Willimann, K., Bioley, G., Levy, N., Eberl, M.*, et al.* (2009). Cross-presenting human γδ T cells induce robust $CD8^+$ αβ T cell responses. ***Proc Natl Acad Sci U S A*** *106*, 2307-2312.

Brandes, M., Willimann, K., Lang, A.B., Nam, K.H., Jin, C.*, et al.* (2003). Flexible migration program regulates γδ T-cell involvement in humoral immunity. ***Blood*** *102*, 3693-3701.

Brandes, M., Willimann, K., and Moser, B. (2005). Professional antigen-presentation function by human γδ T Cells. ***Science*** *309*, 264-268.

Brown, C.E., Starr, R., Martinez, C., Aguilar, B., D'Apuzzo, M.*, et al.* (2009). Recognition and killing of brain tumor stem-like initiating cells by $CD8^+$ cytolytic T cells. ***Cancer Res*** *69*, 8886-8893.

Bruder, J., Siewert, K., Obermeier, B., Malotka, J., Scheinert, P.*, et al.* (2012). Target specificity of an autoreactive pathogenic human γδ-T cell receptor in myositis. ***J Biol Chem*** *287*, 20986-20995.

Bucur, O., Ray, S., Bucur, M.C., and Almasan, A. (2006). APO2 ligand/tumor necrosis factor-related apoptosis-inducing ligand in prostate cancer therapy. ***Front Biosci*** *11*, 1549-1568.

Caccamo, N., Todaro, M., Sireci, G., Meraviglia, S., Stassi, G., *et al.* (2013). Mechanisms underlying lineage commitment and plasticity of human γδ T cells. ***Cell Mol Immunol*** *10*, 30-34.

Campbell, L.L., and Polyak, K. (2007). Breast tumor heterogeneity: cancer stem cells or clonal evolution? ***Cell Cycle*** *6*, 2332-2338.

Capietto, A.H., Martinet, L., and Fournie, J.J. (2011). Stimulated γδ T cells increase the *in vivo* efficacy of trastuzumab in HER-2^+ breast cancer. ***J Immunol*** *187*, 1031-1038.

Carey, L.A., Perou, C.M., Livasy, C.A., Dressler, L.G., Cowan, D., *et al.* (2006). Race, breast cancer subtypes, and survival in the Carolina Breast Cancer Study. ***JAMA*** *295*, 2492-2502.

Casares, N., Pequignot, M.O., Tesniere, A., Ghiringhelli, F., Roux, S., *et al.* (2005). Caspase-dependent immunogenicity of doxorubicin-induced tumor cell death. ***J Exp Med*** *202*, 1691-1701.

Casorati, G., De Libero, G., Lanzavecchia, A., and Migone, N. (1989). Molecular analysis of human γ/δ^+ clones from thymus and peripheral blood. ***J Exp Med*** *170*, 1521-1535.

Chaffer, C.L., Brueckmann, I., Scheel, C., Kaestli, A.J., Wiggins, P.A., *et al.* (2011). Normal and neoplastic nonstem cells can spontaneously convert to a stem-like state. ***Proc Natl Acad Sci U S A*** *108*, 7950-7955.

Chan, K.S., Espinosa, I., Chao, M., Wong, D., Ailles, L., *et al.* (2009). Identification, molecular characterization, clinical prognosis, and therapeutic targeting of human bladder tumor-initiating cells. ***Proc Natl Acad Sci U S A*** *106*, 14016-14021.

Chang, C.C., and Ferrone, S. (2006). NK cell activating ligands on human malignant cells: molecular and functional defects and potential clinical relevance. ***Semin Cancer Biol*** *16*, 383-392.

Chang, M. (2012). Tamoxifen resistance in breast cancer. ***Biomol Ther (Seoul)*** *20*, 256-267.

Chen, H.C., Chou, A.S., Liu, Y.C., Hsieh, C.H., Kang, C.C., *et al.* (2011). Induction of metastatic cancer stem cells from the NK/LAK-resistant floating, but not adherent, subset of the UP-LN1 carcinoma cell line by IFN-γ. ***Lab Invest*** *91*, 1502-1513.

Chen, H.C., Dieli, F., and Eberl, M. (2013). An unconventional TRAIL to cancer therapy. ***Eur J Immunol*** *43*, 3159-3162.

Chen, Z.W., and Letvin, N.L. (2003). Adaptive immune response of Vγ2Vδ2 T cells: a new paradigm. ***Trends Immunol*** *24*, 213-219.

Chou, A.H., Tsai, H.F., Lin, L.L., Hsieh, S.L., Hsu, P.I., *et al.* (2001). Enhanced proliferation and increased IFN-γ production in T cells by signal transduced through TNF-related apoptosis-inducing ligand. ***J Immunol*** *167*, 1347-1352.

Chouaib, S., Janji, B., Tittarelli, A., Eggermont, A., and Thiery, J.P. (2014). Tumor plasticity interferes with anti-tumor immunity. ***Crit Rev Immunol*** *34*, 91-102.

Ciccone, E., Viale, O., Pende, D., Malnati, M., Battista Ferrara, G., *et al.* (1989). Specificity of human T lymphocytes expressing a γ/δ T cell antigen receptor: recognition of a polymorphic determinant of HLA class I molecules by a γ/δ clone. ***Eur J Immunol*** *19*, 1267-1271.

Cleator, S., Heller, W., and Coombes, R.C. (2007). Triple-negative breast cancer: therapeutic options. ***Lancet Oncol*** *8*, 235-244.

Coffelt, S.B., Kersten, K., Doornebal, C.W., Weiden, J., Vrijland, K., *et al.* (2015). IL-17-producing γδ T cells and neutrophils conspire to promote breast cancer metastasis. ***Nature*** *522*, 345-348.

Compte, E., Pontarotti, P., Collette, Y., Lopez, M., and Olive, D. (2004). Frontline: characterization of BT3 molecules belonging to the B7 family expressed on immune cells. ***Eur J Immunol*** *34*, 2089-2099.

Constant, P., Davodeau, F., Peyrat, M.A., Poquet, Y., Puzo, G., *et al.* (1994). Stimulation of human γδ T cells by nonpeptidic mycobacterial ligands. ***Science*** *264*, 267-270.

Cordova, A., Toia, F., La Mendola, C., Orlando, V., Meraviglia, S., *et al.* (2012). Characterization of human γδ T lymphocytes infiltrating primary malignant melanomas. ***PLoS One*** *7*, e49878.

Corvaisier, M., Moreau-Aubry, A., Diez, E., Bennouna, J., Mosnier, J.F., *et al.* (2005). Vγ9Vδ2 T cell response to colon carcinoma cells. ***J Immunol*** *175*, 5481-5488.

Crowley, M.P., Reich, Z., Mavaddat, N., Altman, J.D., and Chien, Y. (1997). The recognition of the nonclassical major histocompatibility complex (MHC) class I molecule, T10, by the γδ T cell, G8. ***J Exp Med*** *185*, 1223-1230.

D'Asaro, M., La Mendola, C., Di Liberto, D., Orlando, V., Todaro, M., *et al.* (2010). Vγ9Vδ2 T lymphocytes efficiently recognize and kill zoledronate-sensitized, imatinib-

sensitive, and imatinib-resistant chronic myelogenous leukemia cells. ***J Immunol*** *184*, 3260-3268.

Dai, Y., Chen, H., Mo, C., Cui, L., and He, W. (2012). Ectopically expressed human tumor biomarker MutS homologue 2 is a novel endogenous ligand that is recognized by human γδ T cells to induce innate anti-tumor/virus immunity. ***J Biol Chem*** *287*, 16812-16819.

Das, H., Groh, V., Kuijl, C., Sugita, M., Morita, C.T.*, et al.* (2001). MICA engagement by human Vγ2Vδ2 T cells enhances their antigen-dependent effector function. ***Immunity*** *15*, 83-93.

De Libero, G., Casorati, G., Giachino, C., Carbonara, C., Migone, N.*, et al.* (1991). Selection by two powerful antigens may account for the presence of the major population of human peripheral γ/δ T cells. ***J Exp Med*** *173*, 1311-1322.

De Libero, G., Lau, S.Y., and Mori, L. (2014). Phosphoantigen presentation to TCR γδ cells, a conundrum getting less gray zones. ***Front Immunol*** *5*, 679.

Dean, M., Fojo, T., and Bates, S. (2005). Tumour stem cells and drug resistance. ***Nat Rev Cancer*** *5*, 275-284.

Decaup, E., Duault, C., Bezombes, C., Poupot, M., Savina, A.*, et al.* (2014). Phosphoantigens and butyrophilin 3A1 induce similar intracellular activation signaling in human TCR $V\gamma9^+$ γδ T lymphocytes. ***Immunol Lett*** *161*, 133-137.

den Hollander, M.W., Gietema, J.A., de Jong, S., Walenkamp, A.M., Reyners, A.K.*, et al.* (2013). Translating TRAIL-receptor targeting agents to the clinic. ***Cancer Lett*** *332*, 194-201.

Deniger, D.C., Maiti, S.N., Mi, T., Switzer, K.C., Ramachandran, V.*, et al.* (2014). Activating and propagating polyclonal γδ T cells with broad specificity for malignancies. ***Clin Cancer Res*** *20*, 5708-5719.

Deniger, D.C., Switzer, K., Mi, T., Maiti, S., Hurton, L.*, et al.* (2013). Bispecific T-cells expressing polyclonal repertoire of endogenous γδ T-cell receptors and introduced CD19-specific chimeric antigen receptor. ***Mol Ther*** *21*, 638-647.

Deryugina, E.I., and Quigley, J.P. (2006). Matrix metalloproteinases and tumor metastasis. ***Cancer Metastasis Rev*** *25*, 9-34.

Devaud, C., Bilhere, E., Loizon, S., Pitard, V., Behr, C.*, et al.* (2009). Antitumor activity of γδ T cells reactive against cytomegalovirus-infected cells in a mouse xenograft tumor model. ***Cancer Res*** *69*, 3971-3978.

Devaud, C., Rousseau, B., Netzer, S., Pitard, V., Paroissin, C., *et al.* (2013). Anti-metastatic potential of human Vδ1$^+$ γδ T cells in an orthotopic mouse xenograft model of colon carcinoma. ***Cancer Immunol Immunother*** *62*, 1199-1210.

Dhar, S., and Chiplunkar, S.V. (2010). Lysis of aminobisphosphonate-sensitized MCF-7 breast tumor cells by Vγ9Vδ2 T cells. ***Cancer Immun*** *10*, 10.

Di Tomaso, T., Mazzoleni, S., Wang, E., Sovena, G., Clavenna, D., *et al.* (2010). Immunobiological characterization of cancer stem cells isolated from glioblastoma patients. ***Clin Cancer Res*** *16*, 800-813.

Dieli, F., Poccia, F., Lipp, M., Sireci, G., Caccamo, N., *et al.* (2003). Differentiation of effector/memory Vδ2 T cells and migratory routes in lymph nodes or inflammatory sites. ***J Exp Med*** *198*, 391-397.

Dieli, F., Vermijlen, D., Fulfaro, F., Caccamo, N., Meraviglia, S., *et al.* (2007). Targeting human γδ T cells with zoledronate and interleukin-2 for immunotherapy of hormone-refractory prostate cancer. ***Cancer Res*** *67*, 7450-7457.

Dokouhaki, P., Han, M., Joe, B., Li, M., Johnston, M.R., *et al.* (2010). Adoptive immunotherapy of cancer using *ex vivo* expanded human γδ T cells: A new approach. ***Cancer Lett*** *297*, 126-136.

Dokouhaki, P., Schuh, N.W., Joe, B., Allen, C.A., Der, S.D., *et al.* (2013). NKG2D regulates production of soluble TRAIL by *ex vivo* expanded human γδ T cells. ***Eur J Immunol*** *43*, 3175-3182.

Dontu, G., and Wicha, M.S. (2005). Survival of mammary stem cells in suspension culture: implications for stem cell biology and neoplasia. ***J Mammary Gland Biol Neoplasia*** *10*, 75-86.

Dudley, M.E., Wunderlich, J.R., Yang, J.C., Sherry, R.M., Topalian, S.L., *et al.* (2005). Adoptive cell transfer therapy following non-myeloablative but lymphodepleting chemotherapy for the treatment of patients with refractory metastatic melanoma. ***J Clin Oncol*** *23*, 2346-2357.

Dull, T., Zufferey, R., Kelly, M., Mandel, R.J., Nguyen, M., *et al.* (1998). A third-generation lentivirus vector with a conditional packaging system. ***J Virol*** *72*, 8463-8471.

Early Breast Cancer Trialists' Collaborative, G. (2005). Effects of chemotherapy and hormonal therapy for early breast cancer on recurrence and 15-year survival: an overview of the randomised trials. ***Lancet*** *365*, 1687-1717.

Eberl, M., Hintz, M., Reichenberg, A., Kollas, A.K., Wiesner, J., *et al.* (2003). Microbial isoprenoid biosynthesis and human γδ T cell activation. ***FEBS Lett*** *544*, 4-10.

Elenbaas, B., Spirio, L., Koerner, F., Fleming, M.D., Zimonjic, D.B., ***et al.*** (2001). Human breast cancer cells generated by oncogenic transformation of primary mammary epithelial cells. ***Genes Dev*** *15*, 50-65.

Faure, F., Jitsukawa, S., Miossec, C., and Hercend, T. (1990). CD1c as a target recognition structure for human T lymphocytes: analysis with peripheral blood γ/δ cells. ***Eur J Immunol*** *20*, 703-706.

Ferlay, J., Soerjomataram, I., Dikshit, R., Eser, S., Mathers, C., ***et al.*** (2015). Cancer incidence and mortality worldwide: sources, methods and major patterns in GLOBOCAN 2012. ***Int J Cancer*** *136*, E359-386.

Fisch, P., Malkovsky, M., Kovats, S., Sturm, E., Braakman, E., ***et al.*** (1990). Recognition by human Vγ9/Vδ2 T cells of a GroEL homolog on Daudi Burkitt's lymphoma cells. ***Science*** *250*, 1269-1273.

Fisher, J.P., Heuijerjans, J., Yan, M., Gustafsson, K., and Anderson, J. (2014). γδ T cells for cancer immunotherapy: A systematic review of clinical trials. ***Oncoimmunology*** *3*, e27572.

Foulkes, W.D., Smith, I.E., and Reis-Filho, J.S. (2010). Triple-negative breast cancer. ***N Engl J Med*** *363*, 1938-1948.

Gao, Y., Yang, W., Pan, M., Scully, E., Girardi, M., ***et al.*** (2003). γδ T cells provide an early source of interferon γ in tumor immunity. ***J Exp Med*** *198*, 433-442.

Gertner, J., Wiedemann, A., Poupot, M., and Fournie, J.J. (2007). Human γδ T lymphocytes strip and kill tumor cells simultaneously. ***Immunol Lett*** *110*, 42-53.

Gertner-Dardenne, J., Bonnafous, C., Bezombes, C., Capietto, A.H., Scaglione, V., ***et al.*** (2009). Bromohydrin pyrophosphate enhances antibody-dependent cell-mediated cytotoxicity induced by therapeutic antibodies. ***Blood*** *113*, 4875-4884.

Gertner-Dardenne, J., Castellano, R., Mamessier, E., Garbit, S., Kochbati, E., ***et al.*** (2012). Human Vγ9Vδ2 T cells specifically recognize and kill acute myeloid leukemic blasts. ***J Immunol*** *188*, 4701-4708.

Ginestier, C., Hur, M.H., Charafe-Jauffret, E., Monville, F., Dutcher, J., ***et al.*** (2007). ALDH1 is a marker of normal and malignant human mammary stem cells and a predictor of poor clinical outcome. ***Cell Stem Cell*** *1*, 555-567.

Ginestier, C., Liu, S., Diebel, M.E., Korkaya, H., Luo, M., ***et al.*** (2010). CXCR1 blockade selectively targets human breast cancer stem cells *in vitro* and in xenografts. ***J Clin Invest*** *120*, 485-497.

Ginestier, C., Monville, F., Wicinski, J., Cabaud, O., Cervera, N.*, et al.* (2012). Mevalonate metabolism regulates basal breast cancer stem cells and is a potential therapeutic target. ***Stem Cells*** *30*, 1327-1337.

Girardi, M., Oppenheim, D.E., Steele, C.R., Lewis, J.M., Glusac, E.*, et al.* (2001). Regulation of cutaneous malignancy by γδ T cells. ***Science*** *294*, 605-609.

Gober, H.J., Kistowska, M., Angman, L., Jeno, P., Mori, L.*, et al.* (2003). Human T cell receptor γδ cells recognize endogenous mevalonate metabolites in tumor cells. ***J Exp Med*** *197*, 163-168.

Gonzalez-Angulo, A.M., Morales-Vasquez, F., and Hortobagyi, G.N. (2007). Overview of resistance to systemic therapy in patients with breast cancer. ***Adv Exp Med Biol*** *608*, 1-22.

Goodell, M.A., Rosenzweig, M., Kim, H., Marks, D.F., DeMaria, M.*, et al.* (1997). Dye efflux studies suggest that hematopoietic stem cells expressing low or undetectable levels of CD34 antigen exist in multiple species. ***Nat Med*** *3*, 1337-1345.

Goodman, T., and Lefrancois, L. (1988). Expression of the γδ T-cell receptor on intestinal $CD8^+$ intraepithelial lymphocytes. ***Nature*** *333*, 855-858.

Green, A.E., Lissina, A., Hutchinson, S.L., Hewitt, R.E., Temple, B.*, et al.* (2004). Recognition of nonpeptide antigens by human Vγ9Vδ2 T cells requires contact with cells of human origin. ***Clin Exp Immunol*** *136*, 472-482.

Greenberg, M.E., Sun, M., Zhang, R., Febbraio, M., Silverstein, R.*, et al.* (2006). Oxidized phosphatidylserine-CD36 interactions play an essential role in macrophage-dependent phagocytosis of apoptotic cells. ***J Exp Med*** *203*, 2613-2625.

Groh, V., Steinle, A., Bauer, S., and Spies, T. (1998). Recognition of stress-induced MHC molecules by intestinal epithelial γδ T cells. ***Science*** *279*, 1737-1740.

Gu, S., Nawrocka, W., and Adams, E.J. (2014). Sensing of Pyrophosphate Metabolites by Vγ9Vδ2 T Cells. ***Front Immunol*** *5*, 688.

Gupta, P.B., Onder, T.T., Jiang, G., Tao, K., Kuperwasser, C.*, et al.* (2009). Identification of selective inhibitors of cancer stem cells by high-throughput screening. ***Cell*** *138*, 645-659.

Halary, F., Pitard, V., Dlubek, D., Krzysiek, R., de la Salle, H.*, et al.* (2005). Shared reactivity of $V\delta2^{neg}$ γδ T cells against cytomegalovirus-infected cells and tumor intestinal epithelial cells. ***J Exp Med*** *201*, 1567-1578.

Hanahan, D., and Weinberg, R.A. (2011). Hallmarks of cancer: the next generation. ***Cell*** *144*, 646-674.

Harding, C.V., and Boom, W.H. (2010). Regulation of antigen presentation by Mycobacterium tuberculosis: a role for Toll-like receptors. ***Nat Rev Microbiol*** *8*, 296-307.

Harly, C., Guillaume, Y., Nedellec, S., Peigne, C.M., Monkkonen, H.*, et al.* (2012). Key implication of CD277/butyrophilin-3 (BTN3A) in cellular stress sensing by a major human γδ T-cell subset. ***Blood*** *120*, 2269-2279.

Harly, C., Peigne, C.M., and Scotet, E. (2014). Molecules and Mechanisms Implicated in the Peculiar Antigenic Activation Process of Human Vγ9Vδ2 T Cells. ***Front Immunol*** *5*, 657.

Harwood, H.J., Jr., Alvarez, I.M., Noyes, W.D., and Stacpoole, P.W. (1991). *In vivo* regulation of human leukocyte 3-hydroxy-3-methylglutaryl coenzyme A reductase: increased enzyme protein concentration and catalytic efficiency in human leukemia and lymphoma. ***J Lipid Res*** *32*, 1237-1252.

Hayday, A.C. (2000). γδ cells: a right time and a right place for a conserved third way of protection. ***Annu Rev Immunol*** *18*, 975-1026.

Heath, W.R., and Carbone, F.R. (2001). Cross-presentation, dendritic cells, tolerance and immunity. ***Annu Rev Immunol*** *19*, 47-64.

Hermann, P.C., Huber, S.L., Herrler, T., Aicher, A., Ellwart, J.W.*, et al.* (2007). Distinct populations of cancer stem cells determine tumor growth and metastatic activity in human pancreatic cancer. ***Cell Stem Cell*** *1*, 313-323.

Himoudi, N., Morgenstern, D.A., Yan, M., Vernay, B., Saraiva, L.*, et al.* (2012). Human γδ T lymphocytes are licensed for professional antigen presentation by interaction with opsonized target cells. ***J Immunol*** *188*, 1708-1716.

Hintz, M., Reichenberg, A., Altincicek, B., Bahr, U., Gschwind, R.M.*, et al.* (2001). Identification of (E)-4-hydroxy-3-methyl-but-2-enyl pyrophosphate as a major activator for human γδ T cells in Escherichia coli. ***FEBS Lett*** *509*, 317-322.

Hollier, B.G., Tinnirello, A.A., Werden, S.J., Evans, K.W., Taube, J.H.*, et al.* (2013). FOXC2 expression links epithelial-mesenchymal transition and stem cell properties in breast cancer. ***Cancer Res*** *73*, 1981-1992.

Holoshitz, J., Vila, L.M., Keroack, B.J., McKinley, D.R., and Bayne, N.K. (1992). Dual antigenic recognition by cloned human γδ T cells. ***J Clin Invest*** *89*, 308-314.

Hsiao, C.H., Lin, X., Barney, R.J., Shippy, R.R., Li, J.*, et al.* (2014). Synthesis of a phosphoantigen prodrug that potently activates Vγ9Vδ2 T-lymphocytes. ***Chem Biol*** *21*, 945-954.

Hsieh, C.H., Hsu, Y.J., Chang, C.C., Liu, H.C., Chuang, K.L.*, et al.* (2009). Total HLA class I loss in a sarcomatoid renal carcinoma cell line caused by the coexistence of distinct mutations in the two encoding β2-microglobulin genes. ***Cancer Immunol Immunother*** *58*, 395-408.

Hu, C., Qian, L., Miao, Y., Huang, Q., Miao, P.*, et al.* (2012). Antigen-presenting effects of effector memory Vγ9Vδ2 T cells in rheumatoid arthritis. ***Cell Mol Immunol*** *9*, 245-254.

Hu, Z., Fan, C., Oh, D.S., Marron, J.S., He, X.*, et al.* (2006). The molecular portraits of breast tumors are conserved across microarray platforms. ***BMC Genomics*** *7*, 96.

Hua, W., Yao, Y., Chu, Y., Zhong, P., Sheng, X.*, et al.* (2011). The $CD133^{+}$ tumor stem-like cell-associated antigen may elicit highly intense immune responses against human malignant glioma. ***J Neurooncol*** *105*, 149-157.

Huang, W.W., Huang, C., Liu, J., Zheng, H.Y., and Lin, L. (2012). Zoledronic acid as an adjuvant therapy in patients with breast cancer: a systematic review and meta-analysis. ***PLoS One*** *7*, e40783.

Hudspeth, K., Silva-Santos, B., and Mavilio, D. (2013). Natural cytotoxicity receptors: broader expression patterns and functions in innate and adaptive immune cells. ***Front Immunol*** *4*, 69.

Hwang-Verslues, W.W., Kuo, W.H., Chang, P.H., Pan, C.C., Wang, H.H.*, et al.* (2009). Multiple lineages of human breast cancer stem/progenitor cells identified by profiling with stem cell markers. ***PLoS One*** *4*, e8377.

Idrees, A.S., Sugie, T., Inoue, C., Murata-Hirai, K., Okamura, H.*, et al.* (2013). Comparison of γδ T cell responses and farnesyl diphosphate synthase inhibition in tumor cells pretreated with zoledronic acid. ***Cancer Sci*** *104*, 536-542.

Ignatiadis, M., and Sotiriou, C. (2013). Luminal breast cancer: from biology to treatment. ***Nat Rev Clin Oncol*** *10*, 494-506.

Ithimakin, S., Day, K.C., Malik, F., Zen, Q., Dawsey, S.J.*, et al.* (2013). HER2 drives luminal breast cancer stem cells in the absence of HER2 amplification: implications for efficacy of adjuvant trastuzumab. ***Cancer Res*** *73*, 1635-1646.

Jachetti, E., Mazzoleni, S., Grioni, M., Ricupito, A., Brambillasca, C.*, et al.* (2013). Prostate cancer stem cells are targets of both innate and adaptive immunity and elicit tumor-specific immune responses. ***Oncoimmunology*** *2*, e24520.

Janeway, C.A., Jr., Jones, B., and Hayday, A. (1988). Specificity and function of T cells bearing γδ receptors. ***Immunol Today*** *9*, 73-76.

Jin, L., Hope, K.J., Zhai, Q., Smadja-Joffe, F., and Dick, J.E. (2006). Targeting of CD44 eradicates human acute myeloid leukemic stem cells. ***Nat Med*** *12*, 1167-1174.

Joffre, O.P., Segura, E., Savina, A., and Amigorena, S. (2012). Cross-presentation by dendritic cells. ***Nat Rev Immunol*** *12*, 557-569.

Johnson, R.M., Lancki, D.W., Sperling, A.I., Dick, R.F., Spear, P.G.*, et al.* (1992). A murine $CD4^-$, $CD8^-$ T cell receptor-γδ T lymphocyte clone specific for herpes simplex virus glycoprotein I. ***J Immunol*** *148*, 983-988.

Jomaa, H., Feurle, J., Luhs, K., Kunzmann, V., Tony, H.P.*, et al.* (1999). Vγ9/Vδ2 T cell activation induced by bacterial low molecular mass compounds depends on the 1-deoxy-D-xylulose 5-phosphate pathway of isoprenoid biosynthesis. ***FEMS Immunol Med Microbiol*** *25*, 371-378.

Kabelitz, D., Wesch, D., Pitters, E., and Zoller, M. (2004). Characterization of tumor reactivity of human Vγ9Vδ2 γδ T cells *in vitro* and in SCID mice *in vivo*. ***J Immunol*** *173*, 6767-6776.

Kalluri, R. (2009). EMT: when epithelial cells decide to become mesenchymal-like cells. ***J Clin Invest*** *119*, 1417-1419.

Kang, N., Zhou, J., Zhang, T., Wang, L., Lu, F.*, et al.* (2009). Adoptive immunotherapy of lung cancer with immobilized anti-TCRγδ antibody-expanded human γδ T-cells in peripheral blood. ***Cancer Biol Ther*** *8*, 1540-1549.

Kato, Y., Tanaka, Y., Tanaka, H., Yamashita, S., and Minato, N. (2003). Requirement of species-specific interactions for the activation of human γδ T cells by pamidronate. ***J Immunol*** *170*, 3608-3613.

Kawasaki, B.T., and Farrar, W.L. (2008). Cancer stem cells, CD200 and immunoevasion. ***Trends Immunol*** *29*, 464-468.

Khan, M.W., Curbishley, S.M., Chen, H.C., Thomas, A.D., Pircher, H.*, et al.* (2014a). Expanded human blood-derived γδ T cells display potent antigen-presentation functions. ***Front Immunol*** *5*, 344.

Khan, M.W., Eberl, M., and Moser, B. (2014b). Potential use of γδ T cell-based vaccines in cancer immunotherapy. ***Front Immunol*** *5*, 512.

Kobayashi, H., Tanaka, Y., Yagi, J., Minato, N., and Tanabe, K. (2011). Phase I/II study of adoptive transfer of γδ T cells in combination with zoledronic acid and IL-2 to patients with advanced renal cell carcinoma. ***Cancer Immunol Immunother*** *60*, 1075-1084.

Kobayashi, H., Tanaka, Y., Yagi, J., Osaka, Y., Nakazawa, H.*, et al.* (2007). Safety profile and anti-tumor effects of adoptive immunotherapy using γδ T cells against advanced renal cell carcinoma: a pilot study. ***Cancer Immunol Immun*** *56*, 469-476.

Kong, Y., Cao, W., Xi, X., Ma, C., Cui, L.*, et al.* (2009). The NKG2D ligand ULBP4 binds to TCRγ9/δ2 and induces cytotoxicity to tumor cells through both TCRγδ and NKG2D. ***Blood*** *114*, 310-317.

Korkaya, H., Paulson, A., Charafe-Jauffret, E., Ginestier, C., Brown, M.*, et al.* (2009). Regulation of mammary stem/progenitor cells by PTEN/Akt/β-catenin signaling. ***PLoS Biol*** *7*, e1000121.

Korkaya, H., Paulson, A., Iovino, F., and Wicha, M.S. (2008). HER2 regulates the mammary stem/progenitor cell population driving tumorigenesis and invasion. ***Oncogene*** *27*, 6120-6130.

Korkaya, H., and Wicha, M.S. (2013). HER2 and breast cancer stem cells: more than meets the eye. ***Cancer Res*** *73*, 3489-3493.

Kozbor, D., Trinchieri, G., Monos, D.S., Isobe, M., Russo, G.*, et al.* (1989). Human TCR-γ^+/δ^+, $CD8^+$ T lymphocytes recognize tetanus toxoid in an MHC-restricted fashion. ***J Exp Med*** *169*, 1847-1851.

Kreso, A., and Dick, J.E. (2014). Evolution of the cancer stem cell model. ***Cell Stem Cell*** *14*, 275-291.

Kunzmann, V., Bauer, E., Feurle, J., Weissinger, F., Tony, H.P.*, et al.* (2000). Stimulation of γδ T cells by aminobisphosphonates and induction of antiplasma cell activity in multiple myeloma. ***Blood*** *96*, 384-392.

Kunzmann, V., Bauer, E., and Wilhelm, M. (1999). γ/δ T-cell stimulation by pamidronate. ***N Engl J Med*** *340*, 737-738.

Kunzmann, V., Smetak, M., Kimmel, B., Weigang-Koehler, K., Goebeler, M.*, et al.* (2012). Tumor-promoting versus tumor-antagonizing roles of γδ T cells in cancer immunotherapy: results from a prospective phase I/II trial. ***J Immunother*** *35*, 205-213.

Kunzmann, V., and Wilhelm, M. (2005). Anti-lymphoma effect of γδ T cells. ***Leuk Lymphoma*** *46*, 671-680.

Kunzmann, V., and Wilhelm, M. (2011). Adjuvant zoledronic acid for breast cancer: mechanism of action? ***Lancet Oncol*** *12*, 991-992.

Lafont, V., Liautard, J., Liautard, J.P., and Favero, J. (2001). Production of TNF-α by human Vγ9Vδ2 T cells *via* engagement of FcγRIIIA, the low affinity type 3 receptor for

the Fc portion of IgG, expressed upon TCR activation by nonpeptidic antigen. ***J Immunol*** *166*, 7190-7199.

Lafont, V., Sanchez, F., Laprevotte, E., Michaud, H.A., Gros, L., ***et al.*** (2014). Plasticity of γδ T Cells: Impact on the anti-tumor response. ***Front Immunol*** *5*, 622.

Lai, D., Wang, F., Chen, Y., Wang, C., Liu, S., ***et al.*** (2012). Human ovarian cancer stem-like cells can be efficiently killed by γδ T lymphocytes. ***Cancer Immunol Immunother*** *61*, 979-989.

Lanca, T., Correia, D.V., Moita, C.F., Raquel, H., Neves-Costa, A., ***et al.*** (2010). The MHC class Ib protein ULBP1 is a nonredundant determinant of leukemia/lymphoma susceptibility to γδ T-cell cytotoxicity. ***Blood*** *115*, 2407-2411.

Landmeier, S., Altvater, B., Pscherer, S., Juergens, H., Varnholt, L., ***et al.*** (2009). Activated human γδ T cells as stimulators of specific $CD8^+$ T-cell responses to subdominant Epstein Barr virus epitopes: potential for immunotherapy of cancer. ***J Immunother*** *32*, 310-321.

Lang, J.M., Kaikobad, M.R., Wallace, M., Staab, M.J., Horvath, D.L., ***et al.*** (2011). Pilot trial of interleukin-2 and zoledronic acid to augment γδ T cells as treatment for patients with refractory renal cell carcinoma. ***Cancer Immunol Immunother*** *60*, 1447-1460.

Le Blanc, K., and Ringden, O. (2007). Immunomodulation by mesenchymal stem cells and clinical experience. ***J Intern Med*** *262*, 509-525.

Li, J., Herold, M.J., Kimmel, B., Muller, I., Rincon-Orozco, B., ***et al.*** (2009). Reduced expression of the mevalonate pathway enzyme farnesyl pyrophosphate synthase unveils recognition of tumor cells by Vγ9Vδ2 T cells. ***J Immunol*** *182*, 8118-8124.

Liang, Y.J., Ding, Y., Levery, S.B., Lobaton, M., Handa, K., ***et al.*** (2013). Differential expression profiles of glycosphingolipids in human breast cancer stem cells *vs*. cancer non-stem cells. ***Proc Natl Acad Sci U S A*** *110*, 4968-4973.

Liao, M.J., Zhang, C.C., Zhou, B., Zimonjic, D.B., Mani, S.A., ***et al.*** (2007). Enrichment of a population of mammary gland cells that form mammospheres and have *in vivo* repopulating activity. ***Cancer Res*** *67*, 8131-8138.

Liao, T., Kaufmann, A.M., Qian, X., Sangvatanakul, V., Chen, C., ***et al.*** (2013). Susceptibility to cytotoxic T cell lysis of cancer stem cells derived from cervical and head and neck tumor cell lines. ***J Cancer Res Clin Oncol*** *139*, 159-170.

Liu, S., Clouthier, S.G., and Wicha, M.S. (2012). Role of microRNAs in the regulation of breast cancer stem cells. ***J Mammary Gland Biol Neoplasia*** *17*, 15-21.

Lo Presti, E., Dieli, F., and Meraviglia, S. (2014). Tumor-infiltrating γδ T lymphocytes: pathogenic role, clinical significance, and differential programing in the tumor microenvironment. ***Front Immunol*** *5*, 607.

Loi, S., Haibe-Kains, B., Desmedt, C., Lallemand, F., Tutt, A.M., *et al.* (2007). Definition of clinically distinct molecular subtypes in estrogen receptor-positive breast carcinomas through genomic grade. ***J Clin Oncol*** *25*, 1239-1246.

Lopez, R.D., Xu, S., Guo, B., Negrin, R.S., and Waller, E.K. (2000). CD2-mediated IL-12-dependent signals render human γδ-T cells resistant to mitogen-induced apoptosis, permitting the large-scale *ex vivo* expansion of functionally distinct lymphocytes: implications for the development of adoptive immunotherapy strategies. ***Blood*** *96*, 3827-3837.

Lu, H., Clauser, K.R., Tam, W.L., Frose, J., Ye, X., *et al.* (2014). A breast cancer stem cell niche supported by juxtacrine signalling from monocytes and macrophages. ***Nat Cell Biol*** *16*, 1105-1117.

Luo, M., Brooks, M., and Wicha, M.S. (2015). Epithelial-mesenchymal plasticity of breast cancer stem cells: implications for metastasis and therapeutic resistance. ***Curr Pharm Des*** *21*, 1301-1310.

Luoma, A.M., Castro, C.D., Mayassi, T., Bembinster, L.A., Bai, L., *et al.* (2013). Crystal structure of Vδ1 T cell receptor in complex with CD1d-sulfatide shows MHC-like recognition of a self-lipid by human γδ T cells. ***Immunity*** *39*, 1032-1042.

Ma, C., Zhang, Q., Ye, J., Wang, F., Zhang, Y., *et al.* (2012). Tumor-infiltrating γδ T lymphocytes predict clinical outcome in human breast cancer. ***J Immunol*** *189*, 5029-5036.

Ma, S., Cheng, Q., Cai, Y., Gong, H., Wu, Y., *et al.* (2014). IL-17A produced by γδ T cells promotes tumor growth in hepatocellular carcinoma. ***Cancer Res*** *74*, 1969-1982.

Ma, Y., Aymeric, L., Locher, C., Mattarollo, S.R., Delahaye, N.F., *et al.* (2011). Contribution of IL-17-producing γδ T cells to the efficacy of anticancer chemotherapy. ***J Exp Med*** *208*, 491-503.

Majeti, R., Chao, M.P., Alizadeh, A.A., Pang, W.W., Jaiswal, S., *et al.* (2009). CD47 is an adverse prognostic factor and therapeutic antibody target on human acute myeloid leukemia stem cells. ***Cell*** *138*, 286-299.

Malkovska, V., Cigel, F.K., Armstrong, N., Storer, B.E., and Hong, R. (1992). Antilymphoma activity of human γδ T-cells in mice with severe combined immune deficiency. ***Cancer Res*** *52*, 5610-5616.

Mani, S.A., Guo, W., Liao, M.J., Eaton, E.N., Ayyanan, A.*, et al.* (2008). The epithelial-mesenchymal transition generates cells with properties of stem cells. ***Cell*** *133*, 704-715.

Mao, C., Mou, X., Zhou, Y., Yuan, G., Xu, C.*, et al.* (2014). Tumor-activated TCR$\gamma\delta^+$ T cells from gastric cancer patients induce the antitumor immune response of TCR$\alpha\beta^+$ T cells *via* their antigen-presenting cell-like effects. ***J Immunol Res*** *2014*, 593562.

Matis, L.A., Fry, A.M., Cron, R.Q., Cotterman, M.M., Dick, R.F.*, et al.* (1989). Structure and specificity of a class II MHC alloreactive γδ T cell receptor heterodimer. ***Science*** *245*, 746-749.

May, C.D., Sphyris, N., Evans, K.W., Werden, S.J., Guo, W.*, et al.* (2011). Epithelial-mesenchymal transition and cancer stem cells: a dangerously dynamic duo in breast cancer progression. ***Breast Cancer Res*** *13*, 202.

Medema, J.P. (2013). Cancer stem cells: the challenges ahead. ***Nat Cell Biol*** *15*, 338-344.

Meraviglia, S., Eberl, M., Vermijlen, D., Todaro, M., Buccheri, S.*, et al.* (2010). *In vivo* manipulation of Vγ9Vδ2 T cells with zoledronate and low-dose interleukin-2 for immunotherapy of advanced breast cancer patients. ***Clin Exp Immunol*** *161*, 290-297.

Meuter, S., Eberl, M., and Moser, B. (2010). Prolonged antigen survival and cytosolic export in cross-presenting human γδ T cells. ***Proc Natl Acad Sci U S A*** *107*, 8730-8735.

Mitra, A., Mishra, L., and Li, S. (2015). EMT, CTCs and CSCs in tumor relapse and drug-resistance. ***Oncotarget*** *6*, 10697-10711.

Miyagawa, F., Tanaka, Y., Yamashita, S., Mikami, B., Danno, K.*, et al.* (2001). Essential contribution of germline-encoded lysine residues in Jγ1.2 segment to the recognition of nonpeptide antigens by human γδ T cells. ***J Immunol*** *167*, 6773-6779.

Monkkonen, H., Ottewell, P.D., Kuokkanen, J., Monkkonen, J., Auriola, S.*, et al.* (2007). Zoledronic acid-induced IPP/ApppI production *in vivo*. ***Life Sci*** *81*, 1066-1070.

Mookerjee-Basu, J., Vantourout, P., Martinez, L.O., Perret, B., Collet, X.*, et al.* (2010). F1-adenosine triphosphatase displays properties characteristic of an antigen presentation molecule for Vγ9Vδ2 T cells. ***J Immunol*** *184*, 6920-6928.

Morel, A.P., Lievre, M., Thomas, C., Hinkal, G., Ansieau, S.*, et al.* (2008). Generation of breast cancer stem cells through epithelial-mesenchymal transition. ***PLoS One*** *3*, e2888.

Morita, C.T., Beckman, E.M., Bukowski, J.F., Tanaka, Y., Band, H.*, et al.* (1995). Direct presentation of nonpeptide prenyl pyrophosphate antigens to human γδ T cells. ***Immunity*** *3*, 495-507.

Moser, B., and Eberl, M. (2007). γδ T cells: novel initiators of adaptive immunity. ***Immunol Rev*** *215*, 89-102.

Moser, B., and Eberl, M. (2011). γδ T-APCs: a novel tool for immunotherapy? ***Cell Mol Life Sci*** *68*, 2443-2452.

Moser, B., Wolf, M., Walz, A., and Loetscher, P. (2004). Chemokines: multiple levels of leukocyte migration control. ***Trends Immunol*** *25*, 75-84.

Muto, M., Baghdadi, M., Maekawa, R., Wada, H., and Seino, K. (2015). Myeloid molecular characteristics of human γδ T cells support their acquisition of tumor antigen-presenting capacity. ***Cancer Immunol Immunother*** *64*, 941-949.

Nakajima, J., Murakawa, T., Fukami, T., Goto, S., Kaneko, T.*, et al.* (2010). A phase I study of adoptive immunotherapy for recurrent non-small-cell lung cancer patients with autologous γδ T cells. ***Eur J Cardiothorac Surg*** *37*, 1191-1197.

Navid, F., Sondel, P.M., Barfield, R., Shulkin, B.L., Kaufman, R.A.*, et al.* (2014). Phase I trial of a novel anti-GD2 monoclonal antibody, Hu14.18K322A, designed to decrease toxicity in children with refractory or recurrent neuroblastoma. ***J Clin Oncol*** *32*, 1445-1452.

Nebbioso, A., Clarke, N., Voltz, E., Germain, E., Ambrosino, C.*, et al.* (2005). Tumor-selective action of HDAC inhibitors involves TRAIL induction in acute myeloid leukemia cells. ***Nat Med*** *11*, 77-84.

Nedellec, S., Bonneville, M., and Scotet, E. (2010a). Human Vγ9Vδ2 T cells: from signals to functions. ***Semin Immunol*** *22*, 199-206.

Nedellec, S., Sabourin, C., Bonneville, M., and Scotet, E. (2010b). NKG2D costimulates human Vγ9Vδ2 T cell antitumor cytotoxicity through protein kinase C θ-dependent modulation of early TCR-induced calcium and transduction signals. ***J Immunol*** *185*, 55-63.

Neefjes, J., Jongsma, M.L., Paul, P., and Bakke, O. (2011). Towards a systems understanding of MHC class I and MHC class II antigen presentation. ***Nat Rev Immunol*** *11*, 823-836.

Nicol, A.J., Tokuyama, H., Mattarollo, S.R., Hagi, T., Suzuki, K.*, et al.* (2011). Clinical evaluation of autologous γδ T cell-based immunotherapy for metastatic solid tumours. ***Br J Cancer*** *105*, 778-786.

Nielsen, T.O., Hsu, F.D., Jensen, K., Cheang, M., Karaca, G.*, et al.* (2004). Immunohistochemical and clinical characterization of the basal-like subtype of invasive breast carcinoma. ***Clin Cancer Res*** *10*, 5367-5374.

Ning, N., Pan, Q., Zheng, F., Teitz-Tennenbaum, S., Egenti, M., *et al.* (2012). Cancer stem cell vaccination confers significant antitumor immunity. ***Cancer Res*** *72*, 1853-1864.

Nishio, N., Fujita, M., Tanaka, Y., Maki, H., Zhang, R., *et al.* (2012). Zoledronate sensitizes neuroblastoma-derived tumor-initiating cells to cytolysis mediated by human γδ T cells. ***J Immunother*** *35*, 598-606.

Nowell, P.C. (1976). The clonal evolution of tumor cell populations. ***Science*** *194*, 23-28.

O'Brien, C.A., Pollett, A., Gallinger, S., and Dick, J.E. (2007). A human colon cancer cell capable of initiating tumour growth in immunodeficient mice. ***Nature*** *445*, 106-110.

O'Reilly, M.S., Boehm, T., Shing, Y., Fukai, N., Vasios, G., *et al.* (1997). Endostatin: an endogenous inhibitor of angiogenesis and tumor growth. ***Cell*** *88*, 277-285.

Oberg, H.H., Peipp, M., Kellner, C., Sebens, S., Krause, S., *et al.* (2014). Novel bispecific antibodies increase γδ T-cell cytotoxicity against pancreatic cancer cells. ***Cancer Res*** *74*, 1349-1360.

Palakodeti, A., Sandstrom, A., Sundaresan, L., Harly, C., Nedellec, S., *et al.* (2012). The molecular basis for modulation of human Vγ9Vδ2 T cell responses by CD277/butyrophilin-3 (BTN3A)-specific antibodies. ***J Biol Chem*** *287*, 32780-32790.

Palucka, K., and Banchereau, J. (2012). Cancer immunotherapy *via* dendritic cells. ***Nat Rev Cancer*** *12*, 265-277.

Pardal, R., Clarke, M.F., and Morrison, S.J. (2003). Applying the principles of stem-cell biology to cancer. ***Nat Rev Cancer*** *3*, 895-902.

Parente-Pereira, A.C., Shmeeda, H., Whilding, L.M., Zambirinis, C.P., Foster, J., *et al.* (2014). Adoptive immunotherapy of epithelial ovarian cancer with Vγ9Vδ2 T cells, potentiated by liposomal alendronic acid. ***J Immunol*** *193*, 5557-5566.

Peng, G., Wang, H.Y., Peng, W., Kiniwa, Y., Seo, K.H., *et al.* (2007). Tumor-infiltrating γδ T cells suppress T and dendritic cell function *via* mechanisms controlled by a unique toll-like receptor signaling pathway. ***Immunity*** *27*, 334-348.

Pereira, P., and Boucontet, L. (2004). Rates of recombination and chain pair biases greatly influence the primary γδ TCR repertoire in the thymus of adult mice. ***J Immunol*** *173*, 3261-3270.

Perou, C.M., Sorlie, T., Eisen, M.B., van de Rijn, M., Jeffrey, S.S., *et al.* (2000). Molecular portraits of human breast tumours. ***Nature*** *406*, 747-752.

Pfeffer, K., Schoel, B., Plesnila, N., Lipford, G.B., Kromer, S., *et al.* (1992). A lectin-binding, protease-resistant mycobacterial ligand specifically activates $V\gamma9^+$ human γδ T cells. ***J Immunol*** *148*, 575-583.

Piggott, L., Omidvar, N., Marti Perez, S., French, R., Eberl, M., *et al.* (2011). Suppression of apoptosis inhibitor c-FLIP selectively eliminates breast cancer stem cell activity in response to the anti-cancer agent, TRAIL. ***Breast Cancer Res** 13*, R88.

Pinto, C.A., Widodo, E., Waltham, M., and Thompson, E.W. (2013). Breast cancer stem cells and epithelial mesenchymal plasticity - Implications for chemoresistance. ***Cancer Lett** 341*, 56-62.

Porcelli, S., Brenner, M.B., Greenstein, J.L., Balk, S.P., Terhorst, C., *et al.* (1989). Recognition of cluster of differentiation 1 antigens by human $CD4^-CD8^-$ cytolytic T lymphocytes. ***Nature** 341*, 447-450.

Poupot, M., Pont, F., and Fournie, J.J. (2005). Profiling blood lymphocyte interactions with cancer cells uncovers the innate reactivity of human γδ T cells to anaplastic large cell lymphoma. ***J Immunol** 174*, 1717-1722.

Psaila, B., Kaplan, R.N., Port, E.R., and Lyden, D. (2006). Priming the 'soil' for breast cancer metastasis: the pre-metastatic niche. ***Breast Dis** 26*, 65-74.

Qin, G., Mao, H., Zheng, J., Sia, S.F., Liu, Y., *et al.* (2009). Phosphoantigen-expanded human γδ T cells display potent cytotoxicity against monocyte-derived macrophages infected with human and avian influenza viruses. ***J Infect Dis** 200*, 858-865.

Rabinovitch, M. (1995). Professional and non-professional phagocytes: an introduction. ***Trends Cell Biol** 5*, 85-87.

Rei, M., Goncalves-Sousa, N., Lanca, T., Thompson, R.G., Mensurado, S., *et al.* (2014). Murine $CD27^-$ $V\gamma6^+$ γδ T cells producing IL-17A promote ovarian cancer growth *via* mobilization of protumor small peritoneal macrophages. ***Proc Natl Acad Sci U S A** 111*, E3562-3570.

Reid, I.R., Gamble, G.D., Mesenbrink, P., Lakatos, P., and Black, D.M. (2010). Characterization of and risk factors for the acute-phase response after zoledronic acid. ***J Clin Endocrinol Metab** 95*, 4380-4387.

Rey, J., Veuillen, C., Vey, N., Bouabdallah, R., and Olive, D. (2009). Natural killer and γδ T cells in haematological malignancies: enhancing the immune effectors. ***Trends Mol Med** 15*, 275-284.

Reya, T., Morrison, S.J., Clarke, M.F., and Weissman, I.L. (2001). Stem cells, cancer, and cancer stem cells. ***Nature** 414*, 105-111.

Rhodes, D.A., Chen, H.C., Price, A.J., Keeble, A.H., Davey, M.S., *et al.* (2015). Activation of human γδ T cells by cytosolic interactions of BTN3A1 with soluble phosphoantigens and the cytoskeletal adaptor periplakin. ***J Immunol** 194*, 2390-2398.

Rhodes, D.A., Stammers, M., Malcherek, G., Beck, S., and Trowsdale, J. (2001). The cluster of BTN genes in the extended major histocompatibility complex. ***Genomics*** *71*, 351-362.

Riano, F., Karunakaran, M.M., Starick, L., Li, J., Scholz, C.J., *et al.* (2014). Vγ9Vδ2 TCR-activation by phosphorylated antigens requires butyrophilin 3 A1 (BTN3A1) and additional genes on human chromosome 6. ***Eur J Immunol*** *44*, 2571-2576.

Ricci-Vitiani, L., Lombardi, D.G., Pilozzi, E., Biffoni, M., Todaro, M., *et al.* (2007). Identification and expansion of human colon-cancer-initiating cells. ***Nature*** *445*, 111-115.

Rich, J.N. (2007). Cancer stem cells in radiation resistance. ***Cancer Res*** *67*, 8980-8984.

Riganti, C., Massaia, M., Davey, M.S., and Eberl, M. (2012). Human γδ T-cell responses in infection and immunotherapy: common mechanisms, common mediators? ***Eur J Immunol*** *42*, 1668-1676.

Rincon-Orozco, B., Kunzmann, V., Wrobel, P., Kabelitz, D., Steinle, A., *et al.* (2005). Activation of Vγ9Vδ2 T cells by NKG2D. ***J Immunol*** *175*, 2144-2151.

Roelofs, A.J., Jauhiainen, M., Monkkonen, H., Rogers, M.J., Monkkonen, J., *et al.* (2009). Peripheral blood monocytes are responsible for γδ T cell activation induced by zoledronic acid through accumulation of IPP/DMAPP. ***Br J Haematol*** *144*, 245-250.

Rouzier, R., Perou, C.M., Symmans, W.F., Ibrahim, N., Cristofanilli, M., *et al.* (2005). Breast cancer molecular subtypes respond differently to preoperative chemotherapy. ***Clin Cancer Res*** *11*, 5678-5685.

Sakamoto, M., Nakajima, J., Murakawa, T., Fukami, T., Yoshida, Y., *et al.* (2011). Adoptive immunotherapy for advanced non-small cell lung cancer using zoledronate-expanded γδ Tcells: a phase I clinical study. ***J Immunother*** *34*, 202-211.

Sallusto, F., Lenig, D., Forster, R., Lipp, M., and Lanzavecchia, A. (1999). Two subsets of memory T lymphocytes with distinct homing potentials and effector functions. ***Nature*** *401*, 708-712.

Sandstrom, A., Peigne, C.M., Leger, A., Crooks, J.E., Konczak, F., *et al.* (2014). The intracellular B30.2 domain of butyrophilin 3A1 binds phosphoantigens to mediate activation of human Vγ9Vδ2 T cells. ***Immunity*** *40*, 490-500.

Santini, D., Martini, F., Fratto, M.E., Galluzzo, S., Vincenzi, B., *et al.* (2009). *In vivo* effects of zoledronic acid on peripheral γδ T lymphocytes in early breast cancer patients. ***Cancer Immunol Immunother*** *58*, 31-38.

Santolaria, T., Robard, M., Leger, A., Catros, V., Bonneville, M.*, et al.* (2013). Repeated systemic administrations of both aminobisphosphonates and human Vγ9Vδ2 T cells efficiently control tumor development *in vivo*. ***J Immunol*** *191*, 1993-2000.

Schatton, T., and Frank, M.H. (2009). Antitumor immunity and cancer stem cells. ***Ann N Y Acad Sci*** *1176*, 154-169.

Schatton, T., Murphy, G.F., Frank, N.Y., Yamaura, K., Waaga-Gasser, A.M.*, et al.* (2008). Identification of cells initiating human melanomas. ***Nature*** *451*, 345-349.

Schatton, T., Schutte, U., Frank, N.Y., Zhan, Q., Hoerning, A.*, et al.* (2010a). Modulation of T-cell activation by malignant melanoma initiating cells. ***Cancer Res*** *70*, 697-708.

Schatton, T., Schutte, U., Frank, N.Y., Zhan, Q., Hoerning, A.*, et al.* (2010b). Modulation of T-cell activation by malignant melanoma initiating cells. ***Cancer Res*** *70*, 697-708.

Scheel, C., and Weinberg, R.A. (2012). Cancer stem cells and epithelial-mesenchymal transition: concepts and molecular links. ***Semin Cancer Biol*** *22*, 396-403.

Schneiders, F.L., Prodohl, J., Ruben, J.M., O'Toole, T., Scheper, R.J.*, et al.* (2014). CD1d-restricted antigen presentation by Vγ9Vδ2-T cells requires trogocytosis. ***Cancer Immunol Res*** *2*, 732-740.

Schoel, B., Sprenger, S., and Kaufmann, S.H. (1994). Phosphate is essential for stimulation of Vγ9Vδ2 T lymphocytes by mycobacterial low molecular weight ligand. ***Eur J Immunol*** *24*, 1886-1892.

Scotet, E., Martinez, L.O., Grant, E., Barbaras, R., Jeno, P.*, et al.* (2005). Tumor recognition following Vγ9Vδ2 T cell receptor interactions with a surface F1-ATPase-related structure and apolipoprotein A-I. ***Immunity*** *22*, 71-80.

Segura, E., and Amigorena, S. (2013). Inflammatory dendritic cells in mice and humans. ***Trends Immunol*** *34*, 440-445.

Segura, E., Touzot, M., Bohineust, A., Cappuccio, A., Chiocchia, G.*, et al.* (2013). Human inflammatory dendritic cells induce Th17 cell differentiation. ***Immunity*** *38*, 336-348.

Seidel, U.J., Vogt, F., Grosse-Hovest, L., Jung, G., Handgretinger, R.*, et al.* (2014). γδ T cell-mediated antibody-dependent cellular cytotoxicity with CD19 antibodies assessed by an impedance-based label-free real-time cytotoxicity assay. ***Front Immunol*** *5*, 618.

Sharma, A., Koldovsky, U., Xu, S., Mick, R., Roses, R.*, et al.* (2012). HER-2 pulsed dendritic cell vaccine can eliminate HER-2 expression and impact ductal carcinoma in situ. ***Cancer*** *118*, 4354-4362.

Shen, Y., Zhou, D., Qiu, L., Lai, X., Simon, M.*, et al.* (2002). Adaptive immune response of Vγ2Vδ2^{+} T cells during mycobacterial infections. ***Science*** *295*, 2255-2258.

Shin, S., El-Diwany, R., Schaffert, S., Adams, E.J., Garcia, K.C.*, et al.* (2005). Antigen recognition determinants of γδ T cell receptors. ***Science*** *308*, 252-255.

Shipitsin, M., Campbell, L.L., Argani, P., Weremowicz, S., Bloushtain-Qimron, N.*, et al.* (2007). Molecular definition of breast tumor heterogeneity. ***Cancer Cell*** *11*, 259-273.

Silva-Santos, B., Serre, K., and Norell, H. (2015). γδ T cells in cancer. ***Nat Rev Immunol*** *15*, 683-691.

Singh, H., Figliola, M.J., Dawson, M.J., Huls, H., Olivares, S.*, et al.* (2011). Reprogramming CD19-specific T cells with IL-21 signaling can improve adoptive immunotherapy of B-lineage malignancies. ***Cancer Res*** *71*, 3516-3527.

Singh, S.K., Hawkins, C., Clarke, I.D., Squire, J.A., Bayani, J.*, et al.* (2004). Identification of human brain tumour initiating cells. ***Nature*** *432*, 396-401.

Smalley, M., Piggott, L., and Clarkson, R. (2013). Breast cancer stem cells: obstacles to therapy. ***Cancer Lett*** *338*, 57-62.

Sorlie, T., Perou, C.M., Tibshirani, R., Aas, T., Geisler, S.*, et al.* (2001). Gene expression patterns of breast carcinomas distinguish tumor subclasses with clinical implications. ***Proc Natl Acad Sci U S A*** *98*, 10869-10874.

Sorlie, T., Tibshirani, R., Parker, J., Hastie, T., Marron, J.S.*, et al.* (2003). Repeated observation of breast tumor subtypes in independent gene expression data sets. ***Proc Natl Acad Sci U S A*** *100*, 8418-8423.

Sotiriou, C., Neo, S.Y., McShane, L.M., Korn, E.L., Long, P.M.*, et al.* (2003). Breast cancer classification and prognosis based on gene expression profiles from a population-based study. ***Proc Natl Acad Sci U S A*** *100*, 10393-10398.

Spada, F.M., Grant, E.P., Peters, P.J., Sugita, M., Melian, A.*, et al.* (2000). Self-recognition of CD1 by γ/δ T cells: implications for innate immunity. ***J Exp Med*** *191*, 937-948.

Spits, H., Paliard, X., Engelhard, V.H., and de Vries, J.E. (1990). Cytotoxic activity and lymphokine production of T cell receptor (TCR)-αβ^{+} and TCR-γδ^{+} cytotoxic T lymphocyte (CTL) clones recognizing HLA-A2 and HLA-A2 mutants: Recognition of

TCR-γδ$^+$ CTL clones is affected by mutations at positions 152 and 156. ***J Immunol*** *144*, 4156-4162.

Steff, A.M., Fortin, M., Arguin, C., and Hugo, P. (2001). Detection of a decrease in green fluorescent protein fluorescence for the monitoring of cell death: an assay amenable to high-throughput screening technologies. ***Cytometry*** *45*, 237-243.

Steinman, R.M., Hawiger, D., and Nussenzweig, M.C. (2003). Tolerogenic dendritic cells. ***Annu Rev Immunol*** *21*, 685-711.

Struckmann, K., Mertz, K., Steu, S., Storz, M., Staller, P., *et al.* (2008). pVHL co-ordinately regulates CXCR4/CXCL12 and MMP2/MMP9 expression in human clear-cell renal cell carcinoma. ***J Pathol*** *214*, 464-471.

Taieb, J., Chaput, N., Menard, C., Apetoh, L., Ullrich, E., *et al.* (2006). A novel dendritic cell subset involved in tumor immunosurveillance. ***Nat Med*** *12*, 214-219.

Tallerico, R., Todaro, M., Di Franco, S., Maccalli, C., Garofalo, C., *et al.* (2013). Human NK cells selective targeting of colon cancer-initiating cells: a role for natural cytotoxicity receptors and MHC class I molecules. ***J Immunol*** *190*, 2381-2390.

Tanaka, Y., Morita, C.T., Tanaka, Y., Nieves, E., Brenner, M.B., *et al.* (1995). Natural and synthetic non-peptide antigens recognized by human γδ T cells. ***Nature*** *375*, 155-158.

Tanaka, Y., Sano, S., Nieves, E., De Libero, G., Rosa, D., *et al.* (1994). Nonpeptide ligands for human γδ T cells. ***Proc Natl Acad Sci U S A*** *91*, 8175-8179.

Thedrez, A., Harly, C., Morice, A., Salot, S., Bonneville, M., *et al.* (2009). IL-21-mediated potentiation of antitumor cytolytic and proinflammatory responses of human Vγ9Vδ2 T cells for adoptive immunotherapy. ***J Immunol*** *182*, 3423-3431.

Thedrez, A., Sabourin, C., Gertner, J., Devilder, M.C., Allain-Maillet, S., *et al.* (2007). Self/non-self discrimination by human γδ T cells: simple solutions for a complex issue? ***Immunol Rev*** *215*, 123-135.

Thiery, J.P., Acloque, H., Huang, R.Y., and Nieto, M.A. (2009). Epithelial-mesenchymal transitions in development and disease. ***Cell*** *139*, 871-890.

Thompson, K., Keech, F., McLernon, D.J., Vinod, K., May, R.J., *et al.* (2011). Fluvastatin does not prevent the acute-phase response to intravenous zoledronic acid in post-menopausal women. ***Bone*** *49*, 140-145.

Todaro, M., D'Asaro, M., Caccamo, N., Iovino, F., Francipane, M.G., *et al.* (2009). Efficient killing of human colon cancer stem cells by γδ T lymphocytes. ***J Immunol*** *182*, 7287-7296.

Todaro, M., Gaggianesi, M., Catalano, V., Benfante, A., Iovino, F., *et al.* (2014). CD44v6 is a marker of constitutive and reprogrammed cancer stem cells driving colon cancer metastasis. ***Cell Stem Cell*** *14*, 342-356.

Todaro, M., Orlando, V., Cicero, G., Caccamo, N., Meraviglia, S., *et al.* (2013). Chemotherapy sensitizes colon cancer initiating cells to Vγ9Vδ2 T cell-mediated cytotoxicity. ***PLoS One*** *8*, e65145.

Toutirais, O., Cabillic, F., Le Friec, G., Salot, S., Loyer, P., *et al.* (2009). DNAX accessory molecule-1 (CD226) promotes human hepatocellular carcinoma cell lysis by Vγ9Vδ2 T cells. ***Eur J Immunol*** *39*, 1361-1368.

Triebel, F., Faure, F., Graziani, M., Jitsukawa, S., Lefranc, M.P., *et al.* (1988a). A unique V-J-C-rearranged gene encodes a γ protein expressed on the majority of $CD3^+$ T cell receptor-α/β^- circulating lymphocytes. ***J Exp Med*** *167*, 694-699.

Triebel, F., Faure, F., Mami-Chouaib, F., Jitsukawa, S., Griscelli, A., *et al.* (1988b). A novel human V δ gene expressed predominantly in the Ti γ A fraction of γ/δ^+ peripheral lymphocytes. ***Eur J Immunol*** *18*, 2021-2027.

Tsai, J.H., and Yang, J. (2013). Epithelial-mesenchymal plasticity in carcinoma metastasis. ***Genes Dev*** *27*, 2192-2206.

Tsuruo, T., and Fujita, N. (2008). Platelet aggregation in the formation of tumor metastasis. ***Proceedings of the Japan Academy*** *84*, 189-198.

Tyler, C.J., Doherty, D.G., Moser, B., and Eberl, M. (2015). Human Vγ9/Vδ2 T cells: Innate adaptors of the immune system. ***Cell Immunol*** *296*, 10-21.

Uccelli, A., Moretta, L., and Pistoia, V. (2008). Mesenchymal stem cells in health and disease. ***Nat Rev Immunol*** *8*, 726-736.

Uldrich, A.P., Le Nours, J., Pellicci, D.G., Gherardin, N.A., McPherson, K.G., *et al.* (2013). CD1d-lipid antigen recognition by the γδ TCR. ***Nat Immunol*** *14*, 1137-1145.

Uno, T., Takeda, K., Kojima, Y., Yoshizawa, H., Akiba, H., *et al.* (2006). Eradication of established tumors in mice by a combination antibody-based therapy. ***Nat Med*** *12*, 693-698.

Urban, E.M., Li, H., Armstrong, C., Focaccetti, C., Cairo, C., *et al.* (2009). Control of CD56 expression and tumor cell cytotoxicity in human Vγ2Vδ2 T cells. ***BMC Immunol*** *10*, 50.

Valachis, A., Polyzos, N.P., Coleman, R.E., Gnant, M., Eidtmann, H., *et al.* (2013). Adjuvant therapy with zoledronic acid in patients with breast cancer: a systematic review and meta-analysis. ***Oncologist*** *18*, 353-361.

Vantourout, P., and Hayday, A. (2013). Six-of-the-best: unique contributions of γδ T cells to immunology. ***Nat Rev Immunol*** *13*, 88-100.

Vantourout, P., Radojkovic, C., Lichtenstein, L., Pons, V., Champagne, E.*, et al.* (2010). Ecto-F(1)-ATPase: a moonlighting protein complex and an unexpected apoA-I receptor. ***World J Gastroenterol*** *16*, 5925-5935.

Vavassori, S., Kumar, A., Wan, G.S., Ramanjaneyulu, G.S., Cavallari, M.*, et al.* (2013). Butyrophilin 3A1 binds phosphorylated antigens and stimulates human γδ T cells. ***Nat Immunol*** *14*, 908-916.

Velasco-Velazquez, M.A., Popov, V.M., Lisanti, M.P., and Pestell, R.G. (2011). The role of breast cancer stem cells in metastasis and therapeutic implications. ***Am J Pathol*** *179*, 2-11.

Vermijlen, D., Ellis, P., Langford, C., Klein, A., Engel, R.*, et al.* (2007). Distinct cytokine-driven responses of activated blood γδ T cells: insights into unconventional T cell pleiotropy. ***J Immunol*** *178*, 4304-4314.

Vesely, M.D., Kershaw, M.H., Schreiber, R.D., and Smyth, M.J. (2011). Natural innate and adaptive immunity to cancer. ***Annu Rev Immunol*** *29*, 235-271.

Viey, E., Fromont, G., Escudier, B., Morel, Y., Da Rocha, S.*, et al.* (2005). Phosphostim-activated γδ T cells kill autologous metastatic renal cell carcinoma. ***J Immunol*** *174*, 1338-1347.

Vincent, M.S., Roessner, K., Sellati, T., Huston, C.D., Sigal, L.H.*, et al.* (1998). Lyme arthritis synovial γδ T cells respond to Borrelia burgdorferi lipoproteins and lipidated hexapeptides. ***J Immunol*** *161*, 5762-5771.

Vincent-Salomon, A., and Thiery, J.P. (2003). Host microenvironment in breast cancer development: epithelial-mesenchymal transition in breast cancer development. ***Breast Cancer Res*** *5*, 101-106.

Visus, C., Ito, D., Amoscato, A., Maciejewska-Franczak, M., Abdelsalem, A.*, et al.* (2007). Identification of human aldehyde dehydrogenase 1 family member A1 as a novel $CD8^+$ T-cell-defined tumor antigen in squamous cell carcinoma of the head and neck. ***Cancer Res*** *67*, 10538-10545.

Visus, C., Wang, Y., Lozano-Leon, A., Ferris, R.L., Silver, S.*, et al.* (2011). Targeting $ALDH^{bright}$ human carcinoma-initiating cells with ALDH1A1-specific $CD8^+$ T cells. ***Clin Cancer Res*** *17*, 6174-6184.

Visvader, J.E., and Lindeman, G.J. (2008). Cancer stem cells in solid tumours: accumulating evidence and unresolved questions. ***Nat Rev Cancer*** *8*, 755-768.

Voduc, K.D., Cheang, M.C., Tyldesley, S., Gelmon, K., Nielsen, T.O.*, et al.* (2010). Breast cancer subtypes and the risk of local and regional relapse. ***J Clin Oncol*** *28*, 1684-1691.

Wang, H., Henry, O., Distefano, M.D., Wang, Y.C., Raikkonen, J.*, et al.* (2013). Butyrophilin 3A1 plays an essential role in prenyl pyrophosphate stimulation of human Vγ2Vδ2 T cells. ***J Immunol*** *191*, 1029-1042.

Webber, J., Steadman, R., Mason, M.D., Tabi, Z., and Clayton, A. (2010). Cancer exosomes trigger fibroblast to myofibroblast differentiation. ***Cancer Res*** *70*, 9621-9630.

Wei, J., Barr, J., Kong, L.Y., Wang, Y., Wu, A.*, et al.* (2010a). Glioblastoma cancer-initiating cells inhibit T-cell proliferation and effector responses by the signal transducers and activators of transcription 3 pathway. ***Mol Cancer Ther*** *9*, 67-78.

Wei, J., Barr, J., Kong, L.Y., Wang, Y., Wu, A.*, et al.* (2010b). Glioma-associated cancer-initiating cells induce immunosuppression. ***Clin Cancer Res*** *16*, 461-473.

Welton, J.L., Marti, S., Mahdi, M.H., Boobier, C., Barrett-Lee, P.J.*, et al.* (2013a). γδ T cells predict outcome in zoledronate-treated breast cancer patients. ***Oncologist*** *18*, e22-23.

Welton, J.L., Morgan, M.P., Marti, S., Stone, M.D., Moser, B.*, et al.* (2013b). Monocytes and γδ T cells control the acute-phase response to intravenous zoledronate: insights from a phase IV safety trial. ***J Bone Miner Res*** *28*, 464-471.

Weninger, W., Crowley, M.A., Manjunath, N., and von Andrian, U.H. (2001). Migratory properties of naive, effector, and memory $CD8^+$ T cells. ***J Exp Med*** *194*, 953-966.

Wesch, D., Peters, C., and Siegers, G.M. (2014). Human γδ T regulatory cells in cancer: fact or fiction? ***Front Immunol*** *5*, 598.

Willcox, C.R., Pitard, V., Netzer, S., Couzi, L., Salim, M., *et al.* (2012). Cytomegalovirus and tumor stress surveillance by binding of a human γδ T cell antigen receptor to endothelial protein C receptor. ***Nat Immunol*** *13*, 872-879.

Winnard, P.T., Jr., Kluth, J.B., and Raman, V. (2006). Noninvasive optical tracking of red fluorescent protein-expressing cancer cells in a model of metastatic breast cancer. ***Neoplasia*** *8*, 796-806.

Wright, M.H., Calcagno, A.M., Salcido, C.D., Carlson, M.D., Ambudkar, S.V.*, et al.* (2008). Brca1 breast tumors contain distinct $CD44^+/CD24^-$ and $CD133^+$ cells with cancer stem cell characteristics. ***Breast Cancer Res*** *10*, R10.

Wrobel, P., Shojaei, H., Schittek, B., Gieseler, F., Wollenberg, B.*, et al.* (2007). Lysis of a broad range of epithelial tumour cells by human γδ T cells: involvement of NKG2D ligands and T-cell receptor- versus NKG2D-dependent recognition. ***Scand J Immunol*** *66*, 320-328.

Wu, P., Wu, D., Ni, C., Ye, J., Chen, W.*, et al.* (2014). γδT17 cells promote the accumulation and expansion of myeloid-derived suppressor cells in human colorectal cancer. ***Immunity*** *40*, 785-800.

Wu, Y., Deng, J., Rychahou, P.G., Qiu, S., Evers, B.M.*, et al.* (2009a). Stabilization of snail by NF-κB is required for inflammation-induced cell migration and invasion. ***Cancer Cell*** *15*, 416-428.

Wu, Y., Wu, W., Wong, W.M., Ward, E., Thrasher, A.J.*, et al.* (2009b). Human γδ T cells: a lymphoid lineage cell capable of professional phagocytosis. ***J Immunol*** *183*, 5622-5629.

Xi, X., Han, X., Li, L., and Zhao, Z. (2013). Identification of a new tuberculosis antigen recognized by γδ T cell receptor. ***Clin Vaccine Immunol*** *20*, 530-539.

Xi, X., Zhang, X., Wang, B., Wang, J., Huang, H.*, et al.* (2011). A novel strategy to screen Bacillus Calmette-Guerin protein antigen recognized by γδ TCR. ***PLoS One*** *6*, e18809.

Xiang, Z., Liu, Y., Zheng, J., Liu, M., Lv, A.*, et al.* (2014). Targeted activation of human Vγ9Vδ2-T cells controls epstein-barr virus-induced B cell lymphoproliferative disease. ***Cancer Cell*** *26*, 565-576.

Xu, B., Pizarro, J.C., Holmes, M.A., McBeth, C., Groh, V.*, et al.* (2011). Crystal structure of a γδ T-cell receptor specific for the human MHC class I homolog MICA. ***Proc Natl Acad Sci U S A*** *108*, 2414-2419.

Xu, J., Lamouille, S., and Derynck, R. (2009a). TGF-β-induced epithelial to mesenchymal transition. ***Cell Res*** *19*, 156-172.

Xu, Q., Liu, G., Yuan, X., Xu, M., Wang, H.*, et al.* (2009b). Antigen-specific T-cell response from dendritic cell vaccination using cancer stem-like cell-associated antigens. ***Stem Cells*** *27*, 1734-1740.

Yang, M.H., Wu, M.Z., Chiou, S.H., Chen, P.M., Chang, S.Y.*, et al.* (2008). Direct regulation of TWIST by HIF-1α promotes metastasis. ***Nat Cell Biol*** *10*, 295-305.

Ye, J., Ma, C., Hsueh, E.C., Eickhoff, C.S., Zhang, Y.*, et al.* (2013). Tumor-derived γδ regulatory T cells suppress innate and adaptive immunity through the induction of immunosenescence. ***J Immunol*** *190*, 2403-2414.

Yehiely, F., Moyano, J.V., Evans, J.R., Nielsen, T.O., and Cryns, V.L. (2006). Deconstructing the molecular portrait of basal-like breast cancer. ***Trends Mol Med*** *12*, 537-544.

Yin, T., Shi, P., Gou, S., Shen, Q., and Wang, C. (2014). Dendritic cells loaded with pancreatic Cancer Stem Cells (CSCs) lysates induce antitumor immune killing effect *in vitro*. ***PLoS One*** *9*, e114581.

Yuasa, T., Sato, K., Ashihara, E., Takeuchi, M., Maita, S., *et al.* (2009). Intravesical administration of γδ T cells successfully prevents the growth of bladder cancer in the murine model. ***Cancer Immunol Immunother*** *58*, 493-502.

Zeng, X., Meyer, C., Huang, J., Newell, E.W., Kidd, B.A., *et al.* (2014). γδ T cells recognize haptens and mount a hapten-specific response. ***Elife*** *3*, e03609.

Zeng, X., Wei, Y.L., Huang, J., Newell, E.W., Yu, H., *et al.* (2012). γδ T cells recognize a microbial encoded B cell antigen to initiate a rapid antigen-specific interleukin-17 response. ***Immunity*** *37*, 524-534.

Zhang, L., Jin, N., Nakayama, M., O'Brien, R.L., Eisenbarth, G.S., *et al.* (2010). γδ T cell receptors confer autonomous responsiveness to the insulin-peptide B:9-23. ***J Autoimmun*** *34*, 478-484.

Appendix: Publications during this PhD

Rhodes DA, **Chen H-C**, Price AJ, Keeble AS Davey MS, James LC, Eberl M and Trowsdale J. Interaction of BTN3A1 with the cytoskeletal adaptor periplakin and the activation of γδ T cells. ***J Immunol*** 194: 2390, 2015

Khan MW, Curbishley S, **Chen H-C,** Thomas A, Pircher H, Mavilio D, Steven N, Eberl M and Moser B. Expanded human blood-derived γδ T cells display potent antigen-presentation functions. ***Front Immunol*** **5**: 344, 2014

Chen H-C, Dieli F, Eberl M. An unconventional TRAIL to cancer therapy. ***Eur J Immunol*** 43: 3159, 2013